

HYDROGEOLOGICAL CHARACTERIZATION OF THE NORTHERN PART
OF THE KIŞLADAĞ GOLD-MINE, UŞAK, TURKEY

A THESIS SUBMITTED TO
THE GRADUATE SCHOOL OF THE NATURAL AND APPLIED SCIENCES
OF
THE MIDDLE EAST TECHNICAL UNIVERSITY

BY

EGEMEN FIRAT

IN PARTIAL FULFILLMENT OF THE REQUIREMENTS
FOR
THE DEGREE OF MASTER OF SCIENCE
IN
GEOLOGICAL ENGINEERING

NOVEMBER 2013

Approval of the thesis:

**HYDROGEOLOGICAL CHARACTERIZATION OF THE NORTHERN PART
OF THE KIŞLADAĞ GOLD-MINE, UŞAK, TURKEY**

submitted by **EGEMEN FIRAT** in partial fulfillment of the requirements for the degree of **Master of Science in Geological Engineering Department, Middle East Technical University** by,

Prof.Dr. Canan Özgen

Dean, Graduate School of **Natural and Applied Science**

Prof.Dr. Erdin Bozkurt

Head of Department, **Geological Engineering**

Prof.Dr. Hasan Yazıcıgil

Supervisor, **Geological Engineering Dept., METU**

Examining Committee Members:

Prof.Dr. Mehmet Ekmekçi

Hydrogeological Engineering Dept., Hacettepe University

Prof.Dr. Hasan Yazıcıgil

Geological Engineering Dept., METU

Prof.Dr. M. Zeki Çamur

Geological Engineering Dept., METU

Assist. Prof. Dr. Koray K. Yılmaz

Geological Engineering Dept., METU

Instr. Dr. Özlem Yağbasan

Geography Teaching, Gazi University

Date: 01/11/2013

I hereby declare that all information in this document has been obtained and presented in accordance with academic rules and ethical conduct. I also declare that, as required by these rules and conduct, I have fully cited and referenced all material and results that are not original to this work.

Name, Last Name: Egemen FIRAT

Signature:

ABSTRACT

HYDROGEOLOGICAL CHARACTERIZATION OF THE NORTHERN PART OF THE KIŞLADAĞ GOLD MINE AREA

Fırat, Egemen

M.S., Department of Geological Engineering

Supervisor: Prof. Dr. Hasan Yazıcıgil

November 2013, 193 pages

The purpose of this study is to characterize the hydrogeological conditions at the northern part of the Kışladağ Gold Mine located in Uşak Province in the West of Turkey. Because of the planned mining activities in the area, it is essential to characterize the system in order to assess the impacts of mining operations on surface and groundwater systems. The characterization studies included hydrological, hydrogeological and hydrochemical analysis of surface and groundwater. Hereby, the relevant measurements from the meteorological stations are taken regularly so as to observe the surface water in the area. After the weirs are set up, surface water level changes are observed and the necessary data is obtained from chemical sampling. By using data collected from meteorological stations and weirs, and information about the land cover and the land use, the hydrological water budget is calculated. Within the scope of groundwater observation studies, some of the existing exploration wells are converted to observation wells, and new wells are drilled in specific places for hydrogeological observation purposes with the aim to observe the desired formations and samples from the wells. By using the drilled observation wells in the area, changes in groundwater levels are observed in the formations, while aquifer parameters of the units are determined by applying aquifer tests in the wells. In addition, hydrological sections are drawn with the help of the well information, and any possible correlations between the hydro-lithological units are determined. Groundwater, surface water, springs and fountains of the area are classified with respect to hydrochemical study by using the parameters obtained from sampling, and further water facies are identified.

Keywords: Kışladağ Gold Mine, Hydrogeological Characterization, Hydraulic Water Budget, Aquifer Test

ÖZ

KIŞLADAĞ ALTIN MADENİNİN KUZEY BÖLÜMÜNÜN HİDROJEOLJİK KARAKTERİZASYONU

Fırat, Egemen

Yüksek Lisans, Jeoloji Mühendisliği Bölümü

Tez Yöneticisi : Prof. Dr. Hasan Yazıcıgil

Kasım 2013, 193 sayfa

Bu çalışma, Türkiye'nin batı bölgesinde yer alan Kışladağ altın madeninin kuzey bölümünün hidrojeolojik karakterizasyonunu ortaya koyma amaçlıdır. Yapılan karakterizasyon çalışması bölgenin yüzey sularını ve yeraltısularının hidrolojik, hidrojeolojik ve hidrojeokimyasal analizlerini içermektedir. Bölgede yapılan madencilik faaliyetleri dolayısıyla yeraltısuları ve yüzey sularının madencilikle nasıl etkileşim içinde olduğunu anlamak gerekmektedir. Bunun sonucu olarak, bölgede bulunan yüzey sularını gözleme amacı ile meteoroloji istasyonlarından ölçümler düzenli olarak alınmış, savaklar kurdurulmuş ve savaklar kullanılarak, yüzey suyu seviyesi değişimleri gözlenmiş ve yapılan kimyasal örneklemelerden gerekli veriler sağlanmıştır. Savak ve meteoroloji istasyonu verileri, bölgenin toprak örtüsü ve tarım alanı bilgileri kullanılarak, hidrolojik su bütçesi hesaplanmıştır. Yeraltısuyunu gözleme amaçlı yapılan çalışmalarda ise, halihazırda bulunan arama kuyularının bazılarını gözlem kuyusuna dönüştürülüp, gözlemek istenilen formasyonlar da baz alınarak, gerekli görülen yerlerde hidrojeolojik gözlem amaçlı yeni kuyular açılmış ve kuyulardan örneklemeler yapılmıştır. Bölgede açılmış olan gözlem kuyuları kullanılarak, formasyonlardaki su seviye değişimleri gözlenmiş ve kuyularda uygulanan akifer testleri ile birimlerin akifer parametreleri saptanmıştır. Bununla birlikte, kuyu bilgileri kullanılarak, hidrolojik kesitler çizilmiş ve hidro-litolojik birimlerin olası uzantıları ilişkilendirilmiştir. Örneklemeden sağlanan parametreler kullanılarak; bölgedeki yeraltısularının, yüzey sularının, kaynak ve çeşmelerin hidrokimyasal sınıflandırılması yapılmış ve su fasiyesleri belirlenmiştir.

Anahtar Kelimeler: Kışladağ Altın Madeni, Hidrojeolojik Karakterizasyon, Hidrolojik Su Bütçesi, Akifer Testi

ACKNOWLEDGMENTS

Foremost, it has been a great honor to have an opportunity to work with Prof. Dr. Hasan Yazicigil through the whole study and benefit from his priceless life time experiences. It is unquestionable that this thesis would not be the same if I was not encouraged, criticized and guided by him whenever I felt stuck.

I would like to express my deepest gratitude to Assistant Prof. Koray K. Yılmaz and Prof Dr. Zeki Çamur who provided me a tremendous opportunity to work with them. I cannot appreciate more their invaluable contributions to my studies.

This master thesis has been conducted as a part of the project named, “Kışladağ Altın Madeni Sahasının Hidrojeolojik Etüdü” and is supported by “Tüprag Metal Madencilik San. ve Tic. A.Ş.”. Therefore, the support provided by Tüprag Metal Madencilik San. ve Tic. A.Ş. is greatly appreciated.

I would also like to show my sincere appreciation to my roommates Burcu Ünsal, Çidem Argunhan, Yağmur Derin and Ayşe Peksezer Sayıt who were with me throughout the study and made me feel supported whenever I needed help.

I cannot thank enough to my beloved friends Sinan Yenigül, Onursal Çatak, Mehmet Hazar and Cansu Kahraman who were intimately involved in this process. Their encouragement and support through the irreplaceable friendship means a lot to me. I would particularly like to thank my lifelong friend İlkey Çevik for the sleepless nights we were working together. I am deeply indebted to him since he made every effort to make things simpler for me.

I am grateful to my parents for providing me the peaceful environment to study and stand behind every decision I made.

Last but certainly not least, I would like to thank Çiğdem Erkılınç who supported me morally and spiritually throughout this process. Her patience and understanding made everything easier and give me the strength to succeed.

TABLE OF CONTENTS

ABSTRACT	v
ÖZ.....	vi
ACKNOWLEDGMENTS.....	vii
TABLE OF CONTENTS.....	viii
LIST OF TABLES	x
LIST OF FIGURES.....	xii
CHAPTERS	
1.INTRODUCTION.....	1
1.1. Purpose and Scope.....	1
1.2. The Location of the Study Area.....	2
1.3 Background and Previous Works	3
1.3.1. Previous Geological Investigations.....	3
1.3.2. Previous Hydrological Investigations	3
1.3.3. Previous Hydrogeological Investigations.....	3
2.SITE DESCRIPTION.....	5
2.1. Physiographic Features	5
2.2. Climate and Meteorology	6
2.2.1. Precipitation	9
2.2.2. Temperature	10
2.2.3. Relative Humidity	12
2.2.4. Evaporation	12
2.3. Geology.....	15
2.3.1. Regional Geology	15
2.3.2. Local Geology.....	16
3.SURFACE WATER HYDROLOGY	23
3.1. Natural Drainage (Drainage Network System).....	23
3.2. Stream Flow Observations.....	23
3.3. Hydrologic Water Budget.....	28

4.HYDROGEOLOGY	41
4.1. Water Points	41
4.1.1. Rivers.....	41
4.1.2. Springs and Fountains.....	41
4.1.3. Wells.....	47
4.2. Groundwater Bearing Units.....	51
4.2.1. Regional Hydrogeological Setting.....	51
4.2.2. Site Hydrogeological Setting.....	55
4.3. Groundwater Levels	67
4.3.1. Spatial Variation in Groundwater Levels	67
4.3.2. Hydrogeological Cross Sections.....	72
5.HYDROCHEMISTRY AND WATER QUALITY.....	79
5.1. Available Data.....	79
5.2. Surface Water Hydrochemistry	81
5.2.1. Observation Points.....	81
5.2.2. The Characteristic Value Determination of Surface Waters.....	81
5.2.3. Hydrochemical Evaluation	83
5.3. Groundwater Hydrochemistry	85
5.3.1. Springs and Fountains.....	85
5.3.2. Wells.....	87
5.4. Water Quality Classifications.....	99
5.4.1. Surface Water Classification	99
5.4.2. Groundwater Classification	103
6.CONCLUSIONS AND RECOMMENDATION.....	117
6.1. Conclusion.....	117
6.2. Recommendation.....	119
REFERENCES	121
APPENDICES	125
A. WELLS IN THE STUDY AREA AND ITS VICINITY	125
B: DETAILED WELL LOGS.....	130
C: AQUIFER TEST RESULTS.....	151

LIST OF TABLES

TABLES

Table 2.1 Meteorological Stations around the Study Area (Yazıcıgil et al., 2013).....	7
Table 3.1 Information about Weir-2 and Weir-6 (Yazıcıgil et al., 2013).....	23
Table 3.2 Watershed and Existing Mine Structure Areas (Yazıcıgil et al., 2013)	24
Table 3.3 Weir Dimension Parameters (Yazıcıgil et al., 2013).....	25
Table 3.4 Hydrologic Soil Groups (Westenbroek et al. 2010)	29
Table 3.5 Data Requirements for Potential Evapotranspiration Methods (Westenbroek et al. 2010).....	29
Table 3.6 Data Requirements for Application of the SWB Model	30
Table 3.7 Land Use/Land Cover Lookup Table and Curve Numbers.....	32
Table 3.8 Groundwater recharge amounts using different evapotranspiration methods in the SWB model	37
Table 3.9 The water budget components obtained from the SWB model.....	38
Table 4.1 Information about springs in the Banaz River Basin (Yazıcıgil et al., 2013).....	43
Table 4.2 Discharge values in the İnay Spring measured by the DSİ (m ³ /s) (Yazıcıgil et al., 2013).....	43
Table 4.3 Discharge values in the Sarıkız Spring as measured by the DSİ (L/s) (Yazıcıgil et al., 2013).....	44
Table 4.4 The springs and fountains in the study area and its vicinity (Yazıcıgil et al., 2013)	47
Table 4.5 The yield and specific yield values of the wells in the study area with respect to their formations (Yazıcıgil et al., 2013)	48
Table 4.6 Aquifer Tests on LP Wells and Well Information.....	61
Table 4.7 Aquifer Tests on HY Wells and Well Information	65
Table 4.8 Calculated Hydraulic conductivity values (m/s) for the planned expansion areas.	66
Table 5.1 Yearly distribution of data belonging to observation point locations (Yazıcıgil et al., 2013).....	79
Table 5.2 The mean ionic charge balance error of observation points (Yazıcıgil et al., 2013)	80
Table 5.3 Location information of surface water quality points (Yazıcıgil et al., 2013)	81

Table 5.4 Information of the surface water point for the determination of characteristic value (Yazıcıgil et al., 2013)	82
Table 5.5 The lower and upper limit characteristic values of the surface water point (Units: mg/l, EC:µS/cm) (Yazıcıgil et al., 2013)	82
Table 5.6 The location information of KWSP-2 and KWSP-9 (Yazıcıgil et al., 2013).....	85
Table 5.7 Location Information of the Observation Points (Yazıcıgil et al., 2013).....	88
Table 5.8 Observation locations in the study area (Yazıcıgil et al., 2013)	96
Table 5.9 Field measurements in the study area (July, 2011) (Yazıcıgil et al., 2013).....	99
Table 5.10 The characteristic value of surface water involving the pre-mining period (BM) and inland water classification by considering the geometric mean values involving the mining period (AM) (YSKYY, 2012) and suitability for human consumption (İTAS, 2005; EU, 1998) Unit: mg/l, EC: µS/cm. pH* alt and pH** for upper limits of the characteristic value. (Yazıcıgil et al., 2013).....	100
Table 5.11 The inland water classification of spring and fountain water according to the geometric mean values (SKKY, 2008; YSKYY, 2012) and suitability for human consumption (İTAS, 2005; EU, 1998) Unit: mg/l, EC: µS/cm. (Yazıcıgil et al., 2013).....	104
Table 5.12 The inland water classification of groundwater (SKKY, 2008; YSKYY, 2012) and suitability for human consumption belonging to the schist unit according to geometric mean values (İTAS, 2005; EU, 1998) Unit: mg/l, EC: µS/cm. (Yazıcıgil et al., 2013).....	108
Table 5.13 The inland water classification of groundwater (SKKY, 2008; YSKYY, 2012) and suitability for human consumption belonging to the volcanic unit according to geometric mean values (İTAS, 2005; EU, 1998) Unit: mg/l, EC: µS/cm. (Yazıcıgil et al., 2013).....	111
Table 5.14 The inland water classification of groundwater (SKKY, 2008; YSKYY, 2012) and suitability for human consumption belonging to the Asartepe Formation according to geometric mean values (İTAS, 2005; EU, 1998) Unit: mg/l, EC: µS/cm. (Yazıcıgil et al., 2013).....	114
Table A.1 Wells in the study area and its vicinity (Yazıcıgil et al., 2013)	126

LIST OF FIGURES

FIGURES

Figure 1.1 Location of the study area.....	2
Figure 2.1 Digital elevation model of the Kışladağ Gold-Mine area (Yazıcıgil et al., 2013) ..	6
Figure 2.2 Meteorological stations and weir locations in the mine area (Yazıcıgil et al., 2013)	8
Figure 2.3 Total precipitation (mm) and the deviation line related with average precipitation (mm) for the Kışladağ region (1975-2012) (Yazıcıgil et al., 2013)	9
Figure 2.4 Average monthly precipitation values of the Kışladağ region (Long Term, 1975- 2012).....	10
Figure 2.5 Average monthly precipitation values of the Kışladağ region (Short Term, 2001- 2012).....	10
Figure 2.6 Average monthly temperature values from the Kışladağ meteorological station (2006-2012).....	11
Figure 2.7 Minimum average monthly temperature values from the Kışladağ meteorological station (2006-2012)	11
Figure 2.8 The maximum average monthly temperature values from the Kışladağ meteorological station (2006-2012)	12
Figure 2.9 Average monthly relative humidity values from the Kışladağ meteorological station (2006-2012)	12
Figure 2.10 Monthly average evaporation values calculated for short term (2001-2012)	13
Figure 2.11 Monthly average evaporation values calculated for long term (1975-2012)	14
Figure 2.12 Monthly distribution of the monthly average precipitation and evaporation values calculated for Kışladağ (1975-2012).....	14
Figure 2.13 The long term annual total evaporation values calculated for Kışladağ (1975- 2012) (Yazıcıgil et al., 2013).....	15
Figure 2.14 Regional geology of the Kışladağ Gold Mine (Yazıcıgil et al., 2000).....	16
Figure 2.15 Geological map of the study area (Yazıcıgil et al., 2013).....	18
Figure 2.16 A possible stratigraphic section of the Northern part of the Kışladağ Gold Mine area (modified from the ARC, 2011)	19
Figure 2.17 Geological cross-sections of the study area (ARC, 2011)	22
Figure 3.1 Cross-Sectional View of the Weirs (Yazıcıgil et al., 2013).....	24
Figure 3.2 December, 2012 (a) Daily Precipitation Data Obtained from the Kışladağ Gold Mine (b) Manual and Automatic Water Level Measurements (Yazıcıgil et al., 2013)	26

Figure 3.3 Daily average flow rates of weirs (06/2005-12/2012) (Yazıcıgil et al., 2013).....	27
Figure 3.4 Daily average flow rates of weirs in logarithmic scale (06/2005-12/2012) (Yazıcıgil et al., 2013)	27
Figure 3.5 Model domain and land use/land cover map	31
Figure 3.6 Hydrologic Soil Groups in the SWB Model Domain	33
Figure 3.7 Flow Chart of the SWB Model (Westenbroek et al., 2010)	34
Figure 3.8 Comparison of Calculated and Observed Flow Values for Weir-5 (2009)	35
Figure 3.9 Unit outflow amounts by using different evapotranspiration methods in the SWB model for Weir-5.....	38
Figure 3.10 The yearly average groundwater recharge amount (mm/year) obtained from the SWB model (2008-2012 average).....	39
Figure 4.1 Regional Hydrogeological Map (Yazıcıgil et al., 2008).....	42
Figure 4.2 Discharge value variations in the Inay Spring as measured by the DSI (Yazıcıgil et al., 2013)	44
Figure 4.3 Discharge value variations in the Sarıkız Spring as measured by the DSI (Yazıcıgil et al., 2013)	45
Figure 4.4 The springs and fountains in the study area and its vicinity (Yazıcıgil et al., 2013)	46
Figure 4.5 Wells in the study area and its vicinity (Yazıcıgil et al., 2013).....	50
Figure 4.6 The groundwater level map of the Ulubey Formation (Yazıcıgil et al., 2008).....	54
Figure 4.7 The well locations in the study area and its vicinity (Yazıcıgil et al., 2013).....	55
Figure 4.8 Calculated hydraulic conductivity values (m/s) for planned areas	67
Figure 4.9 Groundwater level map in the study area (Yazıcıgil et al., 2013)	68
Figure 4.10 Depth to groundwater level map in the study area (Yazıcıgil et al., 2013)	69
Figure 4.11 (a) Temporal Groundwater level changes of the HY-1 and GC-451 wells (b) Temporal Groundwater level changes of HY-3 (c) Temporal Groundwater level changes of HY-4 (d) Temporal Groundwater level changes of HY-8 (e) Temporal Groundwater level changes of the HY-5 and GC-454 wells (f) Temporal Groundwater level changes of the HY-6 and GC-455 wells	72
Figure 4.12 Direction of hydrogeological sections for the extension areas	73
Figure 4.13 Direction of hydrogeological sections and groundwater levels (Yazıcıgil et al., 2013)	74
Figure 4.14 Hydrogeological cross section of AA'	75
Figure 4.15 Hydrogeological cross section of BB'B''	76

Figure 4.16 Hydrogeological cross section of CC'	77
Figure 4.17 Hydrogeological cross section of DD'	78
Figure 5.1 The distribution of the major ion concentration of the characteristic value (BM) and geometric mean of data (AM) of surface water in a Piper Diagram	83
Figure 5.2 Facies distributions of surface waters in the mining period	84
Figure 5.3 The groundwater quality observation locations of the fountains and their facies distribution of mean concentration	86
Figure 5.4 The facies distributions determined by considering the geometric mean of major ion concentration values of KWSP-2 and KWSP-9 in a Piper Diagram	87
Figure 5.5 Well Distribution for Groundwater Quality Observation	89
Figure 5.6 The facies distributions determined by considering the geometric mean of major ion concentration values of the schist unit in a Piper Diagram	90
Figure 5.7 The groundwater facies distribution of mean concentration of the schist unit	91
Figure 5.8 The facies distributions determined by considering the geometric mean of major ion concentration values of the Volcanic unit in a Piper Diagram (the LP-4 well in both volcanic and schist units)	92
Figure 5.9 The groundwater facies distribution of mean concentration of the Volcanic unit (the LP-4 well in both volcanic and schist units)	93
Figure 5.10 The facies distributions as determined by considering the geometric mean of major ion concentration values of the Asartepe Formation in a Piper Diagram	94
Figure 5.11 The groundwater facies distribution of mean concentration of the Asartepe Formation	95
Figure 5.12 The facies distributions as determined by considering the geometric mean of major ion concentration values of the study area in a Piper Diagram	97
Figure 5.13 The facies distributions determined by considering the geometric mean of groundwater levels and well observation points	98
Figure 5.14 The distribution of surface water facies, some parameters, and their classification	101
Figure 5.15 The quality distribution of surface water according to the average SAR and EC values of the characteristic values and the geometric mean during the mining period	102
Figure 5.16 The distribution of spring and fountain water facies, some parameters, and their classification	105
Figure 5.17 The quality distribution of spring and fountain water according to the average SAR and EC values	106
Figure 5.18 The distribution of facies, some parameters, and classification of the wells belonging to the schist unit	109

Figure 5.19 The quality distribution of groundwater belonging to the schist unit according to the average SAR and EC values of the characteristic values	110
Figure 5.20 The distribution of some parameters, facies, and classification of the wells belonging to the volcanic unit	112
Figure 5.21 The quality distribution of groundwater belonging to the Volcanics according to the average SAR and EC values of the characteristic values (LP-4 contains both volcanic and schist units)	113
Figure 5.22 The quality distribution of groundwater belonging to the Asartepe Formation according to the average SAR and EC values of the characteristic values	115
Figure B.1 The detailed well logs of GC-451	130
Figure B.2 The detailed well logs of GC-453	131
Figure B.3 The detailed well logs of GC-454	132
Figure B.4 The detailed well logs of GC-455	133
Figure B.5 The detailed well logs of GC-456	134
Figure B.6 The detailed well logs of GC-457	135
Figure B.7 The detailed well logs of LP-4A	136
Figure B.8 The detailed well logs of LP-5A	137
Figure B.9 The detailed well logs of LP-6	138
Figure B.10 The detailed well logs of LP-7	139
Figure B.11 The detailed well logs of HY-1	140
Figure B.12 The detailed well logs of HY-2	141
Figure B.13 The detailed well logs of HY-3	142
Figure B.14 The detailed well logs of HY-4	143
Figure B.15 The detailed well logs of HY-5	144
Figure B.16 The detailed well logs of HY-6	145
Figure B.17 The detailed well logs of HY-7	146
Figure B.18 The detailed well logs of HY-8	147
Figure B.19 The detailed well logs of HY-9	148
Figure B.20 The detailed well logs of HY-10	149
Figure B.21 The detailed well logs of HY-11	150
Figure C.1 Pumping test result of LP-4A	151
Figure C.2 Slug test result of LP-5A	154
Figure C.3 Pumping test result of LP-6	156

Figure C.4 Slug test result of HY-1.....	160
Figure C.5 Pumping test result of HY-3.....	164
Figure C.6 Slug test result of HY-4.....	167
Figure C.7 Pumping test result of HY-5.....	169
Figure C.8 Pumping test result of HY-6.....	173
Figure C.9 Free flow test result of HY-7.....	178
Figure C.10 Pumping test result of HY-8.....	179
Figure C.11 Pumping test result of HY-9.....	182
Figure C.12 Pumping test result of HY-10.....	187
Figure C.13 Pumping test result of HY-11.....	192

CHAPTER 1

INTRODUCTION

1.1. Purpose and Scope

The Kışladağ Gold Mine, located in the west part of Turkey in Uşak, is the country's biggest gold mine. Mining in the area began in 2006. According to recent studies, it is expected that the total ore extracted from this mine will be approximately 180.6 million tons with an annual average production expected to be nearly 12.5 million tons. The economic life of the Kışladağ Gold Mine is predicted to be approximately 15 years, and includes the planned duration of rehabilitation. As the mining processes continue, new areas should be required. Therefore, within the scope of increasing mine capacity, a new waste rock dump and heap leach pad areas will be needed at the northern part of the existing mine area. These areas have to be hydrologically and hydrogeologically characterized in order to assess the impacts of these mining units on surface and groundwater systems.

This study presents the hydrogeological investigation and characterization of the northern part of the Kışladağ Gold Mine with the aim of producing information to be used for the Environmental Impact Assessment (EIA) studies for the expansion areas. Within the scope of this study, (1) All the previous data collected from the current weirs including, the Kışladağ Gold Mine, the North Waste Rock Dump, and the North Heap Leach Pad areas were evaluated; to determine the hydrological structure of watersheds and surface water potential, a new weir was constructed and operated, and instant flow amounts of all the weirs were measured twice daily during the study; all the measured data were then evaluated. (2) Detailed hydrogeological investigations of the North Waste Rock Dump and the North Heap Leach Pad were performed and the characterizations of physical, chemical and hydraulic parameters of all areas were identified. In this respect, the specific locations were drilled as observation wells. Moreover, core wells which have been previously drilled for exploration purposes were converted into observation wells with casing. Pumping tests and slug tests were conducted in order to determine the hydraulic parameters of aquifers. Groundwater levels were measured for all of the observation wells throughout the study. (3) Water sampling is performed on the wells drilled in the northern part of the mine area and water quality data were obtained. These data were further evaluated with respect to hydrochemical and water quality standards.

The conceptual hydrogeological model of the Kışladağ Gold Mine area was then described by determining aquifer units, the relations of these units with each other, the spatial distribution of hydraulic parameters (hydraulic conductivity and storage coefficients), temporal and spatial change of water levels, temporal and spatial change of water quality, and the hydrological water budget (recharge).

1.2. The Location of the Study Area

The Kışladağ Gold Mine, located in the Aegean Region of Turkey, is positioned approximately 30 km southwest of Uşak and 180 km east of İzmir. The largest residential areas are Ulubey, 13 km southeast, and the town of Eşme, 20 km southwest of the study area. (Figure 1.1) The closest residential areas to the current mine and expansion areas are the Kışla, Gümüşkol, Katrancılar, Bekişli, Karacaömerli, Akçaköy, Emirli and Küçükilyaşlı villages, and Karapınar (District of Katrancılar), Hacıali, Örencik (Districts of Söğütlü) and Güzelköy (District of Karacaömerli) (Figure 2.1).

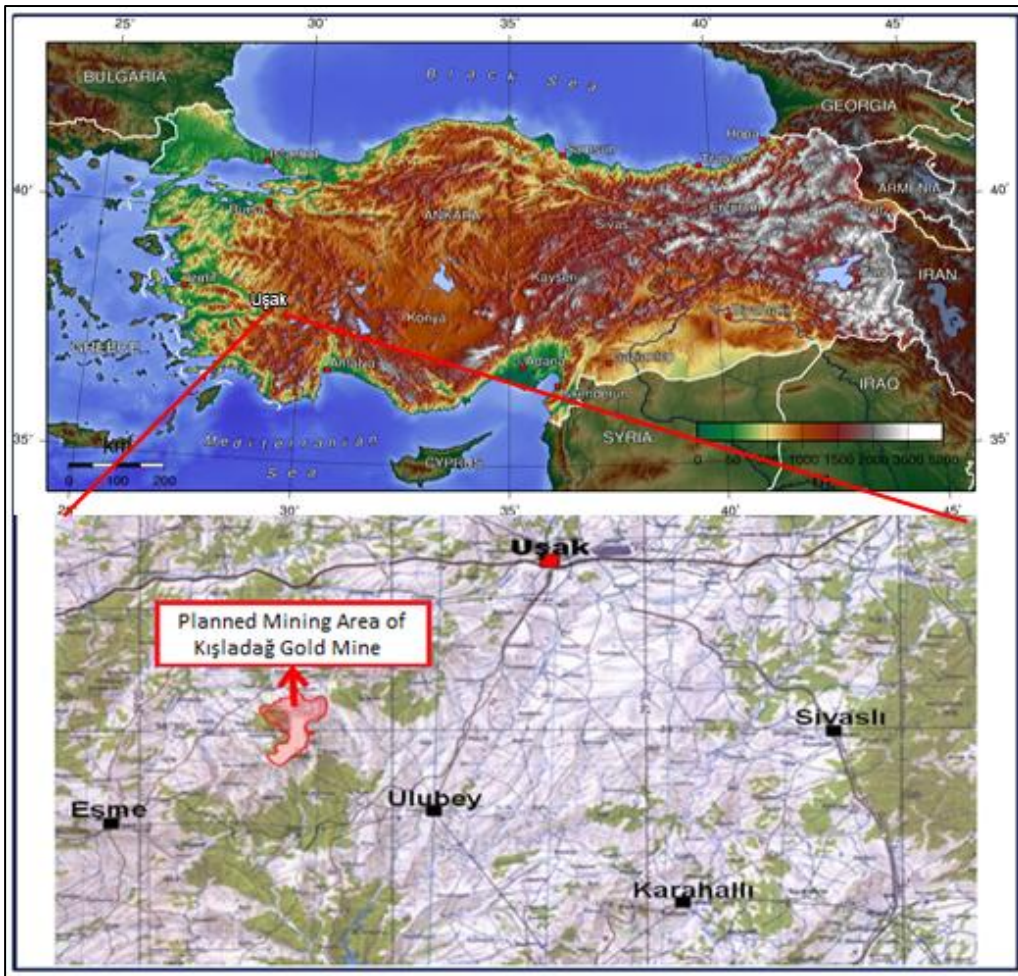


Figure 1.1 Location of the study area

1.3 Background and Previous Works

There are plenty of studies conducted about geology, hydrology and water sources of the Kışladağ Gold Mine area and its vicinity. Some of these studies were regional and some of them focus solely on the Kışladağ Gold Mine area. Below are summaries of the studies conducted as either regional or local.

1.3.1. Previous Geological Investigations

1/50.000 and 1/25.000 scale geological maps of Uşak, Eşme, Ulubey, Banaz, Güre and Sivaslı regions including the Kışladağ Gold Mine area are prepared by the Mineral Research and Exploration General Directorate (MTA).

There are detailed geological studies conducted within the scope of exploration activities. In addition to these, there are various studies particularly concerning structural components, such as: Lewis Geoscience Services Inc., Report on Geological Mapping and Structural Analysis, Kışladağ Gold Project, 2002, Murphy Geological Services, Structural Interpretation of Landsat ETM+ Scene No. 179/33 for West-Central Turkey, 2004, Kuşçu, İ., Structural Mapping of the Open Pit, Kışladağ Gold Mine, 2008, Hudson, M. Donald., Geology of Part of the Kışladağ-Sayacık Area Turkey 2009, Herod O. and Hodkiewicz P., Kışladağ Structural Geology Review, 2010, A.R.C., Geology of Northern Part of the Kışladağ Area (Around Örenköy-Küçükilyaslı-Güzelköy), 2011.

1.3.2. Previous Hydrological Investigations

The detailed hydrological study on the Kışladağ Gold Mine was conducted by Yazıcıgil et al. (2011) in order to determine the surface water potential in area. In this study, runoff coefficients were determined by calculating the flow in the weirs.

1.3.3. Previous Hydrogeological Investigations

The first regional study about this area, conducted in 1955 by The State Hydraulic Works (DSİ), is “Hydrogeological investigation report for drinking water supply to some of the villages in Karahallı and Ulubey districts of Uşak provinces” report. The studies about Hydrogeological investigations of Uşak, Banaz and Sivaslı lowlands were initiated by the DSİ in 1960. According to the results of the report, 13 investigation wells have been drilled. This report, namely the “Hydrogeological investigation report of Uşak, Banaz and Sivaslı Plains” was published by the DSİ in 1976 (Koç et al., 1976). In 1979, “The Hydrogeological Investigation Report for Uşak Springs” was prepared by 2. Regional Directorate of the DSİ (Aysan, 1979). Nine exploration wells were drilled between 1987 and 1990 by the DSİ. Six more exploration wells were drilled after 1989, and the study area of 1985 was expanded towards the south. Consisting of these studies, the “Hydrogeological investigation report of Uşak-Banaz-Sivaslı and Karahallı Plains” was published in 1993 (Kadioğlu, 1993). The last study was conducted within the scope of the Uşak supply water project and it was published as “Drinking Water Project for Uşak Province, Hydrogeological Investigation Report for Uşak Town and Uşak- Susuzören” by Vaytaş Sondaj İnşaat Turizm San. ve Tic. Ltd. Şirketi (Vaytaş, 2006).

Hydrogeological investigations at basin scale and the development of a groundwater management plan for the Ulubey aquifer system, which is the most significant regional aquifer of the area, were conducted by Yazıcıgil et al., (2008). This study, including the Banaz Creek Basin, was performed in an area of 3972 km². Within the scope of this study; the hydrogeological characterization of the units observed in this basin was carried out. The two most important aquifer systems, Ulubey and Asartepe, were designed by a groundwater flow model, and the management plan was created in order to fulfill the water supply of irrigation cooperation and residential areas in the basin within the 20 year planning period.

The first comprehensive hydrogeological study conducted in the Kışladağ Gold Mine and its vicinity by Yazıcıgil et al. (2000), evaluates local alternative water supply areas. Afterward, a series of studies were conducted by the SRK consulting firm, namely: SRK Consulting, Groundwater and Surface Water Monitoring Plan Kışladağ Property, 2002; SRK Consulting, Water Quality Sampling and Analysis Kışladağ Property, 2003; SRK Consulting, Water Supply Studies-Aquifer Test Kışladağ Project, 2003; SRK Consulting, Water Supply Exploration Studies Kışladağ Project, 2005; SRK Consulting, Conceptual Hydrogeological Model, Kışladağ Property, 2005; SRK Consulting, Assessment on Pit Lake Formation & Impacts on Groundwater System Kışladağ Project, 2007; SRK Consulting, Kışladağ Open Pit Dewatering/Depressurization Study, 2012; Yazıcıgil, H., Çamur M.Z., Yılmaz K.K., Ünsal B., Fırat E., 2013; and Hydrogeological Characterization of the Kışladağ Gold-Mine Area, Middle East Technical University.

CHAPTER 2

SITE DESCRIPTION

2.1. Physiographic Features

The Kışladağ Gold-Mine area is separated into two parts by the boundary between the Gediz and Büyük Menderes River Basins. The South Waste Rock Dump area is located in the Büyük Menderes River Basin whereas the Open Pit, South Heap Leach Pad, the North Waste Rock Dump, and the North Heap Leach Pad areas are in the Gediz River Basin. Instead of permanent streams, seasonal streams dominate the area due to the fact that the mine is located on the water divide of these two basins. Since the study area is in the northern part of the existing mine area, the streams are natural tributaries of the Gediz River.

Topographic elevations in the study area vary from a 600-meter- valley bottom to 1300-meter-high hills. In terms of morphology of the region, from west to east, peneplains on the base metamorphic rocks and plateaus originated by Neogene-aged sedimentary rocks are present. Between these features there are extensive volcanic cones namely the Beydağ and Kışla Volcanic Cones in the SW-NE direction. In the northern part of the mine area, topographical elevation ranges from 850 m to 1200 m.

As a result of these detailed topographic measurements within the mine site done by Tüprag, a Digital Elevation Model (DEM) of the study area (Figure 2.1) was prepared by using a topographic map with 1 meter contour intervals. This sensitized map was created by digitizing 1/25000 scale topographic maps.

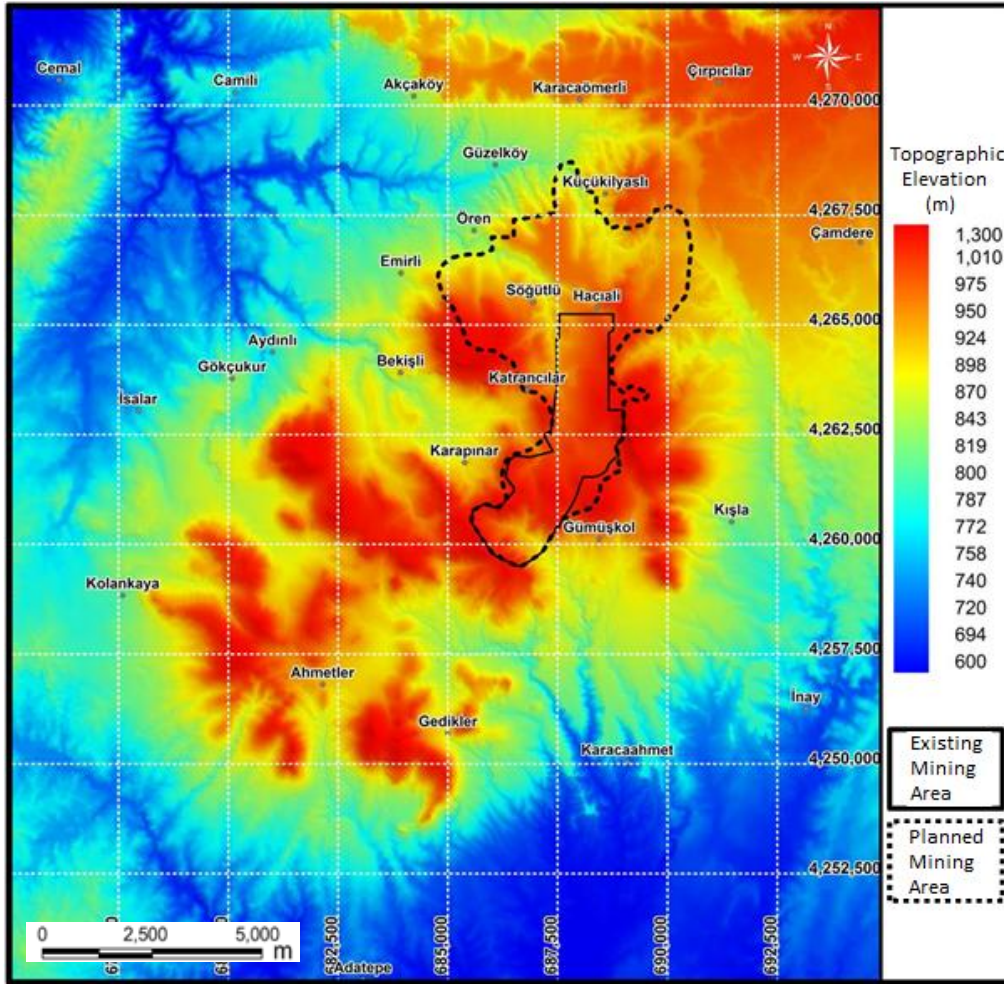


Figure 2.1 Digital elevation model of the Kışladağ Gold-Mine area (Yazıcıgil et al., 2013)

2.2. Climate and Meteorology

The study area geographically is situated between the Aegean and Central Anatolia Regions; therefore, the Mediterranean Transition Climate, which exhibits climatic features of both regions, is dominant (Türkeş, 1966). The Mediterranean Transition Climate receives medium precipitation in both winter and spring. According to the Turkish State Meteorological Services (MGM), the long-term (1975-2012) average rainfall of Uşak is 531.7 mm/year. The highest temperatures are observed in July and August while the lowest ones are in January (www.mgm.gov.tr).

Within the study area, there are 3 active meteorological stations measuring the meteorological parameters (Table 2.1, Figure 2.2). The first station (Met-1) is a manual measurement station installed in April of 2000, between the Open Pit and South Leach Pad Area. In this station, specific parameters such as, air temperature, wet/dry bulb temperatures, wind direction/speed, precipitation and evaporation were measured three times a day (at 7:00, 14:00 and 21:00). The second station (Met-2), the Automated Weather

Observing System (AWOS), situated in the same place as the manual station, has been operating since August of 2005. The AWOS station records air pressure, air temperature, wind direction/speed, possible sunshine and precipitation data every 5 minutes. The other Automated Weather Observing System station, which was the third (Met-3) station in this area installed in the northern part of the Open Pit in April of 2010. Since the third station operates on a short term period, this station was not used within the context of this study.

Table 2.1 Meteorological Stations around the Study Area (Yazıcıgil et al., 2013)

Station ID	Corporation	Coordinates (m)		Elevation (m)	Operation Period
		X	Y		
Kışladağ Manual	TUPRAG	687692	4262462	997	April, 2000-Cont.
Kışladağ AWOS	TUPRAG	687692	4262462	997	August, 2005-Cont.
Kışladağ AWOS (Open Pit)	TUPRAG	687130	4260476	1026	April, 2010-Cont.
Uşak	MGM	708760	4284370	930	1929-Cont.

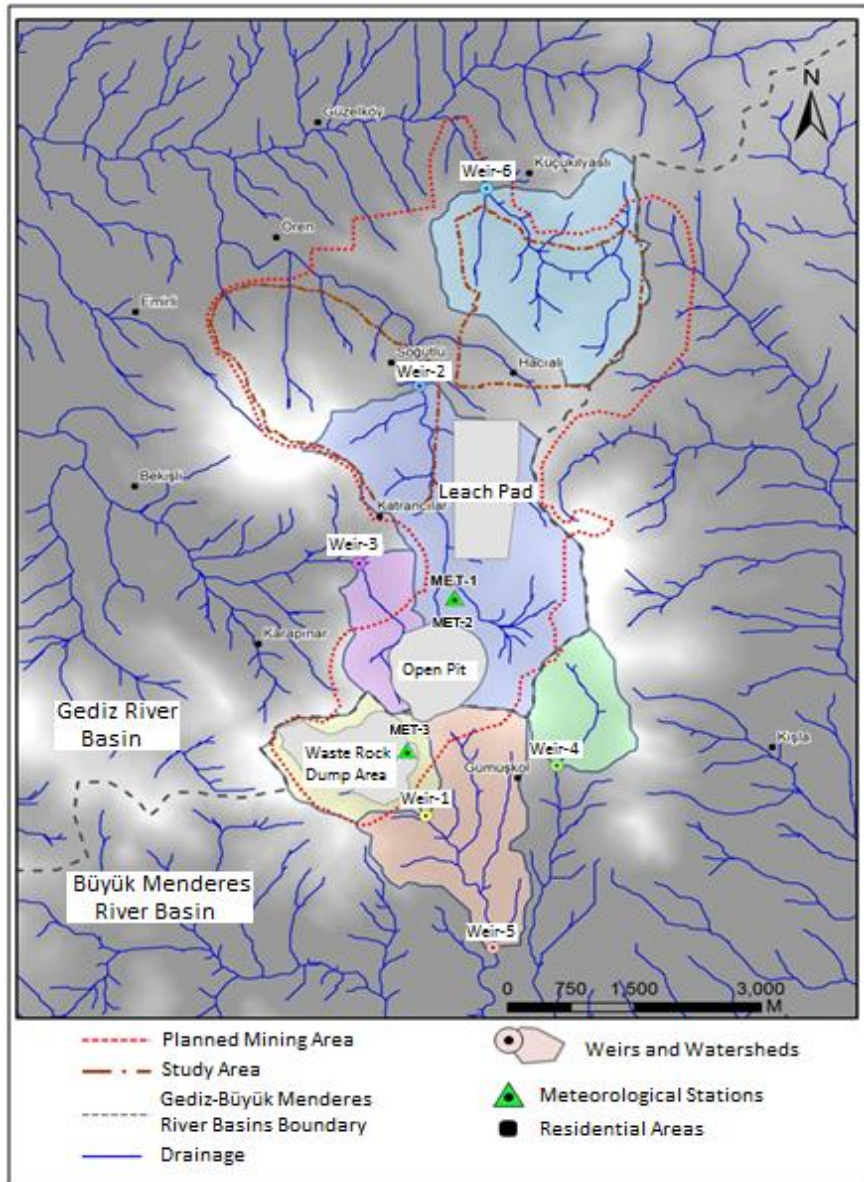


Figure 2.2 Meteorological stations and weir locations in the mine area (Yazıcıgil et al., 2013)

In this study, the data that have been evaluated by Yazıcıgil et al. (2013) using the Kışladağ meteorological stations (2001-2012) are examined. Yazıcıgil et al. (2013) generated long-term (1975-2012) precipitation and evaporation series by using data obtained from the MGM Uşak Meteorological Station (1975-2000). Additionally, temperature and relative humidity data were taken from the Kışladağ AWOS, with an exact operation period between 2006 and 2012.

2.2.1. Precipitation

Precipitation data within the mine area is the combination of the estimated values using the MGM Uşak Meteorological Station (1975-2000) by Yazıcıgil et al. (2011) and the data obtained from the Kışladağ Meteorological Station (2001-2012).

According to Yazıcıgil et al. (2011), due to the short operation period of the Kışladağ meteorological stations (2000-2012), information taken from the MGM Uşak meteorological station was adapted to the Kışladağ mine site in order to observe the long term trend in precipitation. The MGM Uşak meteorological station is located approximately 25 km northeast of the study area. Logically, data obtained from both stations does not show one-to-one correspondence. By comprising a mutual operation period of stations (2000-2012), the mean error values were calculated. Finally, the MGM Uşak meteorological station data (1975 -2000) were revised for the Kışladağ mine area.

The cumulative deviation from average precipitation line and yearly distribution of combined precipitation data (January 1975-March 2000 MGM Uşak Meteorological Station and April, 2000-2012 Kışladağ Meteorological Station) is shown in Figure 2.3. The average total precipitation of combined data was calculated as 493 mm per year whereas the average total precipitation per year equaled 491 mm, if only the Kışladağ meteorological station data (2000-2012) has been evaluated. According to the Kışladağ meteorological station data, 2004 (precipitation: 283 mm/yr.) was the driest and wettest year is detected as 2012 (precipitation: 639 mm/yr.). If the cumulative deviation line shown in Figure 2.3 is examined, it can be said that the study area has periodic dry and wet year intervals. Some of the dry periods are 1984-1996, 2003-2008 and the wet periods involve 1978-1981, 1997-2002, 2009-2012 years. Given the starting year of the mine operation, 2008 is the driest year, and one year later, in 2009, the area can be observed as wet year due to the influence of the large amount of precipitation.

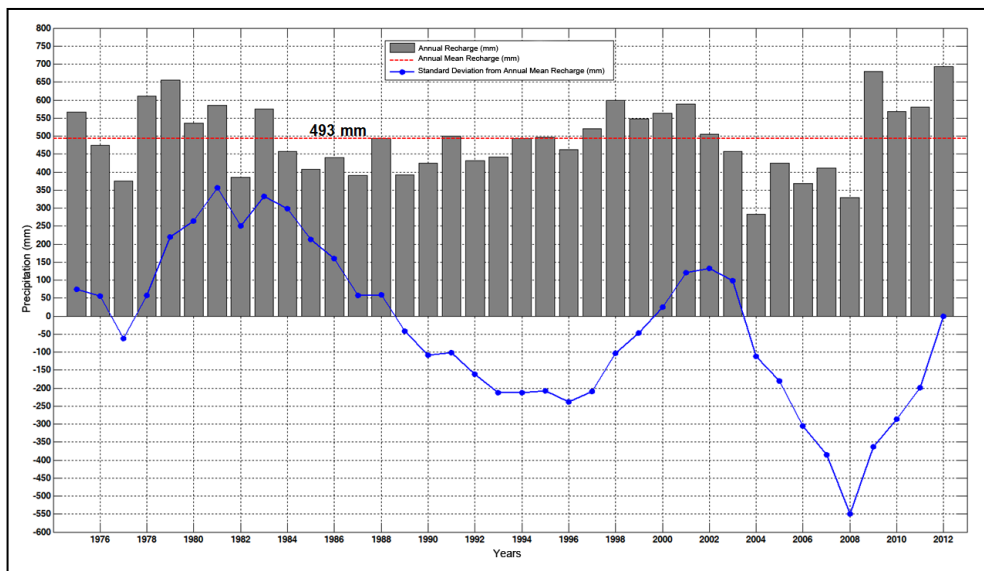


Figure 2.3 Total precipitation (mm) and the deviation line related with average precipitation (mm) for the Kışladağ region (1975-2012) (Yazıcıgil et al., 2013)

When the precipitation values are evaluated on monthly basis for both long-term, 1975-2012, (Figure 2.4) and short-term, 2001-2012, (Figure 2.5) data, it is determined that winter is the wet season while the dry season occurs in summer. The seasonal distribution of the total yearly precipitation consists of 42% in the winter, 26% in the spring, 9% in the summer and 23% in the fall seasons. December indicates the wettest month (71.5 mm) while the driest month is August (9.14 mm).

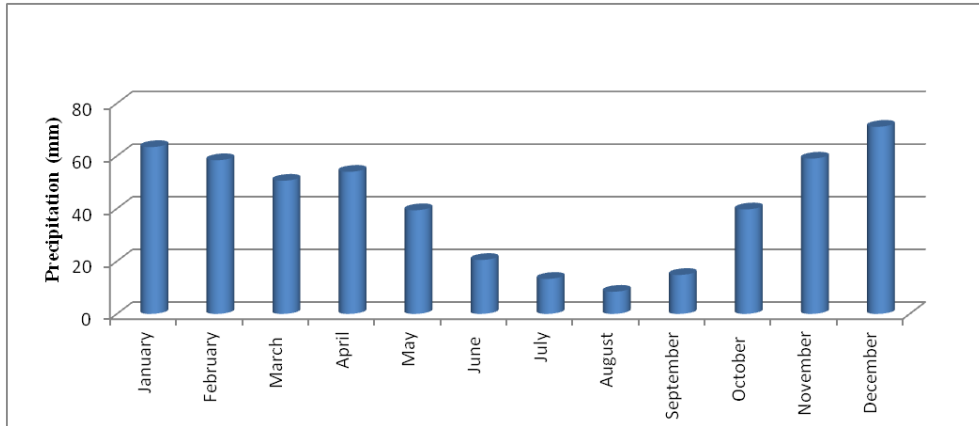


Figure 2.4 Average monthly precipitation values of the Kışladağ region (Long Term, 1975-2012)

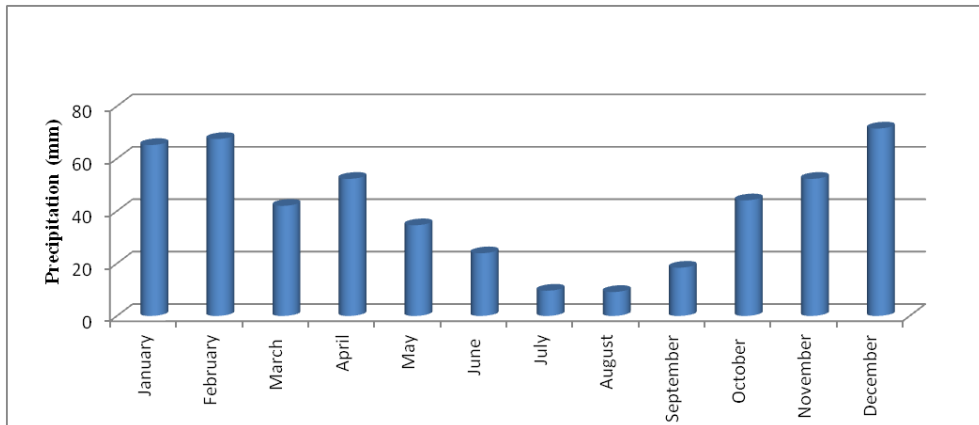


Figure 2.5 Average monthly precipitation values of the Kışladağ region (Short Term, 2001-2012)

2.2.2. Temperature

The seasonal temperature variations in the study area have been evaluated by Yazıcıgil et al. (2013) using the Kışladağ AWOS meteorological station (2006-2012). Figure 2.6 shows the variation of the average temperature values according to month. In this figure, it can be identified that January has the minimum average temperature (2.23 °C) and August has the maximum average temperature (25.2 °C). The mean of the average temperature is calculated as 13.3 °C for the study area. Monthly averages of the minimum temperature as measured by the Kışladağ AWOS meteorological station is presented in Figure 2.7. It is clearly seen that -9.4 °C (January) and -9.6 °C (February) are the minimum values. On the contrary, Figure 2.8

shows the average maximum temperature per month. In this figure, June has the maximum temperature of 37.1 °C.

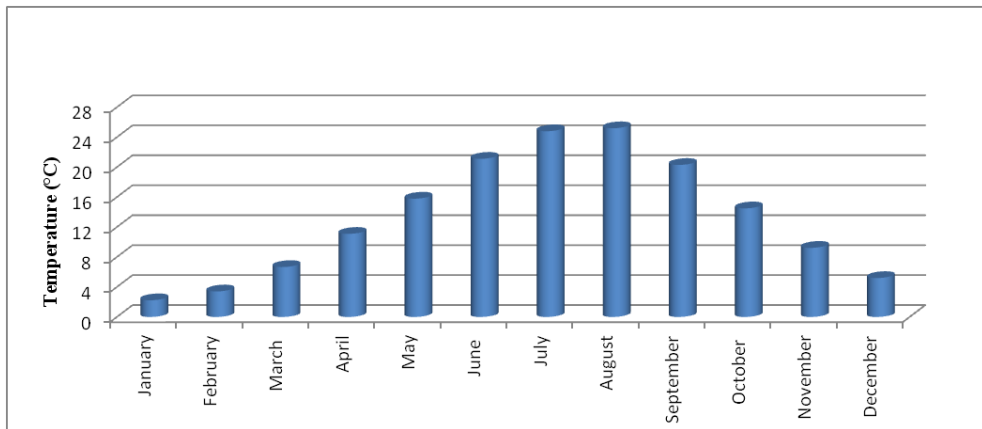


Figure 2.6 Average monthly temperature values from the Kışladağ meteorological station (2006-2012)

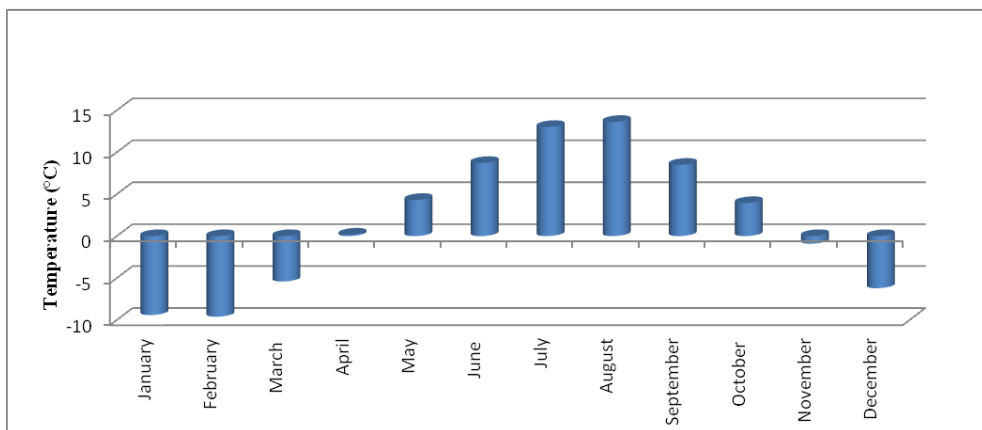


Figure 2.7 Minimum average monthly temperature values from the Kışladağ meteorological station (2006-2012)

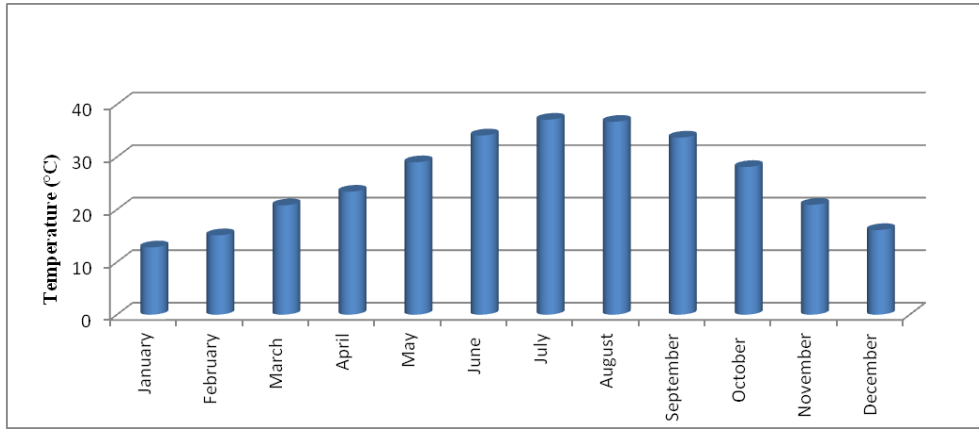


Figure 2.8 The maximum average monthly temperature values from the Kışladağ meteorological station (2006-2012)

2.2.3. Relative Humidity

The relative humidity data variations belonging to the years 2006 and 2012 are shown in Figure 2.9 (Yazıcıgil et al., 2013). In the figure, it is concluded that the average relative humidity is about 75% for the winter season, whereas the relative humidity values are between 38% and 50% in the summer. This is an indication that the area has high air temperature and a dry climate with low precipitation.

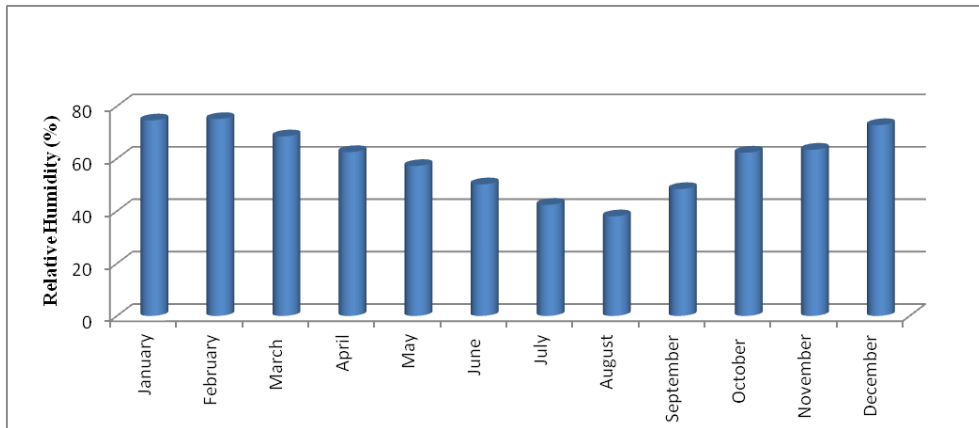


Figure 2.9 Average monthly relative humidity values from the Kışladağ meteorological station (2006-2012)

2.2.4. Evaporation

Evaporation rates for the study area were observed by the Kışladağ Meteorological Station in the years between 2000 and 2012. Generally, the data was procured from April to September. To obtain long term evaporation data, Yazıcıgil et al (2011) converted the MGM Uşak Meteorological Station data (1975-2000) for the study area by using an estimation method. While estimating data from the years 1975 to 2000, average error margins of monthly evaporation amounts were used by considering a mutual time interval (2000-2012) for both the MGM Uşak and the Kışladağ Meteorological Stations. The data procured from

the Uşak Meteorological Station (1975-2000) was corrected and then added to the Kışladağ Meteorological Station data (2000-2012) by considering these error margins.

Short term, monthly evaporation values measured in the Kışladağ Meteorological Station are shown in Figure 2.10, and calculated long term monthly evaporation values (1975-2012) are shown in Figure 2.11. Monthly data shown in Figure 2.10 was recorded for 8 years in 2001-2012. As seen in Figure 2.10 and 2.11, evaporation values for long and short terms were very similar. There is a correlation between evaporation and temperature values as evaporation values reached its highest in the summer days. July and August have the highest values with 233 mm and 226 mm, respectively. In Figure 2.11, it can be seen that evaporation values are reasonably low in the winter period and that December has the lowest monthly average evaporation value of 15.7 mm.

Monthly precipitation and evaporation distribution in Kışladağ is compared in Figure 2.12. As it is seen in this figure, the April-October period has higher evaporation values than precipitation. In contrast, since temperatures are lower in the winter months, evaporation values are lower and precipitation values are much higher. According to this result, it is expected that groundwater recharge for Kışladağ is highest in the winter period.

The long term total yearly evaporation values of Kışladağ are illustrated in Figure 2.13, and indicates values of 1198 mm. In the years between 1990 and 1998, the long term total yearly evaporation values of Kışladağ was lower than the average, while 2000 to 2009, was observed to have an above average value.

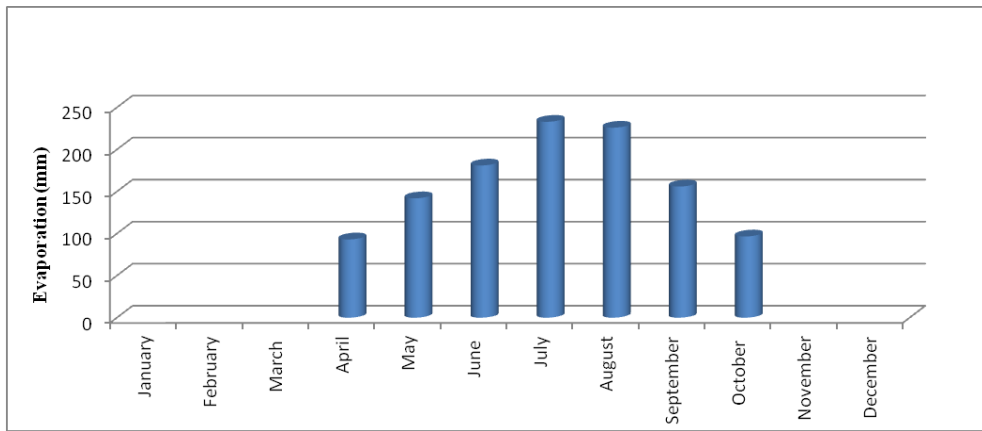


Figure 2.10 Monthly average evaporation values calculated for short term (2001-2012)

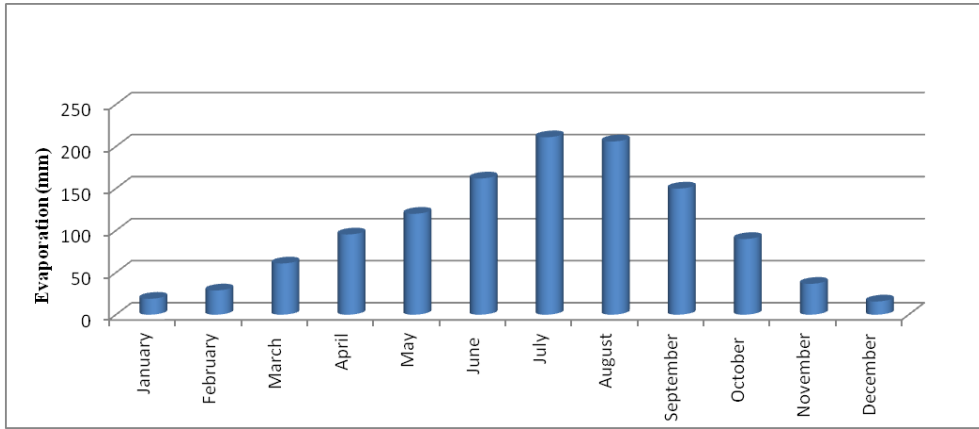


Figure 2.11 Monthly average evaporation values calculated for long term (1975-2012)

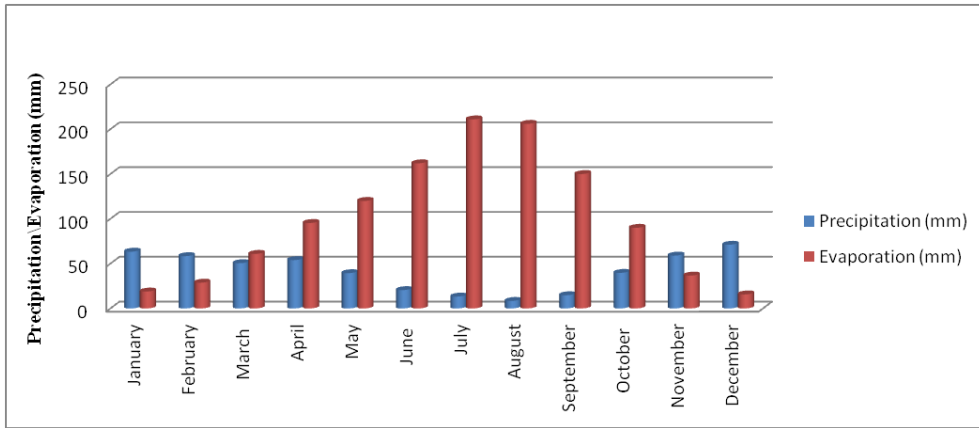


Figure 2.12 Monthly distribution of the monthly average precipitation and evaporation values calculated for Kışladağ (1975-2012)

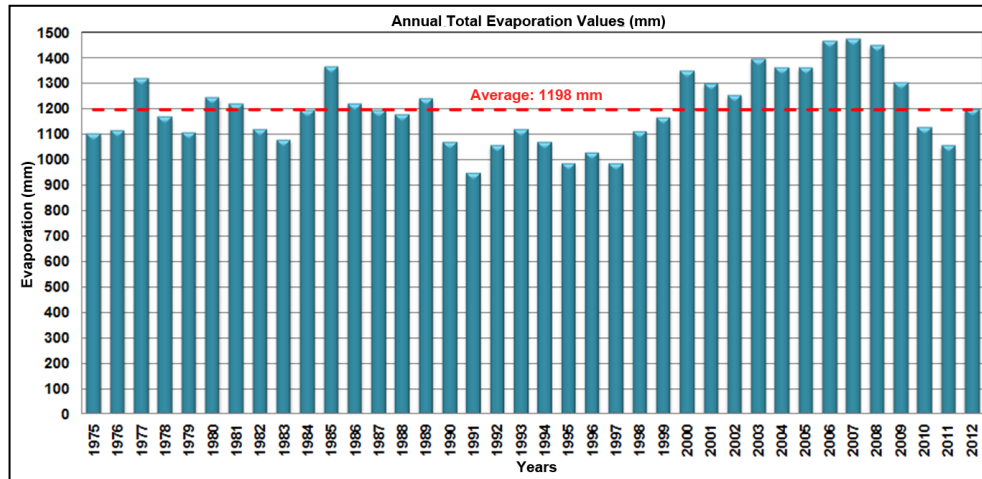


Figure 2.13 The long term annual total evaporation values calculated for Kışladağ (1975-2012) (Yazıcıgil et al., 2013)

2.3. Geology

2.3.1. Regional Geology

The regional geology of the Kışladağ Gold Mine area was studied by Yazıcıgil et al. (2000). As a result of this study, it was concluded that The Menderes Metamorphic Complex, Permo-Triassic aged, is the oldest rock in the region. This complex forming the basement is composed of the Güneyköyü Formation including aplites and granitic gneisses, the Eşme Formation including crystalline/augen gneiss and calcareous schists, and the Musadağı Marbles.

The Tertiary-aged Hacibey Group, consisting of claystone, limestone, conglomerate and sandstone, covers the Menderes Metamorphic Complex. Formations of the Hacibey Group, listed from oldest to youngest are Kurtköy, Küçükderbent and Yeniköy. The Inay Group underlain by the Hacibey Group contains three units: the Ahmetler Formation involving sedimentary rocks, the Beydağı Volcanics and Ulubey Formation covering a widespread area as lacustrine limestone.

The Inay group is overlain with an unconformity plane by the Quaternary-aged Asartepe Formation which consists of siltstones, conglomerates and sandstones of numerous compositions with marl and claystone lenses in some locations. Quaternary-aged Kula Volcanics symbolize the youngest volcanic unit in the region. Clay, silt, sand and gravel deposits along the rivers are represented by the alluvium in the area. The Quaternary deposits involving unconsolidated sediments are composed of these alluviums, as well as other alluvial fan deposits and the colluviums in the region (Figure 2.14).

Miocene, by Karaoğlu et al., 2010, or as Plio-Quaternary by Ercan et al., 1978. Plio-Quaternary, in this study, was labeled as Psc.

A correlation of volcanic units over a wide area is typically difficult to map in stratovolcano complexes (Hudson, 2009). The extension zone of this volcanic activity is represented with more debris avalanche volcanic breccias, and partially in places through the valley as debris conglomerates. The area is mostly covered by farm fields. Particularly, the topographically high areas are covered by agricultural fields that largely have decomposed rock or alluvium and are with considerable disruption of the soils. In the northern part of the study area, schist outcrops are widely seen with thicknesses up to several hundred meters. It has formed before placement of the volcanic sequence. This exposed unit is overlain by partly eroded volcanic sediment

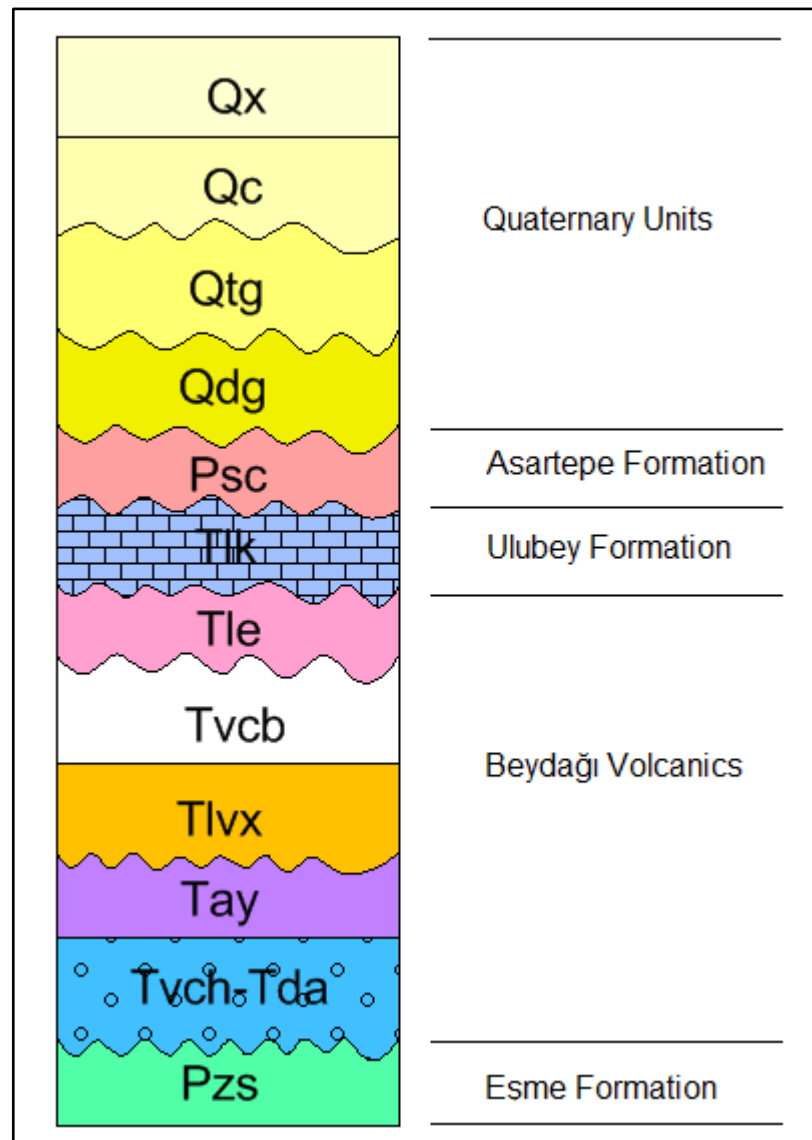


Figure 2.16 A possible stratigraphic section of the Northern part of the Kışladağ Gold Mine area (modified from the ARC, 2011)

Stratigraphic units in the study area

Eşme Formation:

Pzs: The Pzs unit, belonging to Eşme Formation, is the oldest unit exposed in the study area. It consists of Paleozoic garnet-amphibolite, mylonite schist, cerisite quartz schists, mica schist and quartzite. Generally, foliation of this rock is at a low angle, but in some parts it may turn from a low to high angle. There are quartz intrusions cutting the unit along the schistosity.

Beydağı Volcanics:

Tvch: This unit, observed near Haciali, formed with layered volcanoclastics underlies or intercalates with the Tda unit. The Tvch unit consists of latite porphyry conglomerate with rounded clasts up to 50 cm interbedded with laminated volcanic sandstone and fine-grained conglomerate. Some of the finer grained beds show weak graded bedding. At least 60 m of Tvch is exposed overlying schist.

Tda: This unit, composed of debris avalanches, covers the Tlg unit in the study area. In the north part of the Open Pit it overlies the Tla unit. Angular to sub-rounded clasts are rarely up to 4 m across but more typically less than 1 m, and in many exposures, clasts are less than 50 cm. The most part of this unit is exposed to hydrothermal alteration. In some parts, it can be correlated with the Tdab as it has some similarities with this unit.

Tay: Andesitic flow of Yeni Tepe extends from the volcanoclastics of Haciali to the northern part of the study area. In the northeast part, it overlies Pzs unit with at least 50 m of volcanoclastic sediments and some flow breccias at the top. Flow breccias are mostly seen in andesitic composition. The well bedded unit consists of latite porphyry conglomerate with rounded clasts up to 50 cm interbedded with laminated volcanic sandstone, tuff and ignimbrite and lying on the east flank of Yeni Tepe. Beds are typically 5 cm to 50 cm thick. Some of the fine grained beds showing weak-graded bedding include some schist clasts. At least 50 m of Tvch is overlying schist with 10 meters of andesitic flow breccia. The east side of the schist-volcanic boundary is probably likely controlled by a detachment fault, but trace of the fault plane on the metamorphic may have been erased due to an eroded surface.

Tlvx: Tlvx, located in the east of Emirli Tepe, is a channel-filling, light gray, latite porphyry volcanic breccia and debris avalanche. The base of the unit and the northern exposures are mainly debris avalanche deposits with blocks up to 3 m with 10 to 20% matrix, while the bulk of the southern area of exposure is autobreccia with locally flow-banded blocks up to 1.5 m

Tvcb: Volcanoclastics of Bekişli continue through the northwest of Emirli Tepe, and is a channel-filling sequence of latitic debris avalanches and volcanic conglomerates. Typically, rounded blocks up to 4 m are observed, but most of the unit is less than 1 m with parts of blocks having 50 cm maximum height.

Tle: This unit consists of latite and is found near Emirli Tepe. It unconformably overlies Tvcb. The unit includes very dense and resistant, gray, porphyritic latite flow. This latite flow extends towards the northwest trending to follow the ridge.

Ulubey Formation:

Tlk: The Tlk unit is a lacustrine limestone of Karacaömerli. It unconformably overlies schist seen at the northeast of the map. This unit consists of an abundant solution of small cavities.

Asartepe Formation:

Psc: The Asartepe Formation crops in a northern part of the study area. The observable location of the unit is on the east part of the Ömerli village. This unit is composed of conglomerates, pebblestones, sandstones, and clayey-siltstones. The conglomerates at the

base of the unit include several pebbles derived mostly from volcanic sediment, and consist of very few schist gravels.

Quaternary Units:

Qdg: This unit is Quaternary debris outcropping Güzelköy, and is the youngest debris material in the area. It consists of very loose Quaternary lime-tuff clay cements containing schist and alluvium gravels.

Qtg: The Qtg unit is made up of unconsolidated gravels usually perched well above present stream valleys in the west and north of Open Pit. The gravels contain everything from rounded gravel to cobble, to rarely boulder-sized clasts of altered and unaltered volcanic material. These deposits could be as old as Pliocene, but are most likely Quaternary.

Qc: This unit includes unconsolidated colluvial and alluvial gravels which occur in present-day stream valleys and as talus on some steep slopes. This unit may include some disturbed land.

Qx: Areas of disturbance, primarily from agricultural activity, are generally described as Qx. This unit may include some colluviums. Agricultural fields are largely located on decomposed rock or alluvium, and with considerable disruption of the soils, the bedrock of these areas is uncertain and are thus mapped as Qx.

Structural Geology of the Study Area

Although the Kışladağ area has been defined as an almost undeformed region largely lacking faults, according to Hudson (2009), some minor faults were observed in the study area (Figure 2.17). One of them was observed in the eastern part of the region. This fault crosscuts the bedded tuffaceous sediments and volcanoclastics most likely along the schist-volcanic contact at the southeastern part of the study area. The fault having a right lateral strike slip character shows a high angle and N15°E trending. The second main fault crosscutting to the stream valley near the Güzelköy village was observed in the north side of the area. This fault was a normal fault as related to the graben structure. It was observed to be dipping towards the north at a high angle. The southern part of this fault was uplifted and developed by filling with young Plio-Quaternary terrestrial, as well as bedded and undeformed units of Psc sediments. The southern part of this fault includes younger sediments. These consist of mostly debris flow from the sediments and schist fragments. Other structures in the schist, mostly observed in the south of the Küçükilyaslı village, have a high-angle of normal faults cutting the metamorphic basement along N-S and N65°W trending.

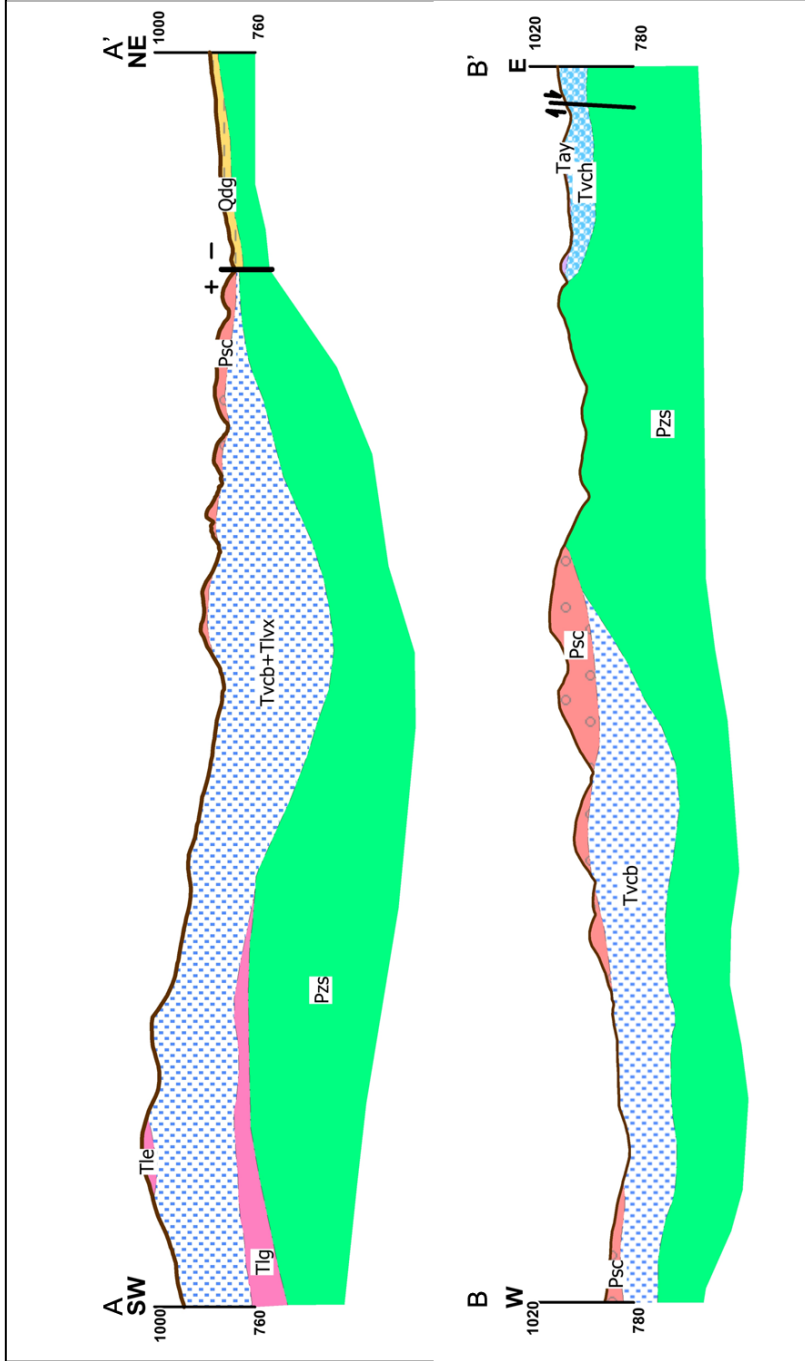


Figure 2.17 Geological cross-sections of the study area (ARC, 2011)

CHAPTER 3

SURFACE WATER HYDROLOGY

3.1. Natural Drainage (Drainage Network System)

As mentioned in section 2.1, the Kışladağ Gold Mine is separated into two parts by the watershed divide between the Gediz and Büyük Menderes River Basins. The study area is part of the Gediz River Basin. Therefore, the drainage system of the area has been connected to the Gediz River in the north. In addition, a radial drainage network system was observed due to volcanic cones in the study area. Seasonal streams are more dominant; however, the streams resulting from sudden precipitations are few and far between in the study area. The topographic elevations of the area vary from 1300 meter to 600 meter.

3.2. Stream Flow Observations

To observe the flow regime of the area, several weirs have been installed in some critical locations by Tüprağ. Figure 2.2 shows the locations and basins of these weirs. Although there are 6 weirs in the area, the study area involves only two of them namely, Weir-2 and Weir-6. The operation time intervals of these weirs were different from each other as they were placed in their locations at different times (Table 3.1). The first record date of Weir-2 is 01/06/2005, whereas 01/11/2011 is the first record date of Weir-6. Operations of both Weir-2 and Weir-6 are still active at the present time. Weir-2 includes the streams between the North Waste Rock Dump Area (Expansion Area), the South Heap Leach Pad, and the Open Pit, and is located near Söğütlü Village. On the other hand, Weir-6 involves streams in almost all of the North Heap Leach Pad area (Expansion Area, between Hacıali and Küçükilyaslı).

Table 3.1 Information about Weir-2 and Weir-6 (Yazıcıgil et al., 2013)

Weir No	Operation Period	Water Level = H (meter) – Flow Rate = Q (L/s) Equations
Weir-2	01.06.2005 - 31.12.2012	$Q=2122 \times H^{2.51}$ (SRK, 2006)
Weir-6	01.11.2011 - 31.12.2012	$Q=2353 \times H^{2.5}$ (Yazıcıgil and Yılmaz, 2011)

The watershed areas for both weirs are shown in Table 3.2. Watershed of Weir-2 involves some parts of existing mine structures (Open Pit and South Waste Rock). The watershed outside the existing mine structures was considered while performing flow observations.

Table 3.2 Watershed and Existing Mine Structure Areas (Yazıcıgil et al., 2013)

Weir No	Total Watershed Area (ha)	Open Pit (ha)	Leach Pad (ha)	Watershed Area (ha)
Weir-2	761.13	67.47	130.21	563.45
Weir-6	506.29	0	0	506.29

The cross-sectional views and dimension parameters of weirs are given in Figure 3.1 and Table 3.3. The equations given in Table 3.1 were used to calculate flow rates for V-notches of the weirs. In cases where water level exceeds the maximum height of a V-notch (D), a contracted weir equation was added to the former equation in order to find the total flow rate.

$$Q=1838*(L-0.2*(H-D))*(H-D)^{1.5} \quad (1)$$

The dimensions of weirs are illustrated below in Figure 3.1 as a cross-sectional view.

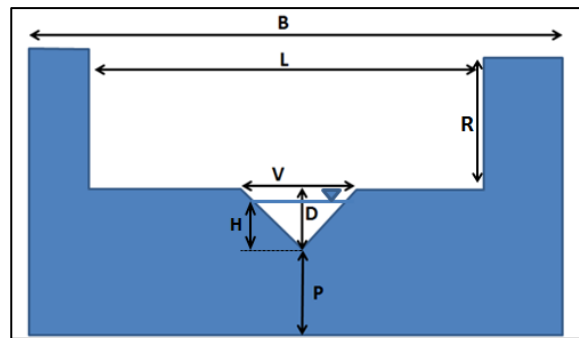


Figure 3.1 Cross-Sectional View of the Weirs (Yazıcıgil et al., 2013)

H: Water Level

L: Sectional Length

B: Canal Width

P: Height from Canal Bottom to V-Section Weir Bottom

D: Maximum Height of V-Section Weir

V: Maximum Width of V-Section Weir

R: Maximum Height of Rectangular Weir

Table 3.3 Weir Dimension Parameters (Yazıcıgil et al., 2013)

Weir No	B (m)	L (m)	V (m)	D (cm)	P (cm)	P (cm)
Weir-2	5.50	3.00	1.04	30.00	24.00	30.00
Weir-6	10.50	2.75	1.03	28.50	90.00	30.00

Water level measurements of weirs were taken manually once a day until 01/11/2010. As of this date, the frequency of measurements was increased to twice daily (morning and afternoon) on the weekdays, but on weekends and holidays, measurements continued to be taken once a day. Also, beginning from 15/11/2011, an automatic pressure gauge was conducted on Weir-6 to take water level measurements in a short interval (every 15 minutes). Manual water level measurements of Weir-6 were compared with automatic ones for December 2012 by Yazıcıgil et al., 2013 (Figure 3.2). According to this comparison, it is concluded that automatic and manual measurements are compatible. Weir flow hydrograph and peak water levels are best observed in automatic measurements rather than manual ones due to the short measurement period (every 15 minutes). Quality controls were done for both automatic and manual measurements. Missing parameters and/or errors in automatic measurements were corrected by using manual ones. Maximum flow values of weirs are specified as the maximum height of the weir (Figure 3.1, D+R), and water levels exceeded this top limit are assumed to be equal the maximum height of the weir (Yazıcıgil et al., 2013).

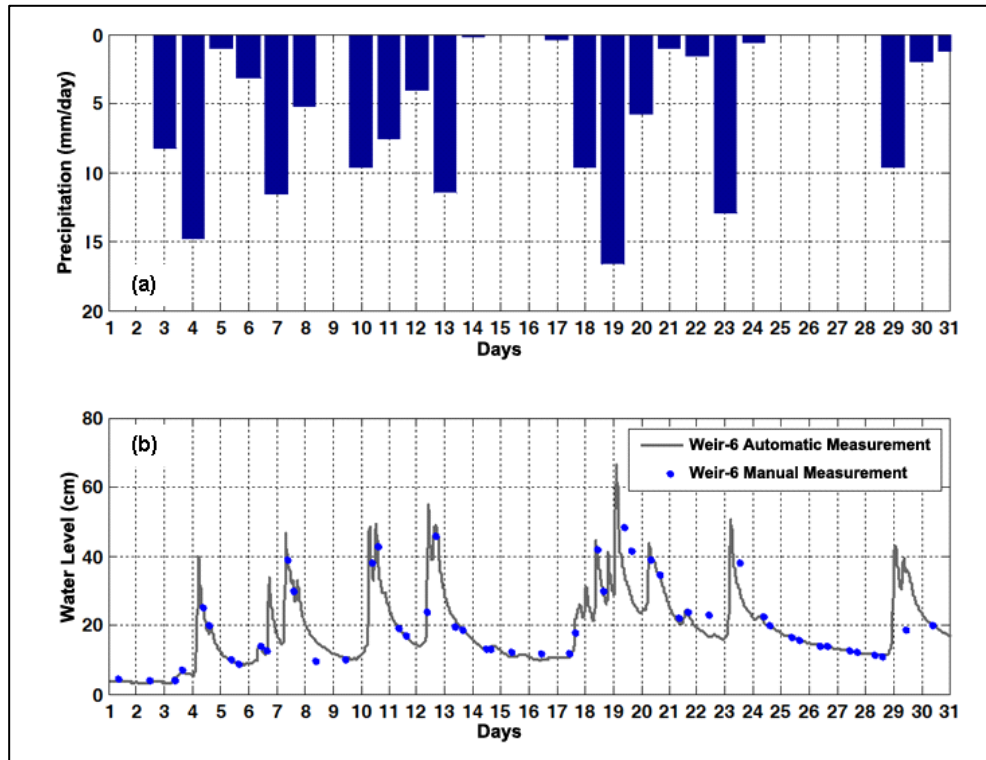


Figure 3.2 December, 2012 (a) Daily Precipitation Data Obtained from the Kışladağ Gold Mine (b) Manual and Automatic Water Level Measurements (Yazıcıgil et al., 2013)

The section of Weir-2 was suppressed by adding a 20-cm plate on 18/08/2011, but was removed from Weir-2 on 25/04/2012. During this time interval, it was assumed that the maximum height of a rectangular weir (R) is 10 cm, but that no change in the water level-discharge equation occurred. The maximum flow amount measured from the weir was also reduced due to this constriction (Yazıcıgil et al., 2013).

By using the data derived from procedures described so far, daily average flow rates (Figure 3.3) were obtained by implementing this data into water level-flow equations by Yazıcıgil et al. (2013). In Figure 3.3, the maximum flow rate was recorded as 1000 L/s and the effects of constriction were seen on 08/2011-04/2012. Generally, flow rates of weirs reached high values in December, January, February and March. The daily flow rates of weirs rarely exceed 200 L/s and reached 1000 L/s only a few times. A logarithmic scale illustration of the daily average flow rates was provided to evaluate low rates more accurately. Therefore, the daily flow rates are given in a logarithmic scale in Figure 3.4. According to this figure, flow rates increased in November to December, reached the maximum values in January and February, and begin to decrease March to July. In the period involving July, August and September, there was no flow recorded in the weirs.

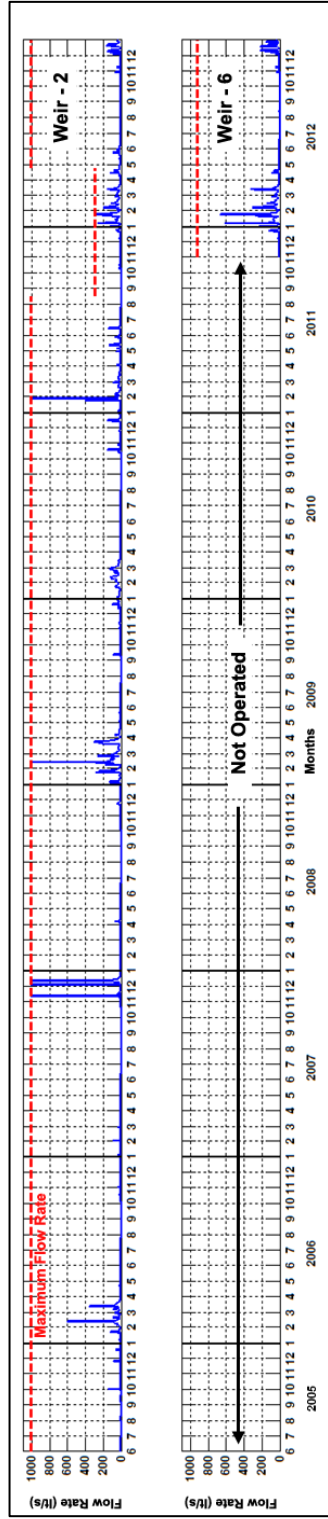


Figure 3.3 Daily average flow rates of weirs (06/2005-12/2012) (Yazıcıgil et al., 2013)

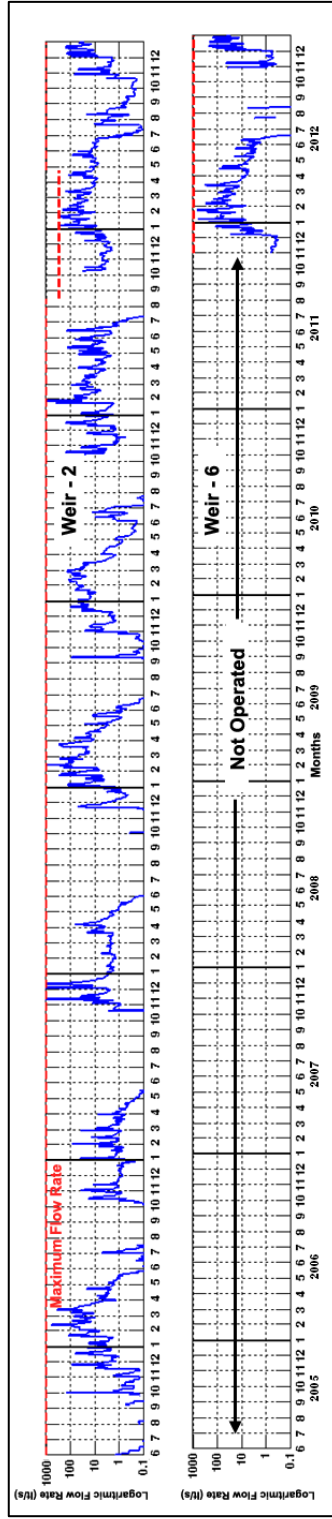


Figure 3.4 Daily average flow rates of weirs in logarithmic scale (06/2005-12/2012) (Yazıcıgil et al., 2013)

3.3. Hydrologic Water Budget

In order to figure out the component of a water budget for the study area, the software, Soil-Water-Balance (SWB; Westenbroek et al. 2010), developed by the United States Geological Survey (USGS) was used. The Soil-Water-Balance (SWB) computer code has been implemented to calculate spatial and temporal variations in groundwater recharge. The SWB model calculates recharge by the use of a commonly available geographic information system (GIS) that combines data layers with tabular climatological data. Recharge calculations are made on a rectangular grid of computational elements that may be easily imported into a regional groundwater-flow model. Recharge estimates calculated by the code may be output as daily, monthly, or annual values (Westenbroek et al. 2010).

The working principle of the SWB model was described by Westenbroek et al. (2010). Recharge is calculated separately for each grid cell in the model domain. Sources and sinks of water within each grid cell are determined on the basis of input climate data and landscape characteristics; recharge is then calculated as the difference between the change in soil-moisture with these sources and sinks (Eq. 2).

$$\mathbf{Recharge} = \mathbf{Sources} \text{ (Precipitation + Snowmelt + Inflow)} - \mathbf{Sinks} \text{ (Interception + Outflow + Evapotranspiration)} - \Delta \mathbf{Soil Moisture} \quad (2)$$

Specific water balance components are discussed briefly below.

Precipitation: Precipitation data were input as daily values either as a time series at a single gage or as a series of daily gridded files.

Snowmelt: Snow was allowed to accumulate and/or melt on a daily basis. The daily mean, maximum and minimum air temperatures were used to determine whether precipitation takes the form of rain or snow. Precipitation that falls on a day when the mean temperature minus one-third the differences between the daily high and low temperatures is less than or equal to the freezing point of water is considered to fall as snow (Dripps and Bradbury, 2005). Snowmelt calculation is based on a temperature-index method.

Inflow: Inflow is calculated by use of a flow-direction grid derived from a digital elevation model to route outflow (surface runoff) to an adjacent down slope grid cells. Inflow is considered to be zero if flow routing is turned off.

Interception: Interception is treated simply by means of a “bucket” model approach, a user specified amount of rainfall is assumed to be trapped and used by vegetation, and evaporated or transpired from plant surfaces. Daily precipitation values must exceed the specified interception amount before any water is assumed to reach the soil surface. Interception values may be specified for each land-use type and season (growing and dormant).

Outflow: Outflow (or surface runoff) from a cell is calculated by use of the U.S. Department of Agriculture, Natural Resources Conservation Services (NRCS) curve number rainfall-runoff relation (Cronshey and others, 1986). This rainfall-runoff relation is based on four basin properties: soil type, land use, surface condition, and antecedent runoff condition. Hydrologic soil type is separated into 4 groups by considering infiltration capacity of soils:

A, B, C and D. From Group A to Group D, infiltration capacity decreases and, consequently, an overland flow potential increases (Table 3.4).

Table 3.4 Hydrologic Soil Groups (Westenbroek et al. 2010)

Soil Group	Infiltration rate
A	> 0.3 inch per hour
B	0.15–0.3 inch per hour
C	0.05–0.15 inch per hour
D	< 0.05 inch per hour

Evapotranspiration: The SWB code can use any of five commonly applied methods to estimate potential evapotranspiration. The methods currently included in the SWB code are: Thornthwaite-Mather (1957), Jensen-Haise (1963), Turc (1961), and Hargreaves and Samani (1985). The data required to calculate potential evapotranspiration component for these methods are summarized in Table 3.5.

Table 3.5 Data Requirements for Potential Evapotranspiration Methods (Westenbroek et al. 2010)

Method	Mean Air Temperature (°F)	Min. Air Temperature (°F)	Max. Air Temperature (°F)	Mean Relative Humidity (%)	Percent Possible Sunshine (%)
Thornthwaite-Mather	√				√
Jensen-Haise	√				√
Turc	√			√	√
Hargreaves-Samani	√	√	√		

Soil Moisture, Δ Soil Moisture: The soil-moisture term represents the amount of water held in storage for a given grid cell. Soil moisture has an upper bound that corresponds to the soils' maximum water-holding capacity (roughly equivalent to the field capacity); soil moisture has a lower bound that corresponds to the soils' wilting capacity.

Data type, description of data and sources of data are indicated in Table 3.6 to run the SWB model for the study area.

Table 3.6 Data Requirements for Application of the SWB Model

Data Type	Description	Source
Gridded (ARC, ASCII or Surfer Grid)	Land Use/Land Cover	1/25000 Scaled National Soil Database
	Flow Direction	Digital Elevation Model, DEM, (Resolution: 25m)
	Hydrologic Soil Group	1/25000 Scaled National Soil Database
	Available Water Capacity	1/25000 Scaled National Soil Database
Tabular	Soil and Land Use Properties Lookup Table	Westenbroek et al. (2010) (Converted by Considering National Soil Database)
	Climate at Single Station	Kışladağ Meteorological Station
	Matrix of Soil-Water Retention for Given Accumulated Potential Water Loss	Westenbroek et al. (2010)

To implement the SWB model on the Kışladağ Gold Mine site, the model domain is selected in a region between 675000E-4252000N and 695000E-4272000N (Figure 3.5). The model contains 666400 cells having dimensions of 25m x 25m. Land use/Land Cover data for the model is provided from 1/25000 scaled National Soil Database (NSDB) (Figure 3.5). By applying NSDB data to the model domain, each cell has a soil/land use property. To use this data in the SWB model, a soil and land use properties lookup table was created by taking NSDB data into consideration. This lookup table is shown at Table 3.7.

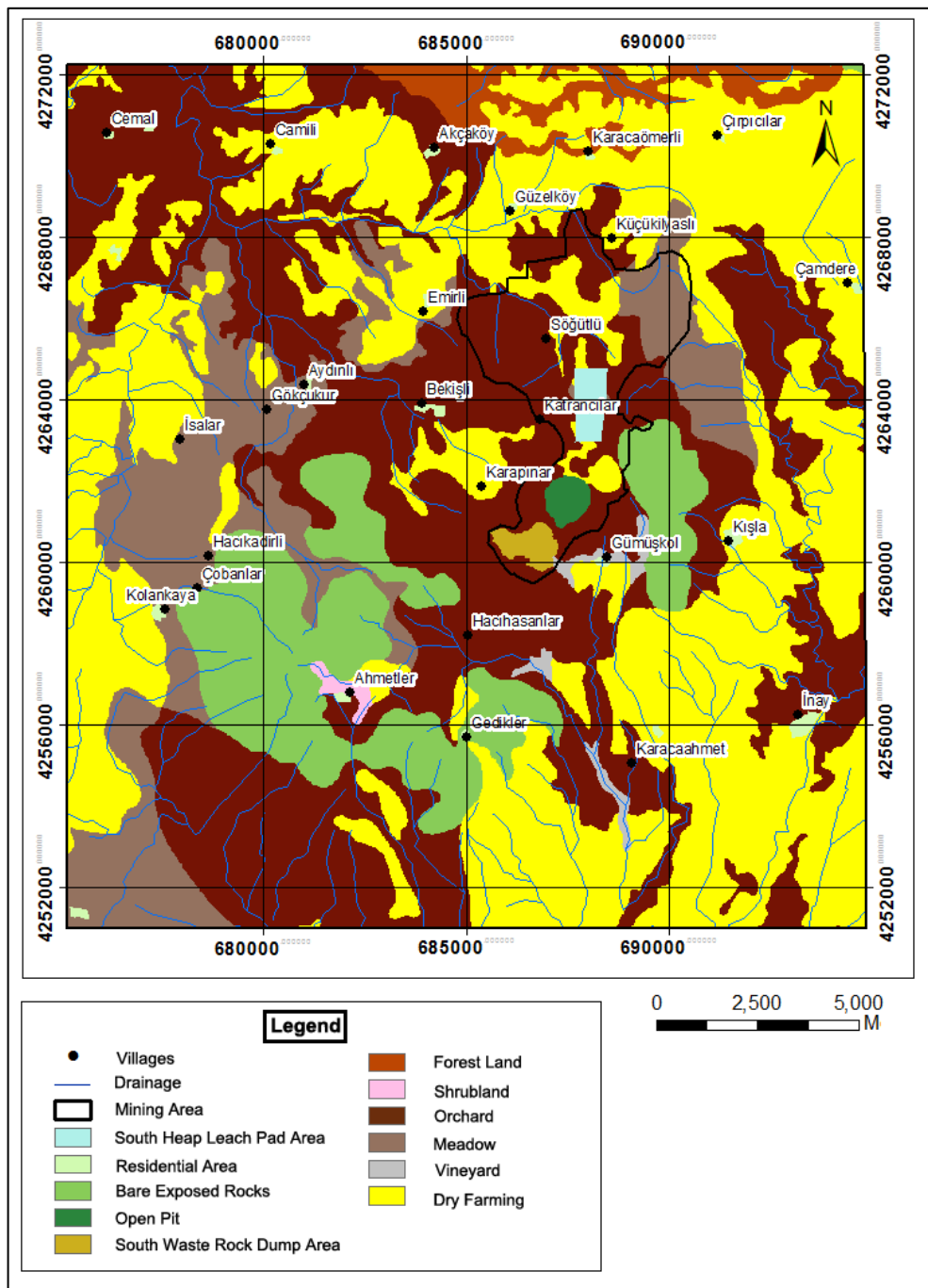


Figure 3.5 Model domain and land use/land cover map

Table 3.7 Land Use/Land Cover Lookup Table and Curve Numbers

Land Use/Land Cover Code	Descriptions	Imperviousness (%)	Hydrologic Soil Groups Curve Numbers			
			Initial		Final	
			C	D	C	D
11	South Heap Leach Pad		100	100	100	100
21	Low Density Residential	30	83.4	85.6	83.4	85.6
31	Bare Exposed		88.1	90.5	88.1	90.5
32	Open Pit		94.7	95.8	94.7	40
33	South Waste Rock Dump		100	100	100	100
43	Mixed Forest		67.8	74.2	67.8	74.2
51	Shrubland		74.8	79.3	74.8	88
61	Orchard		71.7	77.1	71.7	77.1
81	Pasture		88.1	89	88.1	89
82	Row Crops		88.9	89.6	88.9	89.6
83	Small Grains		81.8	84.5	86	89

Soil groups in the model domain are assigned as C and D types because clay loam soil dominates approximately the entire area (Figure 3.6). The slope and depth data taken from the NSDB were also used to determine hydrologic soil groups. Shallow soil with a steep slope is included in group D. The initially assigned curve numbers have been changed until a good match is obtained between the observed and simulated run-off values. The default values; available water capacity value is assumed as 250mm/m and vertical hydraulic conductivities are taken as 7×10^{-8} m/s for C and 3.5×10^{-8} m/s for D. These values are default values suggested by the SWB model. The beginning date of dormant and growing seasons were decided as 15 April and 10 October by reckoning with land cover and agricultural activities in the area. After all data was applied, the SWB model was run in daily steps beginning in 2008 until the end of 2012 (5 years). The working principle of the SWB model is illustrated in Figure 3.7.

The most significant term for the hydrologic studies is *evapotranspiration*. To clarify this, the model was run using 4 different evapotranspiration methods. These methods are Thornthwaite-Mather (1957), Jensen-Haise (1963), Turc (1961), and Hargreaves and Samani (1985) (Table 3.5).

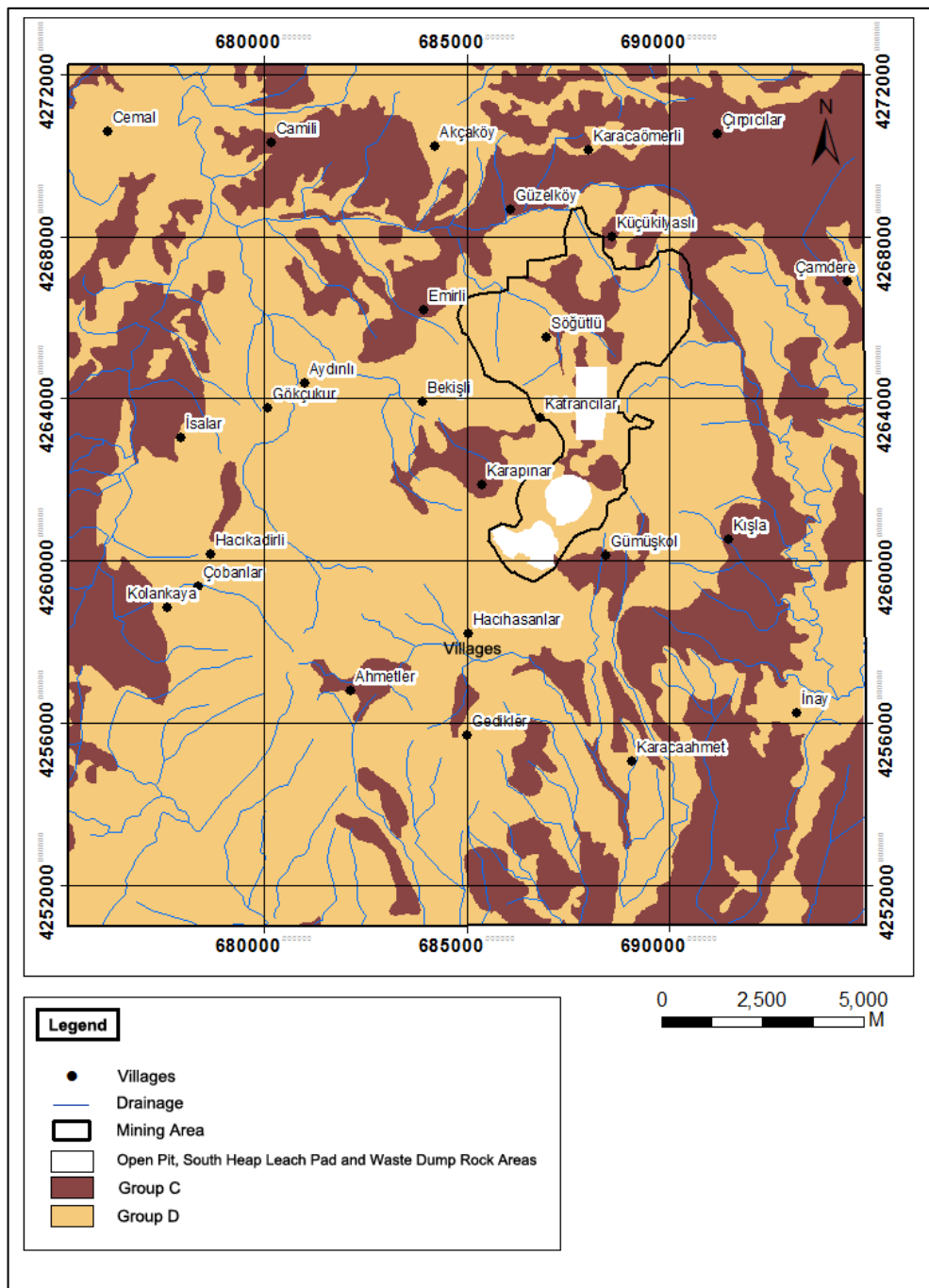


Figure 3.6 Hydrologic Soil Groups in the SWB Model Domain

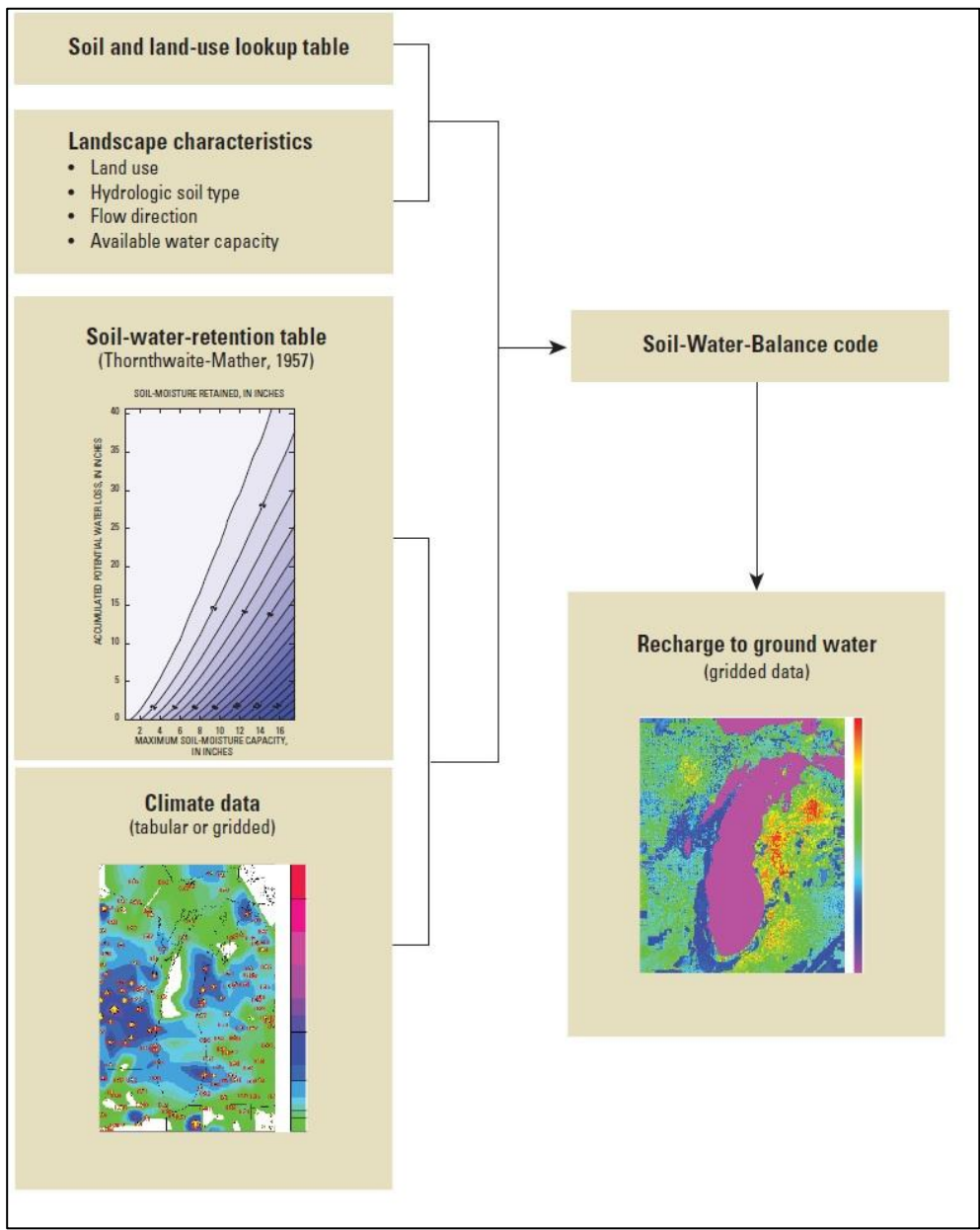


Figure 3.7 Flow Chart of the SWB Model (Westenbroek et al., 2010)

The most important step for modeling is model calibration. It is necessary to make the model results similar within the field observation data by changing the model parameters systematically. For the calibration process, Weir-5 with a 610.04 total watershed area (Yazıcıgil et al., 2013), located in the south side of the study area (Figure 2.2), was used. Calculated flow data (model cell involving the Weir-5) was compared to observed flow data of Weir-5 by modifying Land Use/Land Cover curve numbers to calibrate the model. In addition to this, the year of 2009 was selected to calibrate the model because 2009 was the wettest year for the period between 2008 and 2012. Figure 3.8 indicates the comparison of the calculated and observed flow data on Weir-5 for 2009. The Turc (1961) method was applied to the model in order to calculate the evapotranspiration.

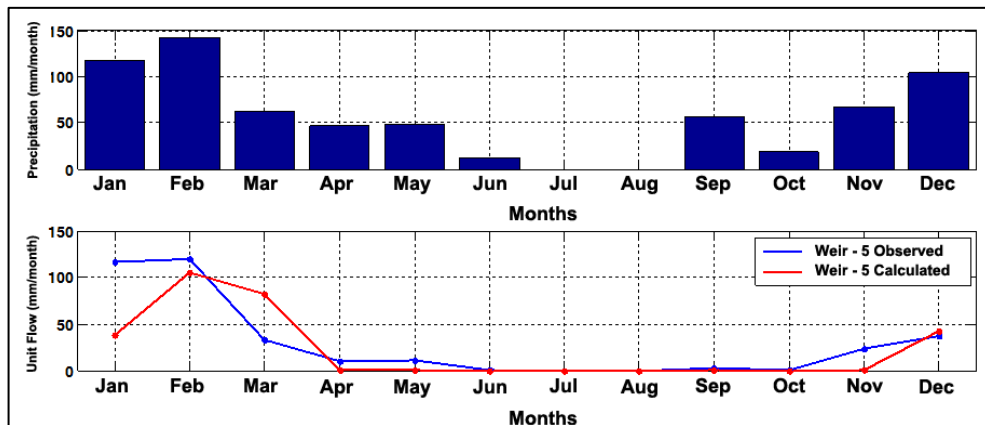


Figure 3.8 Comparison of Calculated and Observed Flow Values for Weir-5 (2009)

Recharge values obtained from the SWB model for the years 2008-2012 are given in Table 3.8. By using four different evapotranspiration estimation methods: Thornthwaite-Mather, Jensen-Haise, Turc, Hargreaves and Samani, the recharge to groundwater amount is determined and compared with each other. It is seen that for the months of December, January, February and March, recharge amounts have higher values when compared to the others. In terms of evapotranspiration methods, The highest recharge value (63.8 mm/year) was calculated in the method in which evapotranspiration were determined by Thornthwaite-Mather approach. The second highest one is 49.94 mm/year by using Jensen-Haise method. If the Turc method is chosen for the calculation of evapotranspiration, the model gives 37.82 mm/year recharge value. The lowest recharge value (33.43 mm/year) was obtained by using Hargreaves-Samani method. If we compare Turc and Hargreaves-Samani methods, the model gives similar results as recharge values calculated from these methods are 6% of the average annual precipitation value. Another output of the SWB model is outflow (surface runoff) amount from the cell. After calculating recharge values, outflow of cells involving Weir-5 was also calculated for each method. These calculated runoff values were compared to the observed outflow amount for Weir-5 over the years 2008 to 2012 in Figure 3.9. According to this figure, the outflow amount in 2008 was very low due to the fact that that the operation time of Weir-5 began in March 2008, which was the driest year by comparison. By examining Figure 3.9, it is clearly seen that the outflow amount differences between calculated and observed values changed for each year. In the SWB model, the maximum

outflow amount was calculated by using the Thornthwaite-Mather evapotranspiration method whereas the minimum was calculated by using the Hargreaves-Samani method. Given the calculated amount of groundwater recharge in Table 3.8, it is calculated significantly higher by using the Thornthwaite-Mather method in comparison to the other methods. Therefore, it can be interpreted that this method is not suitable. Groundwater recharges calculated by using the Hargreaves-Samani and Turc methods give similar results. Moreover, the outflow amounts calculated with these methods were closest to the outflow values observed in 2010 which properly represents the yearly average precipitation (Figure 3.9). Amatya et al. (1995) evaluated the reliability of the Hargreaves and Samani, Makkink, Priestly-Taylor, Turc, and Thornwaite evapotranspiration estimation methods by comparing the estimates with results from the Penman-Monteith method for conditions in eastern North Carolina, and found that Turc's method gave the best daily evapotranspiration estimates. Besides, Irmak et al. (2003) evaluated 21 evapotranspiration estimation methods based on their daily performance under the humid climatic conditions in Florida, among the temperature-based equations; Turc's equation was ranked the best. As a result, the Turc evapotranspiration method is preferred to calculate water budget values using the SWB model (Table 3.9). In Table 3.9, the total yearly average precipitation input for the SWB model, converts to 75.5% of evapotranspiration, 8.5% of surface flow and 6.64% of groundwater recharge. Yearly average groundwater recharge obtained from the SWB model was calculated as 37.8 mm over the modeled area.

Table 3.8 Groundwater recharge amounts using different evapotranspiration methods in the SWB model

THORNTWAITE - MATHER		Groundwater Recharge Values (mm)												Annual Recharge	Annual Precipitation (mm)	Recharge/Precipitation (%)
		Jan	Feb	Mar	Apr	May	June	July	Aug	Sep	Oct	Nov	Dec			
Year																
2008	0	0	0	1.02	0	0	0	0	0	0	0	0	0.51	1.52	329	0.5
2009	13.97	40.13	41.40	10.92	0	0	0	0	0	0	0	0	3.05	109.47	678.8	16.1
2010	13.72	39.88	10.92	0	0	0	0	0	0	0	0	0	0.76	65.28	568.4	11.5
2011	2.54	20.07	7.11	10.67	11.18	3.30	0	0	0	0.25	0	0	0.76	55.88	579.7	9.6
2012	21.34	32.51	20.57	7.87	0	0	0	0	0	0	0	0	4.57	86.87	692.6	12.5
													Average	63.8	569.7	11.2
JENSEN - HAISE		Groundwater Recharge Values (mm)												Annual Recharge	Annual Precipitation (mm)	Recharge/Precipitation (%)
		Jan	Feb	Mar	Apr	May	June	July	Aug	Sep	Oct	Nov	Dec			
Year																
2008	0	0	0	0.25	0	0	0	0	0	0	0	0	0.51	0.76	329	0.2
2009	12.70	36.83	36.83	4.83	0	0	0	0	0	0	0	0	2.54	93.73	678.8	13.8
2010	10.16	33.78	7.62	0	0	0	0	0	0	0	0	0	0.76	52.32	568.4	9.2
2011	1.78	16.26	3.30	4.83	0.76	0.51	0	0	0	0	0	0	0.51	27.94	579.7	4.8
2012	18.03	27.94	20.07	4.83	0	0	0	0	0	0	0	0	4.06	74.93	692.6	10.8
													Average	49.94	569.7	8.8
HARGREAVES - SAMANI		Groundwater Recharge Values (mm)												Annual Recharge	Annual Precipitation (mm)	Recharge/Precipitation (%)
		Jan	Feb	Mar	Apr	May	June	July	Aug	Sep	Oct	Nov	Dec			
Year																
2008	0	0	0	0	0	0	0	0	0	0	0	0	0	0	329	0
2009	7.62	31.75	26.16	0	0	0	0	0	0	0	0	0	1.78	67.31	678.8	9.9
2010	4.06	26.92	4.57	0	0	0	0	0	0	0	0	0	0.25	35.81	568.4	6.3
2011	1.27	7.87	0	0	0	0	0	0	0	0	0	0	0	9.14	579.7	1.6
2012	13.21	22.61	16.00	0	0	0	0	0	0	0	0	0	3.05	54.86	692.6	7.9
													Average	33.43	569.7	5.9
TURC		Groundwater Recharge Values (mm)												Annual Recharge	Annual Precipitation (mm)	Recharge/Precipitation (%)
		Jan	Feb	Mar	Apr	May	June	July	Aug	Sep	Oct	Nov	Dec			
Year																
2008	0	0	0	0.02	0	0	0	0	0	0	0	0.02	0.06	0.1	329	0
2009	7.87	32.77	34.29	2.54	0	0	0	0	0	0	0	0	1.78	79.25	678.8	11.7
2010	4.32	27.69	5.33	0	0	0	0	0	0	0	0	0	0.25	37.59	568.4	6.6
2011	1.27	9.91	0	1.78	0.25	0	0	0	0	0	0	0	0	13.21	579.7	2.3
2012	14.22	23.88	17.78	0	0	0	0	0	0	0	0	0	3.05	58.93	692.6	8.5
													Average	37.82	569.7	6.6

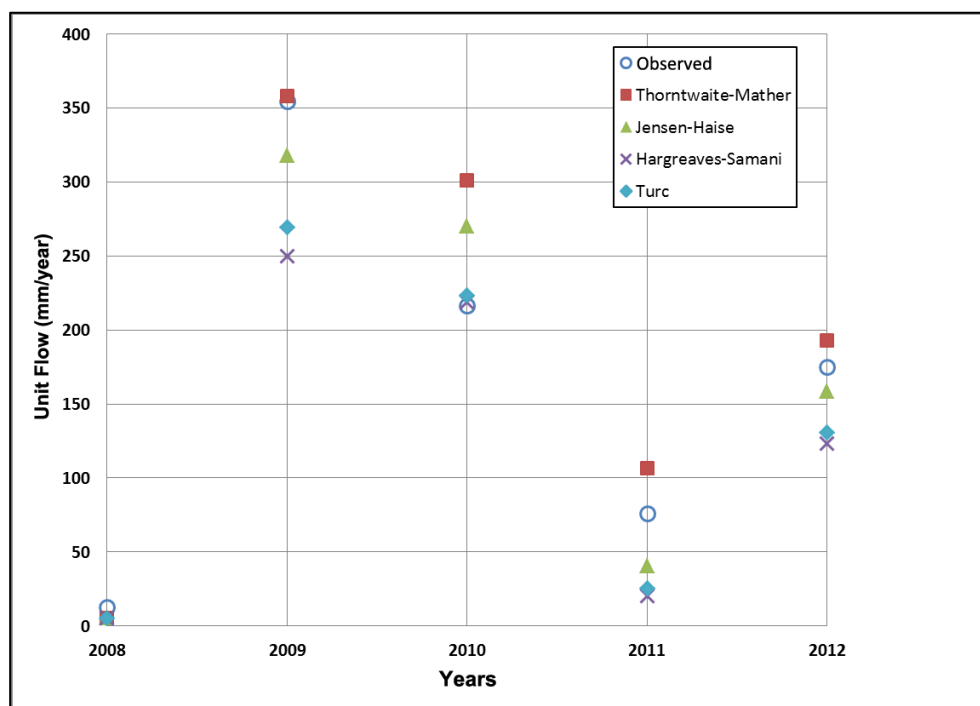


Figure 3.9 Unit outflow amounts by using different evapotranspiration methods in the SWB model for Weir-5

Table 3.9 The water budget components obtained from the SWB model

Water Budget Component	Sources		Sinks				Change in Soil Moisture (mm)	Groundwater Recharge (mm)
	Total Precipitation (mm)	Snowmelt - Snowfall Difference (mm)	Interception (mm)	Outflow (mm)	Runoff Outside (mm)	Actual Evapotranspiration (mm)		
2008	329,00	36.3 - 47.5	29,2	0	2,5	279,7	6,4	0,1
2009	678,80	163.2 - 152	29	59,4	28	437,2	56,9	79,3
2010	568,40	49.4 - 49.4	45,2	19,1	32,5	470,9	-36,9	37,6
2011	579,70	48.8 - 48.8	48,3	12,6	4,3	500,1	1,1	13,2
2012	692,60	154 - 154	41,9	58,3	25,6	463,2	44,5	58,9
Avarege	569,7	0	38,7	29,9	18,6	430,2	14,4	37,8
Avarege / Precipitation (%)	100	0	6,8	5,25	3,26	75,52	2,53	6,64

Areal distribution of average groundwater recharge values during 2008-2012 are given in Figure 3.10. By considering this figure, in the mining area, recharge values were between 0-12.7 mm 12.7-25.4 mm, and locally, the recharge values were between 50.8-76.2 mm. For the study area, groundwater recharge values were between 0-12.7 mm and 12.7-25.4 mm in the North Heap Leach Pad and the North Waste Rock Dump areas, respectively. In the North Heap Leach pad area, meadows and orchards were the dominant land use types, whereas the North Waste Rock Dump is almost only covered with orchard (dry). In addition to this, the dry farming (fallow) region, located between these processing areas, had a 50.8-76.2 mm groundwater recharge value. The South Heap Leach Pad and Waste Rock Dump areas are considered as impermeable and recharge values observed in these areas was zero (Figure 3.10). Generally, it is concluded that groundwater recharge has higher values in dry farming and barred rock/rubble areas. The results obtained from the SWB model can be improved

with field observations and other studies. Since this model covers a very extensive area, the results can be fine-tuned with other observation methods.

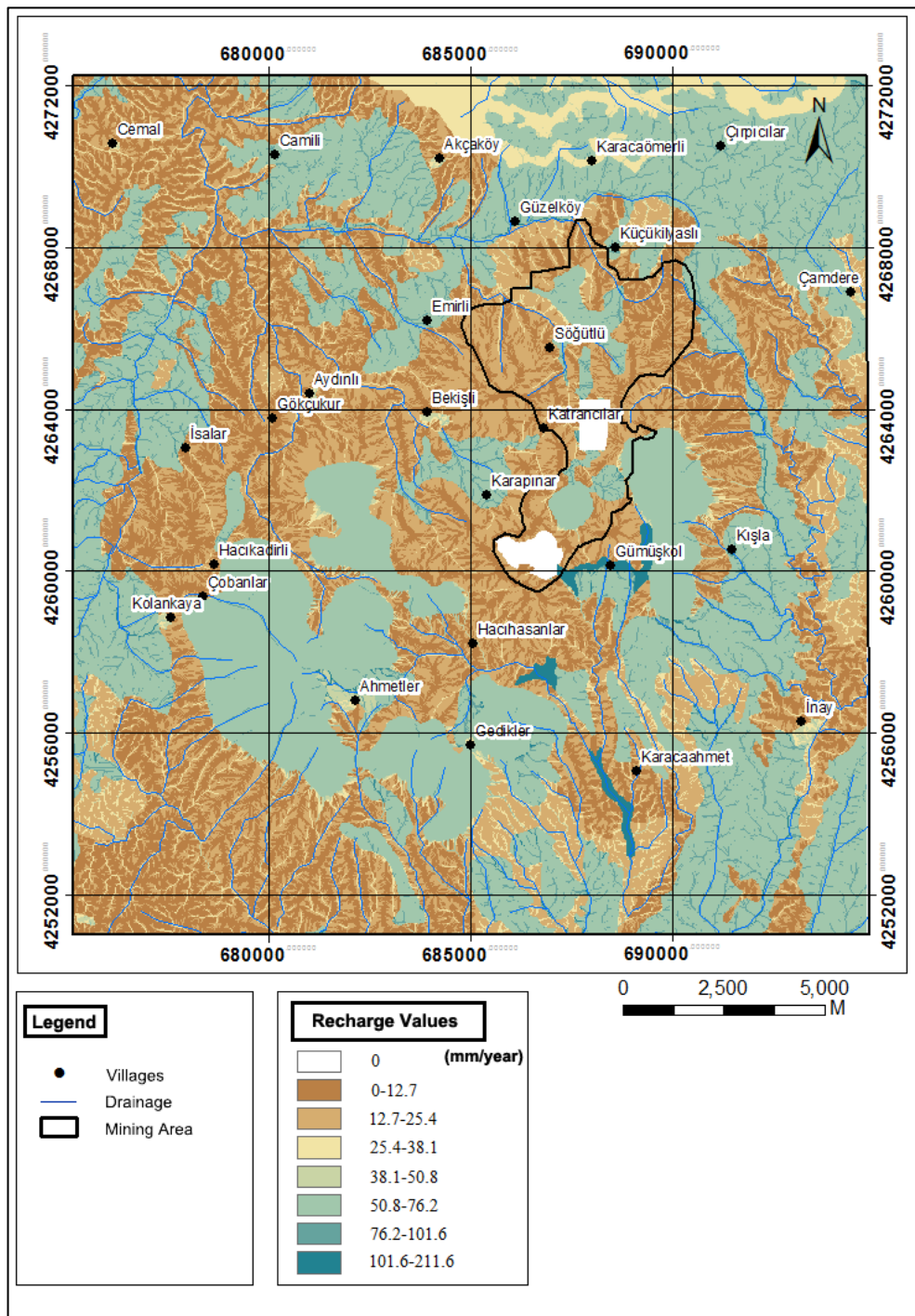


Figure 3.10 The yearly average groundwater recharge amount (mm/year) obtained from the SWB model (2008-2012 average)

CHAPTER 4

HYDROGEOLOGY

4.1. Water Points

4.1.1. Rivers

The Kışladağ Gold Mine area is located on the water divide separating the Gediz and Büyük Menderes basins. The Open Pit and South Heap Leach Pad are located on the Gediz Basin; whereas existing non-economic waste rock dump is situated in the Büyük Menderes Basin. The planned North Waste Rock Dump area and the northward extension of the South Heap Leach Pad are completely situated in the Gediz Basin. Since the mine area is mostly located on a water divide, instead of rivers, which flow continuously and drain the area, there are streams, which flow with rainfall seasonally.

The nearest continuous streams to the study area are the Banaz Stream and its branch the Yavu Creek. (Figure 4.1) The Banaz Creek drains an area of 3475 km², from west of the study region to east of Sivaslı Town; and from the Murat Mountain in the north to the Adıgüzel Dam in the south. According to the data (1986 - 1996) from the DSİ-24 flow gauging station, located on the Banaz Stream, the average discharge was calculated as 4.78 m³/s (150.82 hm³ / year). The EİEİ-735 gauging station, located in the upstream of DSİ-24, has 3227 km² of watershed area with an average flow rate calculated as 5.39 m³/s (169.9 hm³/year) with respect to data collected from 1988 to 2000. This data set corresponds to a wetter period.

The Banaz Stream and its branch Yavu Creek constitute the discharge area of the Ulubey aquifer. The Ulubey aquifer consists of karstic limestones and is located east of the mine area, covering approximately 1700 km². According to the calculations of Yazıcıgil et al (2008) this discharge reached 2.94 m³/s (92.8 hm³ / year).

4.1.2. Springs and Fountains

The source of springs with a high discharge rate (>8-10 L/s) in the investigation area is mostly from the Ulubey aquifer. The locations of these springs are shown in Figure 4.1 and detailed information is presented in Table 4.1. According to Table 4.1, the total discharge from the springs was 44.7 hm³/year. 76% of this total discharge is from the Ulubey aquifer, while 24% is from the Alluvium and Asartepe Formations.

The İnay spring, the nearest spring to the study area at 7.5 km away, meets the drinking and usage water needs of the İnay Village. The discharge rates measured by DSİ from 1986 to 1988 range between 2 L/s (January 1988) and 13 L/s (July 1986); whereas the average discharge rate is 8.5 L/s. The discharge rates of the İnay Spring measured by the DSİ are presented in Table 4.2 and the respective graphs are shown in Figure 4.2.

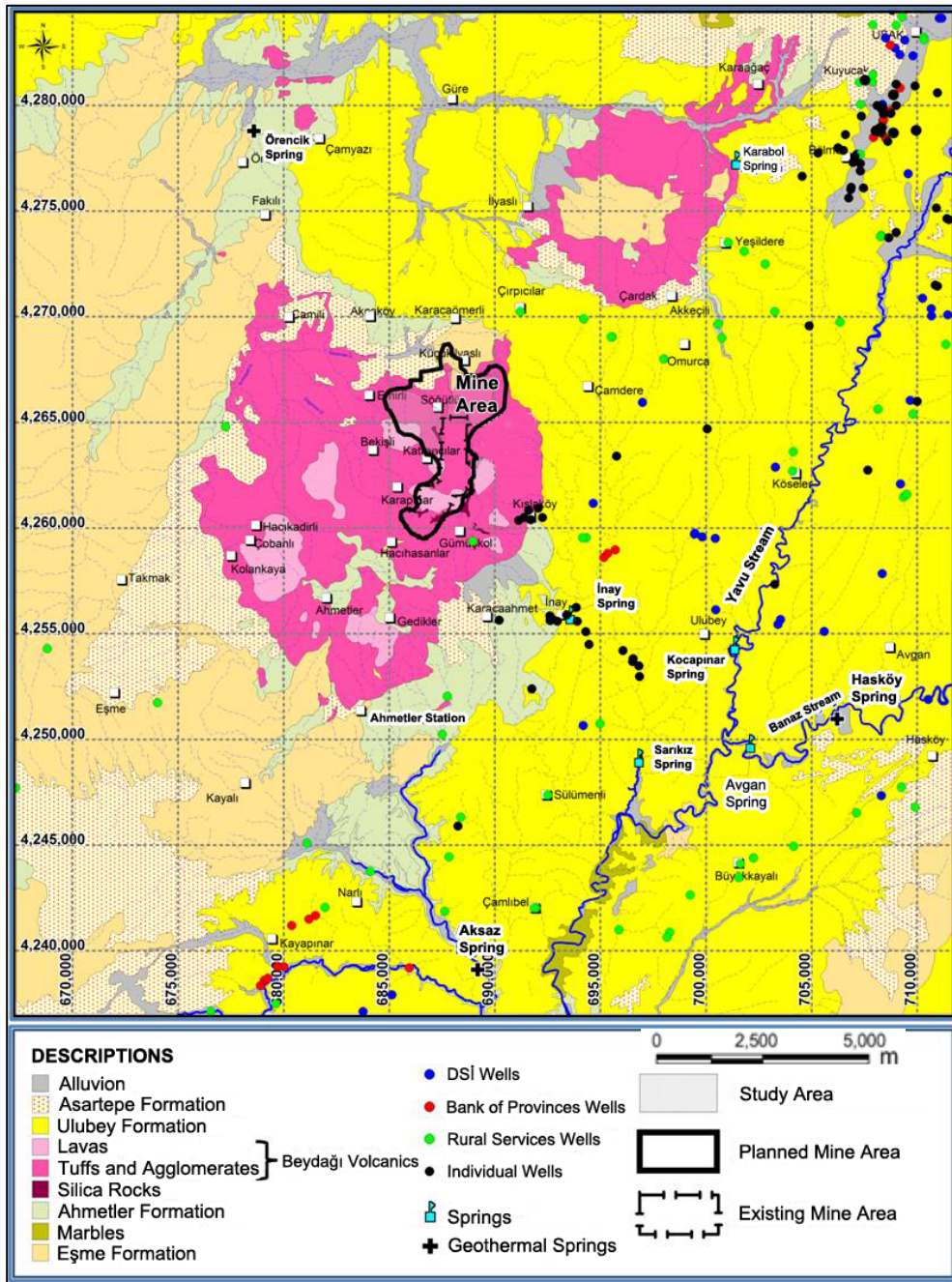


Figure 4.1 Regional Hydrogeological Map (Yazıcıgil et al., 2008)

Table 4.1 Information about springs in the Banaz River Basin (Yazıcıgil et al., 2013)

Springs	Coordinates		Elevation (m)	Units	Average Discharge (L/s)	Approximate Distance to Mine Area (km)
	Easting	Northing				
Gürpınar	737634	4255019	949	Alluvium	260	50
Pınarbaşı 1	734562	4262878	939	Alluvium	21	46
Pınarbaşı 2	736470	4262483	1092	Alluvium	22	48
Evren	736148	4263813	1030	Alluvium	34	48
Sazak	729850	4265520	880	Alluvium	8	41
Karabol	701422	4277464	815	Ulubey	45	18
Avgan	702109	4249863	521	Ulubey	243	18
Sarıköz	696824	4249181	539	Ulubey	165	14.7
Cabar	722500	4257500	715	Ulubey	493	34
İnay	693574	4255946	705	Ulubey	8.5	7.5
Kocapınar	701363	4254525	572	Ulubey	14.7	15
Uyuz	717690	4254230	689	Ulubey	70	30
Hasköy	715667	4253917	647	Ulubey	15	28
Sivashlı 1	733606	4272004	883	Ulubey	1	46
Sivashlı 2	734007	4271898	895	Ulubey	10	46

Table 4.2 Discharge values in the İnay Spring measured by the DSİ (m³/s) (Yazıcıgil et al., 2013)

	Jan	Feb	March	April	May	June	July	Aug	Sept	Oct	Nov	Dec
1986				12	13	12	13	8	7	10	10	9
1987	10	10	10	8	10	4	10	7	5	3	6	5
1988	2	7	4	11	12				7		11	0
2007					10	11	9	9	8	9	9	8
Avg.	6.0	8.5	7.0	10.3	11.3	9.0	10.7	8.0	6.8	7.3	9.0	7.3

The Sarıköz Spring, having an average discharge rate of 165 L/s, is 14.7 km away from the study area, and it is primarily used for irrigation purposes. The discharge rates measured by the DSİ from 1986 to 2007 are illustrated in Table 4.3. Figure 4.3 represents the graph of change in discharge rates with time. The discharge rate of Sarıköz Spring was measured as 111 L/s in 16.08.2007.

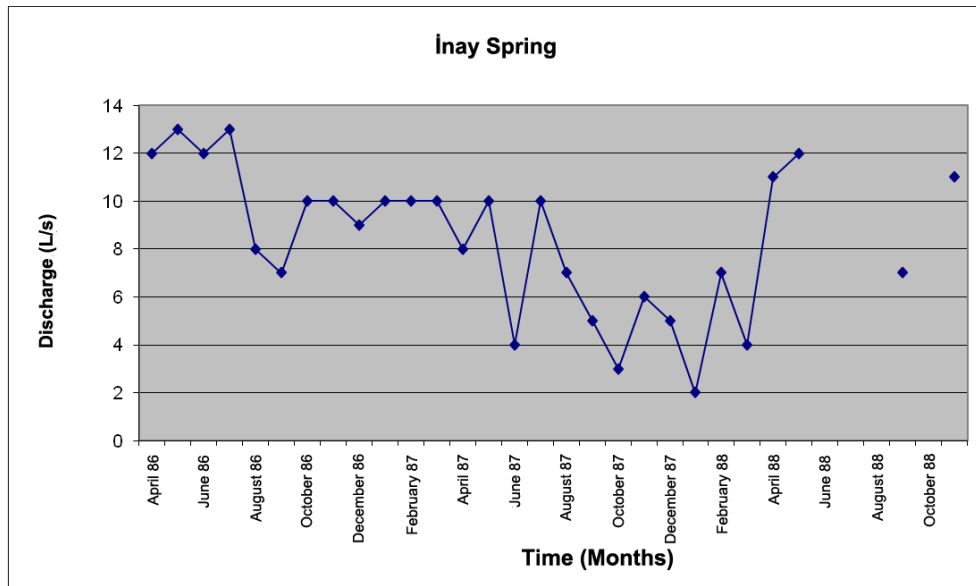


Figure 4.2 Discharge value variations in the Inay Spring as measured by the DSI (Yazıcıgil et al., 2013)

Table 4.3 Discharge values in the Sarıkız Spring as measured by the DSI (L/s) (Yazıcıgil et al., 2013)

	Jan	Feb	March	April	May	June	July	Aug	Sept	Oct	Nov	Dec
1986						185	156	224	140	187	176	182
1987	219	185	271	181	183	145	147	220	198	184	197	
1988	256	248	185	143	164				159		149	
1989				147						138		
1990				139						135		
1991				143						0		
1994				107						51		
1995				204						84		
1996				84						83		
1998				0						103		
1999				76						60		
2000				69						77		
2001				107						99		
2002				100						109		
2003				57						131		
2004				122						133		
2005				95						138		
2006				153						116		
2007					107	115	113	111	92	110	102	94
Average	237.5	216.5	228.0	120.4	151.3	148.3	138.7	185.0	147.3	114.0	156.0	138.0

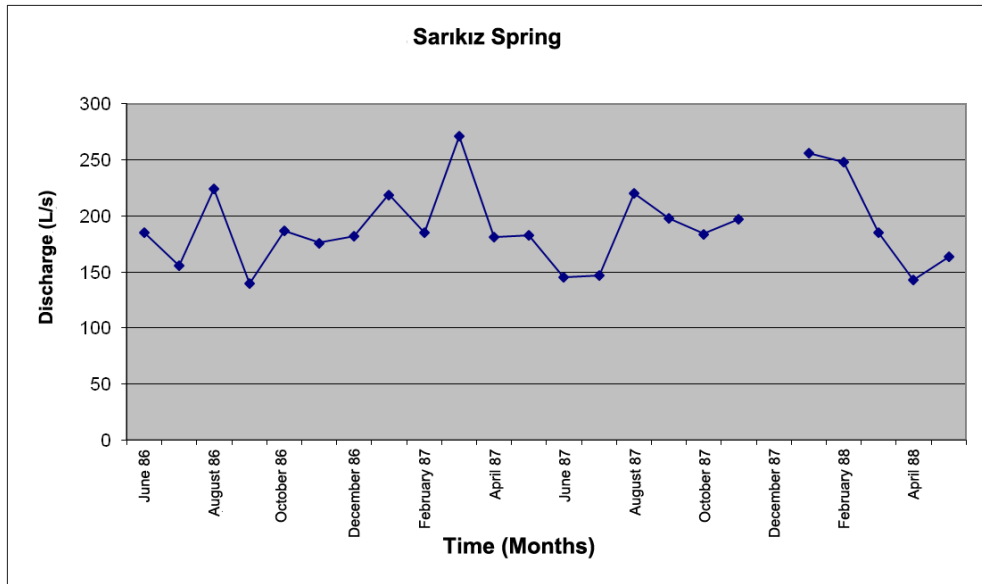


Figure 4.3 Discharge value variations in the Sarıkız Spring as measured by the DSI (Yazıcıgil et al., 2013)

The Kocapınar Spring, originating from the Yavu Creek Valley, is 15 km away from the study area, and has an average discharge rate of 10-13 L/s. This spring was developed by the Bank of Provinces in 1963 and partly fulfills the drinking and water usage needs of the Ulubey town. The Avgan Spring, originating from the Banaz Stream Valley, is located 18 km southeast of the study area. The average discharge rate of this spring was calculated as 243 L/s and formally meets the drinking and water usage needs of the Avgan village. The Karabol Spring, which is situated 18 km northeast of the study area, has a discharge rate of 45 L/s and partially meets the drinking and water usage needs of Uşak.

The springs and fountains which are located within the Kışladağ Gold Mine and vicinity have low discharge rates (<0.25 L/s), and 10 of them are included in the observation program conducted by the Tüprağ. The locations of these springs are demonstrated in Figure 4.4, and detailed information is given in Table 4.4. Studies to determine the hydrogeochemical features and water quality of the study area were initiated by taking monthly water samples from these springs in the year 2000.

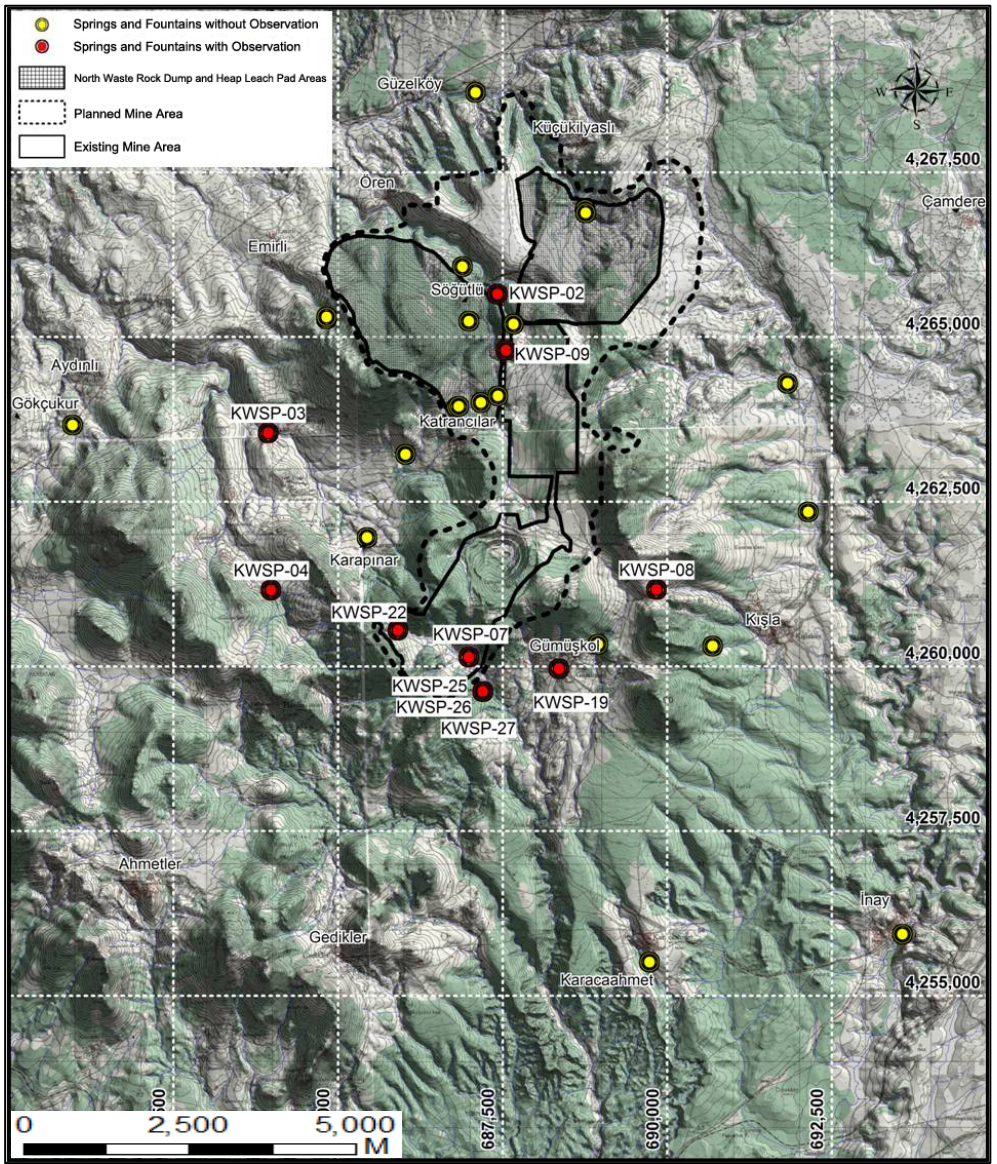


Figure 4.4 The springs and fountains in the study area and its vicinity (Yazıcıgil et al., 2013)

Table 4.4 The springs and fountains in the study area and its vicinity (Yazıcıgil et al., 2013)

Observation Points	Coordinates		Observation Period	Type	Location	Formation
	Easting	Northing				
KWSP-02	687424	4265662	2000-2004	Fountain	South Heap Leach Pad	Volcanoclastics
KWSP-03	683940	4263554	2000-2006	Fountain	Outside the Mine Area	Volcanoclastics
KWSP-04	683983	4261171	2000-Present	Fountain	Outside the Mine Area	Alluvium
KWSP-07	686989	4260150	2000-2005	Fountain	South Waste Rock Dump Area	Intrusives
KWSP-08	689840	4261177	2001-Present	Spring	Outside the Mine Area	Volcanics
KWSP-09	687550	4264809	2001-Present	Fountain	South Heap Leach Pad	Volcanics
KWSP-19	688361	4259974	2003-Present	Tap Water	Outside the Mine Area	Ulubey FM
KWSP-22	685909	4260559	2004-Present	Spring	South Waste Rock Dump Area	Volcanic Conglomerate
KWSP-25	687207	4259632	2005-Present	Fountain	South Waste Rock Dump Area	Volcanic Conglomerate
KWSP-26	687199	4259630	2005-Present	Fountain	South Waste Rock Dump Area	Volcanic Conglomerate
KWSP-27	687203	4259628	2005-Present	Leak	South Waste Rock Dump Area	Volcanic Conglomerate

4.1.3. Wells

The wells located in the Kışladağ Gold Mine and its vicinity is presented in three groups. The first groups of wells were opened by official institutions and were well-logged. These wells were used to determine the general hydrogeological conditions of the Kışladağ Gold Mine and its vicinity. The second group is comprised of individual wells. Information about these wells was based on the data kept in well permit documents. The third and last group includes the wells opened by Tüprağ Metal Madencilik San. ve Tic. A.Ş for exploration, test and observation purposes. According to detailed measurements, tests and analysis, the hydrogeological characterization of the Kışladağ mining area was completed. Below is detailed information about these wells belonging to these three different groups.

Official Institution Wells

Around the Kışladağ Gold Mine, there are 117 wells which were drilled by the DSİ, the Rural Services and the Bank of Provinces. (Figure 4.1) The DSİ has drilled 34 wells, 27 of which were opened for exploration purposes while the others were drilled for water supply purposes. The Rural Services built 64 wells in order to meet the drinking and water usage needs of the surrounding villages. Lastly, the Bank of Provinces drilled 19 wells in order to supply drinking and water usage for the settlements having municipality. The information about these wells are given in Appendix A.

There are 57 wells that have detailed well logs and received water from a single geological unit outcropping in the project area and its vicinity. These wells were evaluated according to their yields and specific capacity by calculating minimum, maximum and average values (Table 4.5). By examining this table, the highest yield and specific capacity values can be

observed in wells which received water from the Asartepe and Ulubey Formations. This leads to the fact that these two formations are aquifers of regional importance.

Table 4.5 The yield and specific yield values of the wells in the study area with respect to their formations (Yazıcıgil et al., 2013)

Formations	Number of Wells	Yield (L/s)			Specific capacity (L/S/M)		
		Minimum	Mean	Maximum	Minimum	Mean	Maximum
Ahmetler FM.	10	dry	7.51	17.00	dry	0.20	0.48
Alluvium	2	1.70	2.85	4.00	0.12	0.19	0.25
Asartepe FM.	5	1.46	11.29	26.00	0.06	4.73	17.54
Eşme FM.	2	2.50	2.75	3.00	0.029	0.032	0.035
Ulubey FM.	37	dry	11.38	30.00	dry	2.78	17.46
Beydağı Volcanics	1	0.20	0.20	0.20	0.002	0.002	0.002

Individual Wells around the Kışladağ Gold Mine area

From the individual wells around the Kışladağ Gold Mine, those having records on the DSI were obtained and evaluated. The locations of all 62 individual wells, except for the five Tüprağ wells pumping water from the Ulubey aquifer, are shown in Figure 4.1. Fifty-four of these wells have been opened for irrigation purposes, whereas 8 of them are used for drinking and usage purposes. Although the information is inadequate, it is estimated that the majority of the wells receive water from the Ulubey aquifer. The amount of the annual DSI allocation for these wells is approximately 100,000 tons.

The Observation Wells Drilled in the Kışladağ Mining Area and Vicinity

There are a total of 82 wells, 33 of which were drilled in 2007. The remaining 49 wells were drilled within the scope of capacity increasing in order to determine the hydrogeological conditions and hydraulic parameters, measure the water level, flow rate and water quality parameters, and to observe changes around the Kışladağ Gold Mine. The locations of the wells are presented in Figure 4.5 and well information is shown in Appendix A including information about the names of the wells, elevations and coordinates, observation periods, operation area, screened units, depths, screen lengths, and hydraulic conductivity coefficients.

Monthly measurements of well parameters such as, water level, pressure, discharge rate (if there is free flow), and water quality were performed by Tüprağ. Monitoring activities initiated in the year 2000 are continuing in 40 active wells. Additionally, with the aim of determining the hydraulic parameters like, hydraulic conductivity and storage coefficients, certain of aquifer tests were conducted. These aquifer tests are composed of packer, pumping, recovery and slug tests. In the light of information obtained from these observation wells, the current hydrogeological features of the study area were defined. These aquifer tests are conducted by Tüprağ.

Among 33 wells drilled before 2007, 13 wells drilled in waste rock dump (6 wells coded as WR) and leach pad (LP-1, LP-2, LP-3, LP-8, LP-9, LP-10 and LP-11) are permanent

observation wells in order to monitor the operational and closure periods. Among the rest of the wells, 6 were drilled in the Open Pit area for geotechnical purposes (PZ coded wells), 6 were drilled in different locations as observation wells, 2 were exploration wells, 2 were drilled for water usage purposes, and lastly, 4 were caisson and shallow wells.

Within the context of the capacity increasing activities planned in the year 2011, the observation wells have been drilled in leach pad (LP-4, LP-5, LP-6 and LP-7), planned waste rock dump and planned heap leach pad (11 wells coded as HY). Additionally, 9 GC coded wells drilled and cased for geotechnical and exploration purposes in 2011 are included in the observation program. Among these 9 wells, 4 of which are around the Open Pit and 4 are located in the expansion area. The shallow wells (DH coded wells) located in the North Heap Leach Pad and vicinity were opened for geotechnical purposes in 2012; however casing has not been installed in these wells. The WR-1 well in the waste rock dump and the LP-4 and LP-5 wells in the leach pad were cancelled (abandoned) and replaced with newly drilled WR-1A, LP-4A and LP-5A wells in 2012. The details about the wells drilled within the scope of capacity increasing activities and the respective tests conducted are represented in Section 4.2.2., where the hydrogeology of the expansion area is addressed.

Additionally, in order to determine the water levels in the Open Pit and hydraulic parameters of the region, 11 wells (KPT, PBPW and PBMW wells) were drilled, and pumping tests were performed.

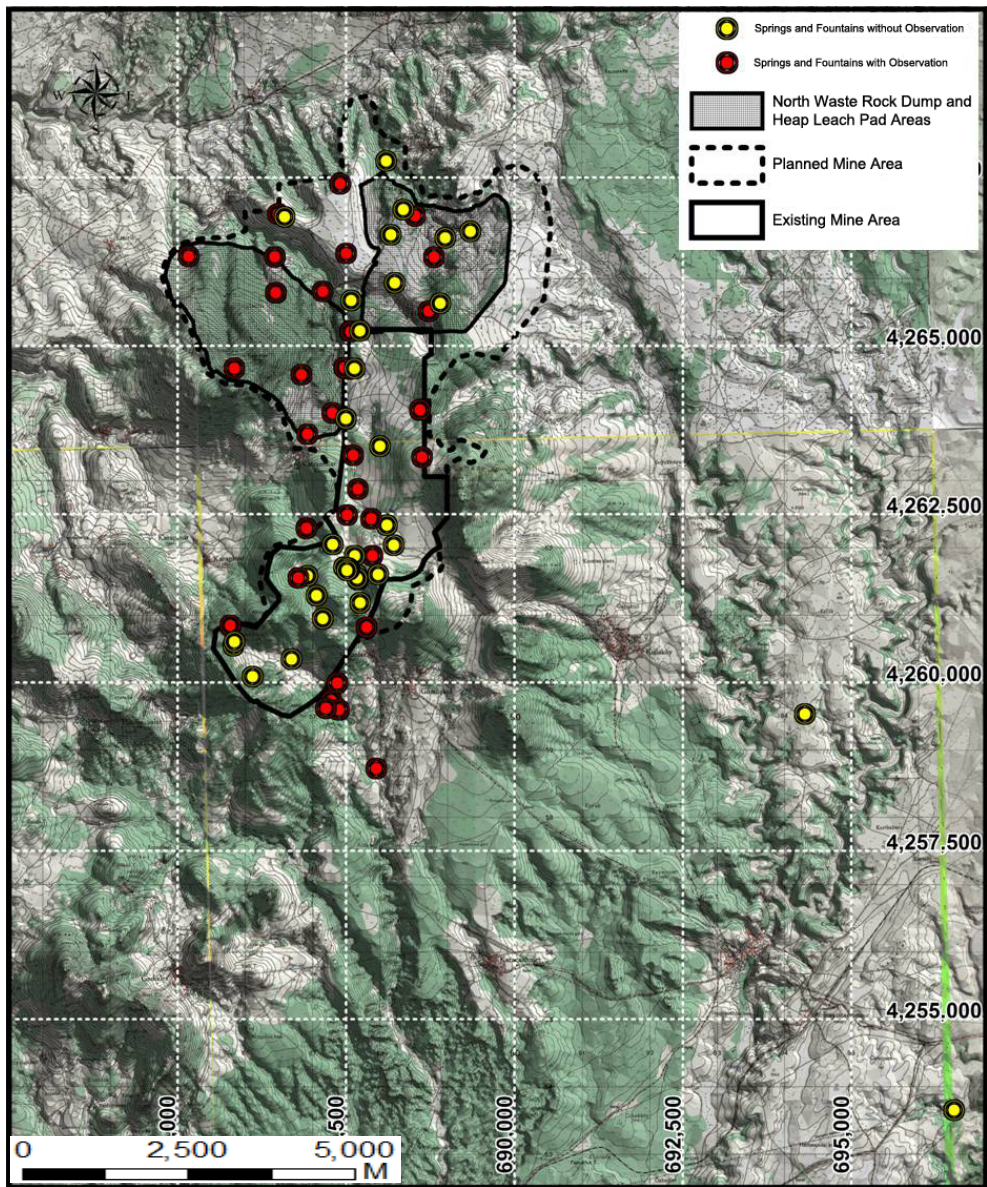


Figure 4.5 Wells in the study area and its vicinity (Yazıcıgil et al., 2013).

4.2. Groundwater Bearing Units

4.2.1. Regional Hydrogeological Setting

According to information from water resources points, hydrogeological properties of the study area and its vicinity were determined. The geological units were classified with respect to their lithological and groundwater bearing properties into 7 main hydro-lithological groups. Figure 4.1 shows the simplified geological setting, existing water wells, springs, and drainage network of the area. The characteristics of hydro-lithological groups are described below.

Schists and Gneisses (Eşme Formation)

The outcrops of this formation forming the crystalline basement of the area are seen at the western part of Kayalı, Takmak and Örencik. At the west and the north part of the mining area, the Eşme formation is overlain by Ahmetler and Asartepe Formations. However, in the mining site, volcanic rocks overlie this formation. The Eşme formation is identified as a poor aquifer as its yields are very low. The well yield of this formation is about 2.5-3.0 L/s. According to the aquifer test evaluation of the wells filtering the Eşme Formation, hydraulic conductivity values range between 1.19×10^{-8} m/s and 2.61×10^{-6} m/s. The geometric mean of the hydraulic conductivity value is 1.81×10^{-7} .

Marbles (Musadağı Formation)

The Musadağı Formation outcropping in the Banaz River Basin is located in the west of the Çamlıbel village. This formation has limited extension, but it is classified as a good aquifer due to its karstic characteristic. As a result of the pumping tests conducted by the State Hydraulic Works, transmissivity of the formation was calculated as varying from 5 m²/day to 11361 m²/day. Furthermore, the hydraulic conductivity values vary between 6.0×10^{-7} m/s and 1.5×10^{-3} m/s (Yazıcıgil et al., 2008). It is foreseen that this aquifer is not suitable enough to supply groundwater because it is contaminated by the highly polluted Yavu Creek and Banaz River (Yazıcıgil et al., 2008).

Volcanic Sequence (Beydağı Volcanics)

This sequence is composed of lava flows, agglomerates, and tuffs. The outcrops are dominantly seen in the mining and study area. In the Kışladağ Gold-Mine, and in the west of this area, schists and gneisses enclose or underlie the Beydağı Volcanics. On the other hand, these volcanic rocks inter-finger with the Ahmetler and Ulubey Formations in the south. It can be said that these rocks have a low groundwater bearing capacity. The hydraulic conductivity values are between 4.56×10^{-9} m/s and 1.61×10^{-6} m/s according to the results of aquifer tests conducted in the area. The geometric mean of these results is 1.05×10^{-7} m/s.

Ahmetler Formation

The Ahmetler Formation, involving Merdivenlikuyu, Balçıklıdere and Gedikler units, is composed of pebblestone, sandstone, siltstone, tuffite, mudstone, marl and limestone. Fine grained clastics are more prevalent in this formation. There are only a few wells supplying groundwater at a very low flow rate. Therefore, the Ahmetler Formation is classified as a poor aquifer but is important because it forms the bottom, impervious boundary of the Ulubey aquifer. This formation is underlain by schist and gneiss at the north and south parts of the mining area.

Ulubey Formation

This sedimentary formation, covering a widespread area (approximately 1700 km²), is the most important aquifer for the region. It consists of thick to very thick, locally massive lacustrine limestones and intercalations of these rocks with marl bands. The thickness of this formation is about 250 m. Having horizontal and/or gently dipping beds, it forms a very broad, synclinal structure around Ulubey. These karstic-type rocks consist of numerous fractures and joints. Fractures in the rock are very rife because of karstic cavities and dissolutions. The Ulubey Formation feeds water to the high capacity water supply wells (15-30L/s) and high yield springs (250-500 L/s) in the area. The yields of 41 wells filtering this aquifer range from dry to 30 L/s, and the average yield value is 11 L/s. Additionally, the specific capacity values vary between 0-17.46 L/s/m and the average specific capacity value is calculated as 2.78 L/s/m. According to the results of pumping tests within the Ulubey Aquifer drilled by State Hydraulic Works and Bank of Provinces, transmissivity values were recorded as 6 m²/day to 5158 m²/day. Hydraulic conductivity values were between 1.04x10⁻⁶ and 1.45x10⁻³. The geometric mean value of the hydraulic conductivity was calculated as 3.58x10⁻⁵ by considering the aquifer tests results of 20 wells. The SRK Consulting company performed an aquifer test on Tüprag water supply wells, which showed that the storage coefficient of the aquifer was 0.059 (SRK, 2003). Yazıcıgil (2000) states that the Ulubey formation contains all types of aquifers with poor, medium and good characteristics. Some parts of the formation having good aquifers are due to the fractured, jointed and fault controlled karstic structures existing in the region.

The Ulubey Formation is an unconfined aquifer underlain by the impervious Ahmetler Formation. On a regional scale, groundwater levels in the northern part of the Ulubey aquifer are about 880-900 m in centrum of Uşak. Moving south towards Ulubey, groundwater levels decrease to 600 m (Figure 4.6) and reach 410 m around the Adıgüzel Dam. The hydraulic gradient of the aquifer is approximately 0.023 near Sivashı, 0.022 around Ulubey, and 0.009 inside the basin between the Banaz and Yavu Creeks (Yazıcıgil et al., 2008). In the southern part of Ulubey, it was observed that the aquifer discharges to the Banaz and Yavu Creeks.

Asartepe Formation

The rarely spread outcrops of the Asartepe Formations are seen in the southwest, southeast and northeast parts of the study area. This formation is mostly observed outside of the study area, near Banaz and Sivaslı (Yazıcıgil et al., 2008). The formation, consisting of fine grained units, was formed by pebblestone, sandstone, siltstone, claystone, and marl alternation. The yields of five wells tapping the Asartepe Formations are between 1.46 L/s and 26 L/s, and the mean value of well yield is 11.3 L/s. The specific capacity varies from 0.06 L/s/m to 17.54 L/s/m and the average value is calculated as 4.7 L/s/m. The transmissivity values of this formation are between 94 m²/day-796 m²/day and hydraulic conductivity values range from 6.50x10⁻⁶ m/s to 1.00x10⁻⁴ m/s as a result of pumping tests conducted by the Hydraulic State Works on 4 wells. Additionally, four wells were drilled in the study area to observe the Asartepe Formation; one of which is a dry well. Slug tests were performed on two of these wells due to a low yield of the formation. According to slug test results, the average hydraulic conductivity value of this formation is 2.8x10⁻⁸ m/s. This is an indication that the Asartepe Formation is an impervious layer on the northern part of the mine area. The Asartepe Formation outcrops cover the widespread areas around Sivaslı on the eastern side of the study area, which has characteristics of the aquifer in this region.

Quaternary Deposits

These deposits are made up of the alluvial cone deposits, terraces of sediments, and alluviums. There are several shallow and man-made wells belonging to individuals who use them for irrigation purposes. The wells in these alluvial aquifers are located around Uşak, Banaz and Güre. Four wells were drilled by the Hydraulic State Works in order to determine aquifer properties of these deposits. As a result of pumping tests performed on these wells, transmissivity values vary from 67 m²/day to 482 m²/day, and hydraulic conductivities were between 3.93x10⁻⁵ m/s and 2.5x10⁻⁴ m/s.

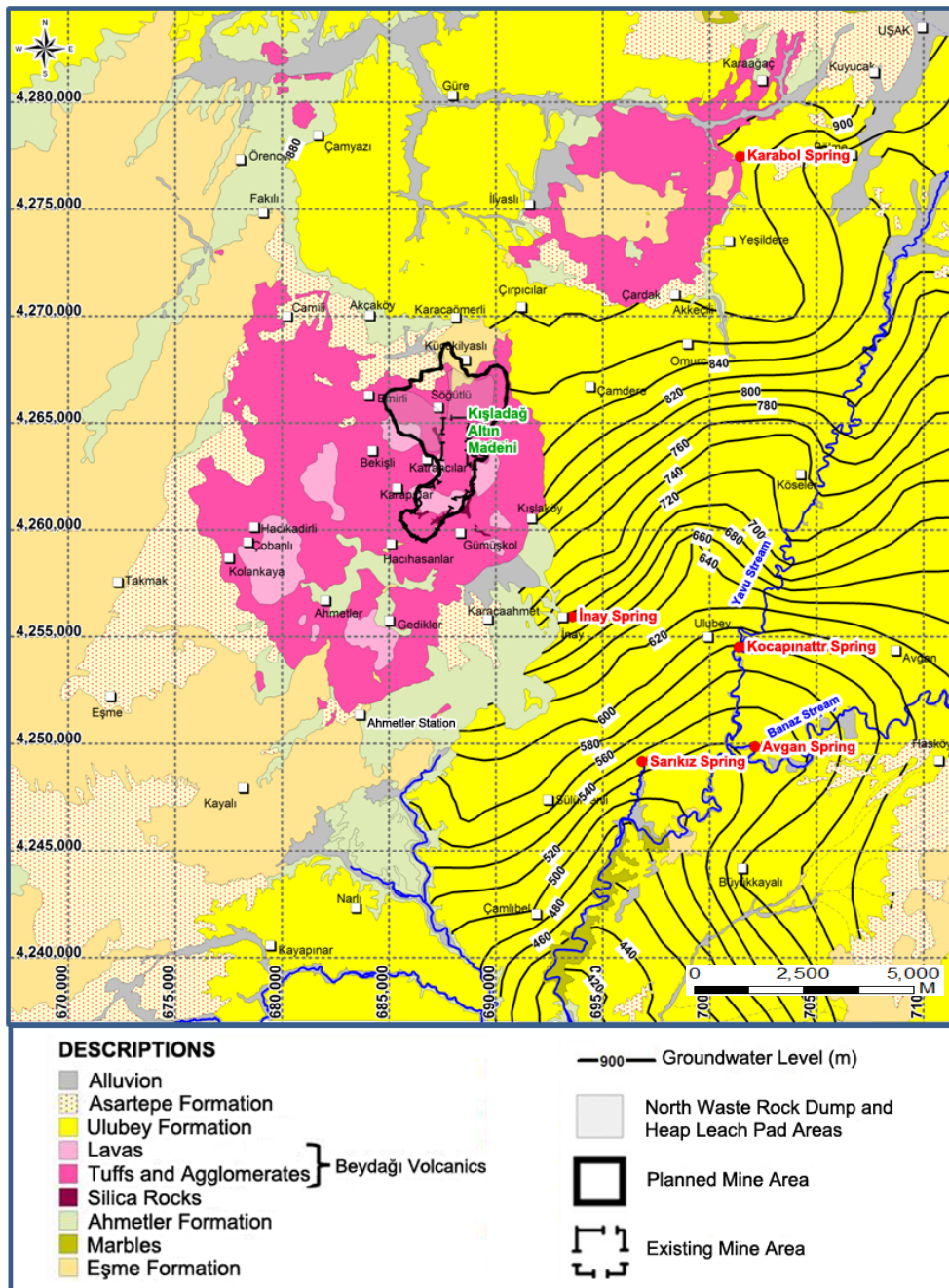


Figure 4.6 The groundwater level map of the Ulubey Formation (Yazıcıgil et al., 2008)

Well Information

Well information including casing details are given in Appendix B.

GC Piezometer Observation Wells

Within the scope of the Project, seven GC Exploration Wells (GC-451, GC-452, GC-453, GC-454, GC-455, GC-456 and GC-457), which were previously drilled for exploration purposes, have been converted to observation wells in order to observe the water level change in the schist unit.

The 7 wells, with diameters of HQ (96 mm), were drilled on different dates between 22 September 2011 and 18 November 2011. These wells were completed using PVC pipe and quartz sand. Some of these wells were filled with quartz sand before installing the PVC casing and screen so that the well screen located in the desired elevation within the schist unit. The PVC length and the volume of the quartz sand, which was needed for completing wells of different depths, were determined so that the schist unit could be filtered.

GC-451: The GC-451 exploration well, which later transformed into the observation well, is located on the north side of the South Heap Leach Pad area. After the development processes were completed, it was filled with quartz sand. By this means, the well depth was reduced from 300.6 meters to 134 meters. Following, the casing and screen were installed, and the construction of the well was completed on 23 September 2011.

GC-452: The GC-452 exploration hole, with a depth of 350.5 meters, was drilled on the northwest border of the planned expansion area, and its drilling was finished on 2 October 2011. However, unexpected PVC squeeze during the process of PVC placement and sand filling activities has led to destruction of the well. As a result, it was decided to cancel the casing of this well.

GC-453: The GC-453 exploration well, located on the north side of the South Heap Leach Pad, was converted to an observation well on 11 October 2011. The well, which was initially 300.1 meters in depth, reached a depth of 124 meters with the help of quartz sand filling. Following this procedure, the well construction was completed with casing and screen.

GC-454: Drilling process of the GC-454 well (located on the north side of the North Waste Rock Dump area) was ceased at 301 meters. Following, development activities were completed, and the bottom of the well was elevated from 301 meters to 250 meters with sand filling. Casing and screen installation was done with respect to this new level and the construction of the well was completed on 20 October 2011.

GC-455: The GC-455 exploration well, located at the North Waste Rock Dump area, has a depth of 287.7 meters. After the drilling process, the well was developed and the depth of the well was adjusted to 230 meters, which finalized the casing process. The transformation of the GC-455 well into an observation well was completed on 25 October 2011.

GC-456: Drilling of the GC-456 well was finished on 12 November 2011 at 302 meters depth on the south side of the North Waste Rock Dump area. As the well makes a 60° angle with the surface, it could not be transformed into an observation well.

GC-457: The GC-457 well is located in the south of the planned North Waste Rock Dump area. After the depth of the well reached 302.5 meters, the well was developed and filled with quartz sand to a new depth of 146 meters. As a last step, casing and screen were completed and the well was converted to an observation well. The construction of the well was finalized on 17 November 2011.

LP Observation Wells

LP-4A: LP-4A, located at the northwest of the South Heap Leach Pad, was drilled as a replacement of the previously drilled LP-4 well. The purpose of opening this well was to observe the schist unit. As a result, the drilling ended at 90 meters and completion was initiated. The LP-4A well, 10.5 inches in diameter, was washed with water 4 times its own volume. Afterwards, the well was developed with 2 hp submersible pumps for 12 hours with flow rates ranging from 1.5 L/s to 0.2 L/s.

LP-5A: The LP-5A well, located next to the LP-4A well, was opened as a substitute to LP-5. LP-5A, which is 34 meters in depth and 10.5 inches in diameter, filters the latite flow and volcanic breccia unit. After the drilling process, the casing and screen were completed and construction terminated. After LP-5A was washed with water 4 times its own volume, the well was developed with a 2 hp submersible pump for 12 hours with flow rates ranging from 1.5 L/s to 0.2 L/s.

LP-6: The LP-6 groundwater observation well, 10.5 inches in diameter, was drilled at the northwest border of the leach pad. The drilling and the installation of casing and screen in LP-6 were completed between 16 September 2011 and 4 October 2011. Since the LP-6 observation well was aimed at the schist unit, drilling continued until the depth reached 183.4 meters from the surface. Following that, the drilling activities were finished and the well washed with 90m³ of fresh water. The development process was performed with a 3 hp submersible pump placed 140 meters depth from the surface for more than 8 hours with approximately 2 L/s flow rate.

LP-7: Drilling and completion of the LP-7 groundwater observation well, positioned next to the LP-6 well at the northwest border of the South Heap Leach Pad, were performed between the dates of 14-18 October 2011. The LP-7 groundwater observation well was designed solely to monitor the Asartepe Formation, which was formed from stream sediments, and consists of tuff and gravels mixed with a clay matrix. Since the general information about the geological units and the groundwater level of the region was previously acquired from the drilling process of the LP-6 well, it was foreseen that the LP-7 well should be at least 60 meters in depth. As a result, drilling of this well was terminated when the depth reached 62 meters from the surface. After the well was drilled with a 10.5 inch diameter downhole hammer, the casing process was completed and the well was washed with 80m³ of fresh water. The well was developed with the 1.5 hp submersible pump, placed 50 meters in depth from the surface for at least 8 hours with 1 L/s flow rate. Since the LP-7 well cannot sustain the 1 L/s flow rate, the development process continued intermittently.

HY Observation Wells

HY-1: The HY-1 well is located west of the North Heap Leach Pad, approximately 4 meters away from the GC-451 well. This well, 10 inches in diameters, was constructed in order to investigate the hydraulic relationship between the Asartepe Formation and the schist unit. Drilling was terminated on 4 April 2012 after 86 meters depth was reached, followed by installation of the casing and screen. As a last step, the well was washed with water more than 3 times its own volume and developed with a 20 bar air compressor and a 2 hp submersible pump.

HY-2: The HY-2 well is located on the northwest border of the planned North Heap Leach Pad and was close to the abandoned GC-452 well. The well, 10 inches in diameter and 68 meters in depth, was drilled to observe the Asartepe Formation. Drilling was terminated at 68 meters depth until the borehole was extended to the boundary of volcanoclastics on 20 April 2012. The HY-2 was developed with only a 20 bar air compressor since there was no water within the well.

HY-3: The HY-3 groundwater monitoring well, 10 inches in diameter, was drilled on the north side of the North Heap Leach Pad in order to observe the schist unit. After the well reached 51 meters in depth, the drilling process was halted on 13 April 2012 and completion began. The well was washed with water more than 3 times its own volume, which was approximately 12 m³ and developed with a 20 bar air compressor and a 2 hp submersible pump.

HY-4: The HY-4 well, drilled at the north border of the expansion area, is 10 inches in diameter, and it filters the Asartepe Formation along with its terminal length of 102 meters. After the drilling of the well, casing and screen installation processes were performed and the construction of the well was completed on 9 April 2012. The well was washed with water 4 times its own volume and was developed with a 20 bar air compressor and a 2 hp submersible pump.

HY-5: The HY-5 well was drilled at the northern border of the North Waste Rock Dump, next to the GC-454 well which filters the schist unit. The construction of the well was completed on 13 June 2012 when the well reached 64 meters in depth and the casings were terminated. The HY-5 observation well, 10 inches in diameter, was drilled in order to determine the hydraulic relations between the schist and volcanoclastic units. After the well was washed with water 3 times its own volume, which is approximately 12 m³, it was developed with a 20 bar air compressor and a 2 hp submersible pump.

HY-6: The HY-6 well, 10 inches in diameter and 100 meters in depth, was opened at the west of the Söğütlü Village, within the North Waste Rock Dump, and near the GC-455 well. The HY-6 observation well was opened to investigate the hydraulic relations between the schist and volcanoclastic units. The construction of the well was completed on 20 June 2012 after the drilling and casing installation. The well was washed with approximately 20 m³ water, which is 3 times its own volume, and development processes were performed with a 20 bar air compressor and a 2 hp submersible pump.

HY-7: The HY-7 well was opened at the northeast side of the North Heap Leach Pad, and was filtered in the schist unit. It is drilled 55.3 meters deep with a 10 inches down-hole hammer. After drilling, it was observed that the well became an artesian well, and therefore, while the installation of the casing continued, the water was pumped by a submersible pump with a 15 L/s flow rate. By this means, the water level was lowered 20 meters below the surface. After the well reached the desired dynamic water level, evacuation of water was performed for 48 hours for the installment of the casing. The construction of the well was completed on 12 June 2012. In order to apply a confined aquifer test, a metal pipe with valve and manometers was fixed on the top of the well. As the free flow was observed within the well, the development process was performed with a 20 bar air compressor. Since the well showed free-flow features, and the values of certain parameters such as As, Fe, Mn, P, Zn, Sb were observed to be higher than expected levels, the well was closed with cement on 30 August 2012.

HY-8: The HY-8 well, 10 inches in diameter and 51 meters in depth, was drilled in the middle of the North Heap Leach Pad so as to observe the schist unit. The casing and screen were completed on 18 April 2012. The well was washed with water more than 3 times its own volume and was developed with a 20 bar air compressor and a 2 hp submersible pump.

HY-9: The HY-9 well, 10 inches in diameter, was drilled at the northwest border of the North Waste Rock Dump to observe the volcanic (latite flow) unit. After the well reached 181 meters in depth, the casing and screen installment process began and the construction of the well was completed on 13 November 2012. The HY-9 well was washed with approximately 30 m³ water and developed with a 20 bar air compressor and a 2 hp submersible pump.

HY-10: The HY-10 well is located at the southeast side of the North Waste Rock Dump area, and it filters the volcanic (latite flow) unit. This well is 101.7 meters deep and 10 inches in diameter. The casing and screen installment process was completed on 17 November 2012. It was washed with water more than 3 times its own volume, and development was performed with a 20 bar air compressor and a 2 hp submersible pump.

HY-11: The HY-11 well, 200 meters in depth and 10 inches in diameter, is situated at the west border of the North Waste Rock Dump in order to observe the volcanic (latite flow) unit. The casing of this well was completed on 21 November 2012. The HY-9 well was washed with 60 m³ water and was developed with a 20 bar air compressor and a 2 hp submersible pump.

Aquifer Tests Conducted

Within the scope of this project, after the wells have been developed, they were subjected to aquifer tests in order to determine the hydraulic conductivity of the different lithological units. Aquifer test evaluations using different methods are given in detail in Appendix C. The details of the test results are shown below:

Aquifer Tests on LP Wells

With the aim of observing the units in the leach pad, four LP coded (LP-4A, LP-5A, LP-6, LP-7) groundwater monitoring wells were drilled in addition to the already existing wells in the area.

Within these wells, a pumping test was performed on LP-4A, which is filtered in the schist unit, and slug tests were performed on LP-5A and LP-6, which tap volcanics and schist units, respectively. The aquifer tests conducted at LP-7 well, filtered in the Asartepe Formation, did not give reliable results because of its insufficient yield. Evaluation results of the aquifer tests are presented in Table 4.6.

LP-4A: After the pre-pump tests were performed with different discharge rates, and, in order to determine the hydraulic conductivity of the schist unit, a pump test was applied for 3 hours with a constant discharge rate of 0.5 L/s. Following the pump test, a recovery test was applied for 25 hours. To be able to calculate the hydraulic conductivity of the confined aquifer featured unit, Cooper & Jacob and Theis methods were applied. Recovery test results were evaluated with Theis Recovery method. According to these methods; the calculated hydraulic conductivity (K) values ranged between 9.6×10^{-9} m/s and 1.89×10^{-7} m/s, and the average K value was calculated as 9.54×10^{-8} m/s (Table 4.6).

LP-5A: The LP-5A well was previously drilled in order to test the volcanic unit in the area. However, as a result of the pre-tests, the well was reported to be insuitable for pump tests because of its insufficient yield, and thus, a slug test was conducted upon LP-5A. The results of the slug test were evaluated by using the Bouwer&Rice and Hvorslev methods and the corresponding hydraulic conductivity (K) values ranged between 8.06×10^{-7} m/s and 9.96×10^{-7} m/s, where 9.01×10^{-7} m/s was the average K value (Table 4.6).

LP-6: To be able to determine the hydraulic conductivity of the filtered schist unit, both the rising and falling head phase slug tests were conducted upon LP-6. The test results show that hydraulic conductivity (K) values, which were calculated with the Bouwer&Rice and Hvorslev methods in two phases, were compatible with each other and varied from 2.23×10^{-6} m/s to 3.21×10^{-6} m/s. The calculated average hydraulic conductivity value was 2.61×10^{-6} m/s (Table 4.6).

Table 4.6 Aquifer Tests on LP Wells and Well Information

Well Name	Elevation(m)	Formation	Top Level of Filter(m)	Bottom Level of Filter(m)	Average GWL Level(m)	Test Type	Method	Calculated K Values (m/s)	Average K Values (m/s)
LP-4A	924.8	Schist	874.8	838.8	914.49	Pumping Test	Theis	9.60E-9	9.54E-8
							Cooper&Jacob	8.74E-8	
							Theis Recovery	1.89E-7	
LP-5A	925.43	Volcanics	911.43	895.43	914.16	Slug T.	Bouwer&Rice	8.06E-7	9.01E-7
							Hvorslev	9.96E-7	
LP-6	939.25	Schist	791.25	763.25	913.34	Slug T.	Bouwer&Rice	2.23E-6	2.61E-6
							Hvorslev	2.64E-6	
							Bouwer&Rice	2.35E-6	
							Hvorslev	3.21E-6	

Aquifer Tests on HY Wells

There are 11 observation wells which were drilled for hydrogeological characterization purposes within the North Waste Rock Dump and Leach Pad areas. Various aquifer tests were applied upon these wells so that the aquifer hydraulic parameters of the lithological units in the northern part could be defined.

The wells are screened in different levels and opened for observing different hydrogeological units: HY-1, HY-2 and HY-4 filter the Asartepe Formation, HY-3, HY-7, H-8 filter the schist unit, and HY-5, HY-6, HY-9, HY-10 and HY-11 filter the volcanics.

Pumping, slug and free flow tests were performed on 10 of these wells. Aquifer tests were not conducted upon the HY-2 well, since the well is dry. In order to determine the aquifer parameters, six pumping tests with different methods were performed on HY-3, HY-6, HY-8, HY-9, HY-10, and HY-11 considering whether the aquifer is confined or unconfined. Three slug tests were applied to HY-1, HY-4 and HY-5 wells, and, according to reactions of the aquifers, rising and falling head phase slug tests performed. Finally, a free flow test was performed on the HY-7 well. Evaluation results of the tests are shown in Table 4.7.

HY-1: In order to determine the hydraulic aquifer parameters, the HY-1 well, which was opened in the Asartepe Formation, was initially exposed to pumping test with a constant discharge rate. According to the results of these 3 different pumping tests with discharge rates of 0.3, 0.1 and 0.03 L/s, it was decided to perform a slug test consisting of 2 phases namely, Rising Head Phase and Falling Head Phase. For both of the phases, Bouwer&Rice and Hvorslev methods were applied and analyses were completed. According to these respective methods, it was calculated that hydraulic conductivity (K) values ranged between 1.47×10^{-9} m/s and 1.20×10^{-7} m/s, where 5.34×10^{-8} m/s was the average K value (Table 4.7).

HY-3: Since the results of the pumping tests with constant discharge rates of 1.5 and 0.7 L/s were evaluated as insufficient, pumping test with a constant discharge rate of 0.2 L/s was applied to the HY-3 well, which filters the schist unit with confined aquifer features for 12 hours. After the pump was shut down, a recovery test was performed for 12 hours. Since the aquifer was confined, Theis and Cooper & Jacob methods were used for analyses and the Theis Recovery method was used for the recovery phase. Calculated hydraulic conductivity (K) values ranged between 4.05×10^{-8} m/s - 1.37×10^{-7} m/s while the average K value was 9.55×10^{-8} m/s. (Table 4.7)

HY-4: HY-4 is the last well which observes the Asartepe Formation and was initially examined by a pumping test with a constant discharge rate of 0.5 L/s. As the test results were evaluated to be inadequate, in order to determine the hydraulic aquifer parameters, a slug test was decided to be conducted. Bouwer&Rice and Hvorslev methods were used for the falling head phase. According to these methods, conductivity (K) values ranged between 2.40×10^{-9} m/s and 2.60×10^{-9} m/s, where the average K value was 2.50×10^{-9} m/s. (Table 4.7)

HY-5: The HY-5 well was opened to monitor volcanic units. A pre-test with a constant discharge rate of 0.5 L/s was attempted in order to determine hydraulic conductivity, however, the test results showed that the water in the well had completely evacuated within approximately 43 minutes. In this respect, a slug test was performed, consisting of a 24 hours

falling head phase and an 8 hours rising head phase. Bouwer&Rice and Hvorslev methods were used for both phases to calculate the hydraulic conductivity (K) values which ranged between 3.37×10^{-8} m/s and 1.15×10^{-7} m/s with an average value of 6.99×10^{-8} m/s (Table 4.7).

HY-6: Another well which monitors the volcanic unit is HY-6. A pre-test designed for this well with a constant discharge rate of 0.732 L/s shows that the water in the well evacuated in approximately 4 hours. Therefore, pumping test with a lower constant discharge rate was applied after waiting 1 day for the well to reach its static water level. A pumping test with a discharge rate of 0.25 L/s was performed for 12 hours, following with the recovery test. As the observed volcanic unit showed unconfined aquifer features, Theis with Jacob, Boulton, Cooper&Jacob, and Neumann methods were used for the pumping test; whereas the Theis Recovery was used for the recovery phase tests to calculate the aquifer parameters. According to these test results, the calculated hydraulic conductivity (K) values ranged between 6.93×10^{-8} m/s and 1.16×10^{-7} m/s, while the average hydraulic conductivity (K) value was 9.22×10^{-8} m/s (Table 4.7)

HY-7: The HY-7 well, opened in the schist unit, shows a free flow feature. Therefore, a free flow test was applied, which is a two-step process. The test lasted for 3 hours: within the first one hour, discharge-against-time measurements were taken, and within the last 2 hours, rising-pressure recovery-versus-time measurements were taken. With respect to the results of these tests, hydraulic conductivity (K) value was calculated as 1.19×10^{-8} m/s (Table 4.7).

HY-8: A pumping test with a constant discharge rate was decided to be conducted on the HY-8 well, which filters the schist unit. After applying the pre-test with a discharge rate of 0.5 L/s, the pumping test with a discharge rate 0.4 L/s was performed for 12 hours. This test was followed by a recovery test for 12 hours. Pumping test results were evaluated with the Theis and Cooper&Jacob methods, whereas the recovery test was evaluated with the Theis Recovery method. The hydraulic conductivity (K) value, which can vary according to the different methods, was calculated as 1.80×10^{-7} m/s as a minimum and 5.97×10^{-7} m/s as a maximum value, and the average value was calculated as 3.79×10^{-7} (Table 4.7).

HY-9: The filter level of the HY-9 well was designed to test the volcanic unit. To define the hydraulic conductivity of the volcanic unit, a pumping test with a variable discharge rate was applied for 28 hours. The water in the well was pumped with a discharge rate of 0.103 L/s for the first 2 hours, 0.0945 L/s for the next 5 hours, and finally 0.084 L/s for the last 21 hours. Following the pumping test, a 19 hours recovery test was conducted. As the unit shows an unconfined aquifer feature, the Theis with Jacob, Boulton, Cooper&Jacob, Neumann methods were used for the pumping period; and the Theis Recovery method for recovery phase was used. According to these methods, the hydraulic conductivity (K) value changed from 2.48×10^{-9} m/s to 7.99×10^{-9} m/s, and 4.56×10^{-9} m/s was the average hydraulic conductivity (K) value (Table 4.7).

HY-10: For the HY-10 well, a pumping test with a variable discharge rate was performed for 27 hours to determine the hydraulic conductivity value of the volcanic unit. The water was pumped with a discharge rate of 0.54 L/s for the first 12 hours and with a 0.5 L /s discharge rate for the following 15 hours. This test was examined using the Theis with Jacob, Boulton, Cooper&Jacob, Neumann methods. After the pumping period, a recovery test was

conducted, and the data was evaluated with the Theis Recovery method. The calculated hydraulic conductivity (K) value ranged between 9.74×10^{-8} m/s and 3.49×10^{-8} m/s, where the average K value was 6.44×10^{-8} m/s (Table 4.7).

HY-11: To calculate the hydraulic conductivity from this well, a pumping test with a variable discharge was performed. After conducting a pumping test with a discharge rate of 0.196 L/s for 4 hours, the well reached the dynamic level. The pumping test was continued with a discharge rate of 0.138 L/s for the next 6 hours. After 11.5 hours of waiting for well to reach its static level again, a rising head phase test was applied. Since the unit shows an unconfined aquifer feature, the Cooper&Jacob and Theis Recovery methods were used to evaluate the K value. With respect to these methods, minimum, maximum and average K values were; 9.11×10^{-8} m/s, 6.57×10^{-8} m/s and 7.84×10^{-8} m/s, respectively.

Table 4.7 Aquifer Tests on HY Wells and Well Information

Well Name	Elevation (m)	Formation	Top Level Filter(m)	Bottom Level Filter(m)	Average GWL Level (m)	Test Type	Method	Calculated K Values (m/s)	Average K Values (m/s)
HY-1	968.39	Asartepe	920.39	888.39	897.624	Slug T.	Falling head phase	Bouwer&Rice	1.47E-9
							Rising head phase	Hvorslev	2.1E-9
HY-2	957.85	Asartepe	925.85	893.85	Dry	-	Bouwer&Rice	9.01E-8	5.34E-8
							Hvorslev	1.2E-7	
HY-3	894.51	Schist	872.51	852.51	891.691	Pumping Test	Thesis	4.05E-8	9.55E-8
							Cooper&Jacob	1.37E-7	
HY-4	971.55	Asartepe	920.55	876.55	883.254	Slug T.	Thesis Recovery	1.09E-7	2.50E-9
							Bouwer&Rice	2.4E-9	
HY-5	893.88	Volcanics	865.88	833.88	865.378	Slug T.	Hvorslev	2.6E-9	6.99E-8
							Bouwer&Rice	3.37E-8	
							Hvorslev	3.95E-8	
							Bouwer&Rice	9.12E-8	
							Hvorslev	1.15E-7	
HY-6	935.95	Volcanics	907.95	839.95	913.448	Pumping Test	Thesis with Jacob	7.74E-8	9.22E-8
							Boulton	6.93E-8	
							Cooper&Jacob	1.16E-7	
							Neumann	9.18E-8	
							Thesis Recovery	1.06E-7	
HY-7	911.26	Schist	883.26	815.26	919.56	Free Flow Test	Rising Pressure	1.19E-8	
							Thesis	1.8E-7	
HY-8	917.35	Schist	890.35	870.35	915.001	Pumping Test	Cooper&Jacob	3.59E-7	
							Thesis Recovery	5.97E-7	
HY-9	888.215	Volcanics	836.215	720.215	806.136	Pumping Test	Thesis with Jacob	4.22E-9	4.56E-9
							Boulton	2.48E-9	
							Cooper&Jacob	7.99E-9	
							Neumann	4.62E-9	
							Thesis Recovery	3.47E-9	
HY-10	973.305	Volcanics	935.305	879.305	946.658	Pumping Test	Thesis with Jacob	6.50E-8	6.44E-8
							Boulton	3.49E-8	
							Cooper&Jacob	9.74E-8	
							Neumann	6.36E-8	
							Thesis Recovery	6.12E-8	
HY-11	1,128.835	Volcanics	1,076.835	936.835	962.014	Pumping Test	Cooper&Jacob	9.11E-8	
							Thesis Recovery	6.57E-8	

The evaluations of the aquifer tests performed on the 13 wells in the planned expansion areas within the scope of capacity increase are presented in Table 4.8. In order to investigate the hydraulic properties of the North Waste Rock Dump and leach pad separately, the wells drilled in the expansion areas were divided into 2 groups; minimum, maximum and geometric average values of the calculated hydraulic conductivity values are presented individually for both groups (Table 4.8). Furthermore, in this evaluation process, units tested for each group were also taken into consideration

Table 4.8 Calculated Hydraulic conductivity values (m/s) for the planned expansion areas

Location	Tested Units	Maximum	Minimum	Geometric Average	
Planned North Waste Rock Dump	Beydağı Volcanics	9.01E-07	4.56E-09	7.15E-08	7.45E-08
	Schists	9.54E-08	9.54E-08	9.54E-08	
Planned North Heap Leach Pad	Asartepe Form.	5.34E-08	2.50E-09	1.16E-08	7.29E-08
	Schists	2.61E-06	1.19E-08	1.83E-07	

In the deep wells drilled within the North Waste Rock Dump, initially, volcanic units were penetrated and later, basement rock of schist unit was entered. Six of the 7 wells (HY-5, HY-6, HY-9, HY-10, HY-11 and LP-5A) within this area represent the volcanic, while 1 of them (LP-4A) represents the schists. With respect to the 6 tests performed on the volcanic units, minimum, maximum and geometric average values of hydraulic conductivity were 4.56×10^{-9} m/s, 9.01×10^{-7} and 7.15×10^{-8} m/s respectively. According to the only test performed on the schist units, the calculated hydraulic conductivity value was 9.54×10^{-8} m/s. Evaluating all the test results together, the geometric average value of hydraulic conductivity (K) within the North Waste Rock Dump was calculated as 7.45×10^{-8} m/s.

It was observed that schists approach the surface in the North Heap Leach Pad and outcrops in these areas. Within the wells, it was observed that some of the schists were either covered with the Asartepe Formation or with volcanic units. Since the volcanic units covering the schists are very thin, the wells had to be filtered in the Asartepe Formation and schist unit. Aquifer tests were conducted to test these geologic units. In the North Heap Leach Pad area, 4 of the 7 wells (HY-3, HY-7, HY-8 ve LP-6) represent schists and 2 of them (HY-1 and HY-4) represent the Asartepe Formation. One of the wells drilled in the Asartepe Formation was found out to be dry. According to the tests performed on the Asartepe Formation, minimum, maximum and geometric average values of hydraulic conductivity were 2.50×10^{-9} m/s, 5.34×10^{-8} m/s and 1.16×10^{-8} m/s, respectively. For the schist unit, minimum, maximum and geometric average values of hydraulic conductivities were 1.19×10^{-8} m/s, 2.61×10^{-6} m/s, and 1.83×10^{-7} m/s, respectively. The geometric average value of hydraulic conductivity in the North Heap Leach Pad area was calculated as 7.29×10^{-8} m/s, considering all the test results from this region.

The graphical illustration of data given in Table 4.8 is displayed in Figure 4.8. As seen from the figure, in both sites, the hydraulic conductivity of schists was higher than both the

Beydağı Volcanics and Asartepe Formation. As mentioned in previous sections, the Asartepe Formation, having extensive outcrops east of the mining area in the Banaz River Basin and showing aquifer features due to high hydraulic conductivity (6.50×10^{-6} - 1.00×10^{-4} m/s), has low levels of conductivity due to the excessive amounts of clay units in this region. Figure 4.8 also shows that hydraulic features of the volcanic and schist units were very similar to each other in the planned expansion areas.

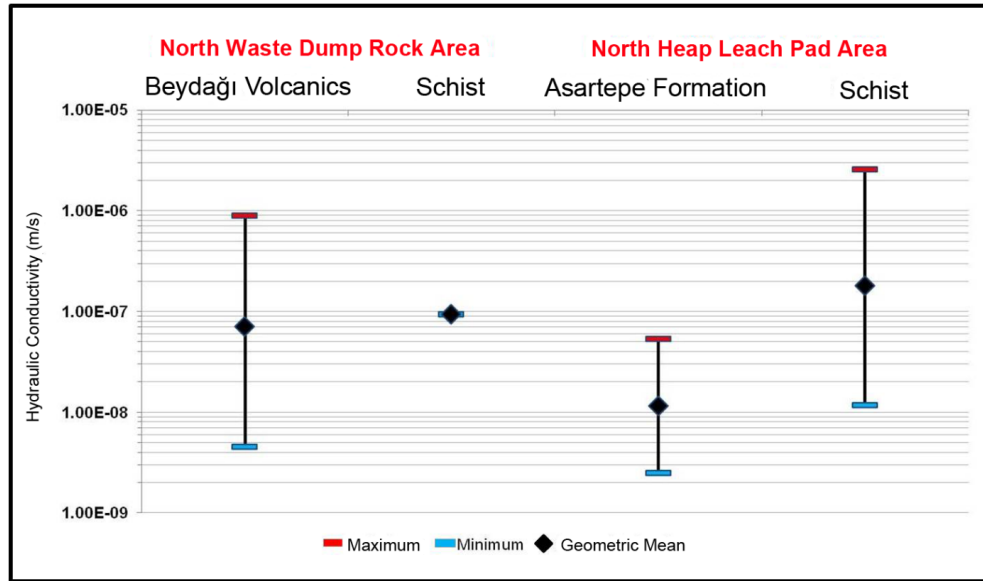


Figure 4.8 Calculated hydraulic conductivity values (m/s) for planned areas

4.3 Groundwater Levels

4.3.1. Spatial Variation in Groundwater Levels

As mentioned in previous chapters, the Kışladağ Gold Mine area is situated on the boundary that separates the Gediz and Büyük Menderes River Basins. Groundwater divide of the area is nearly in the same position. However, the study area is completely on the Gediz River Basin.

Areal distribution of groundwater levels are illustrated in Figure 4.9. According to this map, the maximum groundwater level (1020 m) was observed near the water divide located on the South Heap Leach Pad area. Since the southern area has a high elevation, it was concluded that the recharge amount around this area is naturally high. Moreover, the highest groundwater level was found to be nearly 960 m on the North Waste Rock Dump area due to a high recharge to the system. Towards the north, this level decreases to 810 m, and 920 m west of the North Waste Rock Dump area. For the North Heap Leach Pad area, groundwater levels decreased from 940 m to 870 m along the southeast-northwest direction. The hydraulic gradient was approximately 0.08 for the North Waste Rock Dump area, whereas this value was almost 0.03 for the North Heap Leach Pad.

A depth-to-groundwater level map of the study area was procured by subtraction of the topographic surface from the observed groundwater levels (Figure 4.10). By analyzing this map, it is explained that depth-to-groundwater level ranges from 200-250 for high elevations of the southwest area of the North Waste Rock Dump. Since the topographic elevation progressively decreases towards the north, it is seen that depth-to-groundwater levels also decrease and approaches the surface along the northeast and east of the Söğütlü Creek.

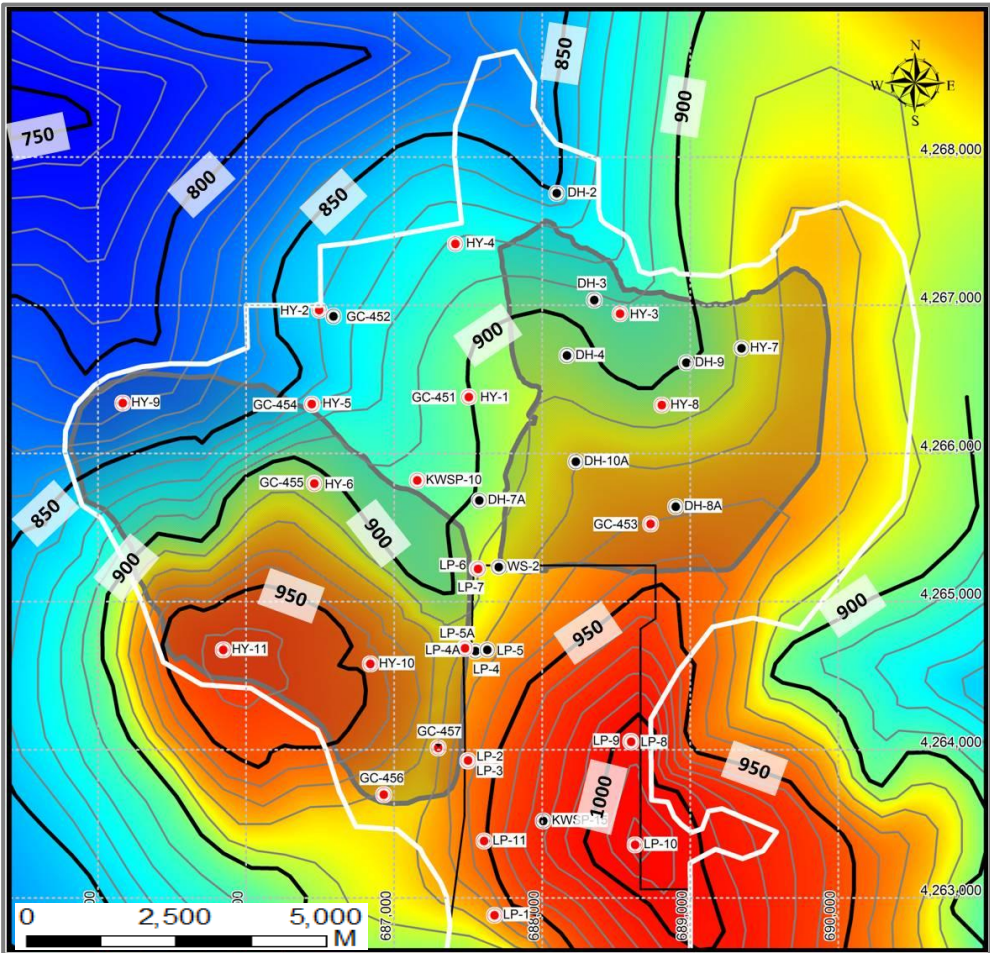


Figure 4.9 Groundwater level map in the study area (Yazıcıgil et al., 2013)

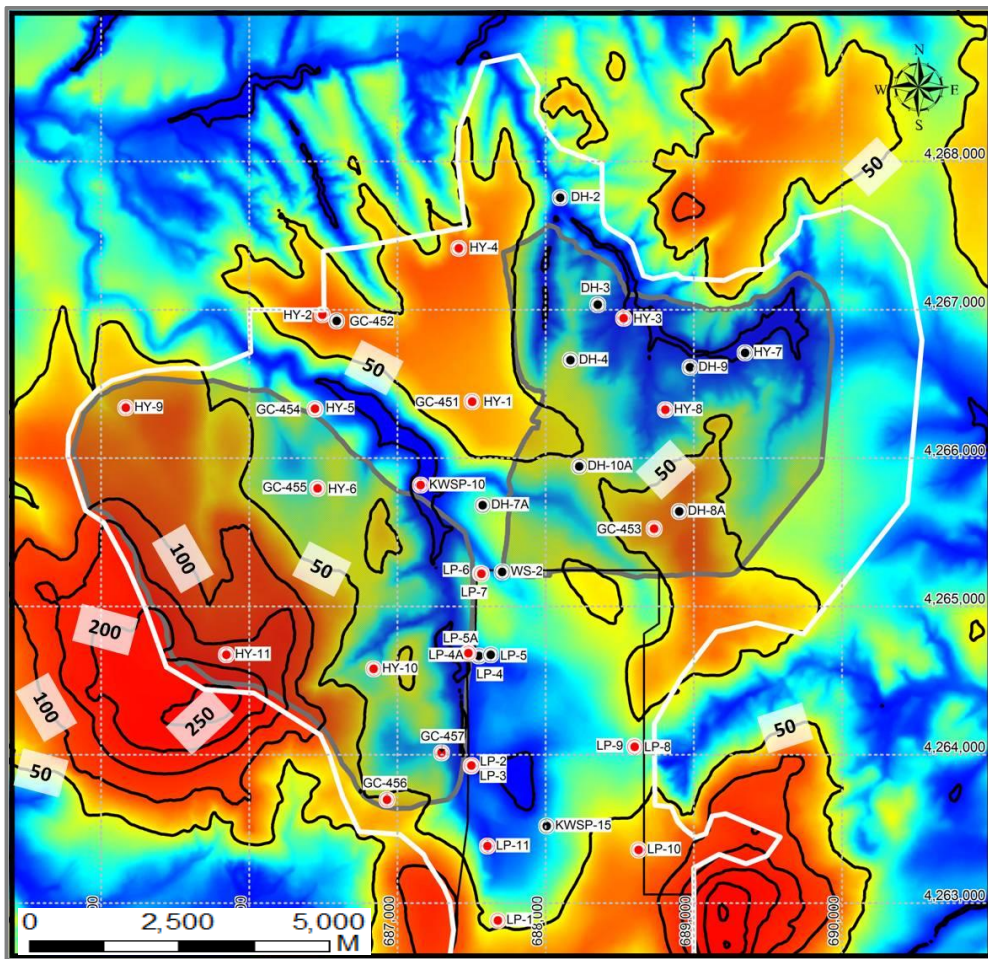


Figure 4.10 Depth to groundwater level map in the study area (Yazıcıgil et al., 2013)

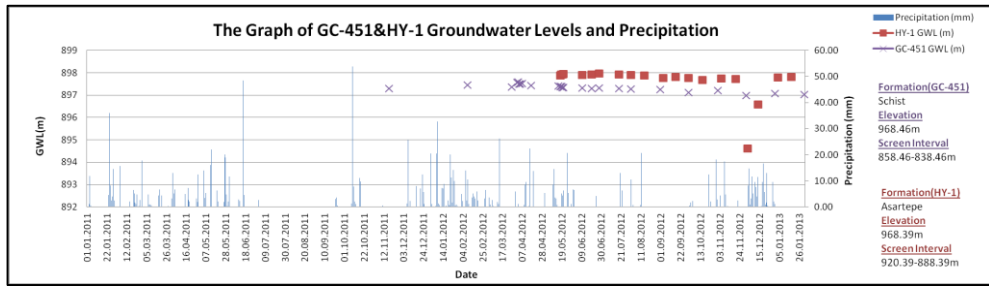
Temporal Variation in Groundwater Levels

As of 2011, within the mine expansion area, eight HY wells were drilled in order to determine its hydrogeological characterization, to observe the spatial distribution of water levels, and to observe water levels changes over time. Among these observation wells, the HY-2 well, which is completed in the Asartepe Formation, was discovered to be dry. Likewise, the HY-7 well, which was drilled in schists, was observed to be an artesian well displaying free-flow conditions. Considering the other six wells, the groundwater level was measured every two weeks. The graphs showing the measured temporal water level changes of the HY wells (and GC wells, which were drilled near the HY wells in different units) are presented in Figure 4.11.a and 4.11.f together with the measured temporal change of rainfall. In addition to these wells, HY-9, HY-10 and HY-11 wells were drilled in the North Waste Rock Dump in 2012; however, these wells have not yet yielded enough data to reveal the groundwater level changes over time.

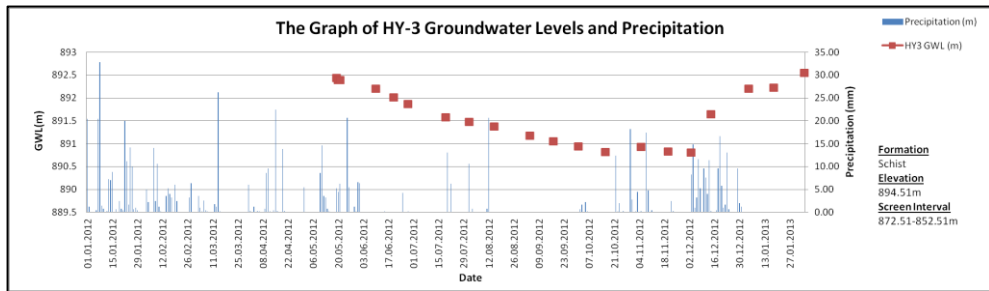
The HY-1 well was drilled near GC-451, which is screened in the schist unit in the mine expansion area, in order to investigate the groundwater levels in the Asartepe Formation and to observe the hydrological relations between the two units. Examining Figure 4.11.a, which shows water level changes over time for these two wells, it is observed that the difference between HY-1 and GC-451 groundwater levels is less than 1 meter. The studies also reveal that the water level in schists of this region was less than those in the Asartepe Formation.

Figures 4.11.b, 4.11.c. and 4.11.d represent the following wells, respectively: the HY3 well, drilled in schists; the HY-4 well, drilled in the Asartepe Formation; and the HY-8 well, drilled in volcanic units. Data from these wells were not collected in long enough periods to reveal the reaction of groundwater levels with seasonal rainfall. By examining Figures 4.11.b, 4.11.c. and 4.11.d, it is observed that these wells, which were drilled approximately at the same time and filtered in different formations, show similar water level trends. In all of these three wells, it was noted that groundwater levels decreased by 1-1.5 meter during the dry season and was followed by a rise in the wet season in response to recharge.

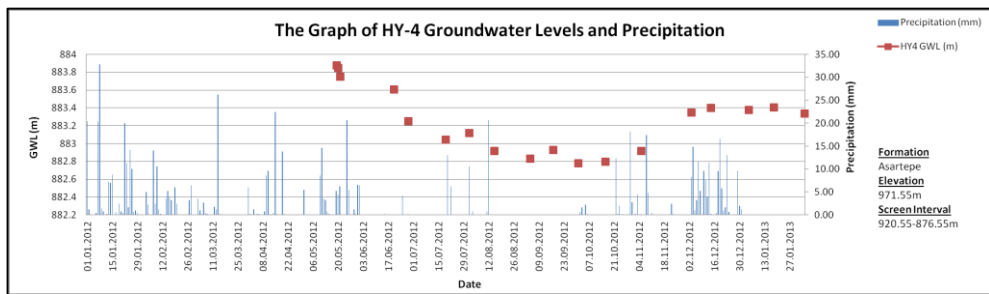
Figure 4.11.e. is a graph of water level changes over time for the HY-5 well, drilled in volcanic units, and the GC-454 well, screened in schist units near the HY-5 well. Similarly, the respective temporal water level changes of the HY-6 well (drilled in volcanic units) and the GC-455 well (screened in the schist unit near the HY-6 well) is presented in Figure 4.11.f. By examining these two graphs, it is observed that the difference between groundwater levels of volcanic and schists units is more than 100 meters. Since this is not observed in any other location, further investigation determined that groundwater levels of volcanic units are compatible with regional groundwater levels. However, as necessary and sufficient development cannot be performed in small diameter GC wells, groundwater levels of GC-454 and GC-455 wells were observed to be low, and it was concluded to be incompatible with regional groundwater levels. Therefore, data from GC-454 and GC-455 was not taken into consideration while defining the hydrogeological characterization of the region.



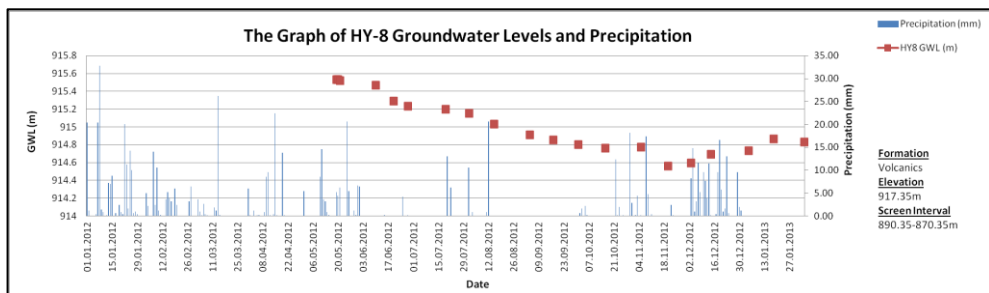
(a) Temporal Groundwater level changes of the HY-1 and GC-451 wells



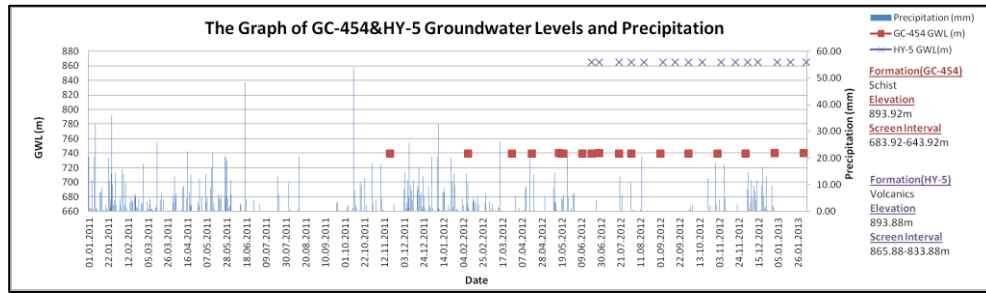
(b) Temporal Groundwater level changes of HY-3



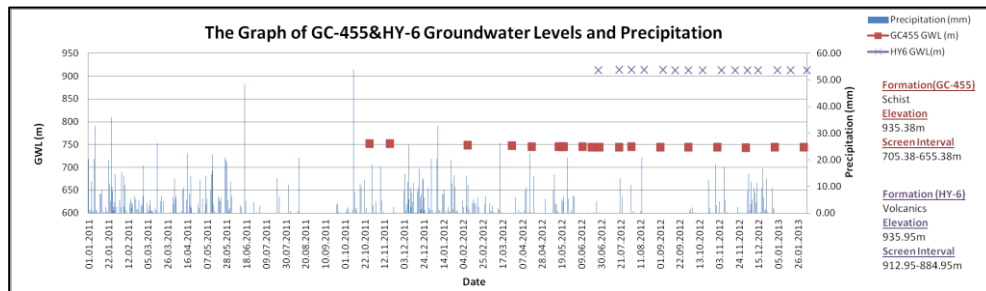
(c) Temporal Groundwater level changes of HY-4



(d) Temporal Groundwater level changes of HY-8



(e) Temporal Groundwater level changes of the HY-5 and GC-454 wells



(f) Temporal Groundwater level changes of the HY-6 and GC-455 wells

Figure 4.11 (a) Temporal Groundwater level changes of the HY-1 and GC-451 wells (b) Temporal Groundwater level changes of HY-3 (c) Temporal Groundwater level changes of HY-4 (d) Temporal Groundwater level changes of HY-8 (e) Temporal Groundwater level changes of the HY-5 and GC-454 wells (f) Temporal Groundwater level changes of the HY-6 and GC-455 wells (cont'd)

4.3.2. Hydrogeological Cross Sections

As the mining area of the Kışladağ Gold Mine will be expanded towards the north, detailed geology of region was also expanded. (ARC, 2011). In this part of the study area, outcrops of basement schist and gneiss, which are identified as the Eşme Formation, the unconformably overlying unit, the Beydağı Volcanics, and the Asartepe formation and quaternary units are seen (Figure 4.14 – Figure 4.17). Furthermore, in order to produce a detailed hydrogeological characterization of the expansion area, numerous wells have been drilled since 2011. Detailed information about these wells is given in part 4.2.2.1. Hydrogeological sections were produced with the help of new information, which was provided by newly drilled wells (Figure 4.14 – Figure 4. 17). Cross section lines and the location of wells in these sections were produced in a geological map in Figure 4.12. Figure 4.13, shows cross section lines in a groundwater level map.

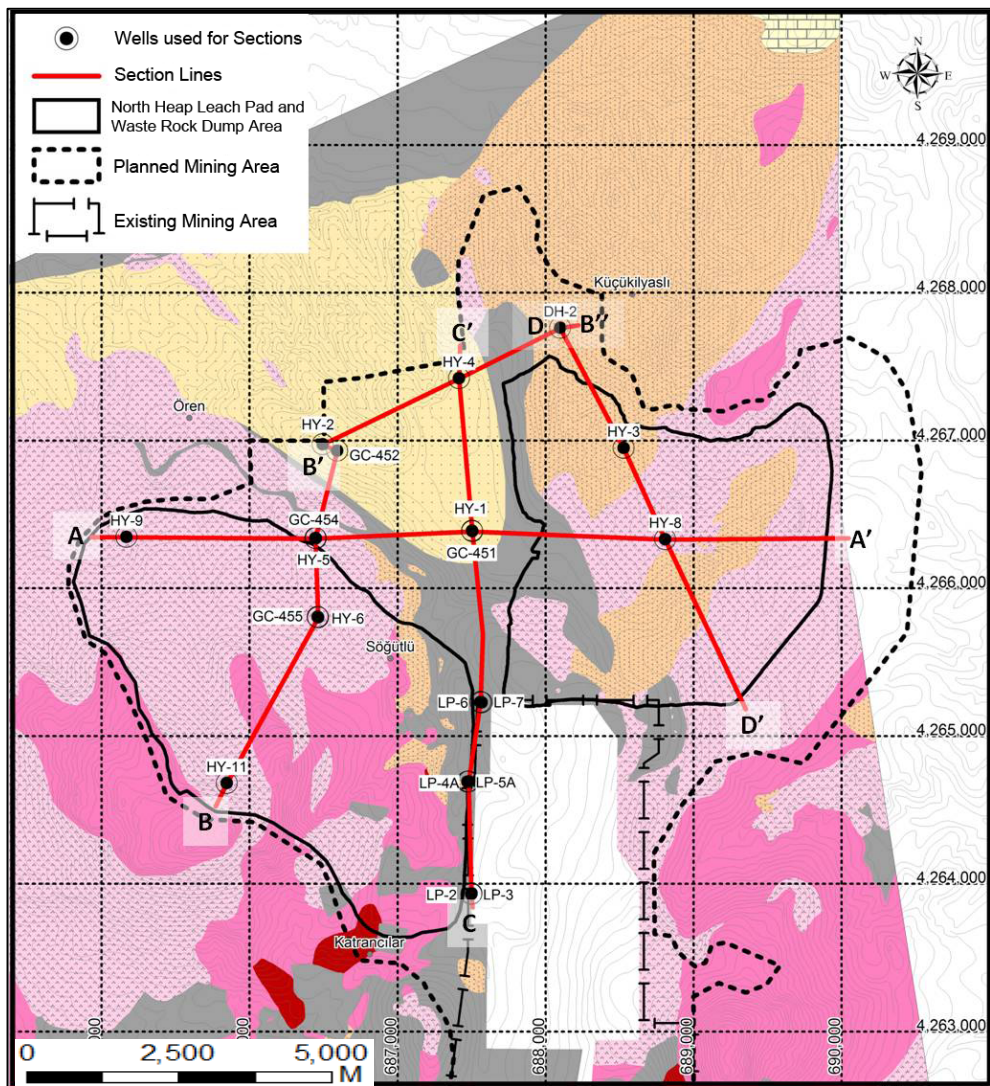


Figure 4.12 Direction of hydrogeological sections for the extension areas

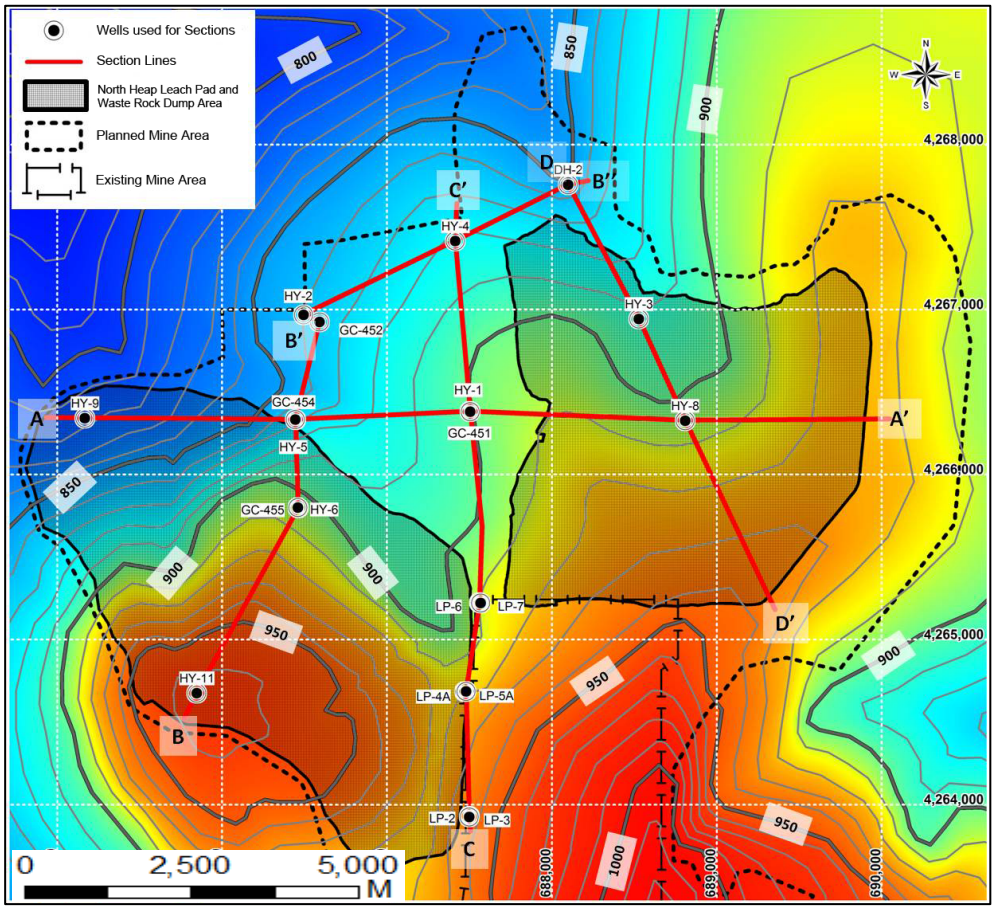


Figure 4.13 Direction of hydrogeological sections and groundwater levels (Yazıcıgil et al., 2013)

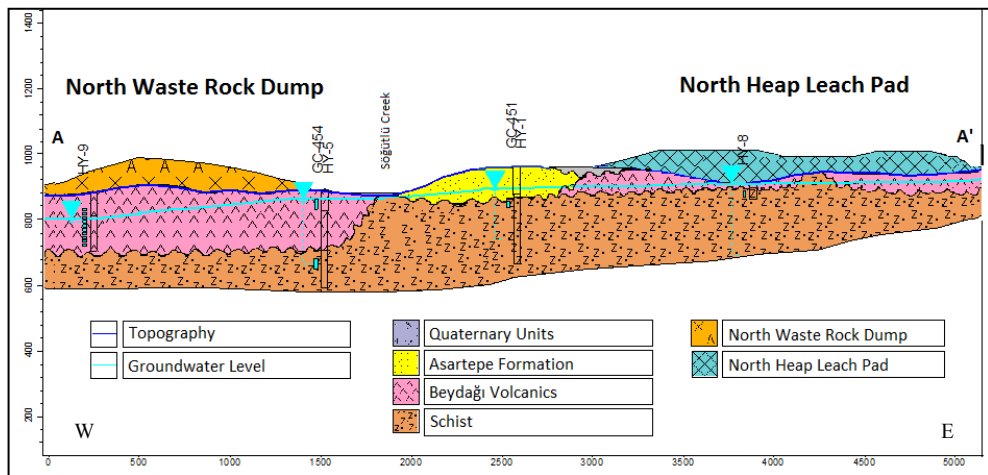


Figure 4.14 Hydrogeological cross section of AA'

A depth-of-water table indicates a decrease towards the east and a convergence towards the surface in the north heap-leach pad, and is about 80 m in the North Waste Rock Dump area. In Figure 4.14, it can be seen that this table, which is about 810 m towards the west part of the section (point A), is increasing throughout towards the eastern direction and reaches 920 m in point A'. It can be seen that the flow direction of ground water in this section is from the North Heap Leach Pad moving towards to the North Waste Rock Dump area, while the hydraulic gradient increases in this same direction.

The hydrogeological cross-section given in Figure 4.14 passes through the north of the planned waste rock dump and the middle of the planned heap leach pad areas along the West-East direction, as shown on Figure 4.13. This cross-section along the A-A' line, is drawn using the data from the boreholes located along this line, namely HY-9, GC-454, HY-5, GC-451, HY-1 and HY-8. As it may be seen from this figure, at the north waste rock dump area, basement schists are overlain by volcanics having almost 200 m of thickness; while schists are either very close to the surface or even outcropping in the vicinity of the north heap leach pad area.

Depth to water table, which is around 80 m at the north waste rock dump area, decreases toward east, where it comes very close to the surface at the north heap leach pad area. As shown in Figure 4.14, groundwater levels are at around 810 m at the western end of the section (north waste rock dump area) and increases eastwards reaching to elevations of around 920 m at the western end of the section (north heap leach pad area). Moreover, it is observed that groundwater flow is directed from the north heap leach pad area towards the north waste rock dump area, with an increasing hydraulic gradient.

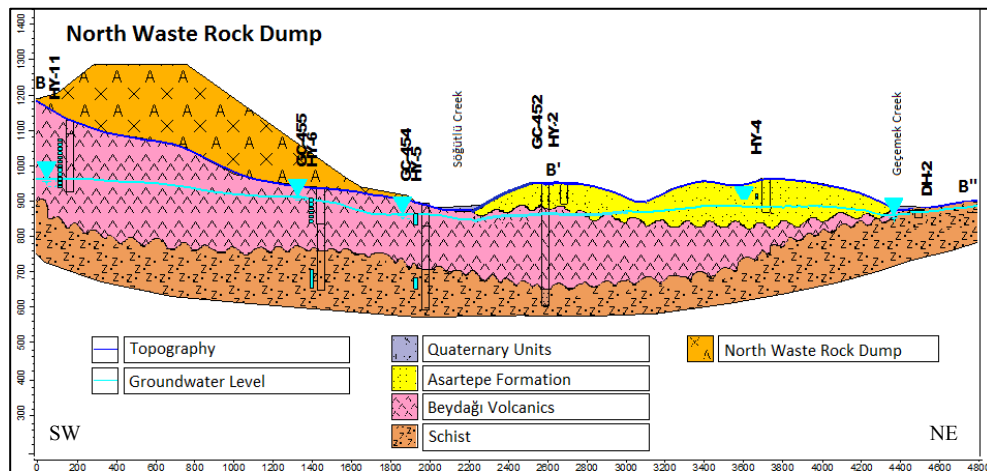


Figure 4.15 Hydrogeological cross section of BB'B''

Figure 4.15 shows the cross-section passing through the BB'B'' line, on which following wells are located: HY-11, GC-455, HY-6, GC-454, HY-5, GC-452, HY-2, HY-4 and DH-2. This section passes through the middle of the planned north waste rock dump area in the SW-NE direction and reaches very close to the northwestern boundary of the planned operation areas. This figure also demonstrates that the planned north waste rock dump area is situated on top of the volcanics having thickness of around 300 m.

Depth to water table is around 160 m at the topographically highest point of the north waste rock dump area (HY-11), while it is very close to the surface in the vicinity of the Söğütlü Creek flowing along the northeastern boundary of the planned waste rock dump area. At the northern side of this valley, depth to groundwater reaches to 80 m. As can be noted from Figure 4.15, along this section, one of the two wells drilled in Asartepete Formation is dry (HY-2 extending to a depth of 68 m), while at the other one (HY-4 extending to a depth of 102 m), depth to groundwater is 81 m. At DH-2 well located at the northeastern end of this cross-section, which is topographically lower, groundwater table is very close to the surface.

Groundwater elevation at HY-11, which is located at the planned north waste rock dump area, is around 960 m. Elevation of the water table declines towards Söğütlü Creek and rises again on the other side of the valley reaching 880 m at HY-4. As it can also be noted from Figure 4.15, this suggests a groundwater flow towards the Söğütlü Creek. When groundwater elevation reach 880 m at HY-4, it is compared to that of DH-2 well (862 m), it can be stated that there is also groundwater flow towards the valley feeding the Geçemek Creek.

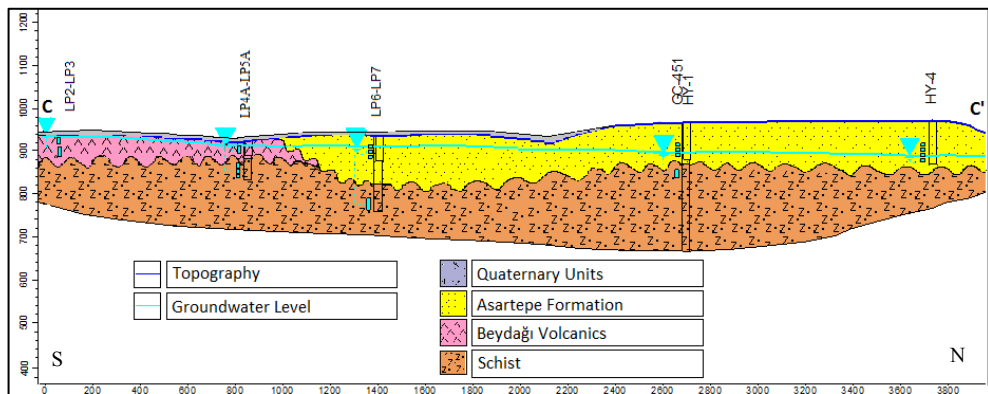


Figure 4.16 Hydrogeological cross section of CC'

Hydrogeological cross-section CC' given in Figure 4.16 passes through the western boundary of the present heap leach pad area (through wells LP-2, LP-3, LP-4A, LP-5A, LP-6, LP-7) and extends to northwards (to GC-451, HY-1 and HY-4). Along this S-N oriented section, basement schists are overlain by the volcanics at the south (around the present heap leach pad area), while they are overlain by the Asartepe Formation at the north; and all these units are covered by a thin layer of alluvium along the valley extending in the NS direction. At this locality, hydraulic conductivity of the Asartepe Formation is low due to its clay content.

Around the southern end of the section, artesian flow conditions are observed at the wells drilled in volcanic units (LP-2 and LP-3). At the wells drilled in Asartepe Formation, depth to water table increases northwards and reaches to 80 m along the section. As it may be noted from Figure 4.13, groundwater elevation decreases northwards from 940 m 880 m, along this section having an approximate length of 3.8 km.

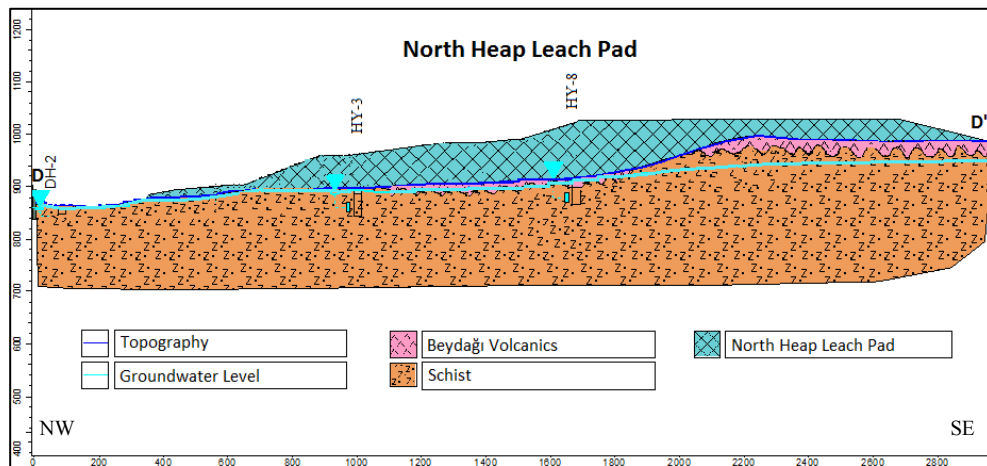


Figure 4.17 Hydrogeological cross section of DD'

Figure 4.17 shows the cross-section passing through the DD' line extends in NNW-SSE direction from the middle parts of the planned north heap leach pad area. Along this section, three wells are located (DH-2, HY-3 and HY-8). As shown in Figure 4.17, basement schists are either locally overlain by a very thin layer of volcanics, or outcrops.

It can be noted from Figure 4.17 that groundwater contained in the schists is very shallow. Especially, at the topographically low northern parts, water table is very close to the surface; therefore artesian flow conditions are expected at the wells that would be drilled along the valley. Figure 4.13 indicates that southern end of the section is located on the groundwater divide and groundwater level is around 930 m, which decreases northwards along the section and reaches to 850 m.

CHAPTER 5

HYDROCHEMISTRY AND WATER QUALITY

5.1 Available Data

While evaluating the study area with respect to hydrochemistry and water quality, the monthly data obtained from field observations were used. Table 5.1 shows the location of observation points and data measurements according to year.

Table 5.1 Yearly distribution of data belonging to observation point locations (Yazıcıgil et al., 2013)

Observation Point ID	2000	2001	2002	2003	2004	2005	2006	2007	2008	2009	2010	2011	2012
HY -1													2
HY-3													3
HY-4													1
HY-5													3
HY-6													3
HY-7													1
HY-8													2
HY-9													1
HY-10													1
HY-11													1
KWSP-2	10	12	12	12	12	5							
KWSP-9		12	12	12	12	11	11	6					
KWSP-10			12	12	12	12	12	12	11	12	12	12	12
LP-4												3	4
LP-4A													8
LP-5												3	4
LP-5A													8
LP-6												1	12
LP-7												1	12
WEIR-2			7	8	7	11	10	8	9	11	9	10	12
WEIR-6												1	3

According to the major ions analysis, the mean value of ionic charge balance error of whole data was 4.92%. The mean errors for each observation points are given in Table 5.2. Generally, ionic charge balance error was less to or around 5%. Therefore, it can be said that the quality of major ions analysis is relatively high and the data was suitable for this evaluation. There was only one sampling for the HY-5 and HY-7 wells, which determined an error slightly more than 10%.

Table 5.2 The mean ionic charge balance error of observation points (Yazıcıgil et al., 2013)

Observation Point ID	%Mean Ionic Charge Balance Error
HY -1	3.3
HY-3	2.1
HY-4	6.9
HY-5	10.1
HY-6	4.5
HY-7	11.0
HY-8	3.5
HY-9	8.2
HY-10	0.4
HY-11	9.0
KWSP-2	7.3
KWSP-9	9.0
KWSP-10	4.6
LP-4	1.6
LP-4A	5.1
LP-5	2.5
LP-5A	5.8
LP-6	1.6
LP-7	1.5
WEIR-2	3.9
WEIR-6	1.5

While evaluating the data, the minimum detection limit of the measurement was considered as long as the measurement did not exceed a Class I value of Inland Water Classification. If it is higher than the Class I values, then the data was not included in the evaluation. The maximum detection limits, $\text{NO}_2 > 0.1$ and $\text{NH}_4 > 0.8$ were considered for the evaluation.

5.2. Surface Water Hydrochemistry

5.2.1 Observation Points

Within the mine area and its vicinity, there are a total of 8 surface water points for the hydrochemical investigation. The northern expansion area contains 2 of them: Weir-2 and Weir-6. Some information about these surface water observation points is presented in Table 5.3.

Table 5.3 Location information of surface water quality points (Yazıcıgil et al., 2013)

Observation Point ID	LATITUDE	LONGITUDE	TYPE	DESCRIPTION	Observation Start time
Weir-2	687293	4265228	Surface Water	Weir	May.02
Weir-6	688074	4267785	Surface Water	Weir	Dec.11

5.2.2. The Characteristic Value Determination of Surface Waters

The characteristic value of water quality parameter for the observation point is the value that does not exceeds a probability of 95%. In order to determine the characteristic value of a pre-mining period, statistical methods given by the Management of Surface Water Quality Regulation (YSKY) (2012) were used considering specific limitations. According to the regulation, if there are 10 sample data taken from different days for the first 3 years, then the Hazen method should be used to evaluate the data. If the sample data is more than 19, then the suggested method is the Weibull method. If the observation period is more than 3 years, then a logarithmic method is practiced. Minimum and maximum are two characteristics determined by quality classification of the lower limit values of oxygen and the lower/upper limit values of ph parameters. In addition, the Weibull method was used for the determination of the lower limit values (Table 5.5).

In order to specify the characteristic values for the pre-mining period, the data belonging to the period up to May 2006 were used. There is only one observation point, Weir-2, covering this period in the study area. Determination of the characteristic value was not performed for the other observation point, Weir-6, because it's operational period began in 2011. The method, data amount and operational period of Weir-2 used for determining its characteristic value is given in Table 5.4.

Table 5.4 Information of the surface water point for the determination of characteristic value (Yazıcıgil et al., 2013)

Observation Point ID	Data Number	Monitoring Year Number	First Used Data Date	Last Used Data Date	Applied Method
WEIR-2	38	5	May.02	May.06	LOG

Table 5.5 The lower and upper limit characteristic values of the surface water point (Units: mg/l, EC:µS/cm) (Yazıcıgil et al., 2013)

WEIR-2	
LOG METHOD	
Al	3.719
As	0.027
Ba	0.1329
Ca	144.6
Cd	0.0007
Cl	40.89
CN	0.0113
Co	0.0054
CO3	4.2
EC	1143.8
Cr	0.007
Cu	0.006
F	0.4
Fe	2.136
HCO3	144.8
Hg	0.00028
Mg	33.2
Mn	0.4632
Na	45.3
Ni	0.0117
N-NO3	2.588
NH4	0.361
NO2	0.026
O2*	4.2-13.9
Pb	0.0115
Ph*	6.80-8.42
P	0.13
Se	0.0017
SO4	569.8
TDS	997.9
TSS	849.2
Zn	0.7

5.2.3. Hydrochemical Evaluation

By using the characteristic value and geometric mean of data belonging to the mining period, surface water quality facies were determined and are illustrated in Figure 5.1 and Figure 5.2. According to the characteristic value of Weir-2, including streams across the Open Pit, the South Heap Leach Pad, and the North Waste Rock Dump, the water facies was determined as Ca-SO₄.

According to the geometric mean of data belonging to the mining period, the facies of Weir-2 are similar to those from the pre-mining period. The water facies of Weir-6, draining the North Heap Leach Pad area, was determined as Ca-HCO₃.

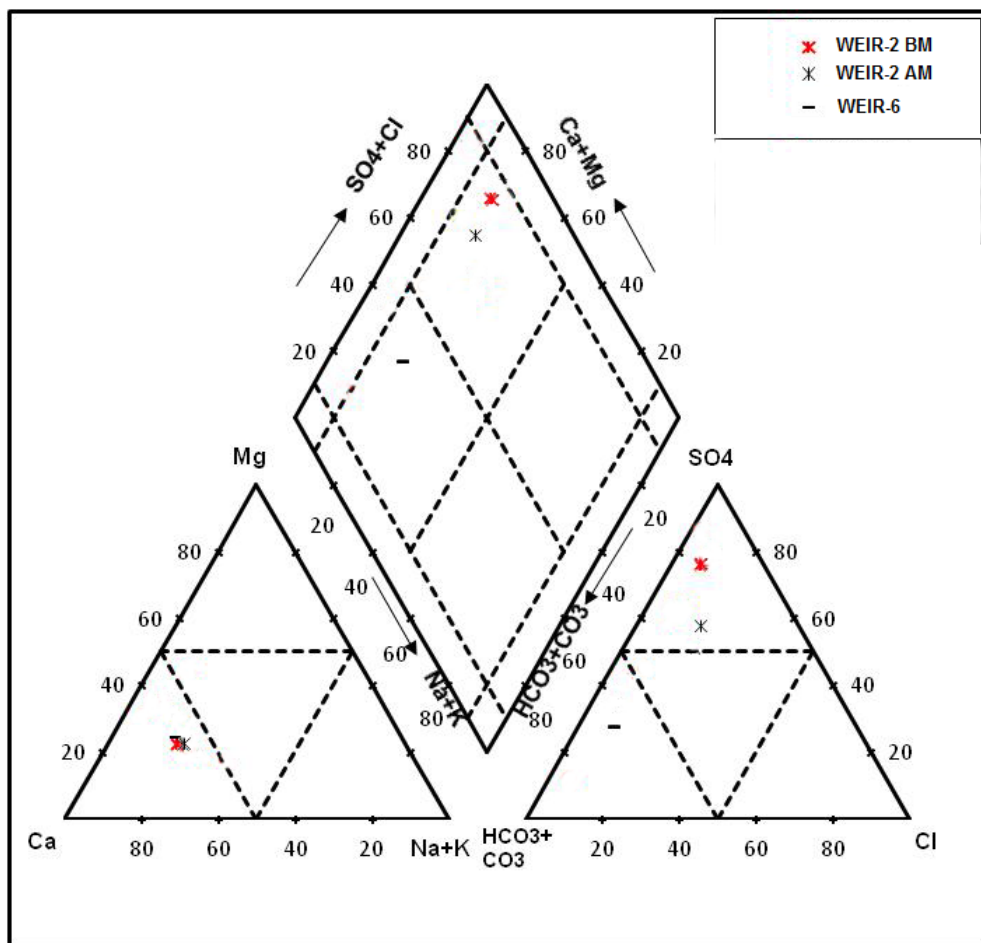


Figure 5.1 The distribution of the major ion concentration of the characteristic value (BM) and geometric mean of data (AM) of surface water in a Piper Diagram

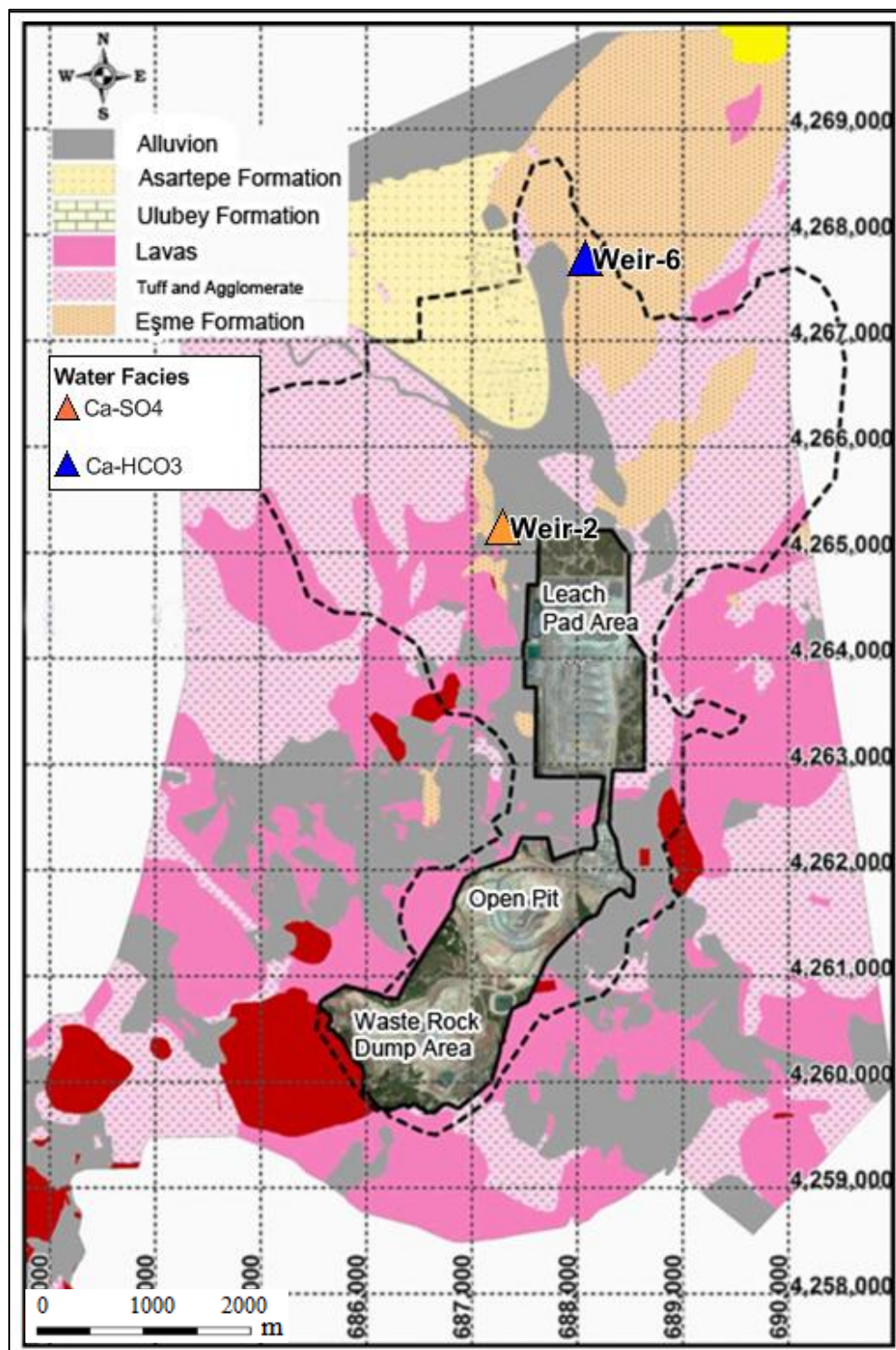


Figure 5.2 Facies distributions of surface waters in the mining period

5.3. Groundwater Hydrochemistry

5.3.1. Springs and Fountains

Observation Points

Although there are 3 springs and 8 fountains in the existing mine area for hydrochemical observation, only 2 fountains are located in the northern expansion area: KWSP-2 and KWSP-9. The location of the observation points are presented in Table 5.6. and shown in Figure 5.3.

Table 5.6 The location information of KWSP-2 and KWSP-9 (Yazıcıgil et al., 2013)

Obs. Point ID	LATITUDE	LONGITUDE	TYPE	FORMATION	DESCRIPTION	Obs. Start	Obs. Finish
KWSP-2	687424	4265662	Fountain	Volcanoclastics	North west of south heap leach pad area	Mar.00	Dec.04
KWSP-9	687550	4264809	Fountain	Volcanic	North of south heap leach pad area	Jan.01	Jun.07

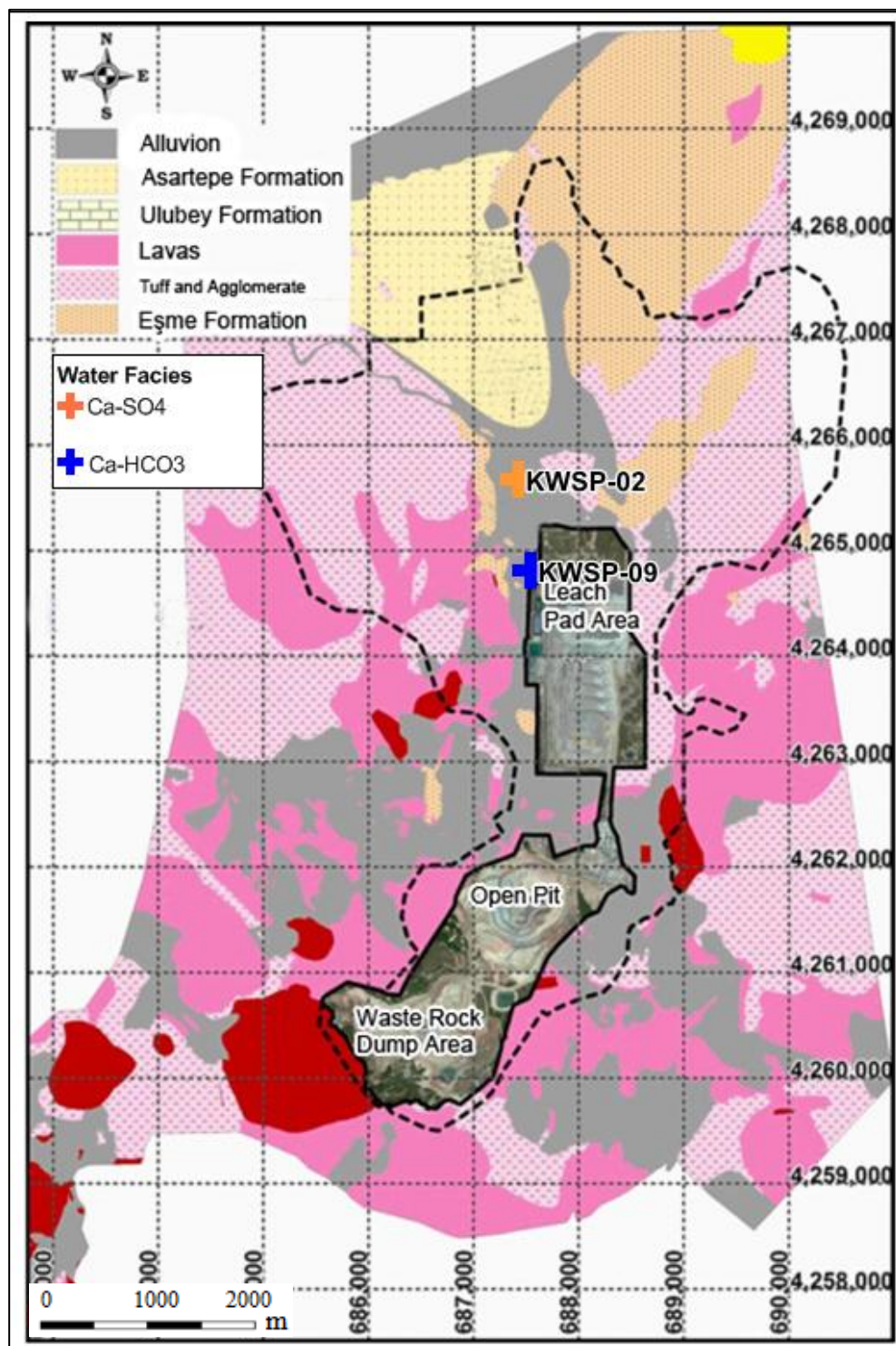


Figure 5.3 The groundwater quality observation locations of the fountains and their facies distribution of mean concentration

Hydrochemical Evaluation

The facies distributions determined by considering the geometric mean of major ion concentration values of KWSP-2 and KWSP-9 is presented in Figure 5.4, and their distributions in the study area are shown in Figure 5.3.

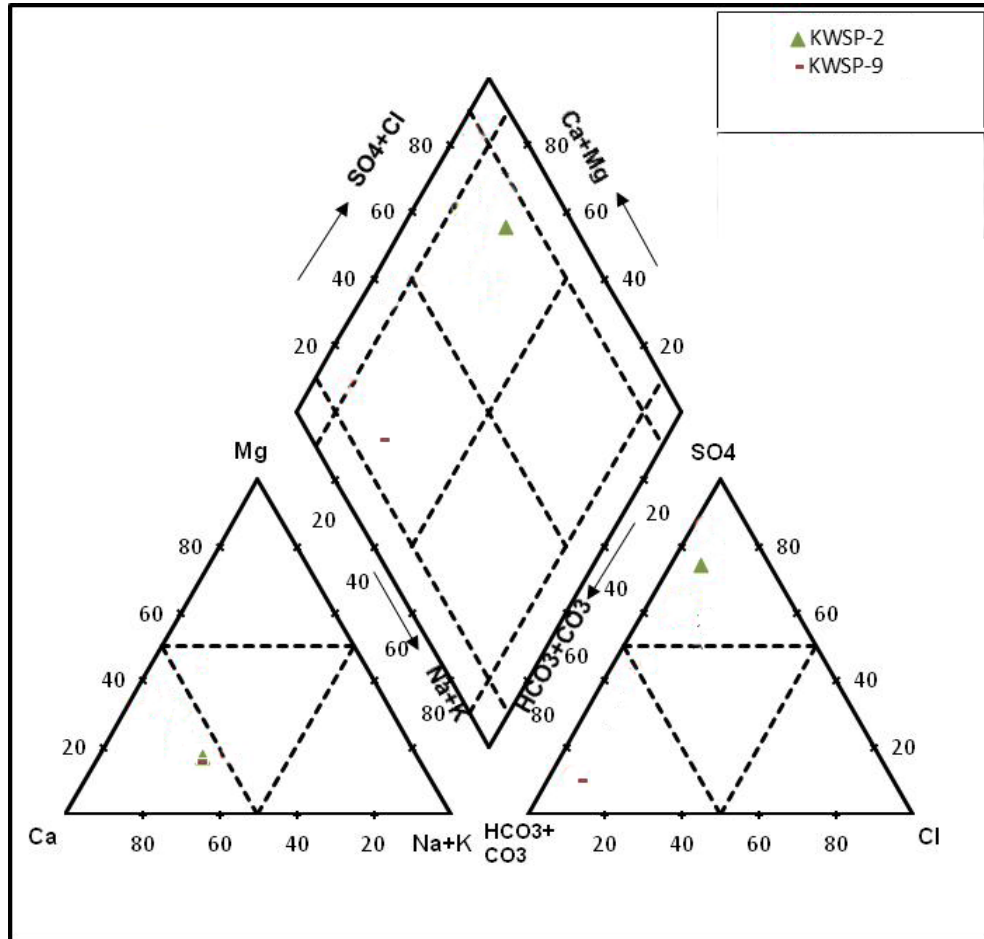


Figure 5.4 The facies distributions determined by considering the geometric mean of major ion concentration values of KWSP-2 and KWSP-9 in a Piper Diagram

The fountains, KWSP-2 and KWSP-9, in the study area are separated into two water facies according to their formations. KWSP-2 originated from volcanoclastic units is in CaSO_4 facies, while KWSP-9 originated in the volcanic rocks is in Ca-HCO_3 facies.

5.3.2. Wells

Observation Points

Hydrochemical observations in the mine area and its vicinity are conducted on 17 wells: 6 were drilled in schists of the Eşme Formation; 7 in the Beydağı Volcanics; 3 in the Asartepi Formation; and 1 drilled in both the Beydağı Volcanics and schists of the Eşme Formation. Table 5.7 provides location information of the wells, and their distributions in the area are shown in Figure 5.5.

Table 5.7 Location Information of the Observation Points (Yazıcıgil et al., 2013)

Observation Point ID	LATITUDE	LONGITUDE	UNITS	Observation Start time	Observation Finish time
HY-1	687504	4266387	Asartepe (Cong., Sands.)	Jun.12	-
HY-4	687415	4267418	Asartepe (Cong., Sands.)	Jun.12	-
LP-7	687568	4265225	Asartepe (Cong., Sands.)	Dec.11	-
HY-5	686448	4266335	Beydağı (Volcanoclastics)	Jun.12	-
HY-6	686463	4265801	Beydağı (Volcanoclastics)	Jun.12	-
LP-5	687630	4264678	Beydağı (Volcanic brec.)	Oct.11	Apr.12
LP-5A	687481	4264689	Beydağı (Volcanic brec.)	May.12	-
HY-9	685169	4266344	Beydağı (Volcanic)	Nov.12	-
HY-10	686841	4264583	Beydağı (Volcanic)	Nov.12	-
HY-11	685847	4264679	Beydağı (Volcanic)	Nov.12	-
HY-3	688528	4266947	Eşme (Schist)	May.12	-
HY-7	689347	4266714	Eşme (Schist)	Jun.12	-
HY-8	688809	4266330	Eşme (Schist)	May.12	-
LP-4A	687473	4264687	Eşme (Schist)	May.12	-
LP-6	687561	4265227	Eşme (Schist)	Dec.11	-
LP-4	687550	4264670	Beydağı (Volcanoclastics)+ Eşme (Schist)	Oct.11	Apr.12
KWSP10	687158	4265822	Eşme (Schist)	02	-

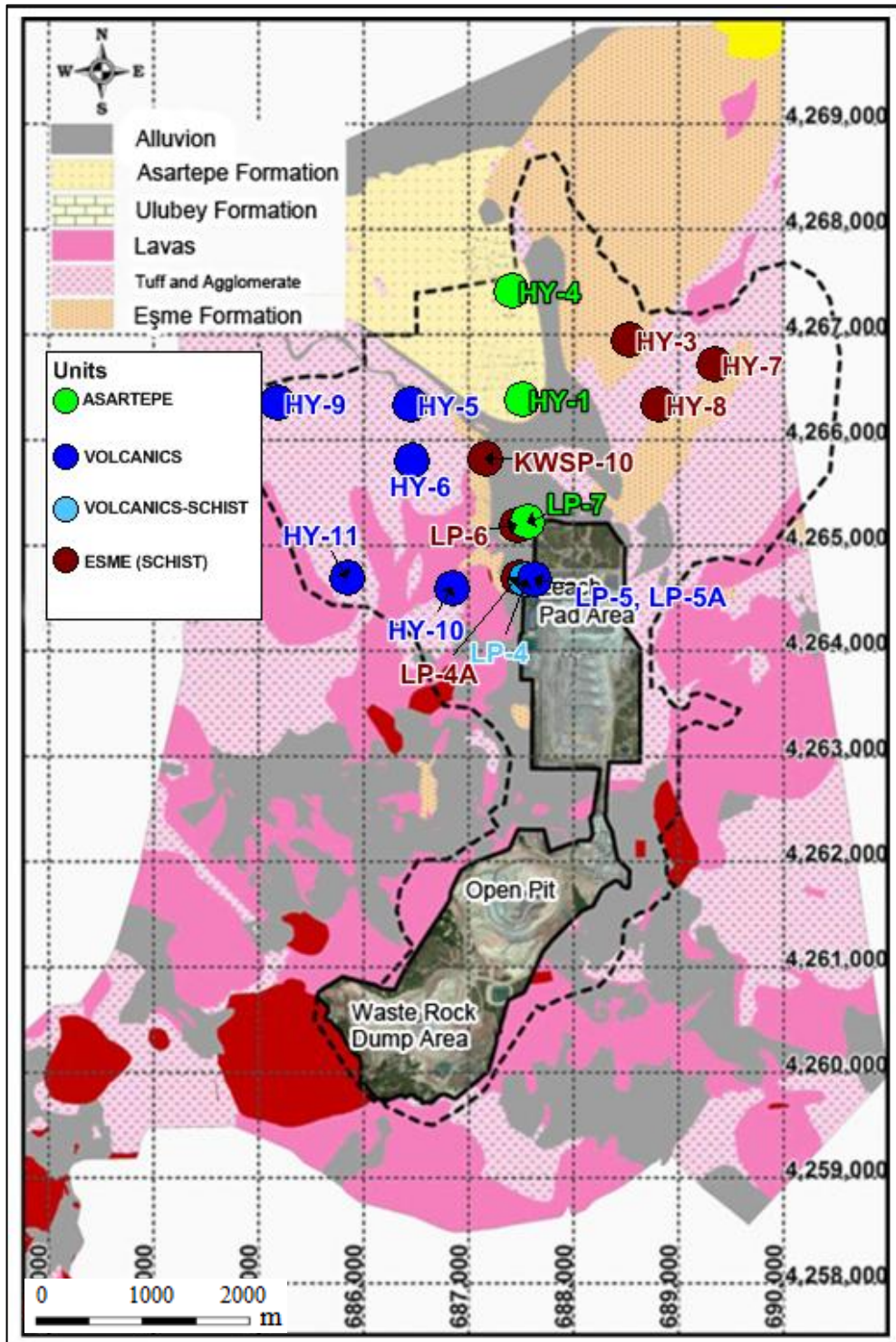


Figure 5.5 Well Distribution for Groundwater Quality Observation

Hydrochemical Evaluations of the Schist Unit

The water facies of the schist unit were determined by considering the geometric mean of the major ion concentration from data obtained from the wells (Figure 5.6). Figure 5.7 shows the distribution of the facies in the study area.

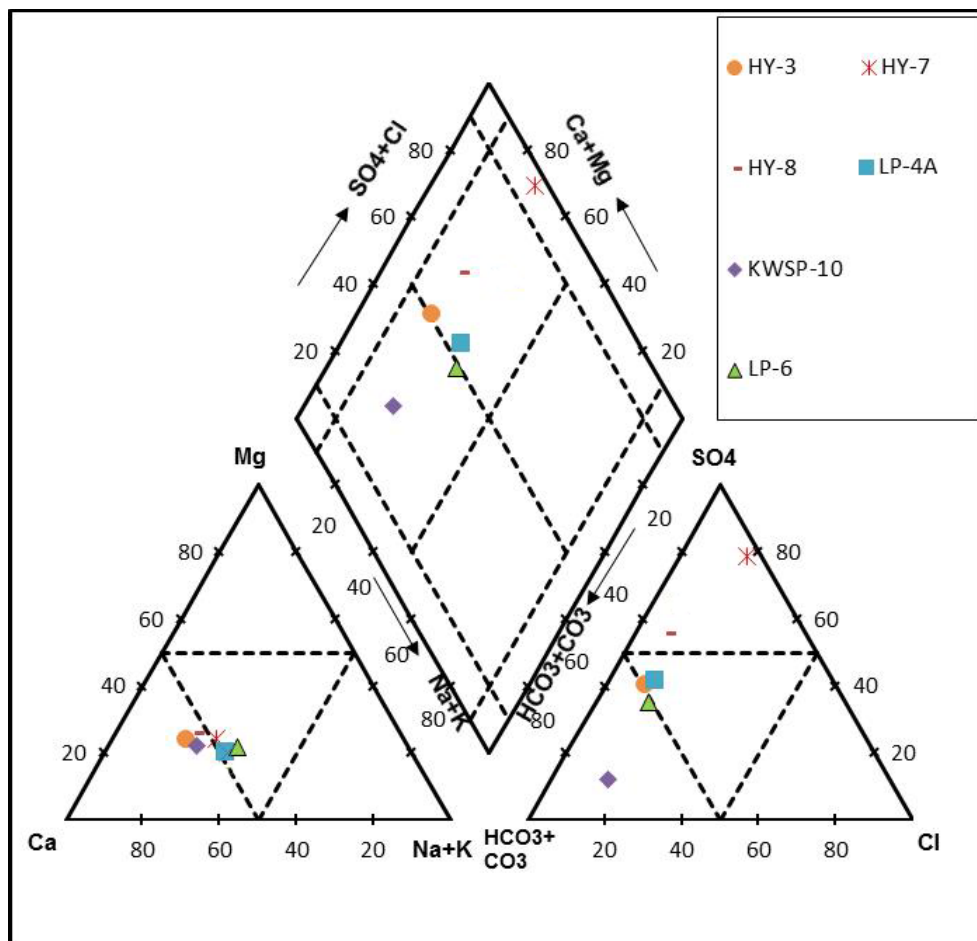


Figure 5.6 The facies distributions determined by considering the geometric mean of major ion concentration values of the schist unit in a Piper Diagram

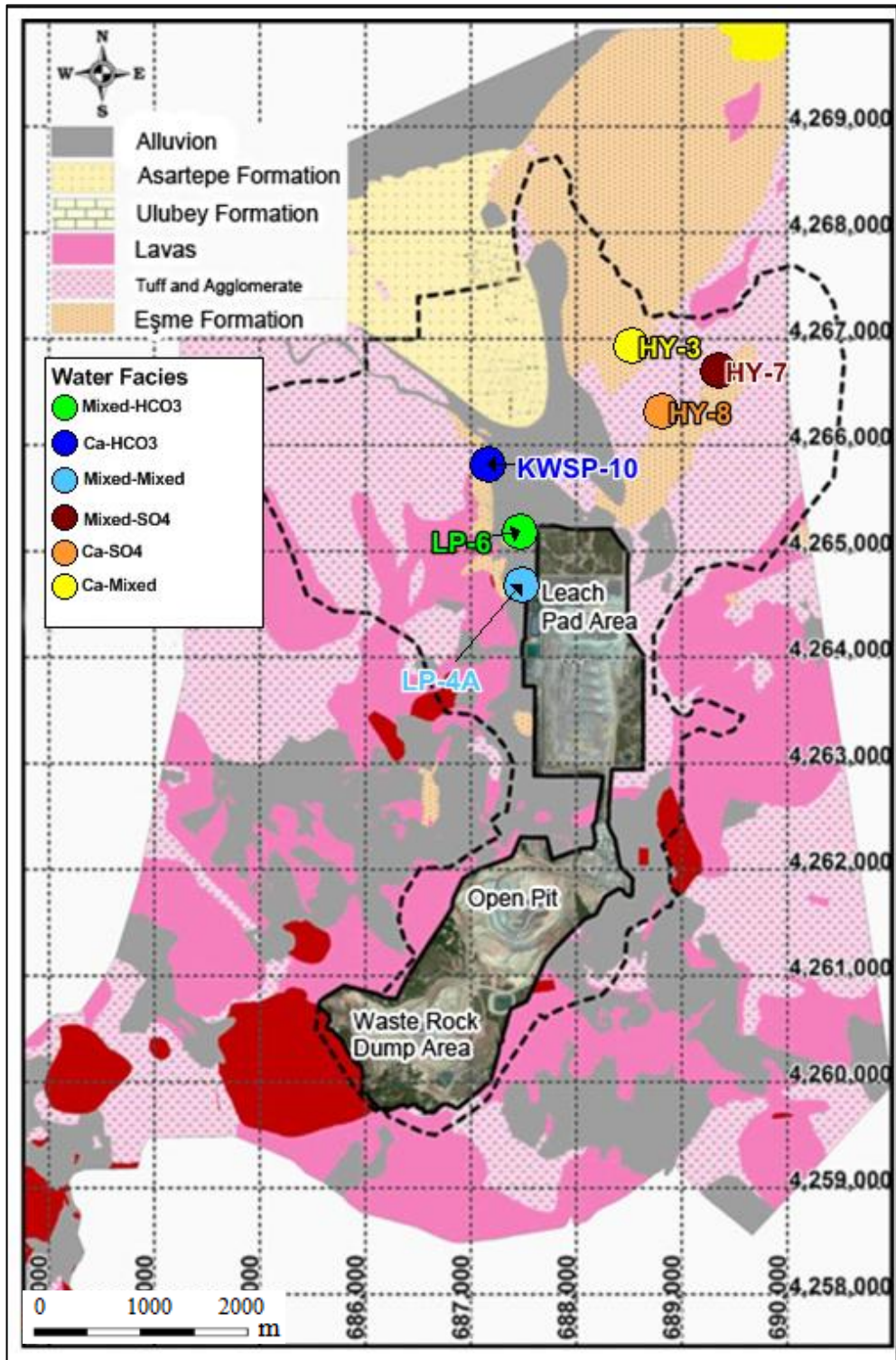


Figure 5.7 The groundwater facies distribution of mean concentration of the schist unit

The groundwater of the schist unit has the major cation as Ca, or mixed type, and the major anion that varies between HCO_3 and SO_4 . Evaluations of the facies of each well separately indicates the following: the KWSP-10, in the northeast part of the North Waste Rock Dump area, is Ca- HCO_3 ; LP-6, in the northwest of the South Heap Leach Pad area, is mixed- HCO_3 ; LP-4 is mixed-mixed; in the North Heap Leach Pad area, HY-7 is mixed- SO_4 ; HY-3 is Ca-mixed; and lastly HY-8 is Ca- SO_4 .

Hydrochemical Evaluations of the Volcanic Unit

Water facies of wells in the volcanic unit, and in both the volcanic and schist units, were determined by considering the geometric mean of major ion concentration of the data obtained from these wells (Figure 5.8). Figure 5.9 shows the distribution of the facies in the study area.

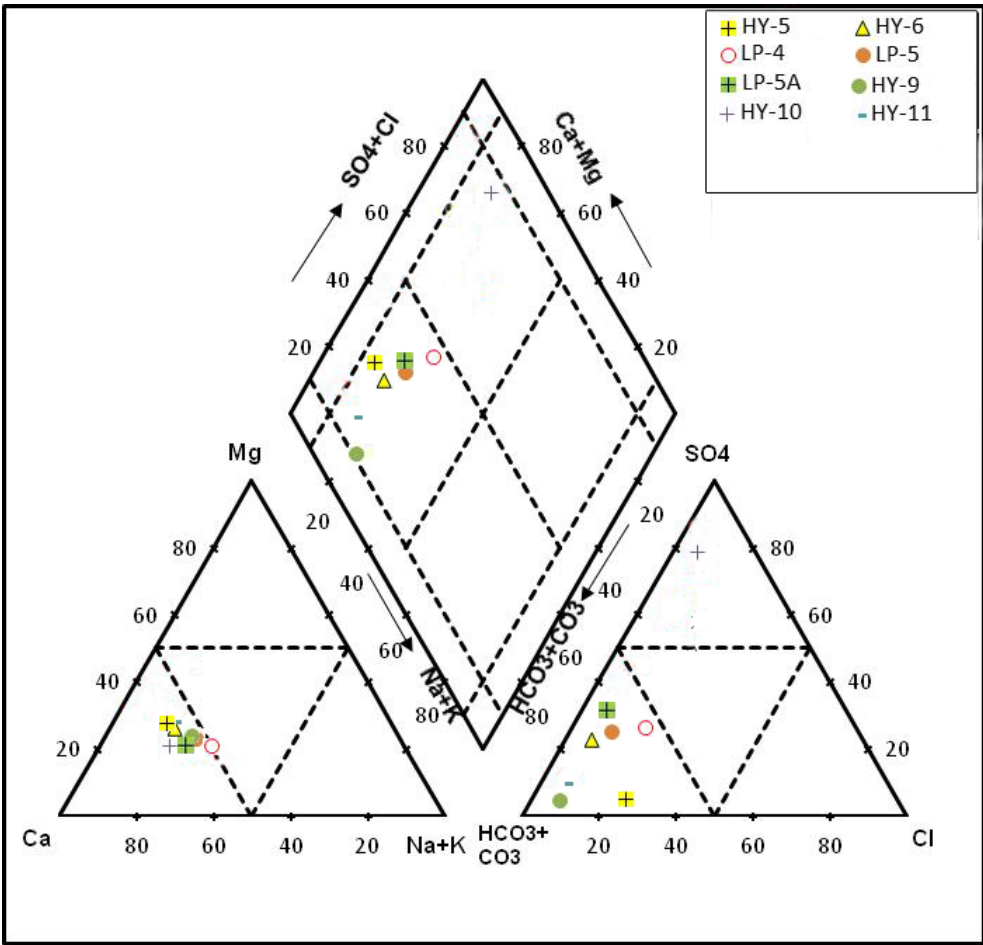


Figure 5.8 The facies distributions determined by considering the geometric mean of major ion concentration values of the Volcanic unit in a Piper Diagram (the LP-4 well in both volcanic and schist units)

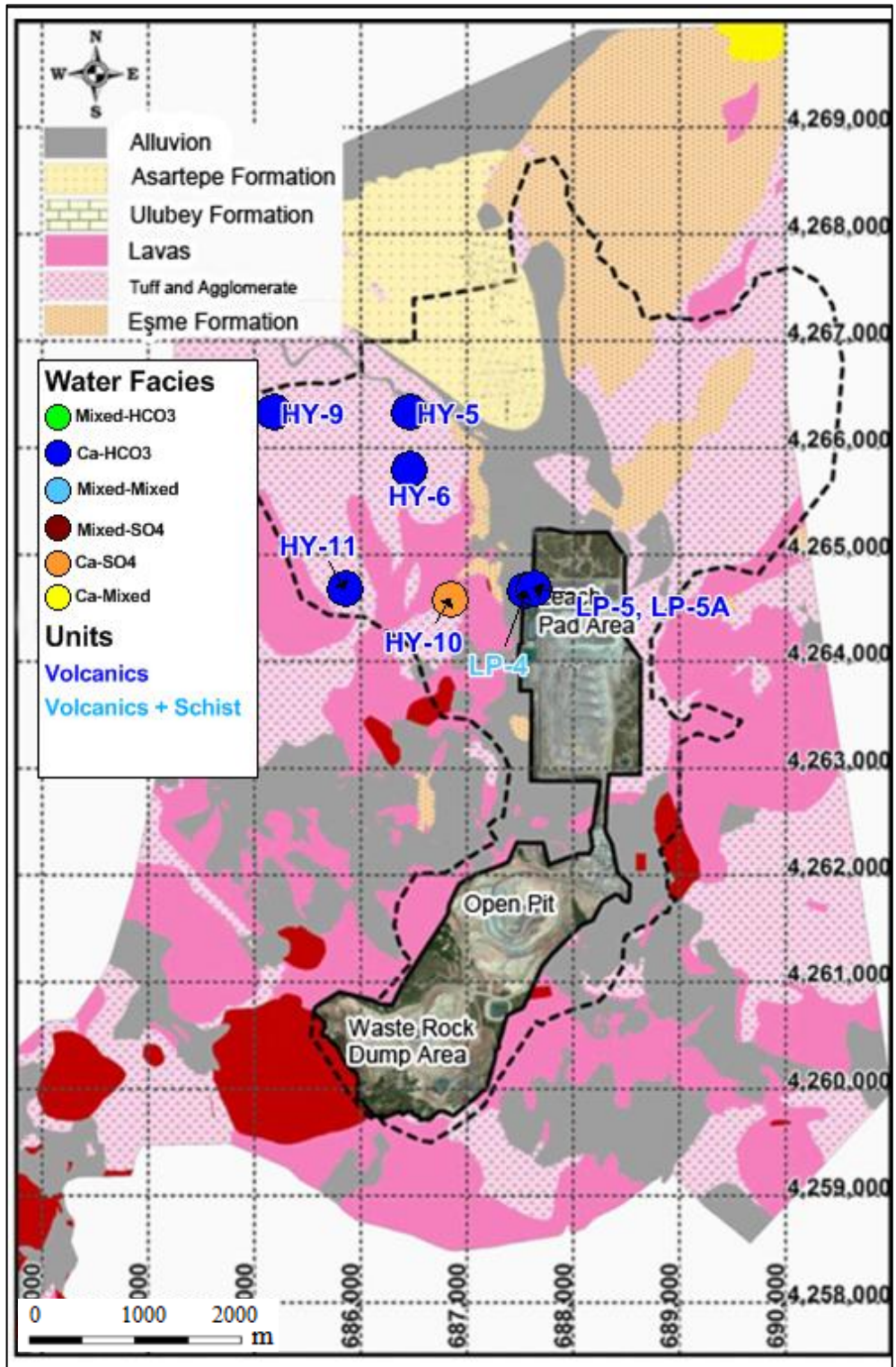


Figure 5.9 The groundwater facies distribution of mean concentration of the Volcanic unit (the LP-4 well in both volcanic and schist units)

In general, the groundwater facies of the volcanic unit shows calcium bicarbonate (Ca-HCO_3) characteristic, especially in the North Waste Rock Dump area. There are two wells having different characteristics while comparing Ca-HCO_3 facies. One of them is the LP-4 well filtering both volcanic and schist units. The groundwater sample obtained from this well has a mixed-mixed type hydrochemical character. Calcium sulphate facies were observed in the HY-10 well, located in the south of the North Waste Rock Dump area.

Hydrochemical Evaluations of the Asartepe Unit

According to evaluation of the geometric mean of major concentration, the facies of the Asartepe Formation was identified as calcium bicarbonate, Ca-HCO_3 (Figure 5.10). The areal distribution of facies in the Asartepe Formation is shown in Figure 5.11.

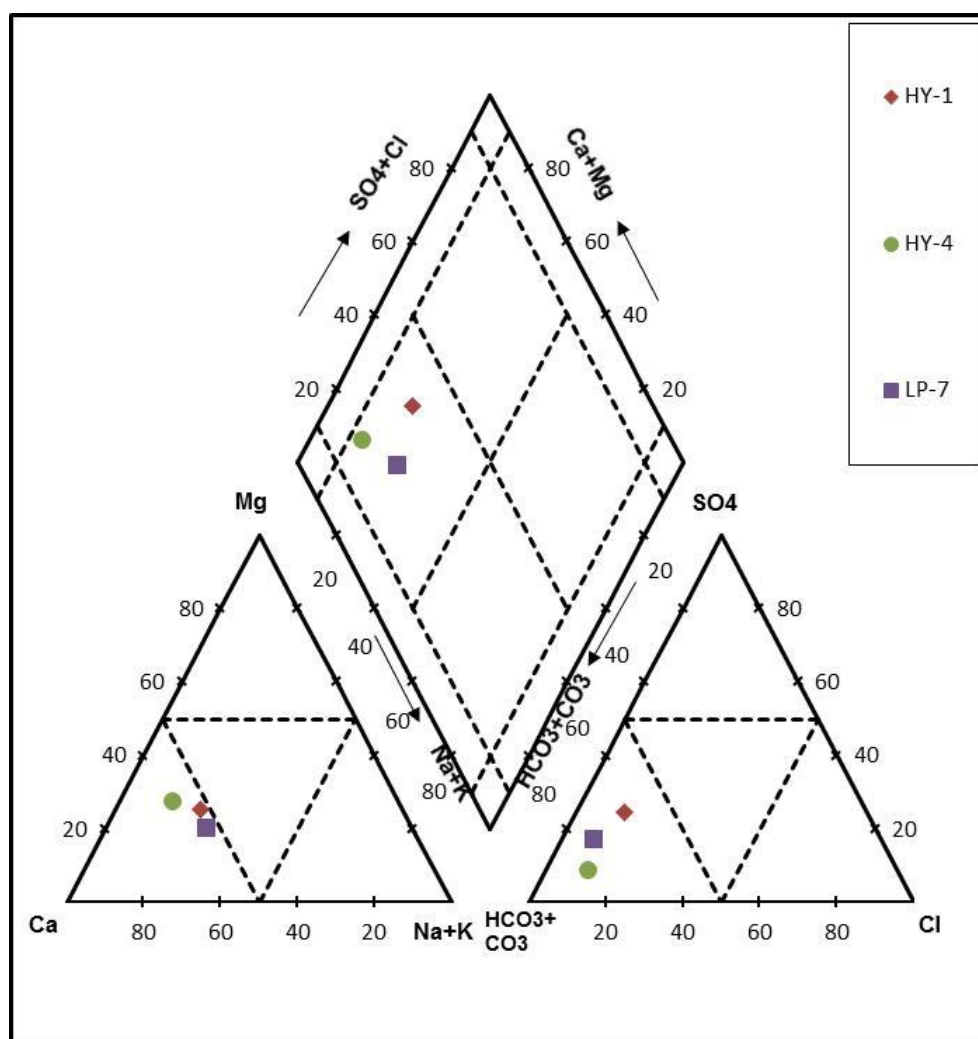


Figure 5.10 The facies distributions as determined by considering the geometric mean of major ion concentration values of the Asartepe Formation in a Piper Diagram

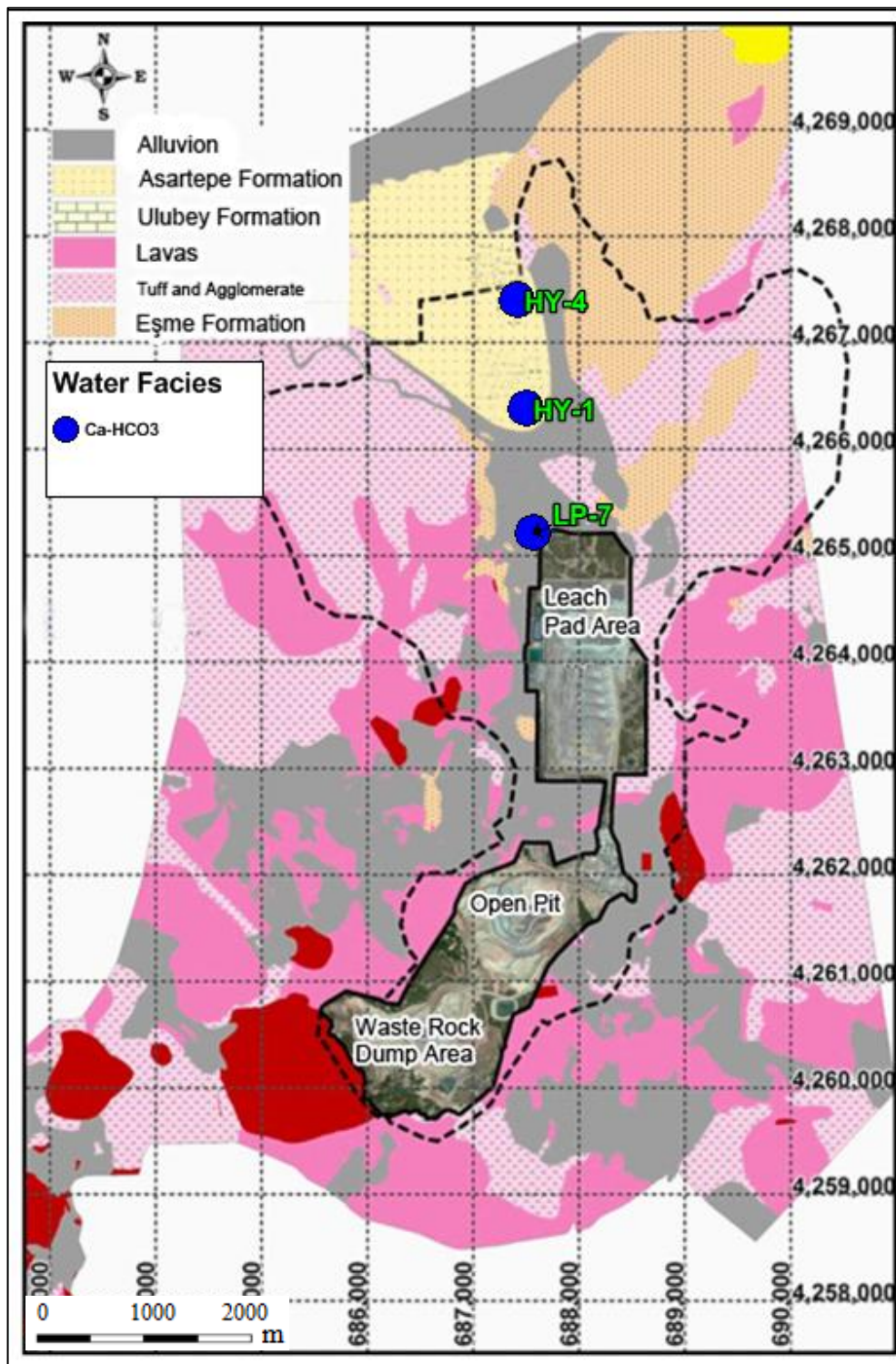


Figure 5.11 The groundwater facies distribution of mean concentration of the Asartepe Formation

General Hydrochemical Evaluation of the Study Area

In the study area involving the North Waste Rock Dump and the Heap Leach Pad, there are 13 locations which are currently under observation. These are given in Table 5.8. The facies distribution in these locations was identified by using the mean of major ion concentration (Figure 5.13).

Table 5.8 Observation locations in the study area (Yazıcıgil et al., 2013)

Observation Point ID	Description
WEIR-2	Weir
WEIR-6	Weir
KWSP-10	Schist
HY-1	Asartepe FM
HY-4	Asartepe FM
HY-3	Schist
HY-7	Schist
HY-8	Schist
HY-5	Volcanoclastics
HY-6	Volcanoclastics
HY-9	Volcanic
HY-10	Volcanic
HY-11	Volcanic

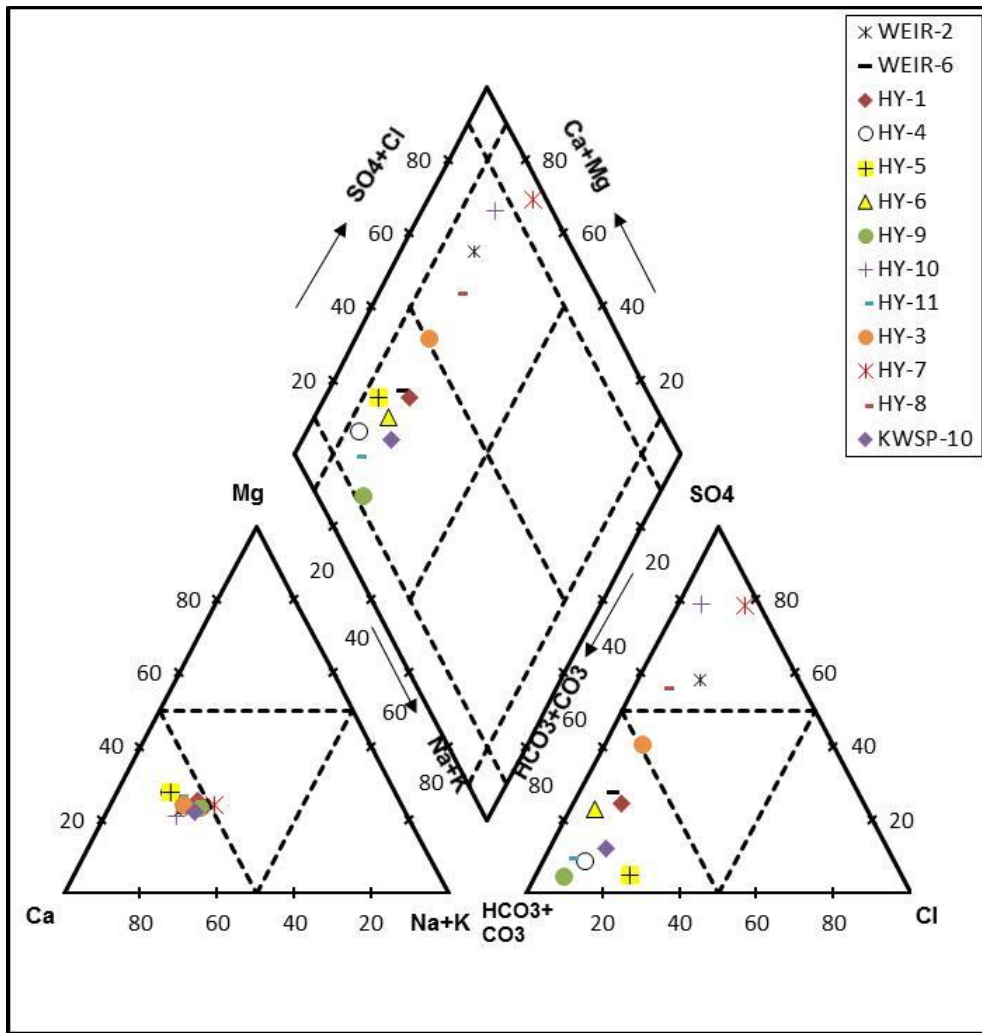


Figure 5.12 The facies distributions as determined by considering the geometric mean of major ion concentration values of the study area in a Piper Diagram

Generally, the groundwater facies consists of calcium, according to cations; however, while examining the anions, the groundwater shows a bicarbonate characteristic, except for observation wells located on the North Heap Leach Pad area. Groundwater facies for those wells are determined as: HY-7 being mixed-SO₄; HY-8, is Ca-SO₄, and HY-3 a Ca-mixed character. The groundwater facies of HY-10 and Weir-2 on the North Waste Rock Dump demonstrate a sulphate characteristic (Figure 5.13).

In addition to observation points in the study area, field parameters were measured from the fountains, cisterns, hand-dug wells, and puddles observed in the field study in July 2011. The measured parameters are given in Table 5.9.

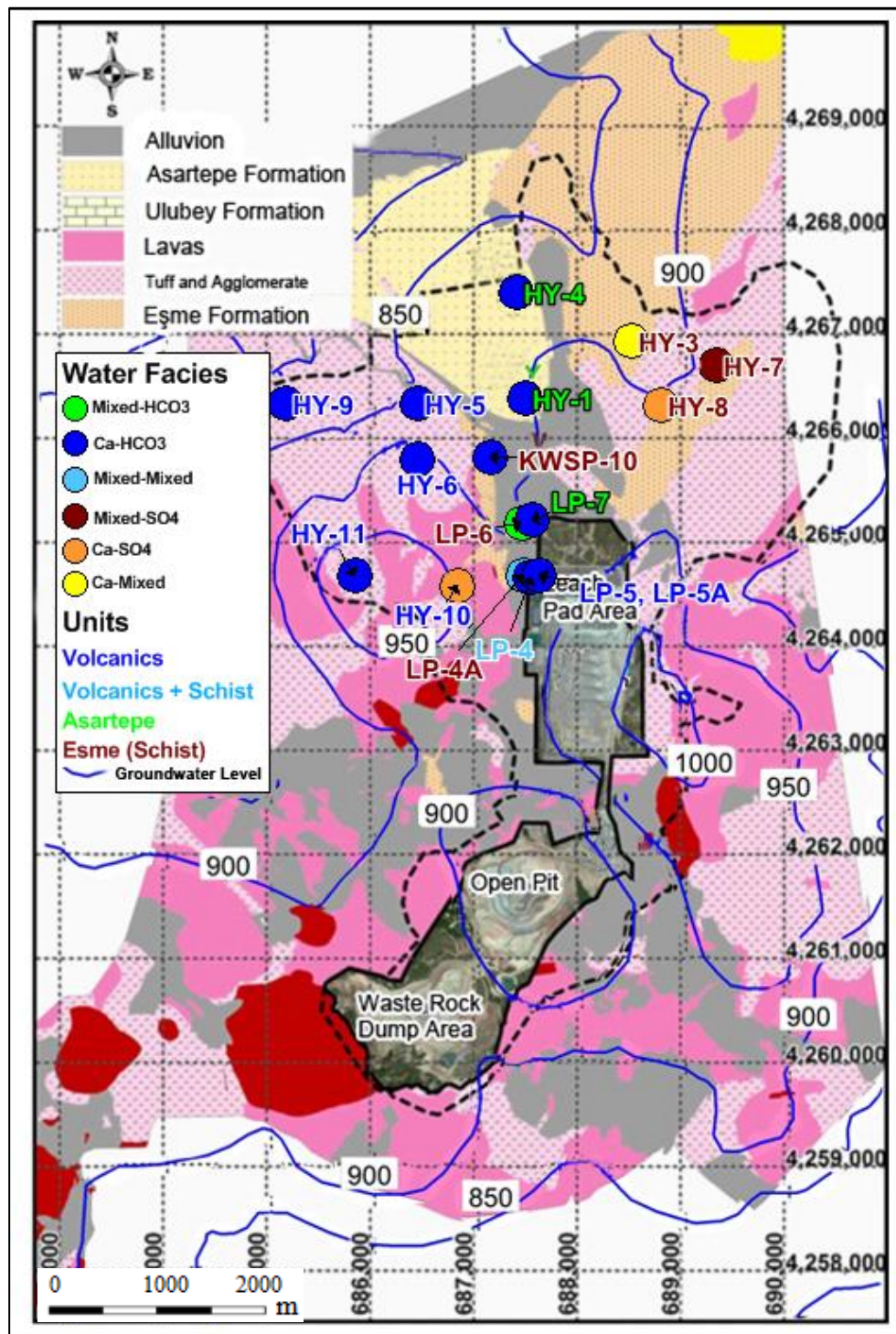


Figure 5.13 The facies distributions determined by considering the geometric mean of groundwater levels and well observation points

Table 5.9 Field measurements in the study area (July, 2011) (Yazıcıgil et al., 2013)

No	Type	Easting	Northing	pH	T (°C)	EC (µS/cm)	TDS (mg/l)	DO%	DO (mg/l)	Discharge (L/s)
1	Puddle	688114	4266604	9	29.1	91.1	39.6			
2	Fountain	688756	4266944	6.6	18.7	50.9	24.6	71.8		0.021
3	Fountain	688763	4266896	7.1	25.1	58.4	27.4			0.04
4	Fountain	687088	4268723	7.3	23.6	267	127.5	64.4		0.057
5	Fountain	687174	4264015	4.3	20.6	117.2	60.8	22.8	1.77	0.023
6	Fountain	687431	4264118	5.8	21.2	88.5	45.3	46.6	3.58	0.021
7	Fountain	684830	4265318	7.2	22.5	60.7	30	99.3	7.5	
8	Fountain	688000	4269687	7.5	17.2	239	137.8			
9	Cistern	686804	4263946	7.1	21.5	47.5	24.1	86.5	6.39	
10	Water Reservoir	684249	4266190	7.9	26.4	69.5	31.3	97.8	6.98	

In No-5 and No-6 fountains, located near the South Heap Leach Pad area, pH and dissolved oxygen values were found to be less than other observation points. As mentioned before, the observation well around these fountains, HY-10 has a sulphate characteristic. The pH value of the No-2 fountain near the HY-3 well is in the interval between acidic-neutral, at 6.59, and another fountain near this well, No-3, has a neutral pH value of 7.07. The HY-3 well filtering the schist has a mixed-anion facies. The other observation points have a basic character and their dissolved oxygen amounts are higher than the No-2, No-3, No-5 and No-6 fountains.

5.4. Water Quality Classifications

5.4.1. Surface Water Classification

According to inland surface water classification (YSKYY, 2012) and drinking water limits for human consumption, the characteristic value of the observation points were identified by considering average temperature values. The geometric mean values belonging to the mining period were used to determine water classification. The results are given in Table 5.10. Inland surface water quality distribution is shown in Figure 5.14.

Table 5.10 The characteristic value of surface water involving the pre-mining period (BM) and inland water classification by considering the geometric mean values involving the mining period (AM) (YSKYY, 2012) and suitability for human consumption (İTAS, 2005; EU, 1998) Unit: mg/l, EC: $\mu\text{S/cm}$. pH* alt and pH** for upper limits of the characteristic value. (Yazıcıgil et al., 2013)

Surface Water	Inland Water Classification				Human Consumption	WEIR-2 BM	WEIR-2 AM	WEIR-6
Parameters	Class I	Class II	Class III	Class IV	upper limit	CLASS III	CLASS II	CLASS II
Temperature ($^{\circ}\text{C}$)	25	25	30	> 30		14.4	13.5	14.6
Cd	0.002	0.005	0.007	> 0.007	0.005	0.0007	0.0016	0.0001
Cu	0.02	0.05	0.2	> 0.2	2	0.006	0.006	0.004
Hg	0.0001	0.0005	0.002	> 0.002	0.001	0.00028	0.00005	0.00005
Ni	0.02	0.05	0.2	> 0.2	0.02	0.0117	0.0107	0.0028
N-NO ₂	0.002	0.01	0.05	> 0.05	0.15	0.0079	0.0076	0.0022
N-NO ₃	5	10	20	> 20	11.5	2.59	0.15	0.03
Pb	0.01	0.02	0.05	> 0.05	0.01	0.0115	0.0011	0.0005
P	0.03	0.16	0.65	> 0.65		0.13	0.01	0.012
Zn	0.2	0.5	2	> 2		0.07	0.073	0.081
As					0.01	0.027	0.008	0.009
Ba					0.7	0.13	0.08	0.06
CN					0.05	0.0113	0.0051	0.005
Cr					0.05	0.007	0.001	0.001
F					1.5	0.37	0.33	0.23
Se					0.01	0.0017	0.0015	0.001
Indicator Parameters								
Al					0.2	3.719	0.108	0.065
Cl					250	40.9	38.5	7.6
EC	400	1000	3000	> 3000	2500	1143.8	670.5	228.7
Fe					0.2	2.136	0.184	0.179
Mn					0.05	0.463	0.217	0.052
Na					200	45.35	27.92	8.79
N-NH ₄	0.2	1	2	> 2	0.39	0.28	0.13	0.12
O ₂	8	6	3	< 3	5	4.2	8.81	8.93
pH*	6.5-8.5	6.5-8.5	6.5-8.5	6.5-8.5	≥ 6.5 and ≤ 9.5	6.8		
pH**	6.5-8.5	6.5-8.5	6.5-8.5	6.5-8.5	≥ 6.5 and ≤ 9.5	8.42	7.29	7.13
SO ₄					250	569.8	189.67	32.92

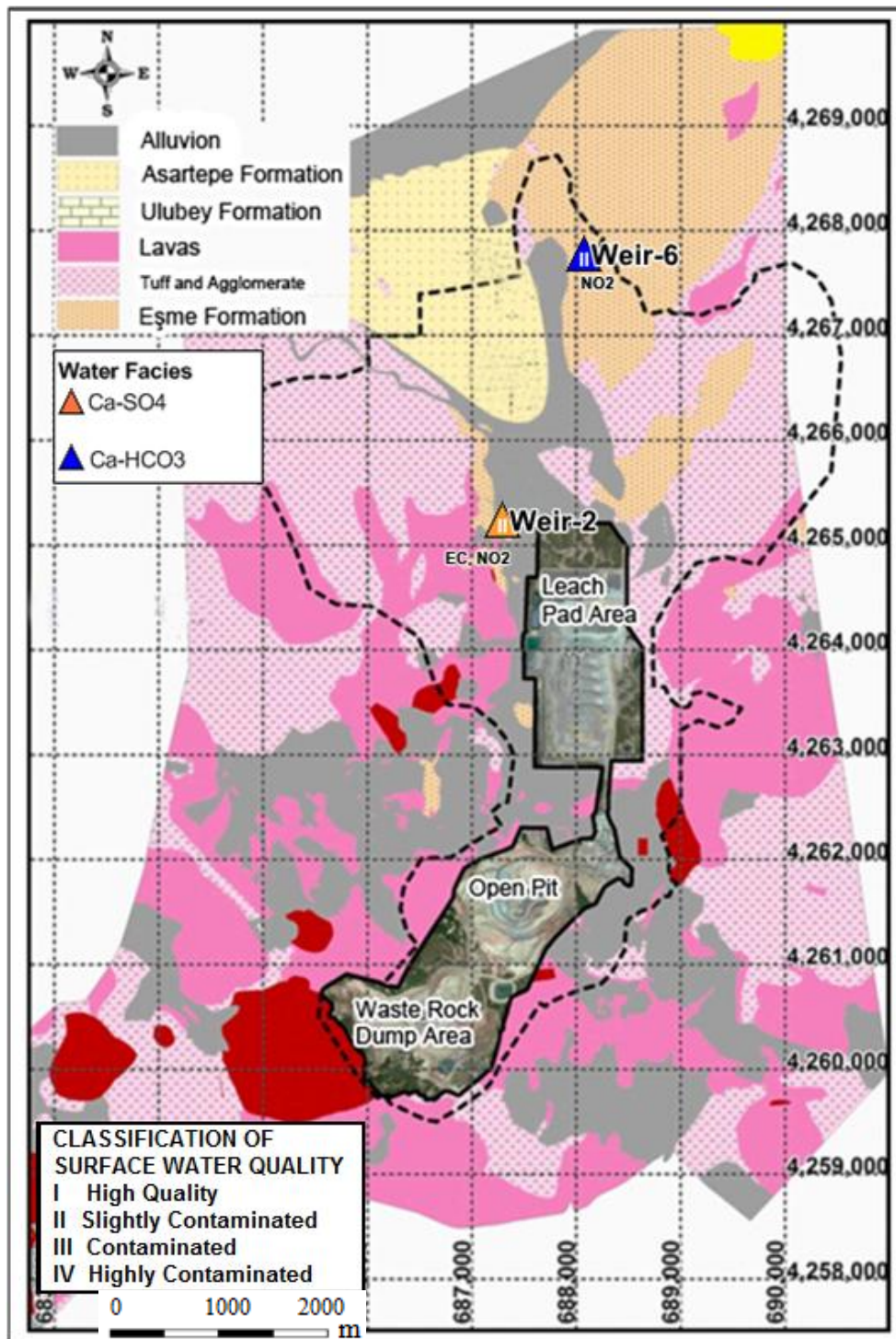


Figure 5.14 The distribution of surface water facies, some parameters, and their classification

According to EC and O₂ values, Weir-2 is identified as Class III water. While examining the mining period, it was determined that the Weir-2 class converted to a Class II, moderately contaminated, by considering the geometric mean of EC and O₂ in this period. Likewise, Weir-6 was classified as Class II by using its geometric mean of NO₂ concentration during the mining period.

As a result of these evaluations, Weir-2 and Weir-6 are considered suitable for human consumption. The distribution of irrigation water quality are shown according to SAR and EC values in Figure 5.15.

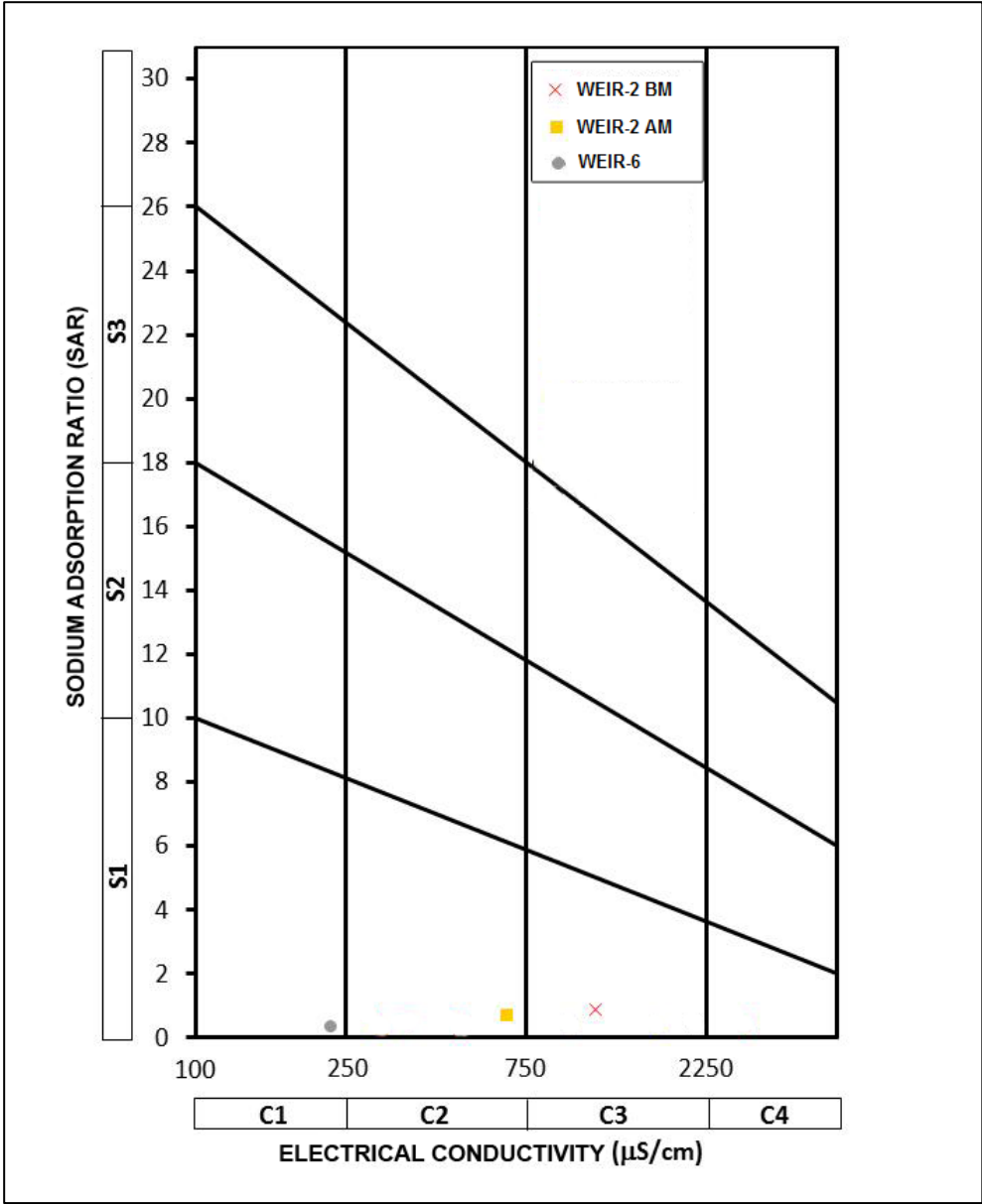


Figure 5.15 The quality distribution of surface water according to the average SAR and EC values of the characteristic values and the geometric mean during the mining period.

5.4.2 Groundwater Classification

The protection of groundwater against pollution regulations involve the criteria for groundwater quality classification and deterioration (YKBKK, 2012) and was repealed for water quality classification criteria. In order to evaluate the groundwater quality of the study area, quality classification limits (SKKY, 2008) were used by considering the changed parameters in YSKYY (2012) because the groundwater quality standard was not previously determined by the General Directorate of Water Management.

Spring and Fountains

The geometric mean of chemical composition of springs and fountains are given in Table 5.11, and were determined according to the inland groundwater classification system (SKKY, 2008; YSKYY, 2012), and the drinking water limits for human consumption (İTAS, 2005; EU, 1998). Figure 5.16 shows the distribution of water quality classification in the study area.

As a result of this classification, KWSP-9, near the South Heap Leach Pad area, was determined to be Class II according to the inland water classification limits. By considering the measurement average values, it was observed that KWSP-2 is suitable for human consumption. Figure 5.17 shows the irrigation water quality description of these locations by SAR and EC values.

Table 5.11 The inland water classification of spring and fountain water according to the geometric mean values (SKKY, 2008; YSKYY, 2012) and suitability for human consumption (İTAS, 2005; EU, 1998) Unit: mg/l, EC: µS/cm. (Yazıcıgil et al., 2013)

Groundwater	Inland Water Classification			Human Consumption	KWSP-2	KWSP-9
	Class I	Class II	Class III			
Parameters				upper limit	Class III	Class II
Temperature (°C)	25	25	> 25		12.8	12.9
As	0.02	0.05	> 0.05	0.01	0.004	0.036
Ba	1	2	>2	0.7	0.04	0.1
Cd	0.002	0.005	> 0.005	0.005	0.0003	0.0001
CN	0.01	0.05	> 0.05	0.05	0.0071	0.0065
Co	0.01	0.02	> 0.02		0.0021	0.0003
Cr	0.02	0.05	> 0.05	0.05	0.003	0.001
Cu	0.02	0.05	> 0.05	2	0.002	0.001
F	1	1.5	> 1.5	1.5	0.34	0.27
Hg	0.0001	0.0005	> 0.0005	0.001	0.00004	0.00005
Ni	0.02	0.05	> 0.05	0.2	0.0122	0.0012
N-NO2	0.002	0.01	> 0.01	0.15	0.0016	0.0014
N-NO3	5	10	> 10	11.5	1.2	0
Pb	0.01	0.02	> 0.02	0.01	0.0005	0.0007
P	0.03	0.16	> 0.16		0.024	0.027
Se	0.01	0.01	> 0.01	0.01	0.0018	0.0013
TDS	500	1500	> 1500		354	176
Zn	0.2	0.5	> 0.5		0.051	0.007
Indicator Parameters						
Al	0.3	0.3	> 0.3	0.2	0.247	0.157
Cl	25	200	> 200	250	11.2	7.5
EC	400	1000	> 1000	2500	421.8	213.2
Fe	0.3	1	> 1	0.2	0.191	0.126
Mn	0.1	0.5	> 0.5	0.05	0.067	0.005
Na	125	125	> 125	200	25.15	12.9
N-NH4	0.2	1	> 1	0.39	0.06	0.06
O2	8	6	< 6	5	6.84	6.92
pH	6.5-8.5	6.5-8.5	< 6->9	≥ 6.5 and ≤ 9.5	6.36	7.37
SO4	200	200	> 200	250	158.95	13.68

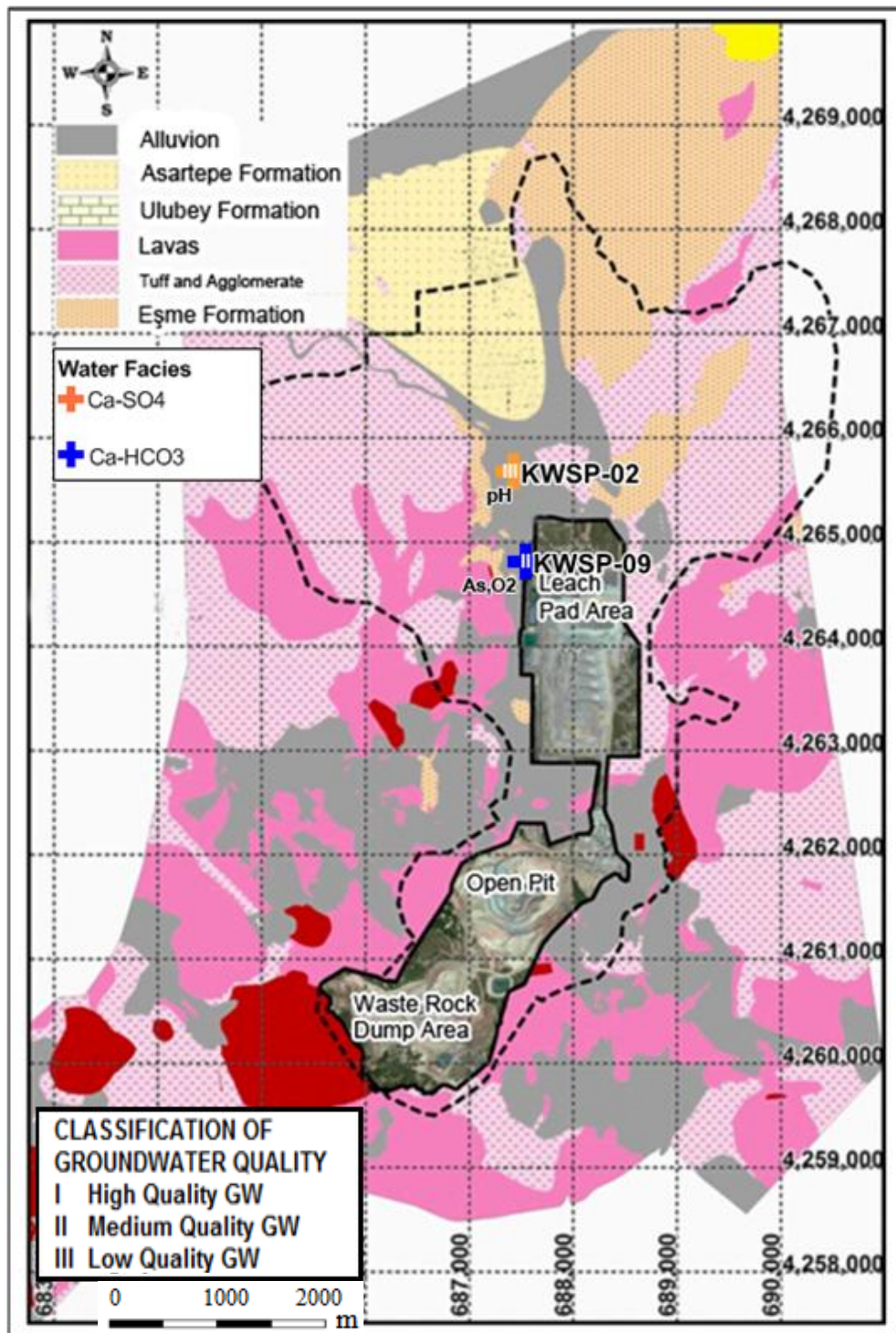


Figure 5.16 The distribution of spring and fountain water facies, some parameters, and their classification

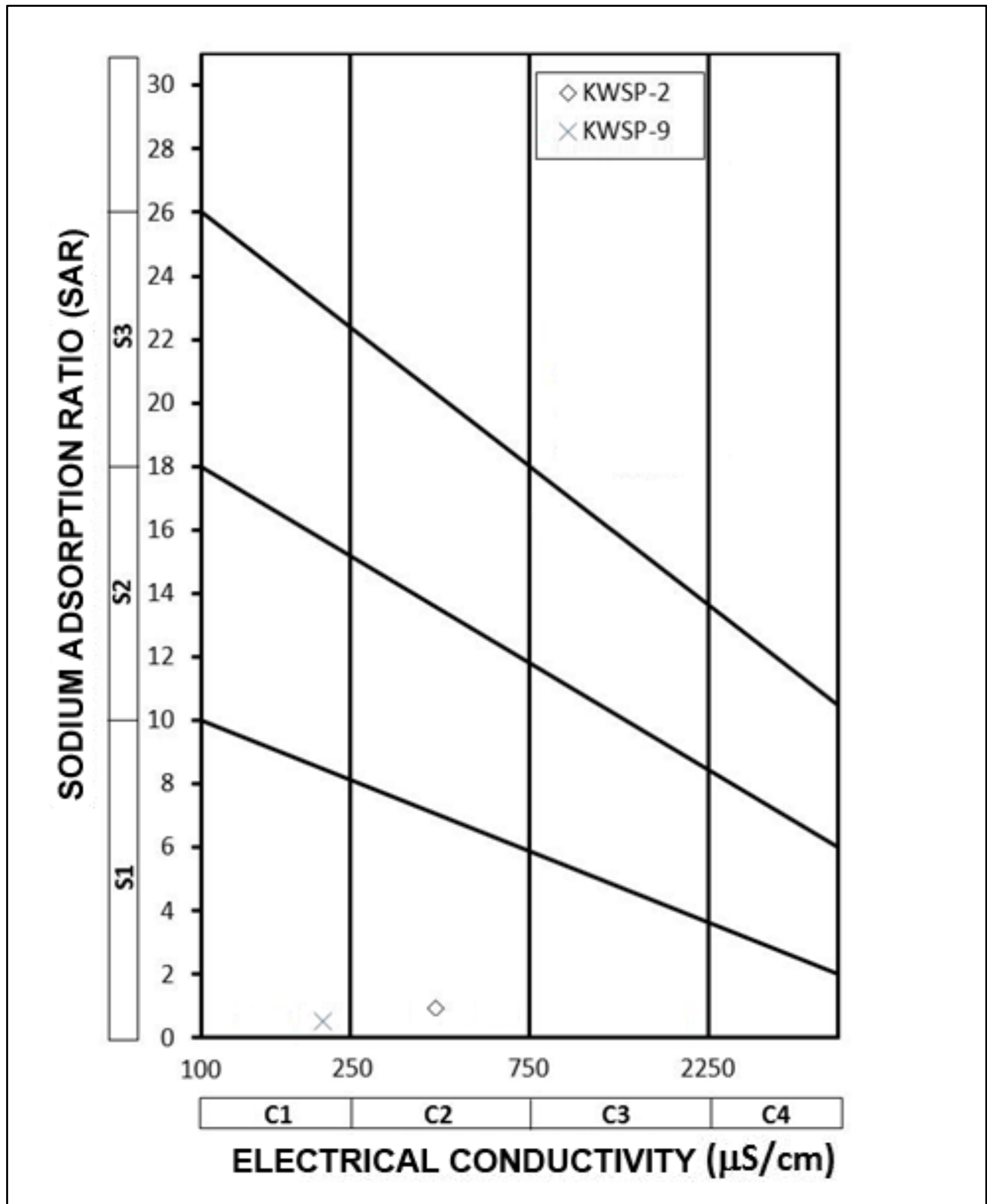


Figure 5.17 The quality distribution of spring and fountain water according to the average SAR and EC values

Wells

The quality classification of the lithological units was done by considering the inland water classification (SKKY, 2008; YSKYY, 2012) and human consumption limits (ITAS, 2005; EU, 1998).

Schist Unit

All wells filtering the schist unit were identified as Class III by using the geometric mean of the measurements. It was observed that O₂ concentration is low in all of the wells. These wells are not suitable for human consumption because they have values exceeding the upper limits for human consumption. In addition, the HY-7 well, has an acidic character with concentrations of As, Fe, Mn, O₂, P, Zn, which are over the limits.

Table 5.12 shows these classification limits and the geometric mean values of the measurements from the wells in the schist unit. The areal distribution of the classification is illustrated in Figure 5.18. SAR and EC value distributions are shown in Figure 5.19.

Table 5.12 The inland water classification of groundwater (SKKY, 2008; YSKYY, 2012) and suitability for human consumption belonging to the schist unit according to geometric mean values (İTAS, 2005; EU, 1998) Unit: mg/l, EC: $\mu\text{S/cm}$. (Yazıcıgil et al., 2013)

Groundwater	Inland Water Classification			Human Consumption	HY-3	HY-7	HY-8	KWSP-10	LP-4A	LP-6
	Class I	Class II	Class III		upper limit	Class III	Class III	Class III	Class III	Class III
Parameters	Class I	Class II	Class III	upper limit	Class III	Class III	Class III	Class III	Class III	Class III
Temperature (°C)	25	25	> 25		15.4	22.9	16.9	12.8	18.6	15.9
As	0.02	0.05	> 0.05	0.01	0.021	0.173	0.075	0.024	0.074	0.025
Ba	1	2	> 2	0.7	0.05	0.04	0.03	0.09	0.03	0.1
Cd	0.002	0.005	> 0.005	0.005	0.0003	0.0004	0.0013	0.0001	0.0001	0.0001
CN	0.01	0.05	> 0.05	0.05	0.005	0.005	0.005	0.0055	0.005	0.005
Co	0.01	0.02	> 0.02		0.0031	0.0028	0.0019	0.0002	0.0014	0.0011
Cr	0.02	0.05	> 0.05	0.05	0.001	0.001	0.001	0.001	0.001	0.001
Cu	0.02	0.05	> 0.05	2	0.001	0.002	0.002	0.001	0.001	0.001
F	1	1.5	> 1.5	1.5	0.54	0.42	0.55	0.24	0.46	0.55
Hg	0.0001	0.0005	> 0.0005	0.001	0.00003	0.00002	0.00002	0.00007	0.00005	0.00005
Ni	0.02	0.05	> 0.05	0.2	0.0216	0.0102	0.0065	0.0014	0.0076	0.0018
N-NO2	0.002	0.01	> 0.01	0.15	0.0025	0.002	0.0021	0.0056	0.0019	0.001
N-NO3	5	10	> 10	11.5	0.1	0.5	0.1	4.7	0	0
Pb	0.01	0.02	> 0.02	0.01	0.0005	0.005	0.0011	0.0003	0.0004	0.0008
P	0.03	0.16	> 0.16		0.004	0.163	0.004	0.142	0.376	0.01
Se	0.01	0.01	> 0.01	0.01	0.0022	0.01	0.0032	0.0011	0.001	0.001
TDS	500	1500	> 1500		507	356	342	306	337	335
Zn	0.2	0.5	> 0.5		0.034	0.582	0.017	0.009	0.033	0.043
Indicator Parameters										
Al	0.3	0.3	> 0.3	0.2	0.015	0.013	0.012	0.019	0.038	0.172
Cl	25	200	> 200	250	26.3	17.3	12.7	19.6	19.5	21.2
EC	400	1000	> 1000	2500	702.7	548	460.6	371.5	411.3	407.1
Fe	0.3	1	> 1	0.2	0.229	11.5	2.875	0.049	0.755	0.384
Mn	0.1	0.5	> 0.5	0.05	0.951	2.56	1.025	0.012	0.303	0.401
Na	125	125	> 125	200	29.13	16	16.58	17.1	24.63	30.14
N-NH4	0.2	1	> 1	0.39	0.19	0.04	0.12	0.06	0.11	0.1
O2	8	6	< 6	5	2	1	1.06	5.13	1.77	1.93
pH	6.5-8.5	6.5-8.5	< 6->9	≥ 6.5 and ≤ 9.5	6.88	3.57	6.86	6.94	6.6	6.88
SO4	200	200	> 200	250	146.63	107	117.96	22.44	93.77	74.03

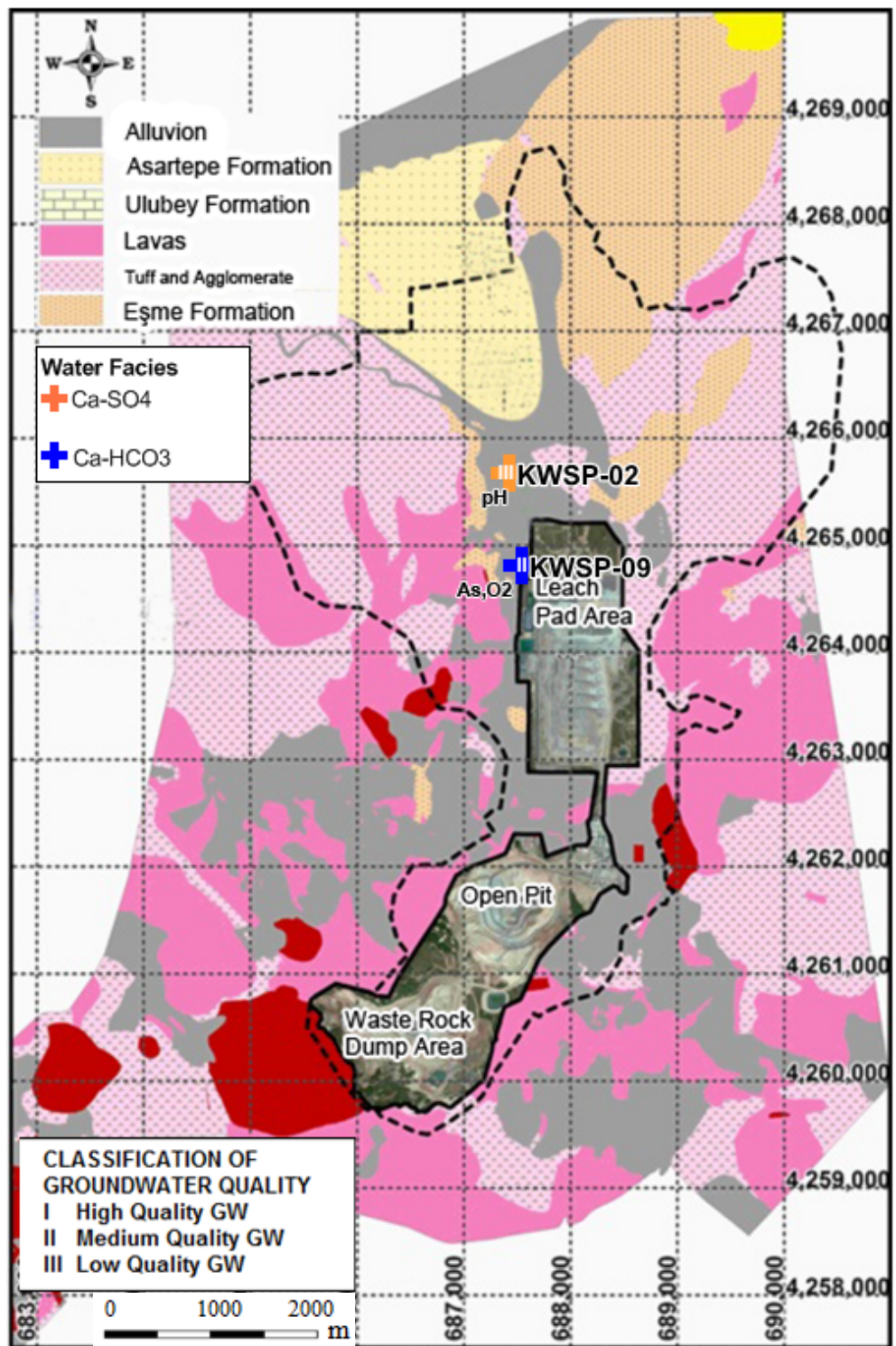


Figure 5.18 The distribution of facies, some parameters, and classification of the wells belonging to the schist unit

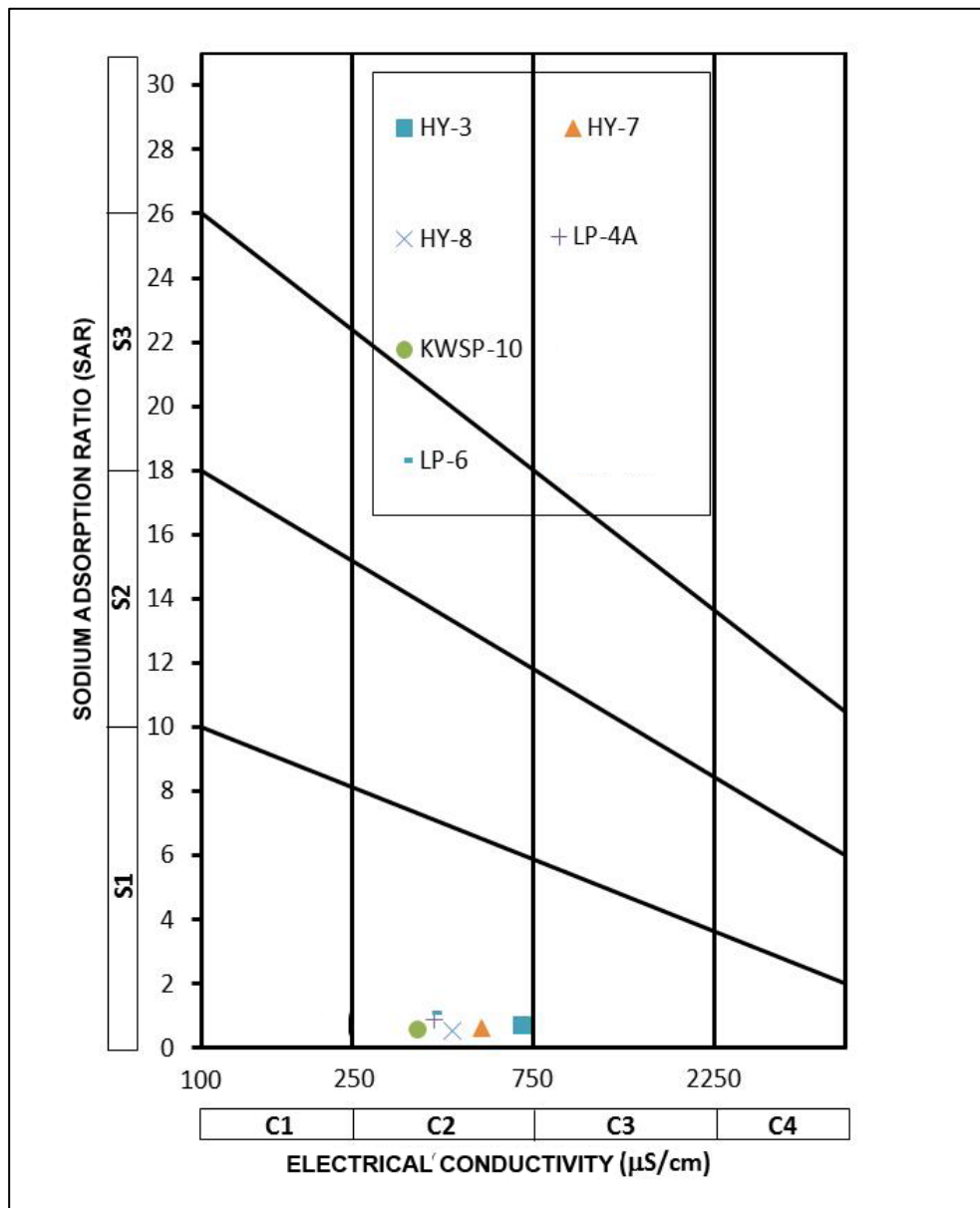


Figure 5.19 The quality distribution of groundwater belonging to the schist unit according to the average SAR and EC values of the characteristic values

Volcanic Unit

All of the wells were determined as Class III. The values marked in red indicate Class III values (Table 5.13). Some wells are not suitable for human consumption because the parameters, As, Cd, Cr, F, Ni, Pb were found to be higher than the uppermost limits. However, LP-5 and HY-11 wells satisfactorily fulfilled the conditions for human consumption according to geometric mean values. The screen interval of LP-4 is on both volcanic and schist units. The facies, classification, and some parameters distributions are illustrated in Figure 5.20. SAR and EC value distributions are shown in Figure 5.21.

Table 5.13 The inland water classification of groundwater (SKKY, 2008; YSKYY, 2012) and suitability for human consumption belonging to the volcanic unit according to geometric mean values (İTAS, 2005; EU, 1998) Unit: mg/l, EC: $\mu\text{S}/\text{cm}$. (Yazıcıgil et al., 2013)

Groundwater	Unit	Inland Water Classification			Human Consumption Upper Limit	HY-5	HY-6	LP-5	LP-5A	HY-9	HY-10	HY-11	LP-4 (Volcanic + Schist)
		Class I	Class II	Class III		Class III	Class III	Class III	Class III	Class III	Class III	Class III	Class III
Temperature	(°C)	25	25	>25		17.1	18.1	17.3	17.7	22.6	18.2	20.4	17.6
As	mg/L	0.02	0.05	>0.05	0.01	0.020	0.041	0.005	0.029	0.025	0.119	0.009	0.025
Ba	mg/L	1	2	>2	0.7	0.12	0.04	0.09	0.05	0.04	0.04	0.03	0.07
Cd	mg/L	0.002	0.005	>0.005	0.005	0.0002	0.0002	0.0009	0.0012	0.0005	0.0036	0.0005	0.0004
CN	mg/L	0.01	0.05	>0.05	0.05	0.0050	0.0050	0.0050	0.0050	0.0050	0.0050	0.0050	0.0050
Co	mg/L	0.01	0.02	>0.02		0.0005	0.0006	0.0004	0.0005	0.0020	0.0215	0.0020	0.0005
Cr	mg/L	0.02	0.05	>0.05	0.05	0.001	0.001	0.001	0.001	0.001	0.001	0.001	0.001
Cu	mg/L	0.02	0.05	>0.05	2	0.002	0.002	0.002	0.002	0.002	0.002	0.002	0.002
F	mg/L	1	1.5	>1.5	1.5	0.36	0.24	0.95	1.31	0.25	0.77	0.21	1.24
Hg	mg/L	0.0001	0.0005	>0.0005	0.001	0.00003	0.00003	0.00005	0.00005	0.00001	0.00002	0.00001	0.00072
Ni	mg/L	0.02	0.05	>0.05	0.2	0.0035	0.0042	0.0069	0.0055	0.0030	0.0498	0.0020	0.0036
N-NO2	mg/L	0.002	0.01	>0.01	0.15	0.0474	0.0060	0.0025	0.0054	0.0054	0.0126	0.0020	0.0019
N-NO3	mg/L	5	10	>10	11.5	8.9	0.0	1.2	2.2	1.4	0.5	0.8	0.1
Pb	mg/L	0.01	0.02	>0.02	0.01	0.0015	0.0011	0.0004	0.0008	0.0050	0.0050	0.0050	0.0021
P	mg/L	0.03	0.16	>0.16		0.010	0.087	0.006	0.014	0.069	0.010	0.069	0.051
Se	mg/L	0.01	0.01	>0.01	0.01	0.0022	0.0022	0.0015	0.0010	0.0100	0.0100	0.0100	0.0010
TDS	mg/L	500	1500	>1500		498	274	759	493	228	393	239	511
Zn	mg/L	0.2	0.5	>0.5		0.020	0.022	0.086	0.062	1.380	1.360	0.802	0.065
Indicator Parameters													
Al	mg/L	0.3	0.3	>0.3	0.2	0.014	0.027	0.038	0.038	0.010	0.106	0.010	0.114
Cl	mg/L	25	200	>200	250	50.1	8.0	37.8	13.4	8.1	12.5	5.4	43
EC	$\mu\text{S}/\text{cm}$	400	1000	>1000	2500	641.7	351.3	751.6	601.1	352	571	268	617.7
Fe	mg/L	0.3	1	>1	0.2	0.012	0.023	0.122	0.042	0.005	0.018	0.003	0.1
Mn	mg/L	0.1	0.5	>0.5	0.05	0.014	0.026	0.016	0.012	0.052	0.408	0.009	0.019
Na	mg/L	125	125	>125	200	18.64	11.28	55.26	32.39	15.8	19.9	8.12	41.11
N-NH4	mg/L	0.2	1	>1	0.39	0.05	0.07	0.06	0.05	0.04	0.04	0.04	0.06
O2	mg/L	8	6	<6	5	3.11	2.23	3.51	3.88	3.41	2.28	4.99	2.31
pH	-	6.5-8.5	6.5-8.5	<6-9.0	≥ 6.5 and ≤ 9.5	7.42	7.36	7.04	6.94	8.06	7.11	8.03	7.06
SO4	mg/L	200	200	>200	250	14.45	39.57	120.4	93.06	6.89	220.60	10.90	86.10

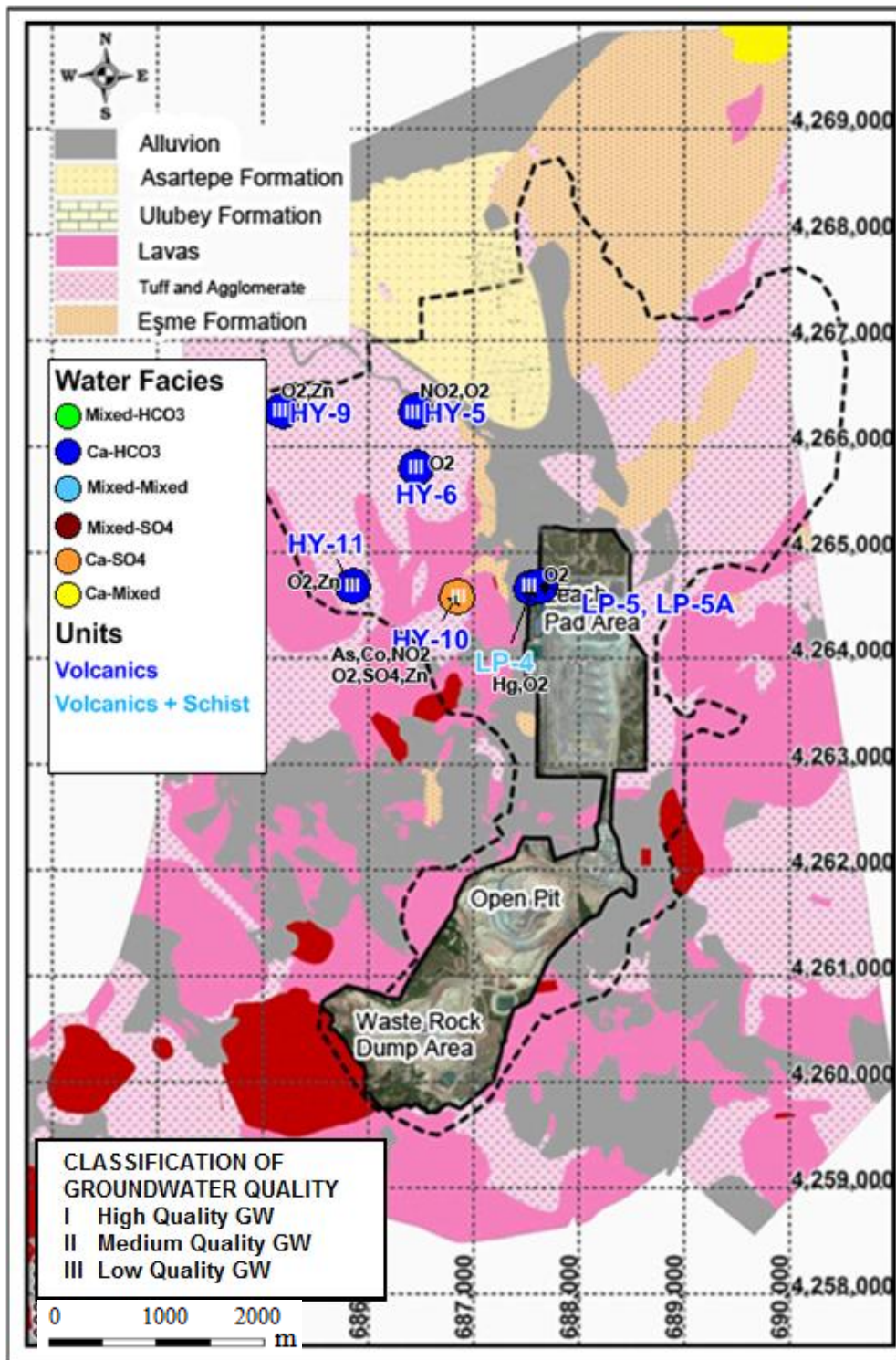


Figure 5.20 The distribution of some parameters, facies, and classification of the wells belonging to the volcanic unit

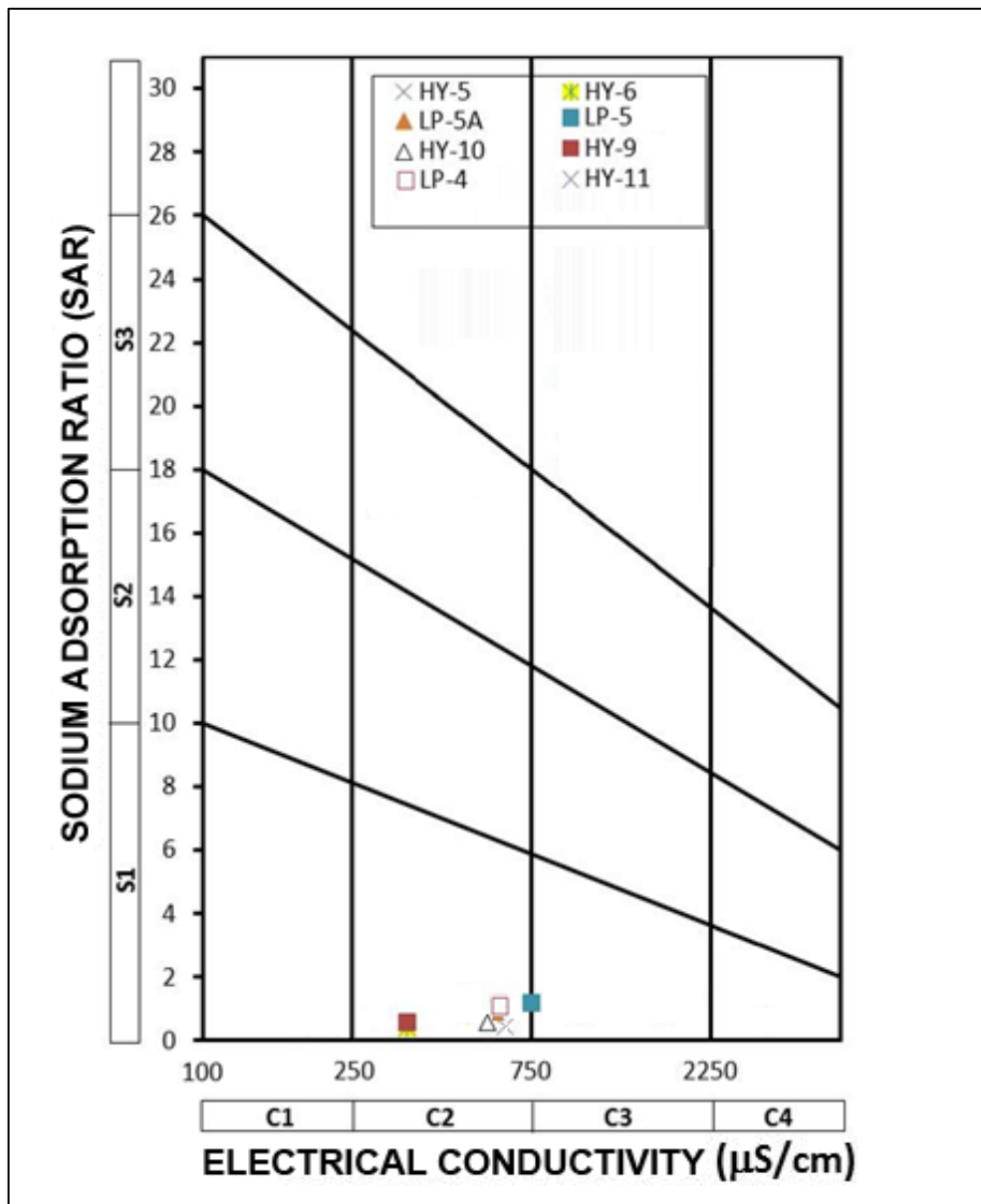


Figure 5.21 The quality distribution of groundwater belonging to the Volcanics according to the average SAR and EC values of the characteristic values (LP-4 contains both volcanic and schist units)

Asartepe Unit

While examining Table 5.14, it is observed that all wells on the Asartepe Formation are classified as Class III due to their low O_2 parameters. Moreover, the wells have high arsenic concentration, and therefore, it can be said that Asartepe is not suitable for human consumption. Irrigation water quality is shown in Figure 5.22 according to their SAR and EC values.

Table 5.14 The inland water classification of groundwater (SKKY, 2008; YSKYY, 2012) and suitability for human consumption belonging to the Asartepe Formation according to geometric mean values (İTAS, 2005; EU, 1998) Unit: mg/l, EC: $\mu\text{S/cm}$. (Yazıcıgil et al., 2013)

Groundwater	Unit	Inland Water Classification			Human Consumption Upper Limit	HY-1	HY-4	LP-7
		Class I	Class II	Class III		Class III	Class III	Class III
Temperature	(°C)	25	25	> 25		19.2	20.4	16.9
As	mg/L	0.02	0.05	> 0.05	0.01	0.015	0.014	0.023
Ba	mg/L	1	2	> 2	0.7	0.12	0.13	0.10
Cd	mg/L	0.002	0.005	> 0.005	0.005	0.0004	0.0004	0.0001
CN	mg/L	0.01	0.05	> 0.05	0.05	0.0050	0.0050	0.0050
Co	mg/L	0.01	0.02	> 0.02		0.0008	0.0020	0.0003
Cr	mg/L	0.02	0.05	> 0.05	0.05	0.001	0.002	0.001
Cu	mg/L	0.02	0.05	> 0.05	2	0.004	0.002	0.001
F	mg/L	1	1.5	> 1.5	1.5	0.33	0.51	0.85
Hg	mg/L	0.0001	0.0005	> 0.0005	0.001	0.00002	0.00001	0.00005
Ni	mg/L	0.02	0.05	> 0.05	0.2	0.0125	0.0020	0.0024
N-NO2	mg/L	0.002	0.01	> 0.01	0.15	0.0071	0.0032	0.0022
N-NO3	mg/L	5	10	> 10	11.5	0.2	1.6	0.0
Pb	mg/L	0.01	0.02	> 0.02	0.01	0.0020	0.0050	0.0007
P	mg/L	0.03	0.16	> 0.16		0.007	0.010	0.009
Se	mg/L	0.01	0.01	> 0.01	0.01	0.0032	0.0100	0.0010
TDS	mg/L	500	1500	> 1500		663	506	397
Zn	mg/L	0.2	0.5	> 0.5		0.017	0.002	0.036
Indicator Parameters								
Al	mg/L	0.3	0.3	> 0.3	0.2	0.065	0.010	0.036
Cl	mg/L	25	200	> 200	250	43.1	28.7	15.8
EC	$\mu\text{S/cm}$	400	1000	> 1000	2500	945.9	856.0	482.4
Fe	mg/L	0.3	1	> 1	0.2	0.041	0.017	0.092
Mn	mg/L	0.1	0.5	> 0.5	0.05	0.087	0.003	0.085
Na	mg/L	125	125	> 125	200	50.23	24.60	31.45
N-NH4	mg/L	0.2	1	> 1	0.39	0.04	0.04	0.07
O2	mg/L	8	6	< 6	5	1.57	3.79	2.39
pH	-	6.5-8.5	6.5-8.5	< 6->9.0	≥ 6.5 and ≤ 9.5	7.52	7.75	7.13
SO4	mg/L	200	200	> 200	250	116.84	33.00	46.74

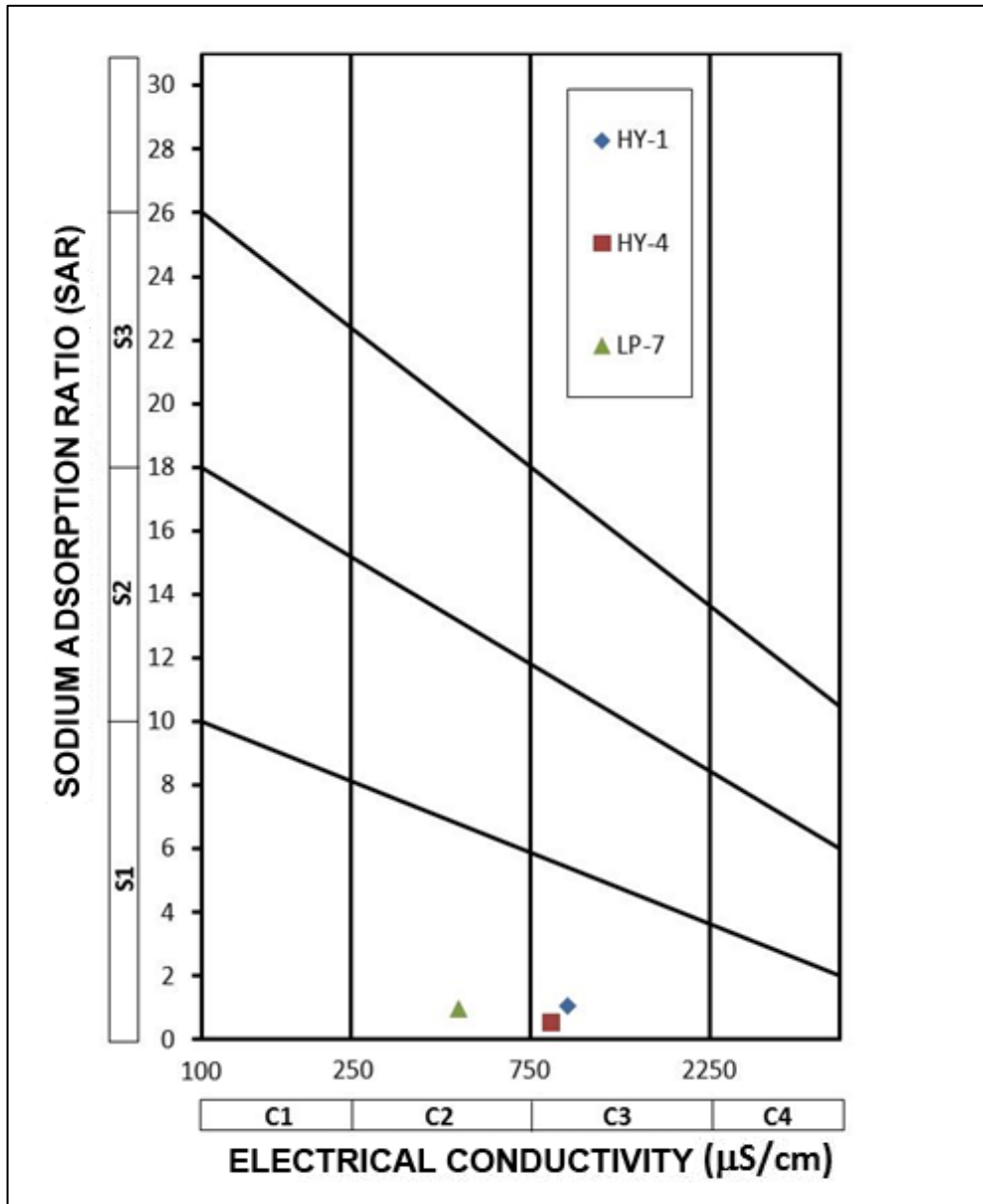


Figure 5.22 The quality distribution of groundwater belonging to the Asartepe Formation according to the average SAR and EC values of the characteristic values

CHAPTER 6

CONCLUSIONS AND RECOMMENDATION

6.1. Conclusion

This study combines the hydrogeological and hydrological investigation results of the northern part of the Kışladağ Gold Mine area where an expansion due to capacity increase is planned. The demography, meteorology, topography, hydrology, hydrogeology and water quality information obtained from previous studies were examined and analyzed, and further hydrological and hydrogeological investigations have been conducted in detail since July 2011. The data obtained from these investigations were evaluated and some conclusions can be reached.

In order to figure out the component of a water budget for the study area, the software, Soil-Water-Balance (SWB; Westenbroek et al. 2010), developed by the United States Geological Survey (USGS) was used. A Soil-Water-Balance (SWB) computer code has been developed to calculate spatial and temporal variations in groundwater recharge by using meteorological data, land use, curve number for runoff, and evaporation calculated by the Turc method. According to the SWB result, it was concluded that the annual average precipitation values are composed of: 75.5% evaporation, 8.5% surface runoff, and 6.64% groundwater recharge. The average annual recharge value was calculated as 37.8 mm for the entire area. However, for the specific study area, groundwater recharge values were found to be between 0-12.7 mm and 12.7-25.4 mm in the North Heap Leach Pad and the North Waste Rock Dump areas, respectively. In the North Heap Leach pad area, meadows and orchards are the dominant land use types, whereas the North Waste Rock Dump is covered mostly by orchard (dry). In addition to this, the dry farming (fallow) region located between these processing areas has a 50.8-76.2 mm groundwater recharge value.

In the planned northern expansion areas which include a waste dump and a leach pad, a total of 31 test and observation wells have been drilled since July 2011 to characterize the hydrogeological setting. Aquifer tests consisting of pumping, recovery and slug tests have been conducted on 13 of these wells in order to determine the hydraulic conductivity of the various lithological units underlying the planned facilities. At the planned north waste rock dump area, schist basement is overlain by volcanic units. Among the seven wells drilled at this location, six wells (HY-5, HY-6, HY-9, HY-10, HY-11 and LP-5A) were completed within the volcanics while one (LP-4A) extended down to the schists. The minimum, maximum and geometric mean of the hydraulic conductivity value for the volcanic units were determined as 4.56×10^{-9} m/s, 9.01×10^{-7} and 7.15×10^{-8} m/s, respectively. Meanwhile, the single test conducted at schists indicated a hydraulic conductivity value of 9.54×10^{-8} m/s for this unit. On the other hand, when all the test results are considered, geometric mean of the hydraulic conductivity value is calculated as 7.45×10^{-8} m/s for the planned waste rock dump area at the north.

At the planned north heap leach pad area, basement schists are either very close to the surface and overlain by Asartepe Formation or by volcanic; or at the surface as extensive outcrops. Due to the fact that at this locality volcanics can only be observed as a thin layer overlying schists, this geologic unit is not monitored or tested. Rather, wells drilled at this location are screened at Asartepe Formation and schists in order to monitor and test these units. Among the 7 wells drilled at this location, four wells (HY-3, HY-7, HY-8 and LP-6) were completed within the schists while three wells (HY-1, HY-2 and HY-4) were completed within the Asartepe Formation, one of which is dry (HY-2). The minimum, maximum and geometric mean of the hydraulic conductivity value for the Asartepe Formation were determined as 2.50×10^{-9} m/s, 5.34×10^{-8} m/s and 1.16×10^{-8} m/s, respectively. Meanwhile, the same parameters were calculated as 1.19×10^{-8} m/s, 2.61×10^{-6} m/s and 1.83×10^{-7} m/s for the schists. Finally, considering all the aquifer test results, geometric mean of the hydraulic conductivity value is calculated as 7.29×10^{-8} m/s for the heap leach pad area planned at the north.

The overall evaluation of the aquifer test results suggests that schists are the most conductive unit at both of these planned operation areas (north waste rock dump area and north heap leach pad area). Furthermore, hydraulic conductivity of the volcanics is very close to the schists. On the contrary, the Asartepe Formation, a widespread aquifer outside the study area within the Banaz Stream Basin, has lower hydraulic conductivity owing to its clayey content at the planned north heap leach pad area.

The Kışladağ Gold Mine area is located on the boundary that separates the Gediz and Büyük Menderes River Basins. The groundwater divide of the area is nearly in the same position, and the planned expansion areas are completely located on the Gediz River Basin. Highest groundwater level (1020 m) at this locality is observed at the present heap leach pad area located on the water divide where higher recharge occurs as a result of elevated topography. Groundwater levels at the planned north heap leach pad area decrease from 940 m to 870 m from southeast to northwest. At the west of the planned north waste rock dump where Emirli Hill is located, groundwater levels are also higher (960m) due to high elevation that results in higher recharge. Groundwater levels at this area decreases towards northwestern boundary to 810 m and towards eastern boundary to 920 m. Hydraulic gradient at the planned north heap leach pad and waste rock areas are about 0.03 and 0.08, respectively.

For the same area by digitally subtracting the groundwater elevation surface from the topographical surface, a depth to groundwater level map is generated (Figure 4.10). Examining this map, it is noted that at the topographically elevated southwestern parts of the planned north waste rock area, depth to groundwater is around 200-250 m. By declining topographical elevation towards north, water table depth decreases to 50 m, while towards the northeastern and eastern parts, along the valley of Söğütlü Creek, water table gets closer to the ground surface. At the planned north heap leach pad area, depth to water table is around 50 m in the vicinity of the present heap leach pad area and decreases towards north reaching close to the ground surface.

The groundwater facies was determined to be calcium, according to cations; however, while examining the anions, a bicarbonate characteristic is evident except for the observation wells

located on the North Heap Leach Pad area, which are: HY-7 is mixed-SO₄, HY-8 is Ca-SO₄, and HY-3 has a Ca-mixed character. Furthermore, the water facies of HY-10 and Weir-2 on the North Waste Rock Dump have a sulphate characteristic. The sulphate characters of waters are due to mineralization. Weir-2 and Weir-6 are identified as Class II. In the study area, there are 4 water points which are suitable for human consumption, and these are LP-5, HY-11, Weir-2 and Weir-6. Arsenic, cadmium, fluoride, nickel and lead are some of the parameters exceeding the limits for human consumption.

6.2 Recommendation

As a result of this study, it is recommended that wells drilled within the scope of this study in the North Waste Rock Dump and North Heap Leach Pad areas should be monitored continuously until the mining operations begin to provide sufficient baseline data. After obtaining permission for mining operations, some of the wells will need to be properly closed during the construction period, and new wells will be required in order to observe the impacts of facilities during operation and closure periods.

Quality control processes should be conducted by periodically evaluating all data collected from surface and groundwater (water levels, flow rates, water quality, meteorological etc.) in the scope of monitoring activities.

Results obtained from the Soil Water Balance (SWB) model can be further developed with field observations and other studies. Since this model covers a very extensive area, the results can be fine-tuned with additional observations while taking into consideration groundwater modeling.

Within the context of “Management of Surface Water Quality Regulation” (YSKYY, 2012), water quality measurements should be continued by re-evaluating the parameters of surface water and measurement frequency.

Within the scope of “Groundwater Pollution Control Regulation” (YKBKK, 2012), preliminary studies should be conducted before the parameter and threshold determination is completed by the General Directorate of Water Management.

REFERENCES

- ARC, 2011, Geology of Northern Part of the Kışladağ Area (Around Örenköy-Küçükyaşlı-Güzelköy).
- Aysan, 1979, The Hydrogeological Investigation Report for Uşak Springs. Devlet Su İşleri Gen. Müd., Ankara.
- Cronshey, R., McCuen, R., Miller, N., Rawis, W., Robbins, S., and Woodward, D., 1986, Urban Hydrology for Small Watersheds-TR-55 (2nd ed.): Washington, D.C., U.S. Dept. of Agriculture, Soil Conservation Service, Engineering Division, Technical Release 55, 164 p.
- Dalgün, N., 1988, Penman Formülüyle Potansiyel Evapotranspirasyon Değerlerinin Bulunması ve Türkiye'deki Dağılımları, Devlet Meteoroloji İşleri Genel Müdürlüğü (DMİ), Ankara.
- DSİ, 1955, Hydrogeological Investigation Report for Drinking Water Supply to Some of the Villages in Karahallı and Ulubey Districts of Uşak Provinces. Devlet Su İşleri Gen. Müd., Ankara.
- DSİ, 1976, Uşak, Banaz ve Sivashlı Ovaları Hidrojeolojik Etüt Raporu. Devlet Su İşleri Gen. Müd., Ankara.
- DSİ, 1993, Uşak, Banaz, Ulubey, Sivashlı ve Karahallı Ovaları Hidrojeolojik Etüt Raporu. Devlet Su İşleri Gen. Müd. II. Bölge, İzmir.
- Encon, Knight Piesold, Planning Alliance, 2011, Kışladağ Altın Madeni Kapasite Artırımı Çevresel Etki Değerlendirmesi Raporu. Çevre ve Orman Bakanlığı, Ankara.
- Ercan, T., Dinçel, A., Metin, S., Türkecan, A., ve Günay, E., 1978, Uşak Yöresindeki Neojen Havzalarının Jeolojisi. TJK Bülteni, 21, 97-106.
- EU, 1998, On Quality of Water Intended for Human Consumption, Council Directive 98/83/EC of 3 November 1998. Official Journal of European Communities.
- Hargreaves, G.H., and Samani, Z.A. (1985), "Reference Crop Evapotranspiration from Temperature." Applied Eng. in Agric., 1(2):96-99.
- Herod O., Hodkiewicz P., 2010, Kışladağ Structural Geology Review.
- Hudson, M. Donald., 2009, Geology of Part of the Kışladağ-Sayacık Area Turkey.
- İl Özel İdaresi, 2000, Hane Sayıları.
- İTAS, 2005. İnsani Tüketim Amaçlı Sular Hakkında Yönetmelik, Resmi Gazete No: 25730.
- Jensen, M.E., and Haise, R.H., 1963, Estimating Evapotranspiration from Solar Radiation. Journal of Irrigation and Drainage Division, American Society of Civil Engineers, v.89, p.15-41.
- Kadioğlu, 1993, Hydrogeological Investigation Report of Uşak-Banaz-Sivashlı and Karahallı Plains

- Karaođlu, Ö., Helvacı C., Ersoy, E.Y., 2010. Petrogenesis and $^{40}\text{Ar}/^{39}\text{Ar}$ Geochronology of the NE–SW-trending Uşak–Güre basin, western Türkiye
- Kuşçu, İ., 2008, Structural Mapping of the Open Pit, Kışladağ Gold Mine.
- Lewis Geoscience Services Inc., Report on Geological Mapping and Structural Analysis, Kışladağ Gold Project, 2002.
- MTA, 2002, 1:500.000 Ölçekli Türkiye Jeoloji Haritası, MTA Genel Md. Yayınları, Ankara.
- Murphy Geological Services, Structural Interpretation of Landsat ETM+ Scene No. 179/33 for West-Central Turkey, 2004.
- SKKY, 2008, Su kirliliđi Kontrol Yönetmeliđinde Deđişiklik Yapılmasına Dair Yönetmelik, Resmi Gazete No: 267856.
- SRK Consulting, Groundwater and Surface Water Monitoring Plan Kışladağ Property, 2002.
- SRK Consulting, Water Quality Sampling and Analysis Kışladağ Property, 2003.
- SRK Consulting, Water Supply Studies-Aquifer Test Kışladağ Project, 2003.
- SRK Consulting, Water Supply Exploration Studies Kışladağ Project, 2005.
- SRK Consulting, Conceptual Hydrogeological Model, Kışladağ Property, 2005.
- SRK Consulting, Manual for Automatic Stage Gauges, January, 2006.
- SRK Consulting, Assessment on Pit Lake Formation & Impacts on Groundwater System Kışladağ Project, 2007.
- SRK Consulting, Kışladağ Open Pit Dewatering/Depressurization Study, 2012.
- Thornthwaite, C.W.; Mather, J.R., 1957, Instructions and Tables for Computing Potential Evapotranspiration and the Water Balance. Publications in Climatology 10, No.3: p. 185-311.
- Turc, L., 1961, Evaluation des Besoins en Eau D'irrigation, Evapotranspiration Potentielle, Formule Climatique Simplifee et Mise a Jour. (In French: original not seen). Annales Agronomiques 12(1):13-49.
- TÜİK (Türkiye İstatistik Kurumu), 2012, Genel Nüfus Sayımı Sonuçları.
- Türkeş, M., 1996, Spatial and Temporal Analysis of Annual Rainfall Variations in Turkey, International Journal of Climatology, Vol. 16, 1057-1076.
- Vaytaş, 2006, Uşak İli İçme Suyu Projesi, Uşak-Merkez ve Uşak-Merkez-Susuzören Lokasyonu, Hidrojeolojik Etüt Raporu.
- Westenbroek, S.M., Kelson, V.A., Dripps, W.R., Hunt, R.J., and Bradbury, K.R., 2010, SWB—A modified Thornthwaite-Mather Soil-Water-Balance code for estimating groundwater recharge: U.S. Geological Survey Techniques and Methods 6–A31, 60 p.
- Yazıcıgil, H., Doyuran, V., Yılmaz K.K., Yeşilnacar, E., Kansu, E., 2000, Determination of Areas with Potential to Supply Water to the Gümüşkol Mine Project of Tüprağ Metal Mining Company, Proje No: 00-0309-2-00-03, Middle East Technical University.

Yazıcıgil, H., Toprak V., Çamur M.Z., Süzen M.L., Ünsal-Erdemli, B., Sevilmiş V., 2008, Uşak-Ulubey Akiferleri Hidrojeolojik Etüdü ve Yeraltıları Yönetim Planı, Proje No: 07-03-09-2-00-04 & 07-03-09-2-00-07, Orta Doğu Teknik Üniversitesi.

Yazıcıgil, H., Yılmaz, K.K., Ünsal-Erdemli, B., 2011, Surface Water Supply Investigation for Kışladağ Gold Mine, Middle East Technical University, Geological Engineering Department, METU Project No: 10-03-09-2-00-16, 66 pages.

Yazıcıgil, H. ve Yılmaz, K.K., 2011, Technical Memorandum: Design Specifications for Weir-6, Report submitted to TÜPRAG, 16 pages.

Yazıcıgil, H., Çamur M.Z., Yılmaz K.K., Ünsal B., Fırat E., 2013, Hydrogeological Characterization of the Kışladağ Gold-Mine Area, Project No: 11-03-09-2-00-17, Middle East Technical University.

YKBKK, 2012, Yeraltılarının Kirlenme ve Bozulmaya Karşı Korunması Hakkında Yönetmelik, Resmi Gazete No. 28257.

YSKYY, 2012, Yüzeysel Su Kalitesi Yönetimi Yönetmeliği, Resmi Gazete No: 28483.

WHO, 2011, Guide Lines for Drinking Water Quality. World Health Organization.

APPENDIX A

WELLS IN THE STUDY AREA AND ITS VICINITY

Table A.1 Wells in the study area and its vicinity (Yazicigil et al., 2013)

Observation Points	Coordinates		Elevation (m)	Observation Period	Type	Location	Formation	Depth (m)	Screen Interval	Hydraulic Conductivity K (m/s)
	Easting	Northing								
KWSP-1	688211	4262054	1000.000	2000-2005	Caisson Well	Open Pit	Volcanics	10.0	-	
KWSP-10	687158	4265822	886.000	2002-Present	Water Well	North Waste Rock Dump Area	Schist		-	
KWSP-11	694314	4259546	820.000	2002-2005	Water Well	Outside the Mine Area	Ulubey FM		-	
KWSP-15	688008	4263524	998.283	2002-2005	Observation Well	South Heap Leach Pad Area	Volcanics - Schist		32.7-45.7	
KWSP-16	688109	4262350	1002.651	2002-2011	Observation Well	Open Pit	Intrusives	100.0	-	
KWSP-17	687473	4261725	1013.780	2002-2005	Exploration Well	Open Pit	Ore Zone	250.0	180-240	4.07E-09
KWSP-18	686694	4260361	922.848	2003-2006	Exploration Well	South Waste Rock Dump Area	Volcanic Conglomerate		0-70	2.00E-08
KWSP-20	696527	4253663	690.000	2003-2004	Water Well	Outside the Mine Area	Ulubey FM		-	
KWSP-21	685832	4260561	1009.782	2003-2004	Observation Well	South Waste Rock Dump Area	Volcanic Conglomerate	40.0	-	
KWSP-23	685848	4260617	1009.841	2004-2005	Observation Well	South Waste Rock Dump Area	Volcanic Conglomerate	20.0	-	
KWSP-24	686115	4260100	992.151	2004-2009	Observation Well	South Waste Rock Dump Area	Volcanic Conglomerate	20.0	-	
WR-1	685785	4260862	1056.500	2005- Present	Observation Well	South Waste Rock Dump Area	Volcanics	32.0	8-28	
WR-1A	685787	4260851	1056.670	2012- Present	Observation Well	South Waste Rock Dump Area	Volcanics	61.0	12-60	
WR-2	687283	4259743	881.660	2005- Present	Observation Well	South Waste Rock Dump Area	Volcanic Conglomerate	52.5	16-52	3.66E-07
WR-3	687396	4259609	876.910	2005- Present	Observation Well	South Waste Rock Dump Area	Volcanic Conglomerate	51.0	14-50	2.55E-07
WR-4	687375	4260004	920.060	2005- Present	Observation Well	South Waste Rock Dump Area	Volcanics	40.5	16-40	1.61E-06
WR-5	687204	4259630	890.000	2005- Present	Observation Well	South Waste Rock Dump Area	Porphyry Latite Lava	40.5	16-40	5.02E-07
WR-6	687953	4258737	844.740	2005- Present	Observation Well	South Waste Rock Dump Area	Volcanic Conglomerate	32.0	12-31	2.17E-07
LP-1	687679	4262887	975.560	2005- Present	Observation Well	South Heap Leach Pad Area	Volcanoclastics	51.0	14-50	2.39E-07
LP-2	687501	4263932	938.150	2005- Present	Observation Well	South Heap Leach Pad Area	Schist	51.0	28-50	2.00E-07
LP-3	687499	4263927	937.990	2005- Present	Observation Well	South Heap Leach Pad Area	Volcanic Breccia	21.0	6-20	1.70E-07
LP-4A	687473	4264687	924.800	2012- Present	Observation Well	South Heap Leach Pad Area	Schist	90.0	50-86	9.54E-08

Table A.1 Wells in the study area and its vicinity (continued)

Observation Points	Coordinates		Elevation (m)	Observation Period	Type	Location	Formation	Depth (m)	Screen Interval	Hydraulic Conductivity	
	Eastings	Northing								K	(m/s)
LP-4	687550	4264670	930.830	2011-2012	Observation Well	South Heap Leach Pad Area	Volcanic Breccia - Schist	54.0	16-48	1.18E-07	
LP-5A	687481	4264689	925.430	2012- Present	Observation Well	South Heap Leach Pad Area	Volcanic Breccia	34.0	14-30	9.01E-07	
LP-5	687630	4264678	941.822	2011-2012	Observation Well	South Heap Leach Pad Area	Volcanic Breccia	34.0	13.5-33.5	8.65E-09	
LP-6	687561	4265227	939.250	2011- Present	Observation Well	South Heap Leach Pad Area	Schist	180.0	148-176	2.61E-06	
LP-7	687568	4265225	939.680	2011- Present	Observation Well	South Heap Leach Pad Area	Asartepe FM	62.0	24-56		
LP-8	688602	4264058	1033.120	2005- Present	Observation Well	South Heap Leach Pad Area	Volcanic- Schist	150.0	130-150	1.80E-07	
LP-9	688599	4264061	1032.990	2005- Present	Observation Well	South Heap Leach Pad Area	Volcanoclastics	85.0	20-80	1.45E-07	
LP-10	688629	4263363	1085.610	2005- Present	Observation Well	South Heap Leach Pad Area	Volcanoclastics	80.0	20-80	1.49E-07	
LP-11	687609	4263388	953.550	2005- Present	Observation Well	South Heap Leach Pad Area	Schist	51.0	14-50	5.85E-07	
PZ-2	687981	4261617	1051.660	2007-2012	Observation Well	Open Pit	Pyroclastics	310.0	145-305		
PZ-3	687895	4261897	1013.560	2007- Present	Observation Well	Open Pit	Pyroclastics	286.0	136-280		
PZ-4	687303	4262066	1003.290	2007-2011	Observation Well	Open Pit	Pyroclastics - Schist	312.0	103-307		
PZ-5	687064	4261303	1039.470	2007-2009	Observation Well	Open Pit	Pyroclastics	340.0	139-335		
PZ-6	686930	4261600	995.530	2007-2010	Observation Well	Open Pit	Pyroclastics - Ore Zone	288.0	94-282		
PZ-7	687715	4261196	1056.830	2007-2010	Observation Well	Open Pit	Pyroclastics - Ore Zone	336.0	153-329		
WS-1	687501	4263932	938.431	-	Water Well	South Heap Leach Pad Area	Volcanics-Schist	200.0	12-196	1.09E-07	
WS-2	687708	4265237	933.954	-	Water Well	South Heap Leach Pad Area	Schist	200.0	40-196	1.02E-07	
WS-3	686916	4262303	946.130	2007- Present	Observation Well	Outside the Mine Area	Volcanics- Schist	200.0	56-196	2.24E-09	
HY-1	687504	4266387	968.390	2012- Present	Observation Well	Study Area	Asartepe FM	86.0	48-80	5.34E-08	
HY-2	686495	4266971	957.850	2012- Present	Observation Well	Study Area	Asartepe FM	68.0	32-64	dry	
HY-3	688528	4266947	894.510	2012- Present	Observation Well	North Heap Leach Pad Area	Schist	51.0	22-42	9.55E-08	
HY-4	687415	4267418	971.550	2012- Present	Observation Well	Study Area	Asartepe FM	102.0	51-95	2.50E-09	

Table A.1 Wells in the study area and its vicinity (continued)

Observation Points	Coordinates		Elevation (m)	Observation Period	Type	Location	Formation	Depth (m)	Screen Interval	Hydraulic Conductivity	
	Easting	Northing								K	(m/s)
HY-5	686448	4266335	893.880	2012- Present	Observation Well	North Waste Rock Dump Area	Volcanoclastics	64.0	28-60		6.99E-08
HY-6	686463	4265801	935.950	2012- Present	Observation Well	North Waste Rock Dump Area	Volcanoclastics	100.0	28-96		9.22E-08
HY-7	689347	4266714	911.260	2012-2012	Observation Well	North Heap Leach Pad Area	Schist	55.3	23.3-51.3		1.19E-08
HY-8	688809	4266330	917.350	2012- Present	Observation Well	North Heap Leach Pad Area	Schist	51.0	27-47		3.79E-07
HY-9	685169	4266344	888.215	2012- Present	Observation Well	North Waste Rock Dump Area	Porphyry Latite - Volcanic Breccia	181.0	52-168		4.56E-09
HY-10	686841	4264583	973.305	2012- Present	Observation Well	North Waste Rock Dump Area	Pyroclastics	101.7	37.7-93.7		6.44E-08
HY-11	685847	4264679	1128.835	2012- Present	Observation Well	North Waste Rock Dump Area	Volcanic Breccia	200.0	52-192		7.84E-08
GC-445	687520	4262499	984.690	2011- Present	Observation Well	Open Pit	Pyroclastics	292.9	140.5-190.5		
GC-446	687631	4261897	979.558	2011	Geotechnical Well	Open Pit		461.5	-		
GC-447	687874	4262449	986.010	2011- Present	Observation Well	Open Pit	Pyroclastics	848.5	310-360		
GC-448	687159	4260961	1046.401	2011	Observation Well	Open Pit	Pyroclastics	500.5	251-301		
GC-449	686797	4261567	1006.340	2011- Present	Observation Well	Open Pit	Intrusives	419.5	128-178		
GC-450	687659	4261617	925.615	2011	Geotechnical Well	Open Pit		500.0	-		
GC-451	687506	4266384	968.460	2011- Present	Observation Well	Study Area	Schist	300.6	110-130		
GC-452	686592	4266929	955.841	2011	Geotechnical Well	Study Area		350.5	-		
GC-453	688733	4265528	1005.330	2011- Present	Observation Well	North Heap Leach Pad Area	Schist	300.1	100-120		
GC-454	686445	4266336	893.920	2011- Present	Observation Well	North Waste Rock Dump Area	Schist	301.0	210-242		
GC-455	686461	4265803	935.380	2011- Present	Observation Well	North Waste Rock Dump Area	Schist	287.7	230-280		
GC-456	686931	4263701	974.681	2011- Present	Exploration Well	North Waste Rock Dump Area		302.0	-		
GC-457	687299	4264017	938.530	2011- Present	Observation Well	North Waste Rock Dump Area	Schist	302.5	114-142		
KPT-1	687809	4260836	1039.050	2012- Present	Observation Well	Open Pit	Pyroclastics	498.0	94-498		2.10E-08
KPT-2	687677	4261558	940.010	2012-2012	Observation Well	Open Pit	Intrusives	262.0	54-262		1.10E-06

Table A.1 Wells in the study area and its vicinity (continued)

Observation Points	Coordinates		Elevation (m)	Observation Period	Type	Location	Formation	Depth (m)	Screen Interval	Hydraulic Conductivity	
	Eastings	Northing								K (m/s)	
KPT-3	687679	4261541	940.110	2012-2012	Observation Well	Open Pit	Intrusives	316.0	60-280	7.83E-07	
KPT-4	687667	4261564	939.900	2012-2012	Observation Well	Open Pit	Intrusives	153.0	0-1.53	1.07E-06	
PBPW-01	687538	4261699	869.939	2012	Observation Well	Open Pit	Intrusives	35.45	13.45-35.45		
PBMW-01	687551	4261699	870.001	2012	Observation Well	Open Pit	Intrusives	33.07	21.07-33.07		
PBMW-02	687527	4261700	870.016	2012	Observation Well	Open Pit	Intrusives	26.79	6.79-26.79		
PBMW-03	687539	4261687	869.883	2012	Observation Well	Open Pit	Intrusives	28.75	6.75-28.75		
PBMW-04	687534	4261714	870.109	2012	Observation Well	Open Pit	Intrusives	37.02	15.02-37.02		
PBMW-05	687518	4261711	870.149	2012	Observation Well	Open Pit	Intrusives	32.74	10.74-32.74		
PBMW-06	687518	4261681	869.639	2012	Observation Well	Open Pit	Intrusives	35.57	23.57-35.57		
DH-2	688100	4267760	864.961	2012	Geotechnical Well	Study Area	Schist	22.0	No Casing		
DH-3	688353	4267039	911.150	2012	Geotechnical Well	North Heap Leach Pad Area	Schist	29.0	No Casing		
DH-4	688168	4266665	944.320	2012	Geotechnical Well	North Heap Leach Pad Area	Schist	28.0	No Casing		
DH-7A	687577	4265687	934.700	2012	Geotechnical Well	Study Area	Alluvium - Volcanic Breccia	30.0	No Casing		
DH-8A	688902	4265645	1007.830	2012	Geotechnical Well	North Heap Leach Pad Area	Schist	20.0	No Casing		
DH-9	688975	4266616	910.986	2012	Geotechnical Well	North Heap Leach Pad Area	Volcanic Conglomerate	30.0	No Casing		
DH-10A	688227	4265948	967.880	2012	Geotechnical Well	North Heap Leach Pad Area	Volcanic Breccia	22.0	No Casing		

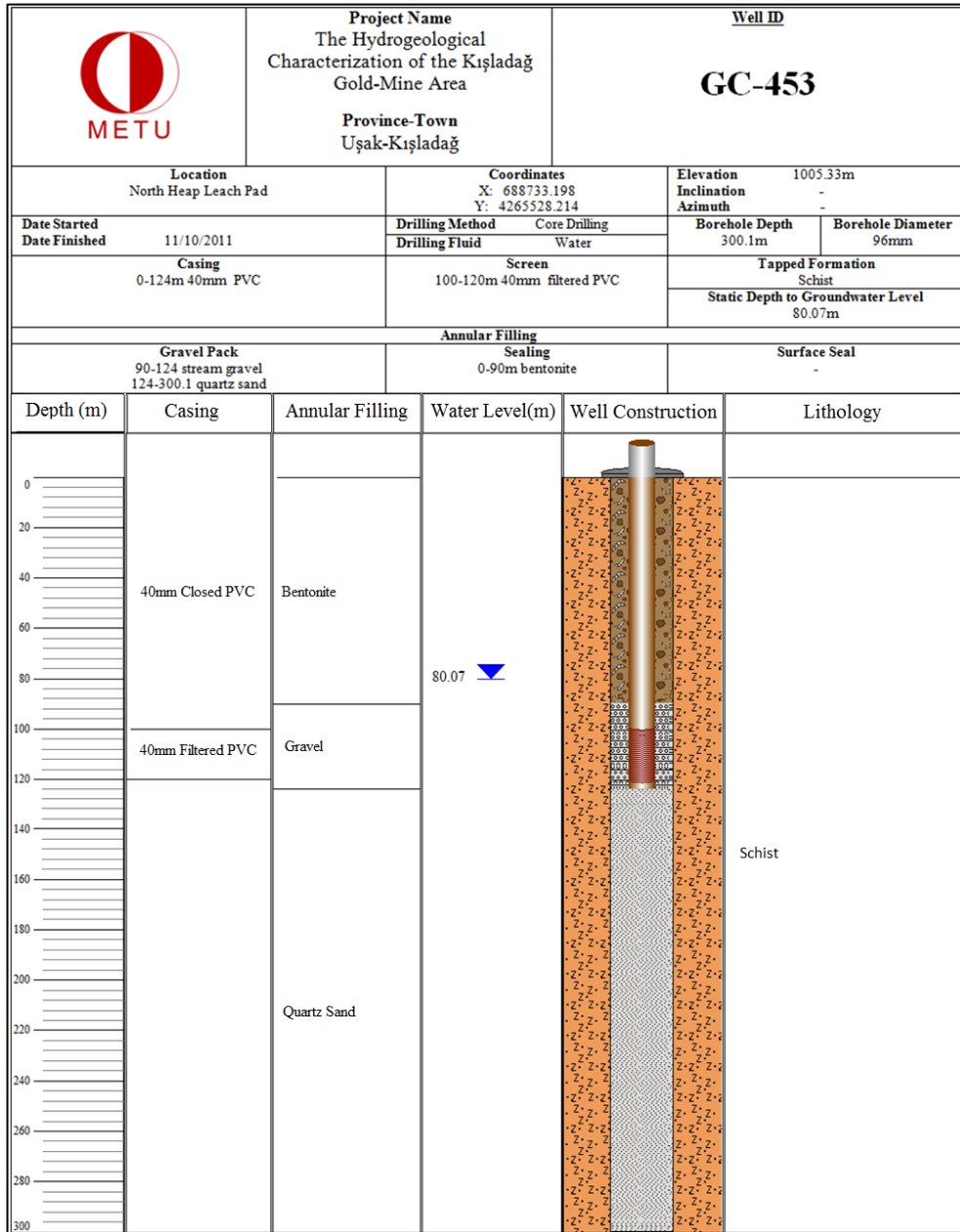


Figure B.2 The detailed well logs of GC-453

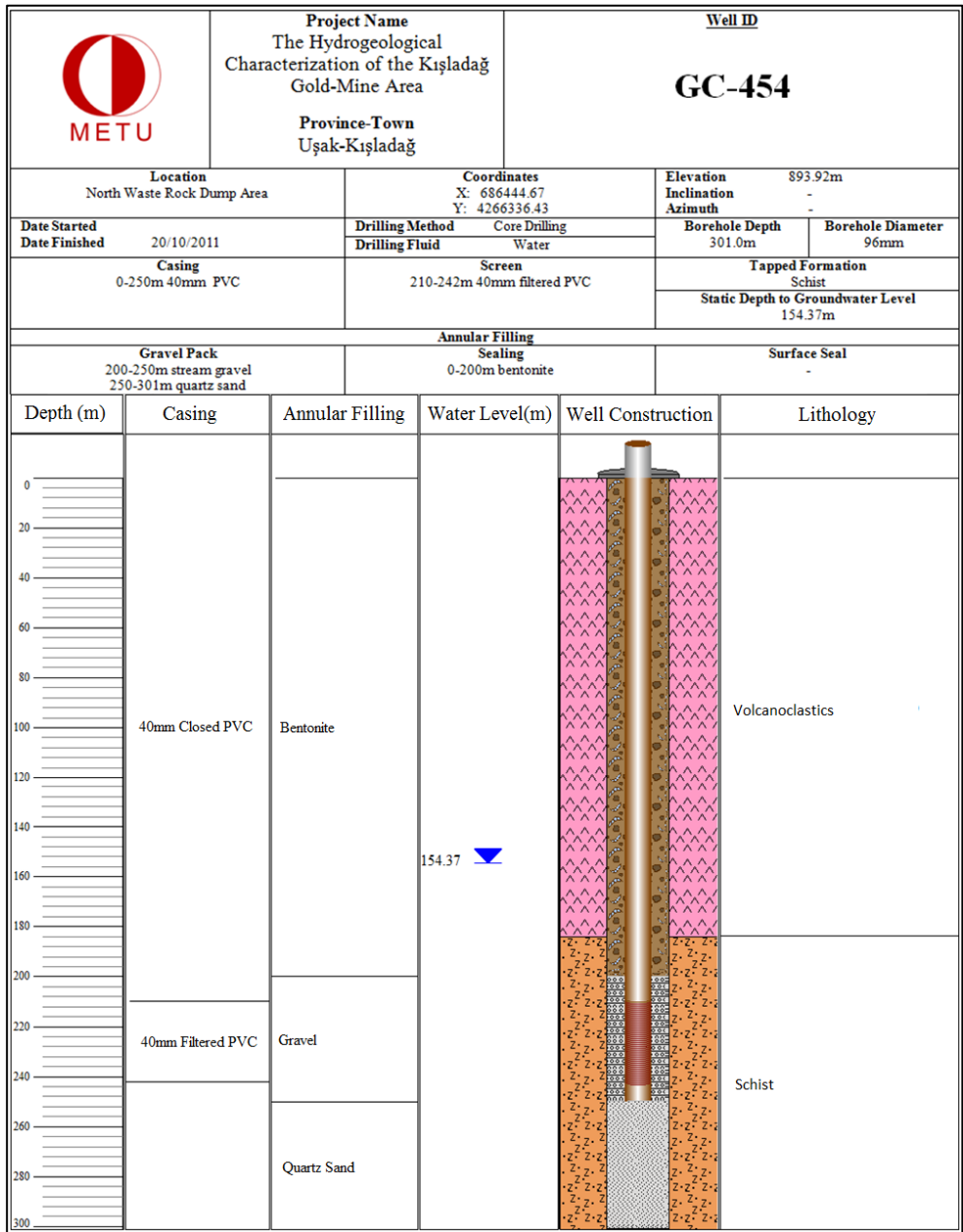


Figure B.3 The detailed well logs of GC-454

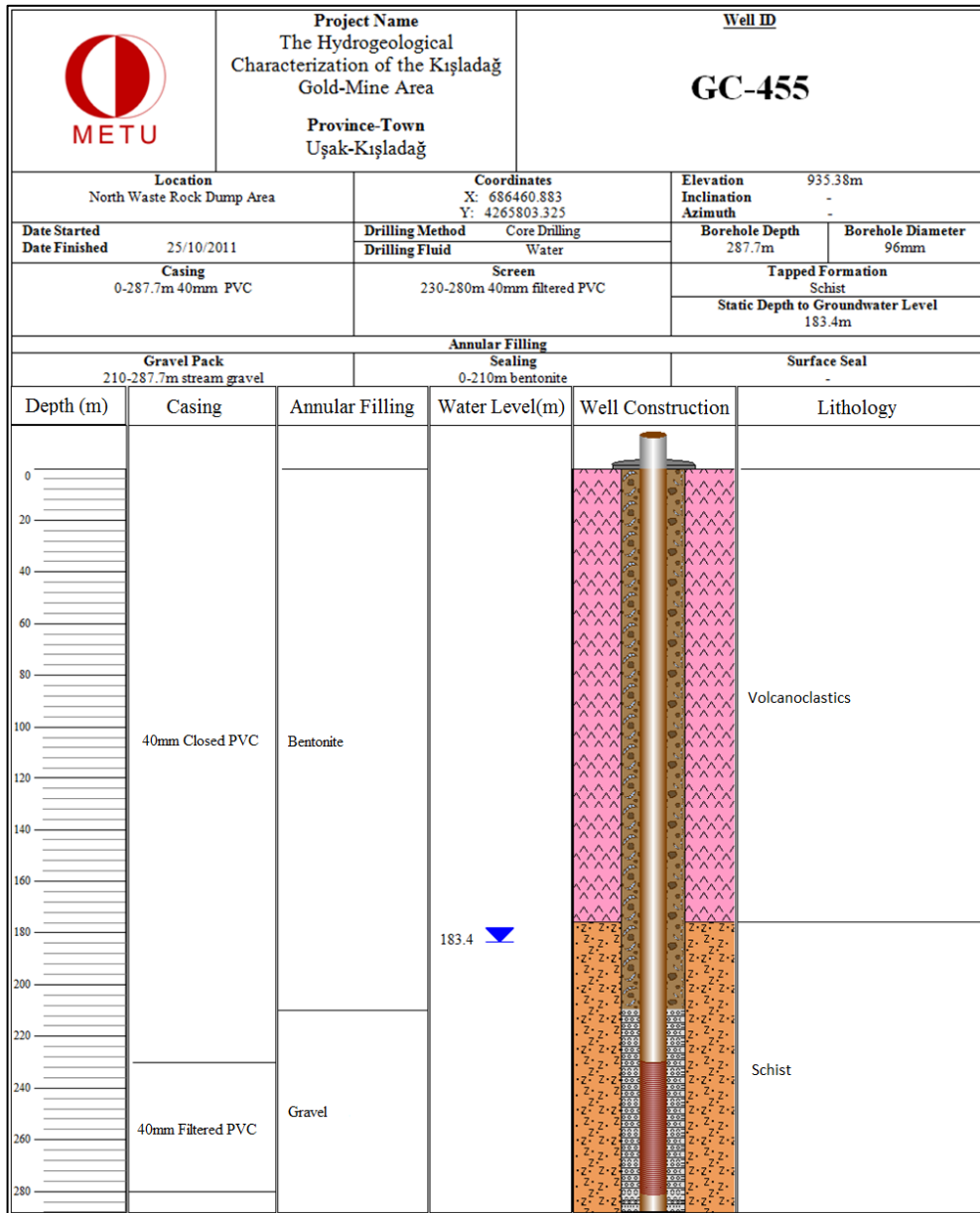


Figure B.4 The detailed well logs of GC-455

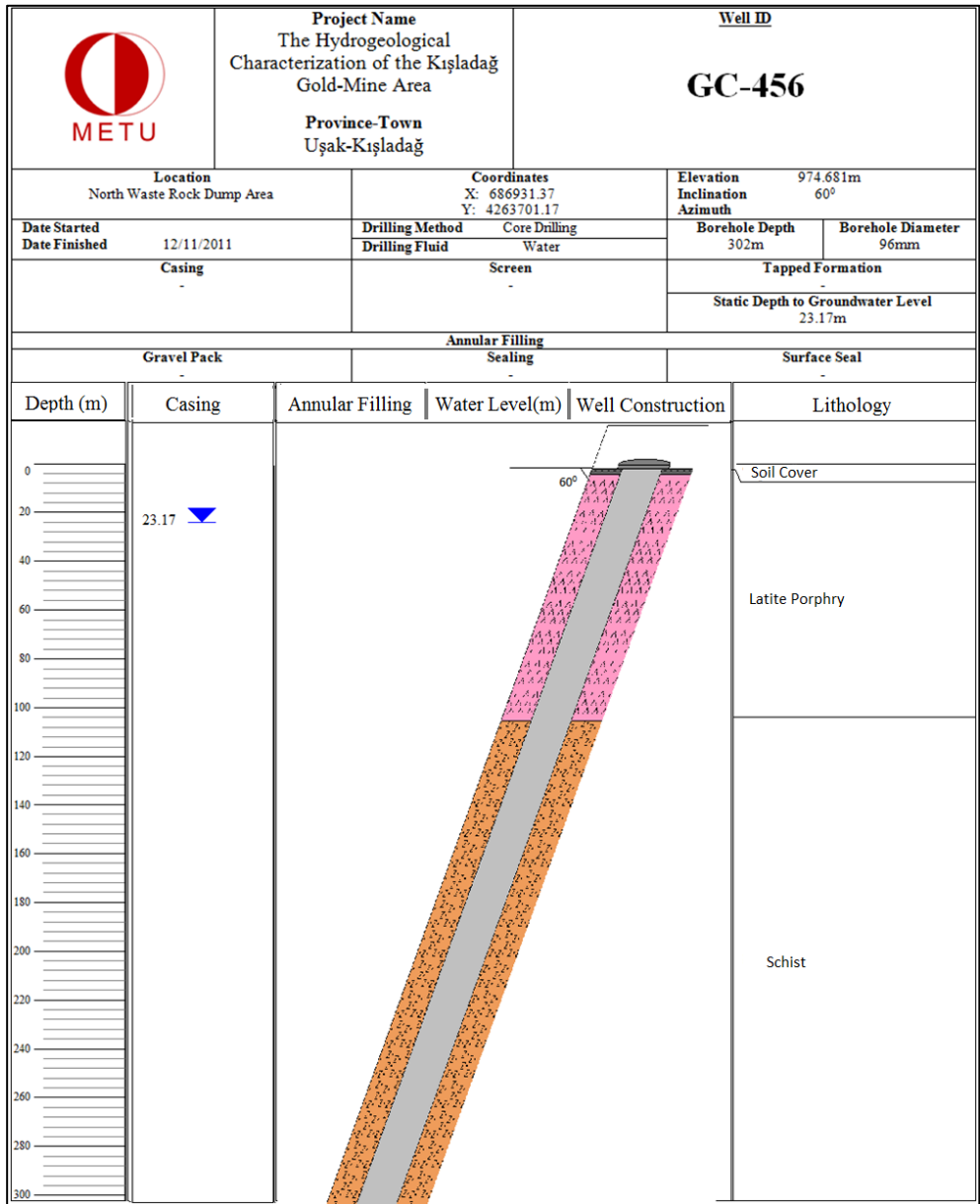


Figure B.5 The detailed well logs of GC-456

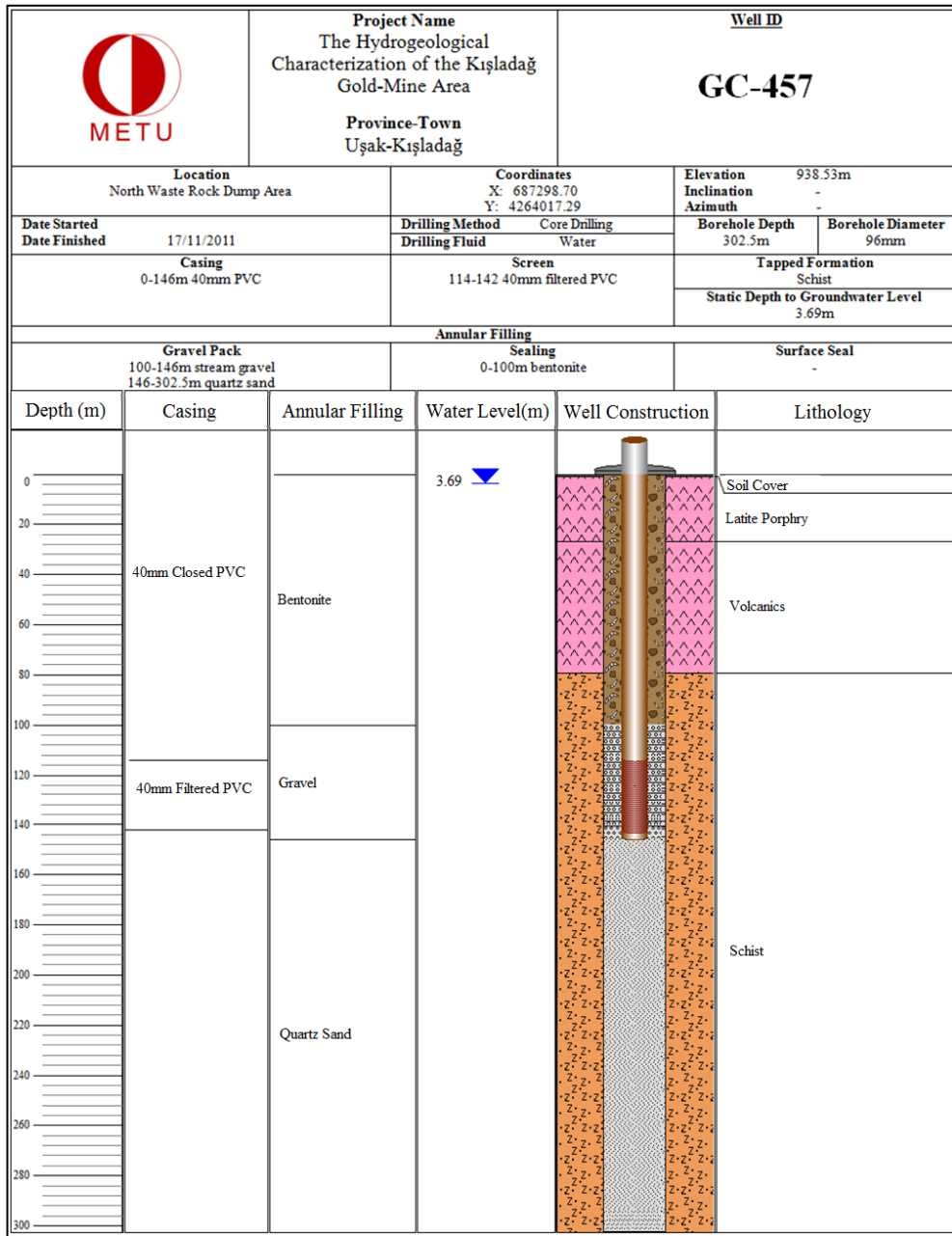


Figure B.6 The detailed well logs of GC-457

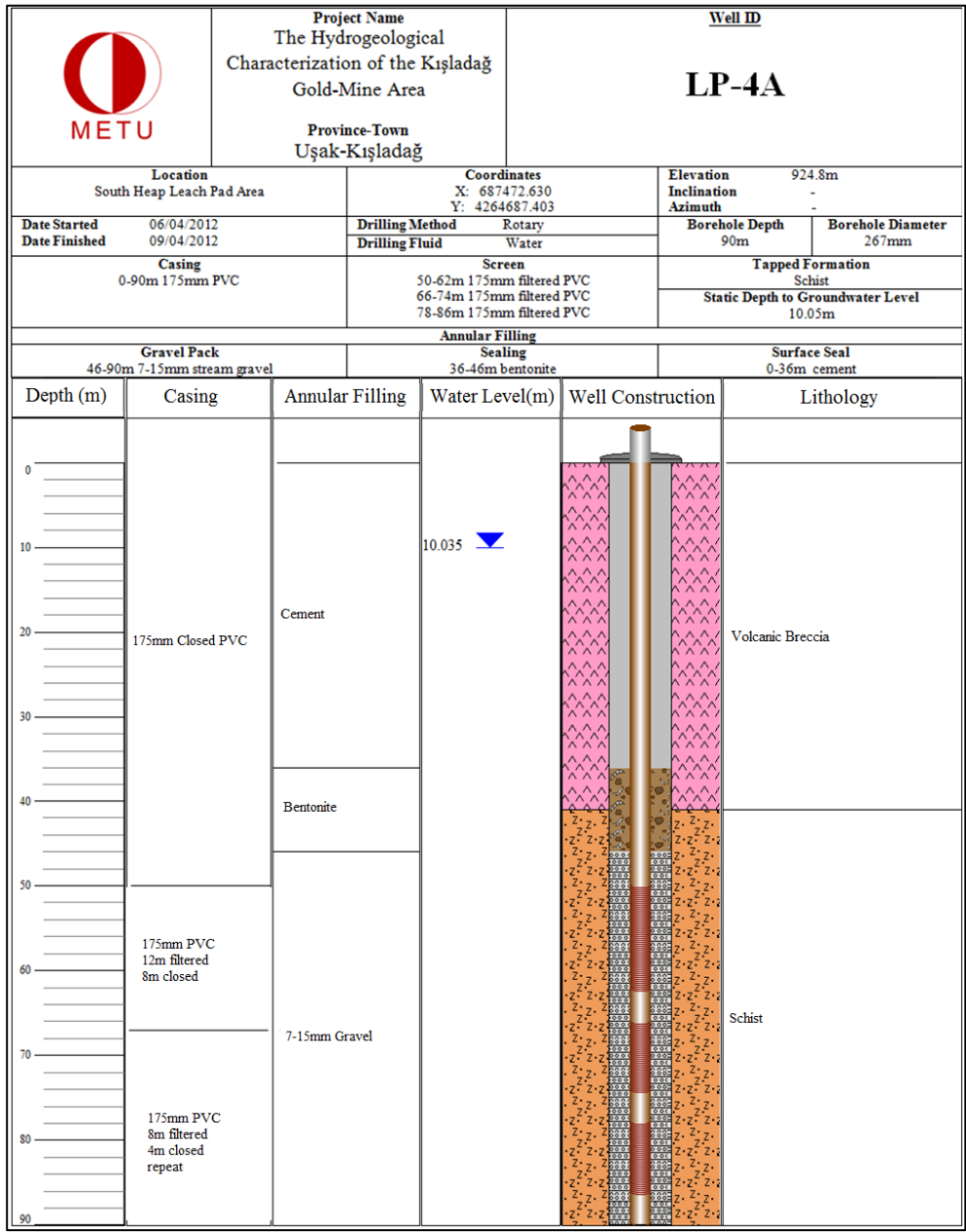


Figure B.7 The detailed well logs of LP-4A

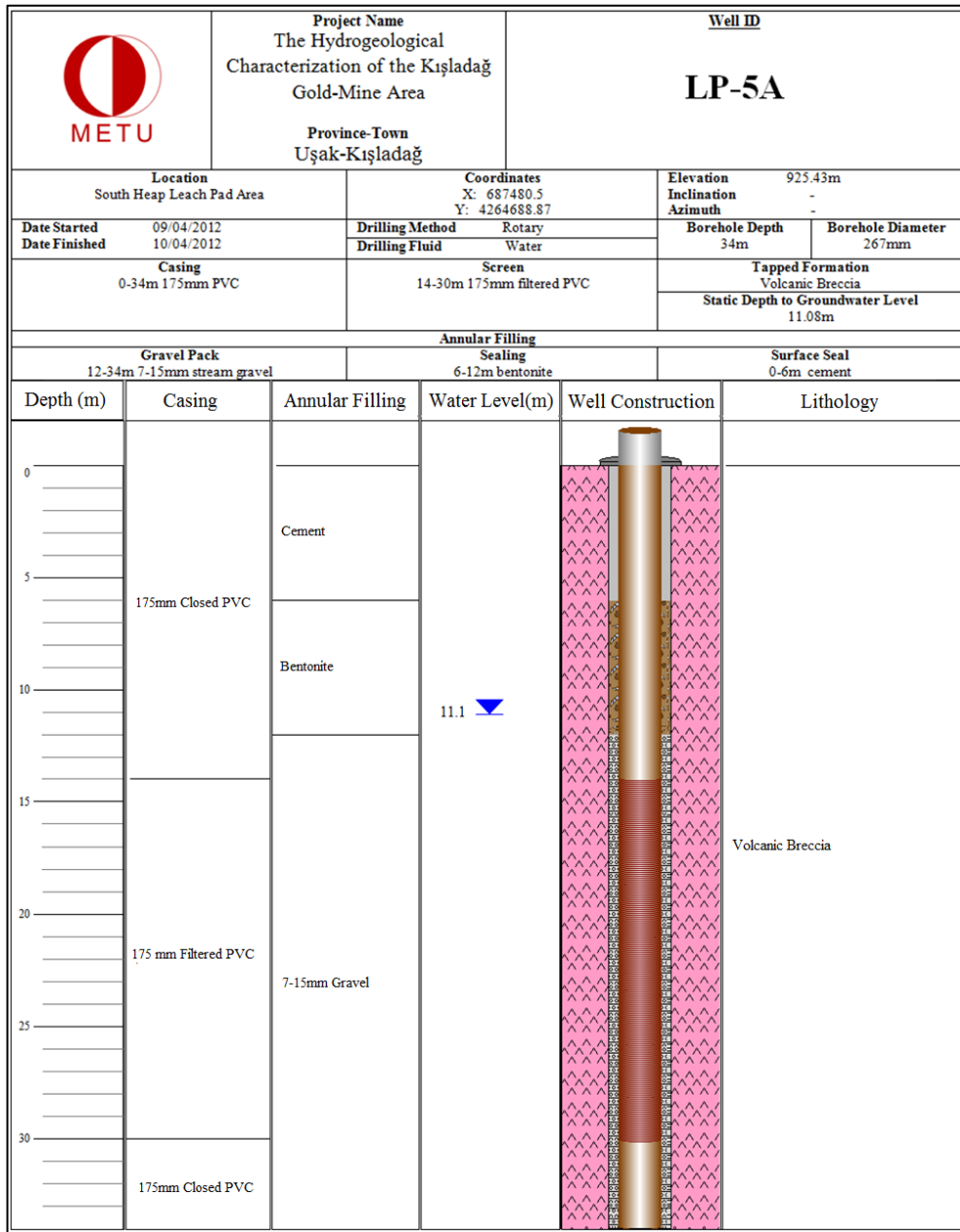


Figure B.8 The detailed well logs of LP-5A

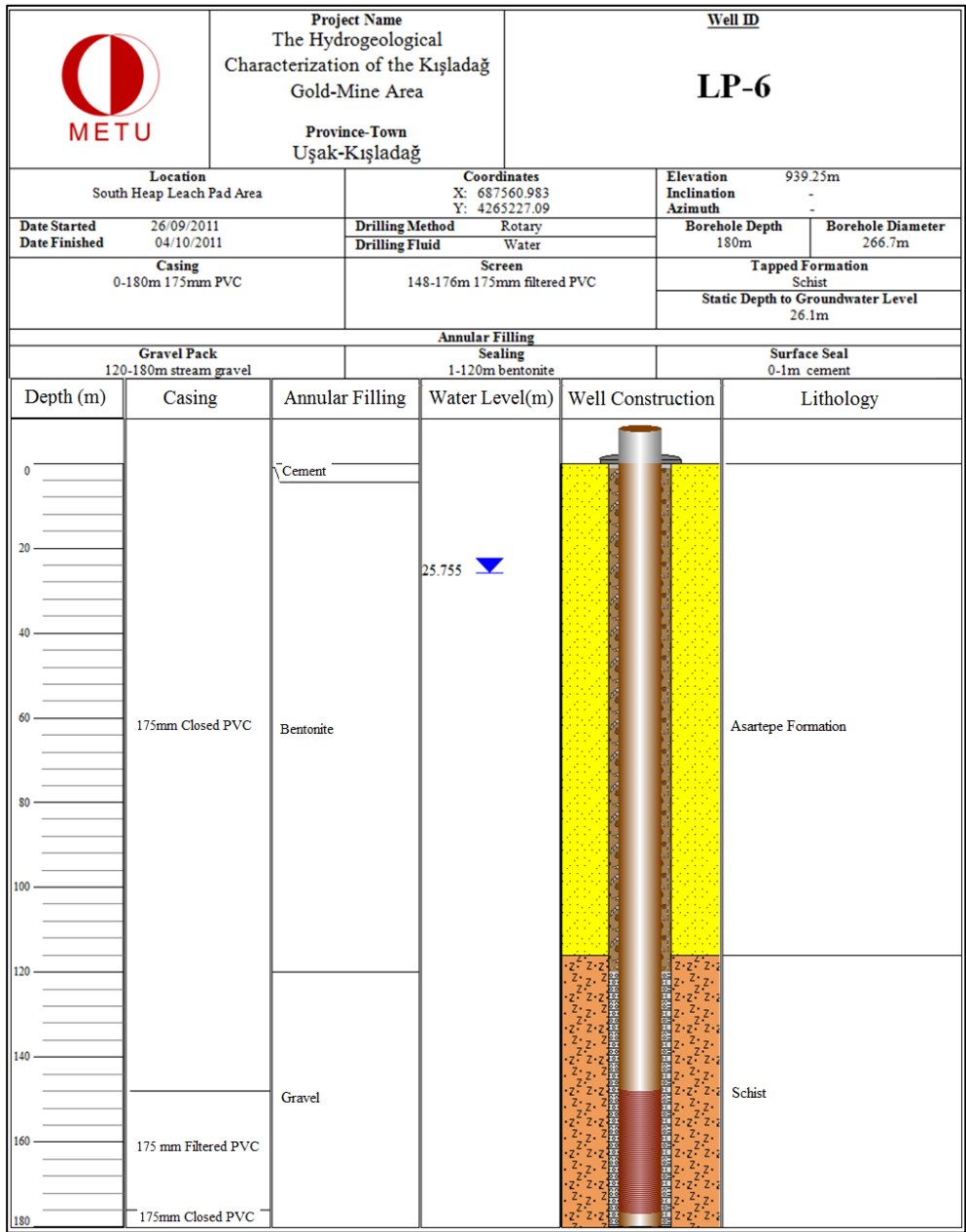


Figure B.9 The detailed well logs of LP-6

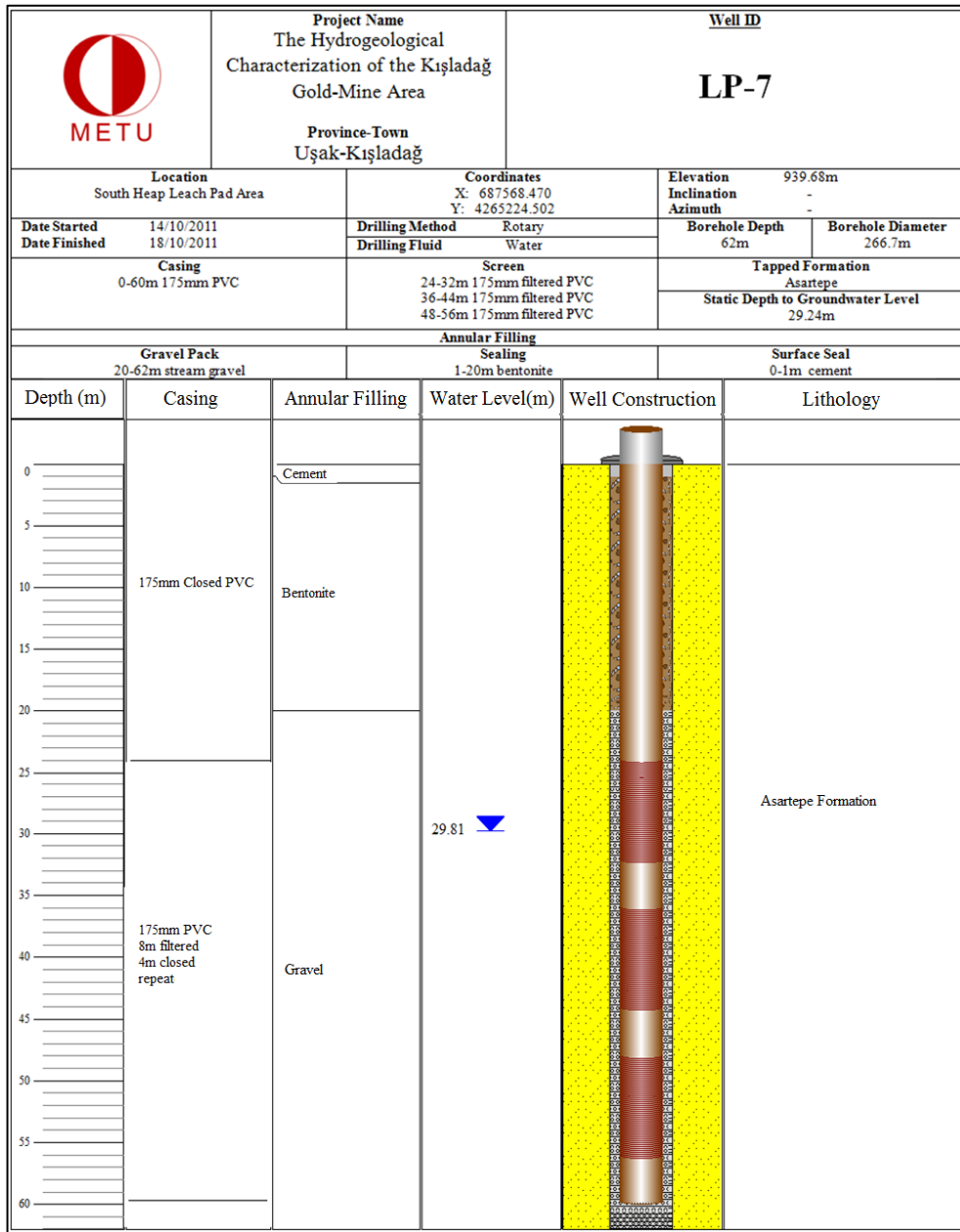


Figure B.10 The detailed well logs of LP-7

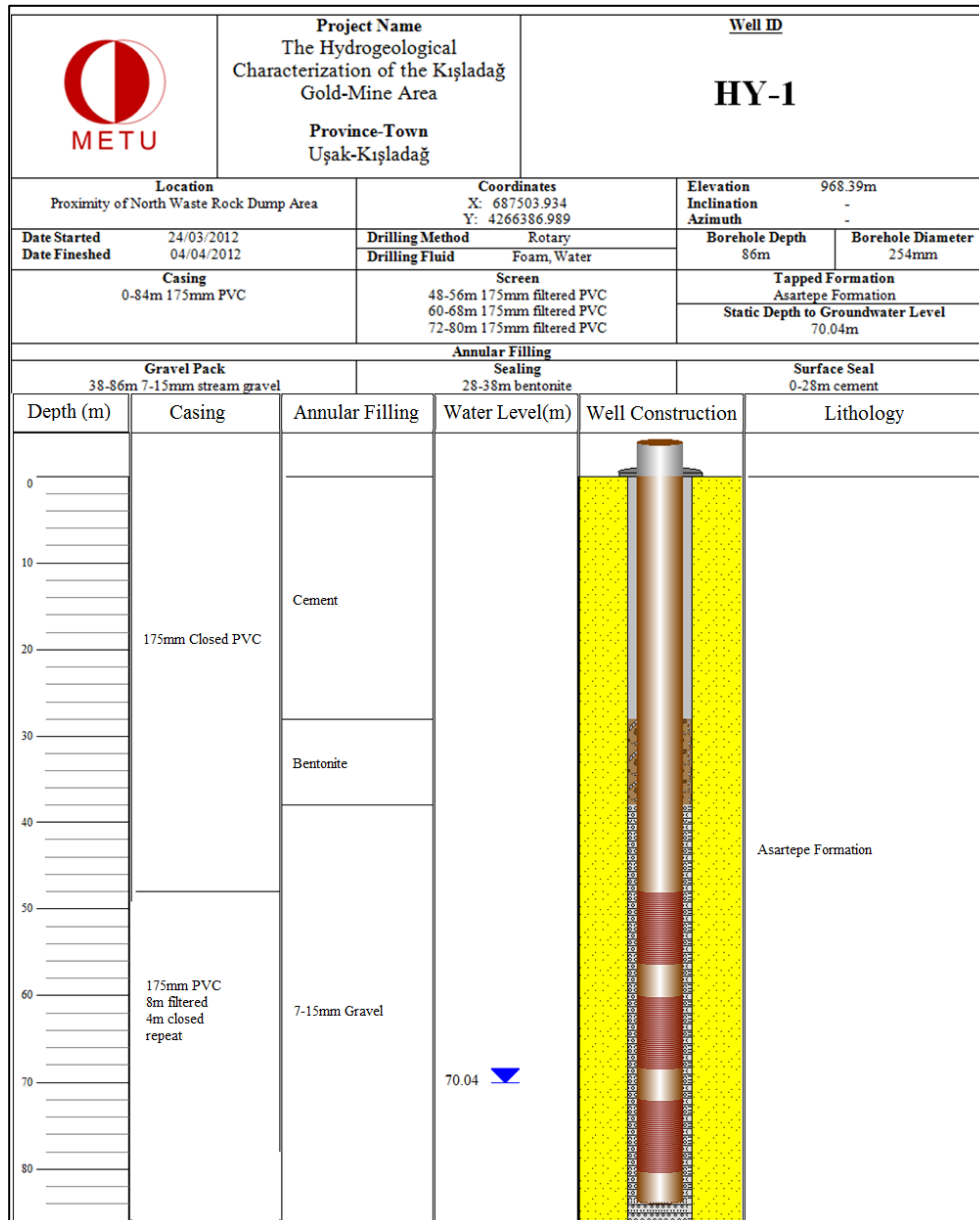


Figure B.11 The detailed well logs of HY-1

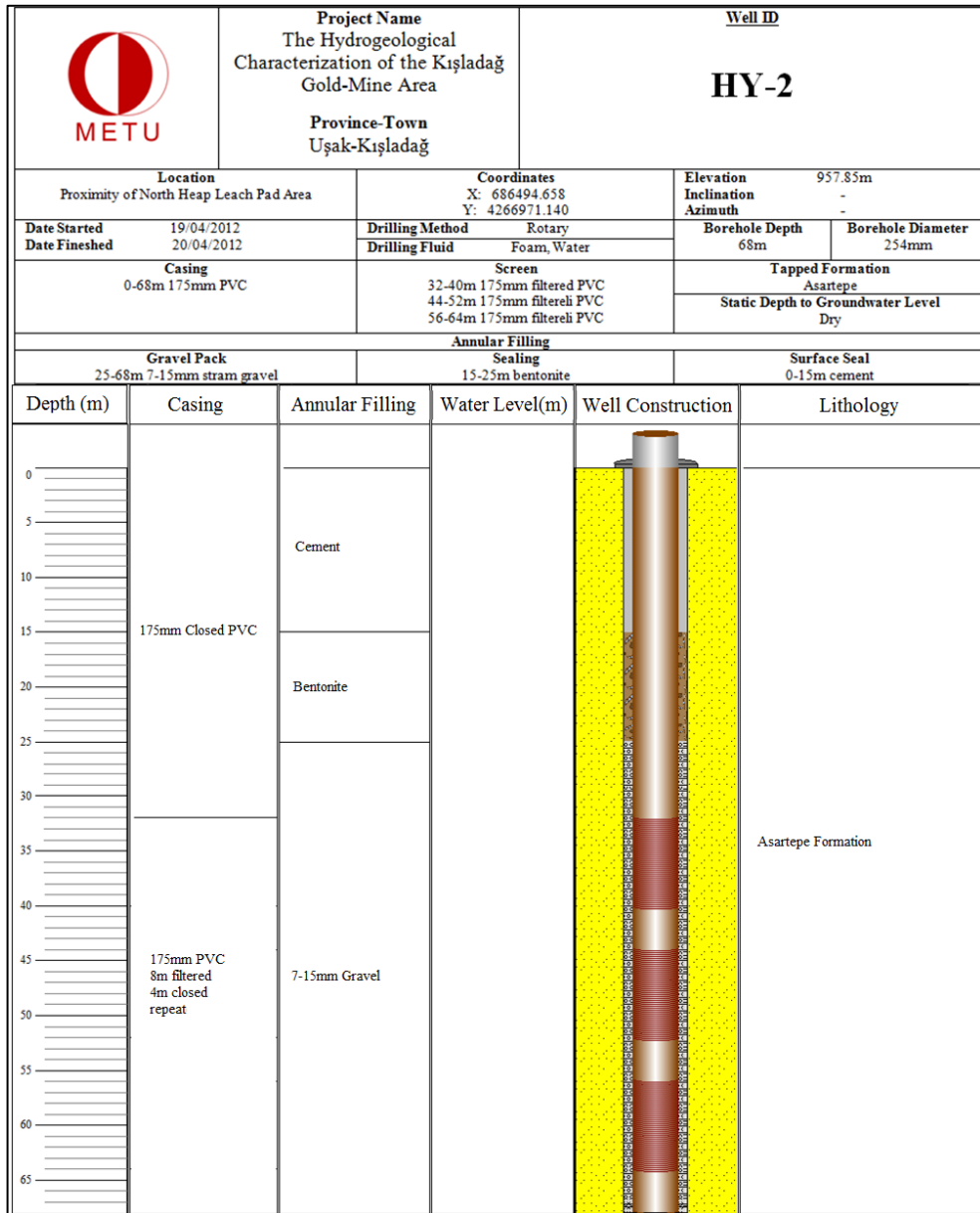


Figure B.12 The detailed well logs of HY-2

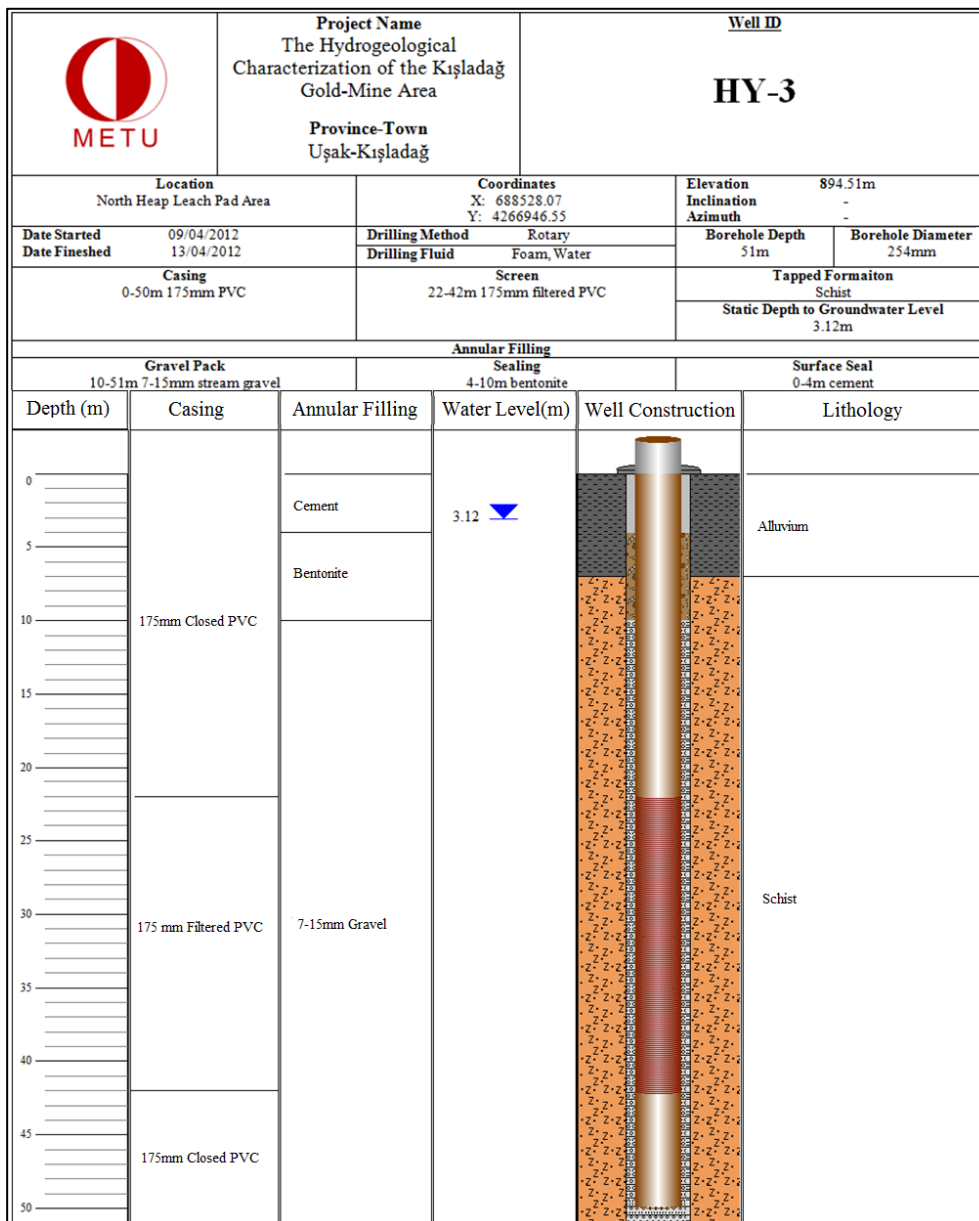


Figure B.13 The detailed well logs of HY-3

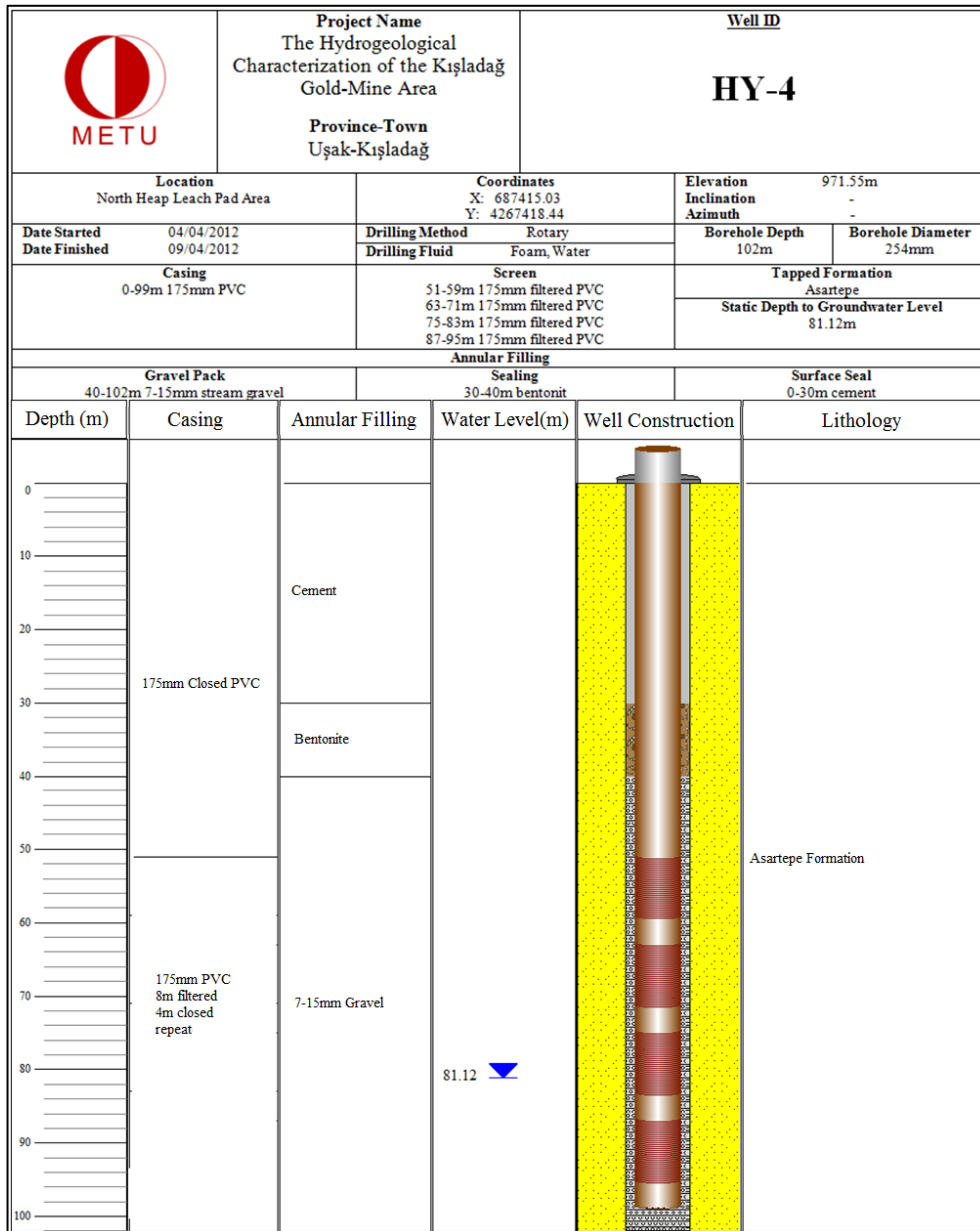


Figure B.14 The detailed well logs of HY-4

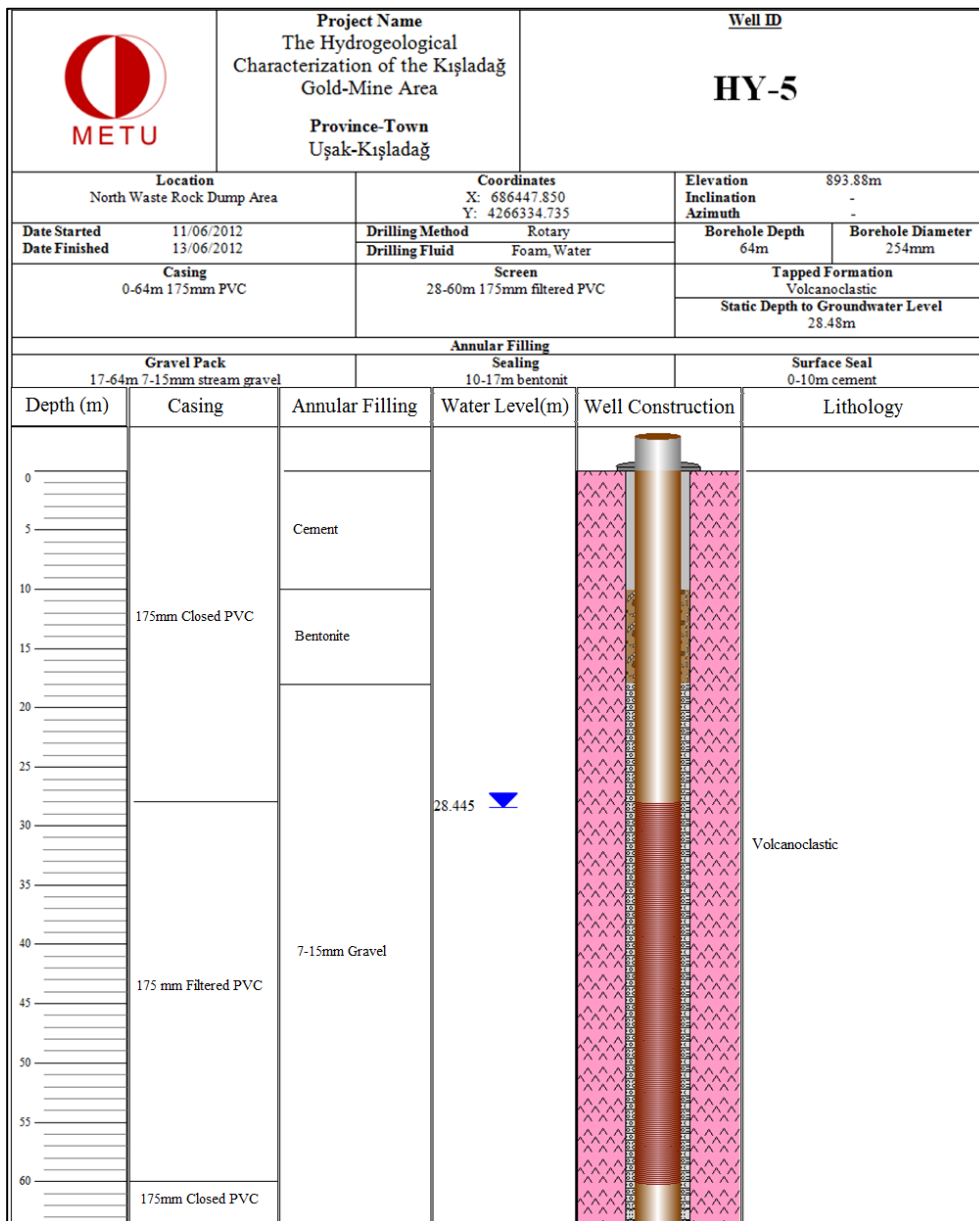


Figure B.15 The detailed well logs of HY-5

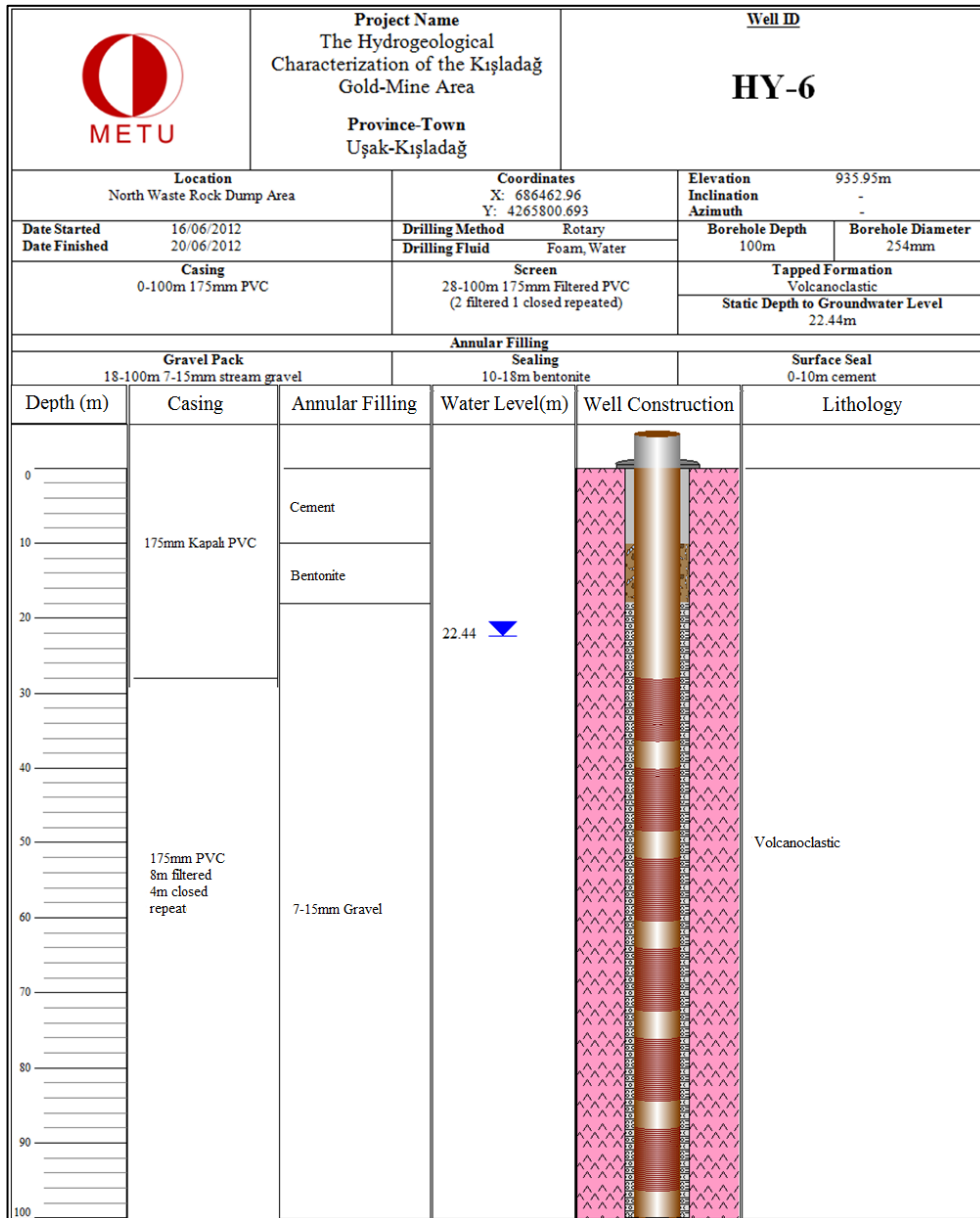


Figure B.16 The detailed well logs of HY-6

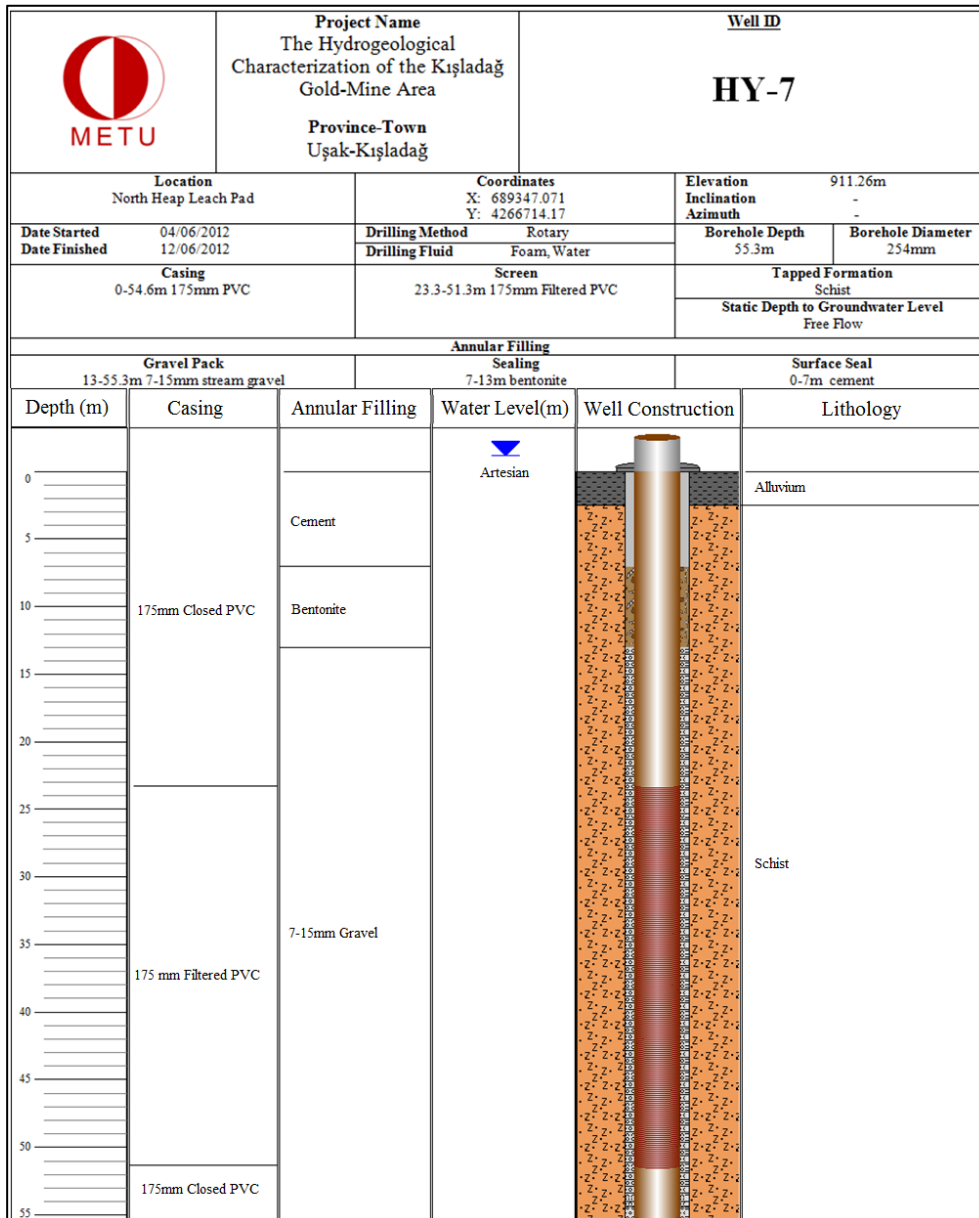


Figure B.17 The detailed well logs of HY-7

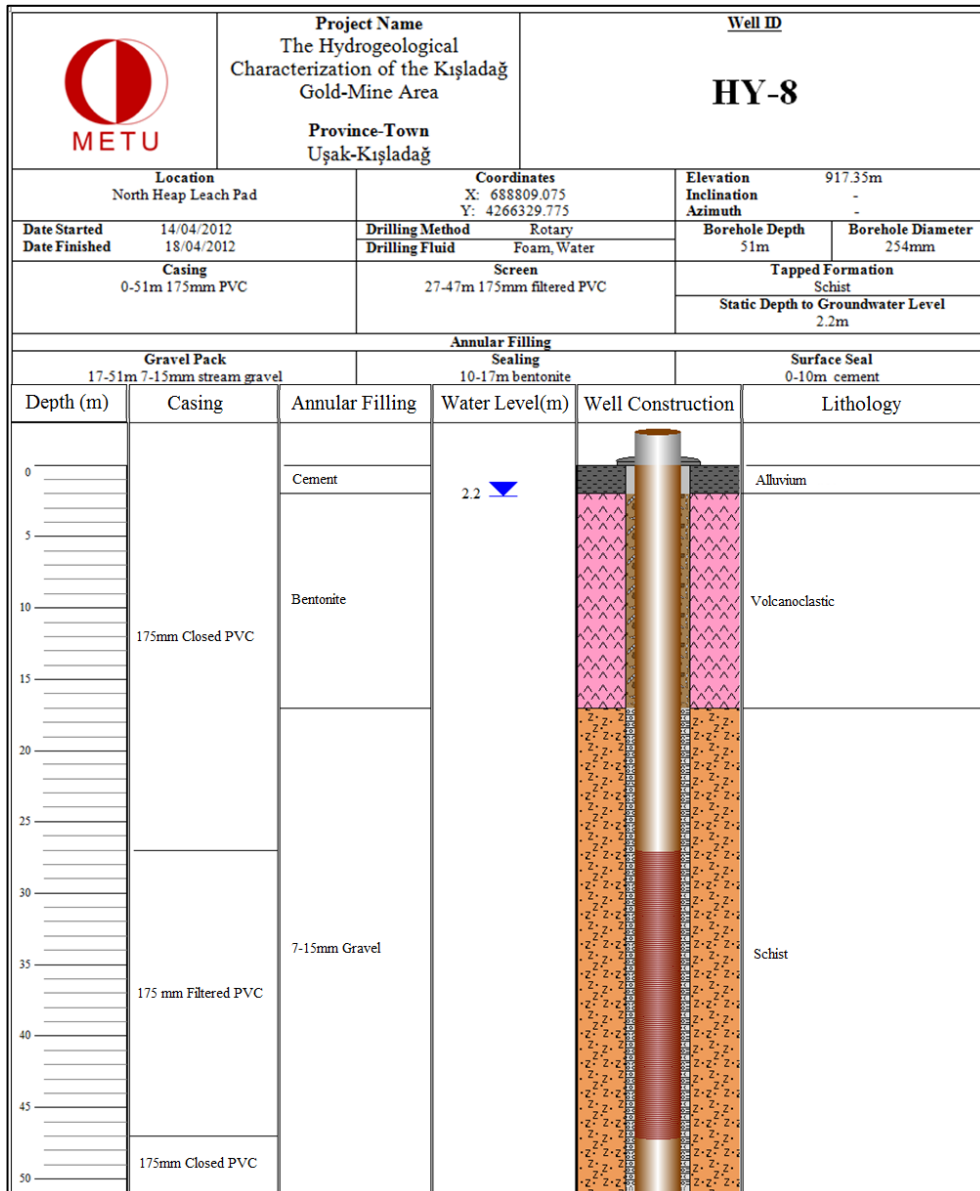


Figure B.18 The detailed well logs of HY-8

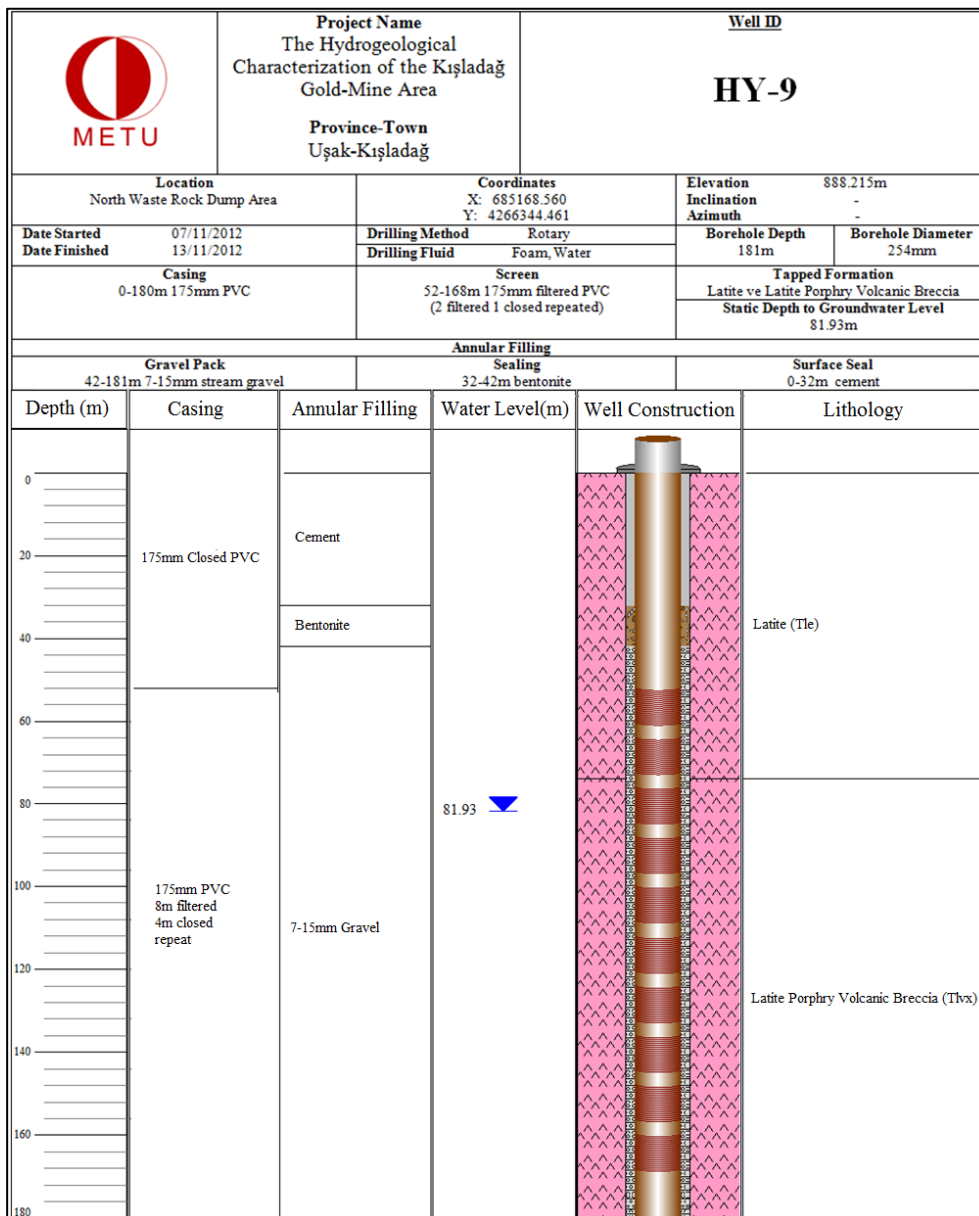


Figure B.19 The detailed well logs of HY-9

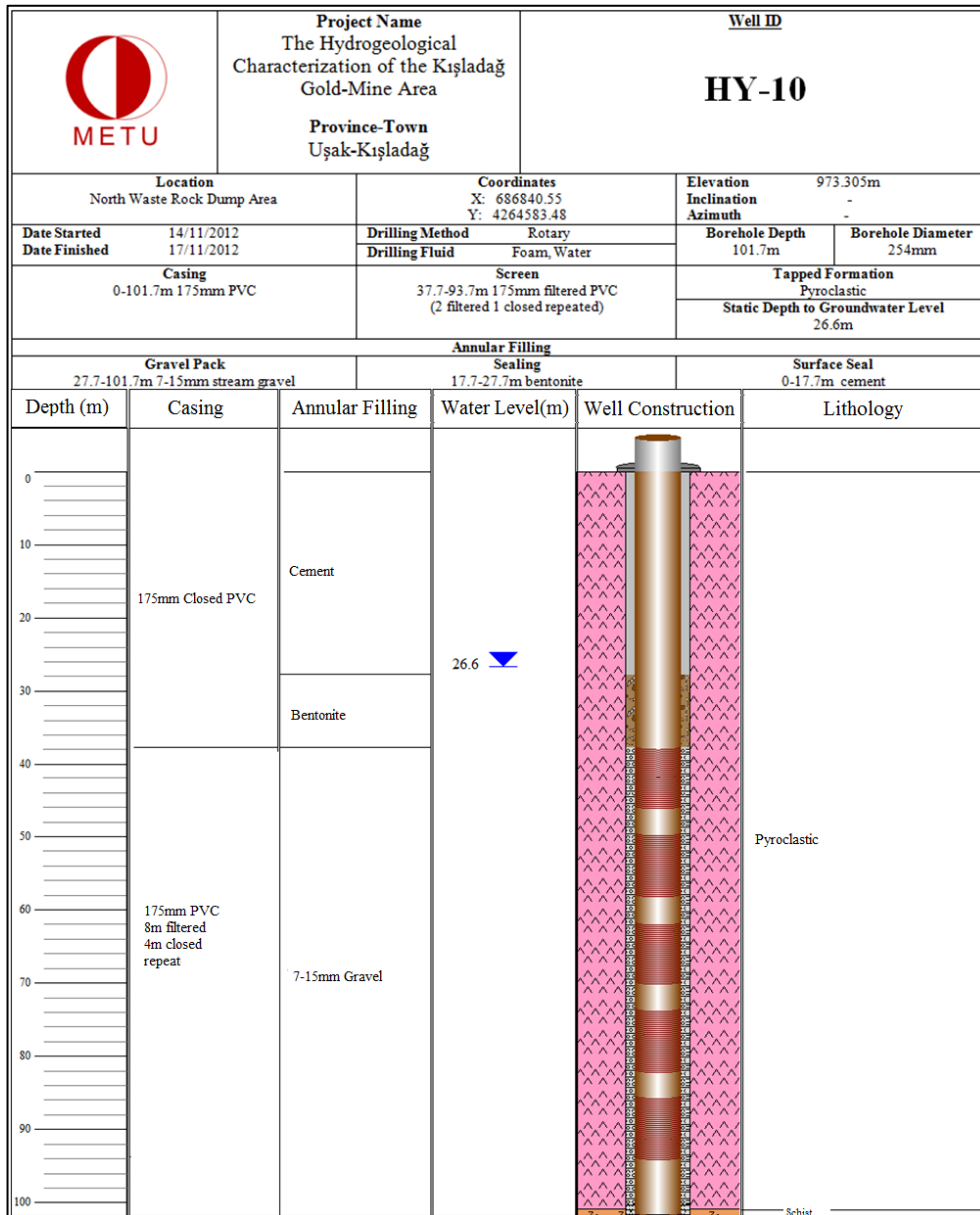


Figure B.20 The detailed well logs of HY-10

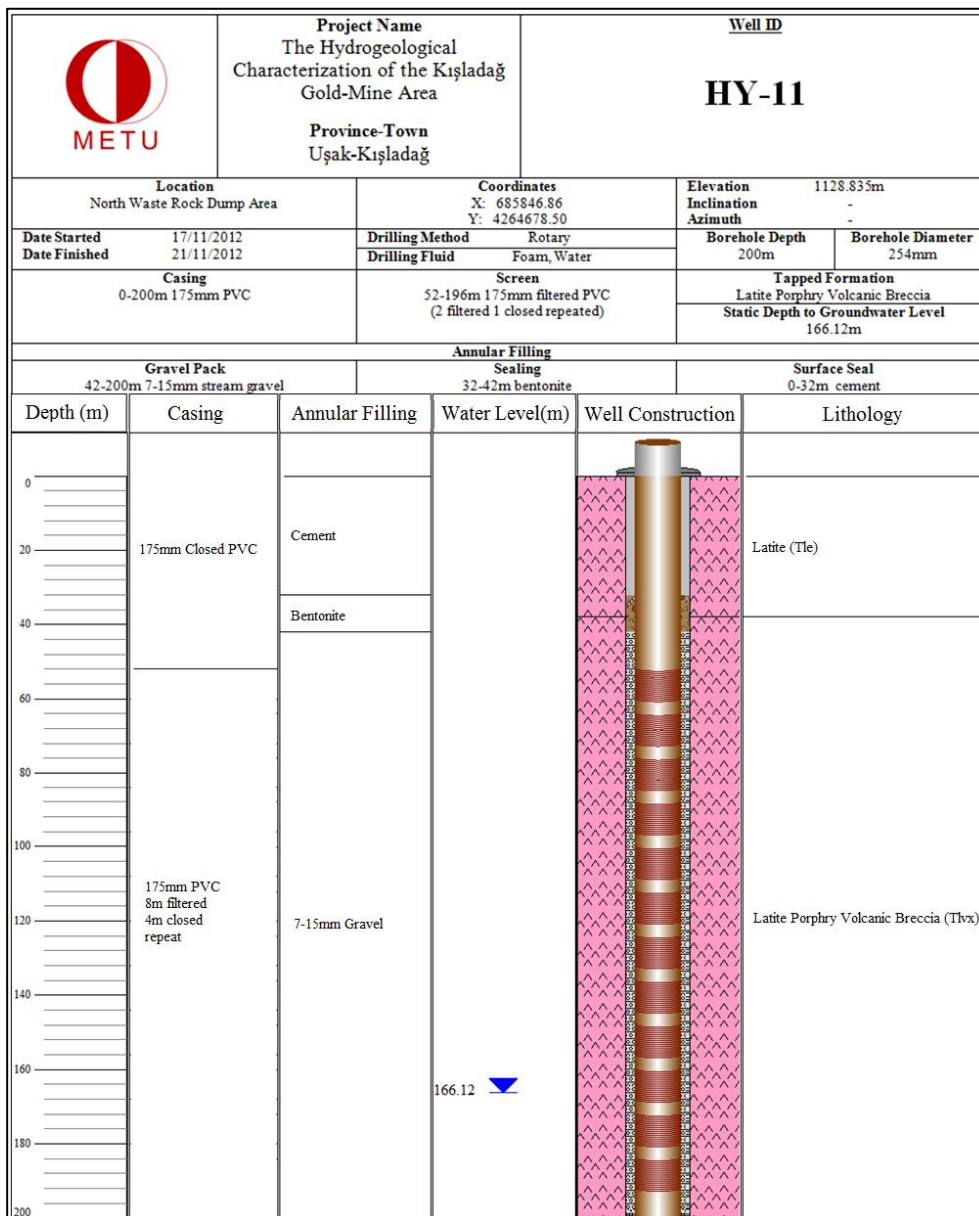


Figure B.21 The detailed well logs of HY-11

APPENDIX C:

AQUIFER TEST RESULTS

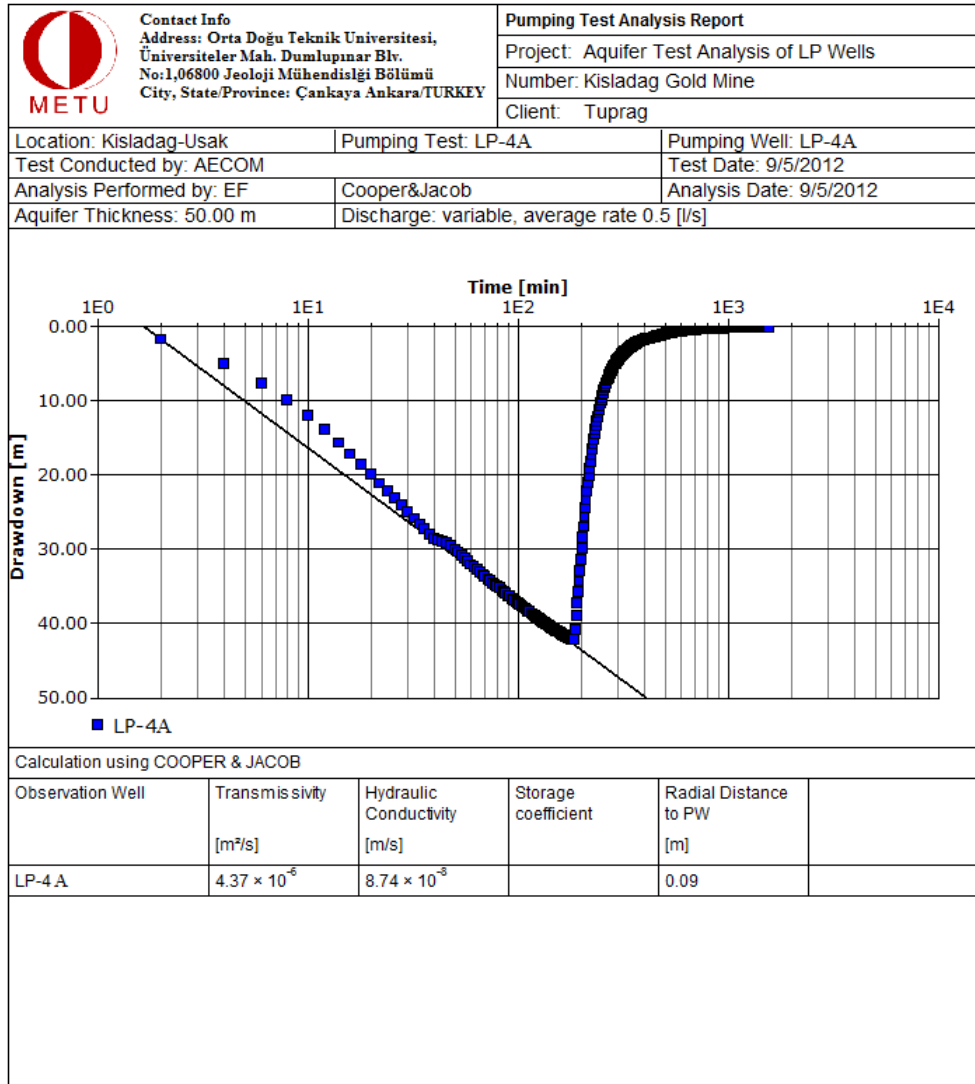


Figure C.22 Pumping test result of LP-4A

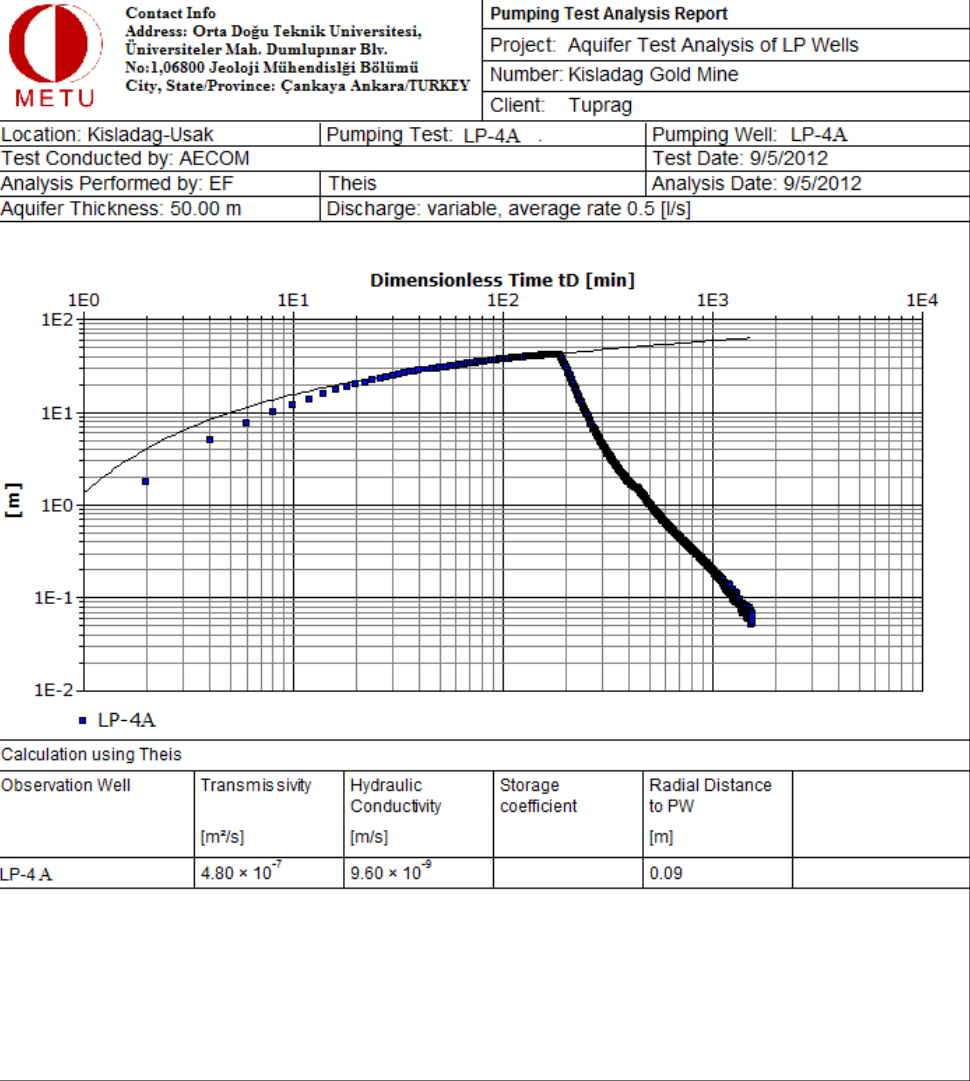


Figure C.1 Pumping test result of LP-4A (cont'd)

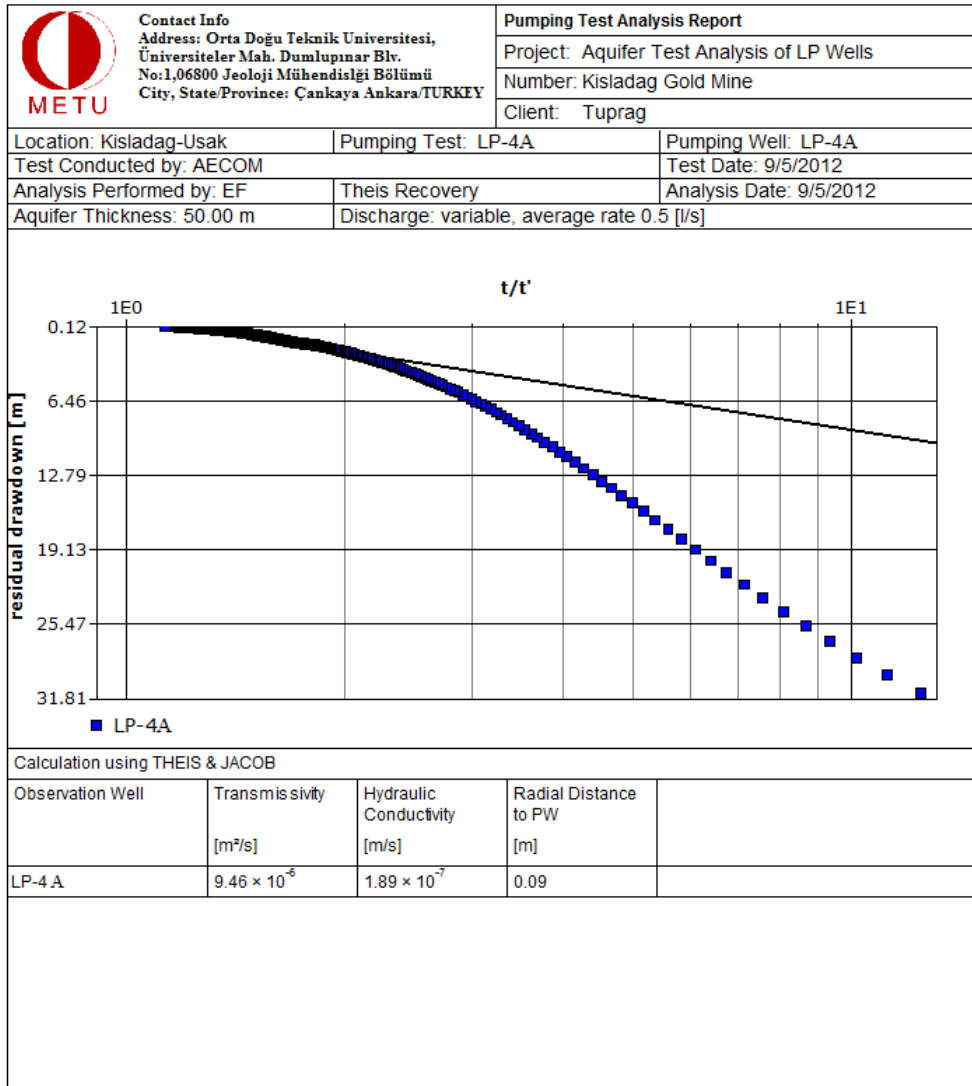


Figure C.1 Pumping test result of LP-4A (cont'd)

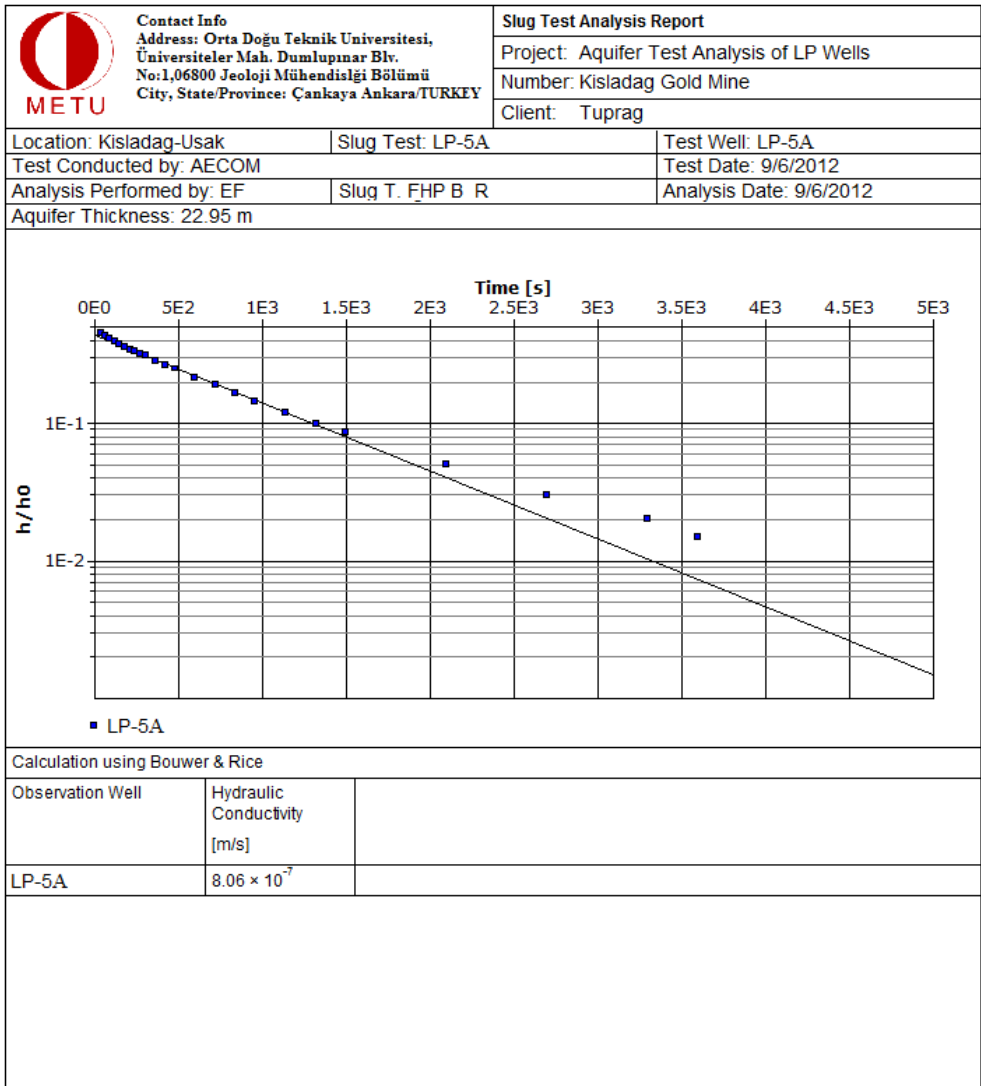


Figure C.23 Slug test result of LP-5A

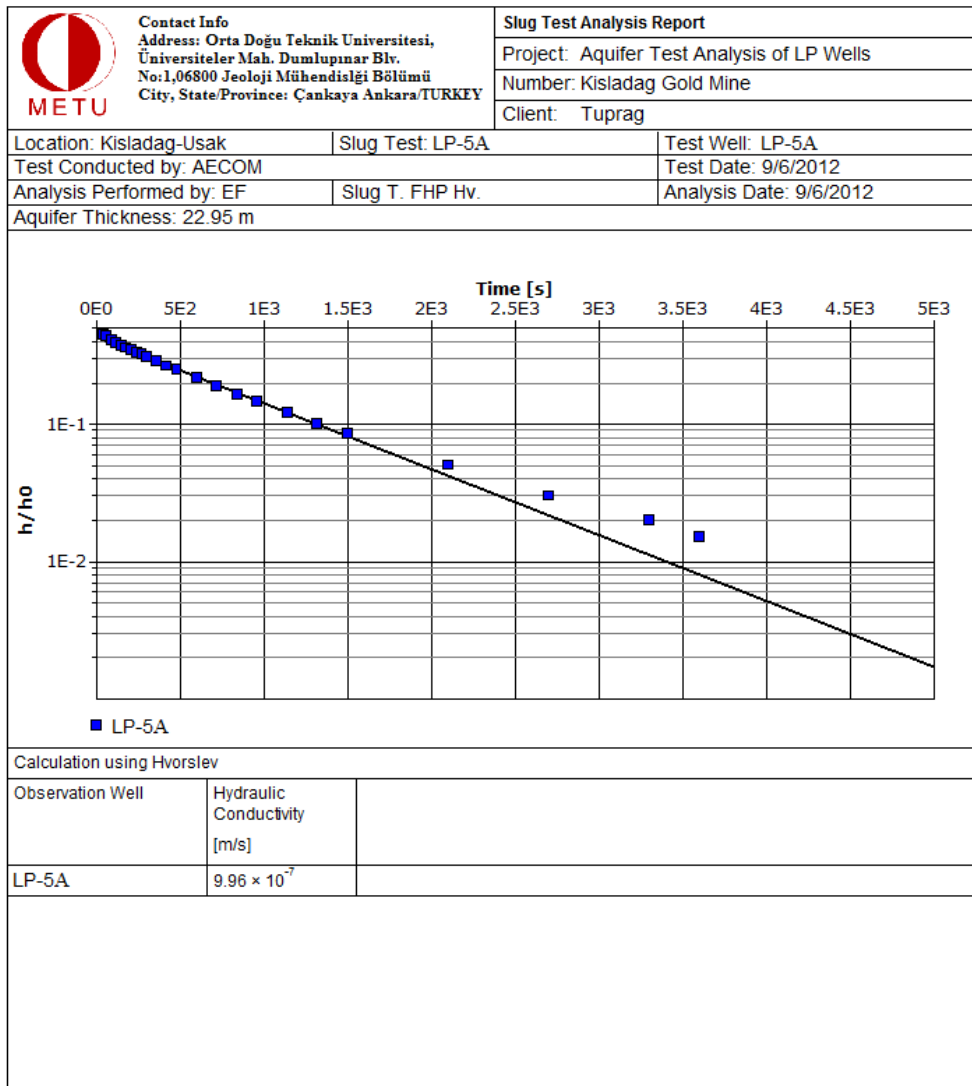


Figure C.2 Slug test result of LP-5A (cont'd)

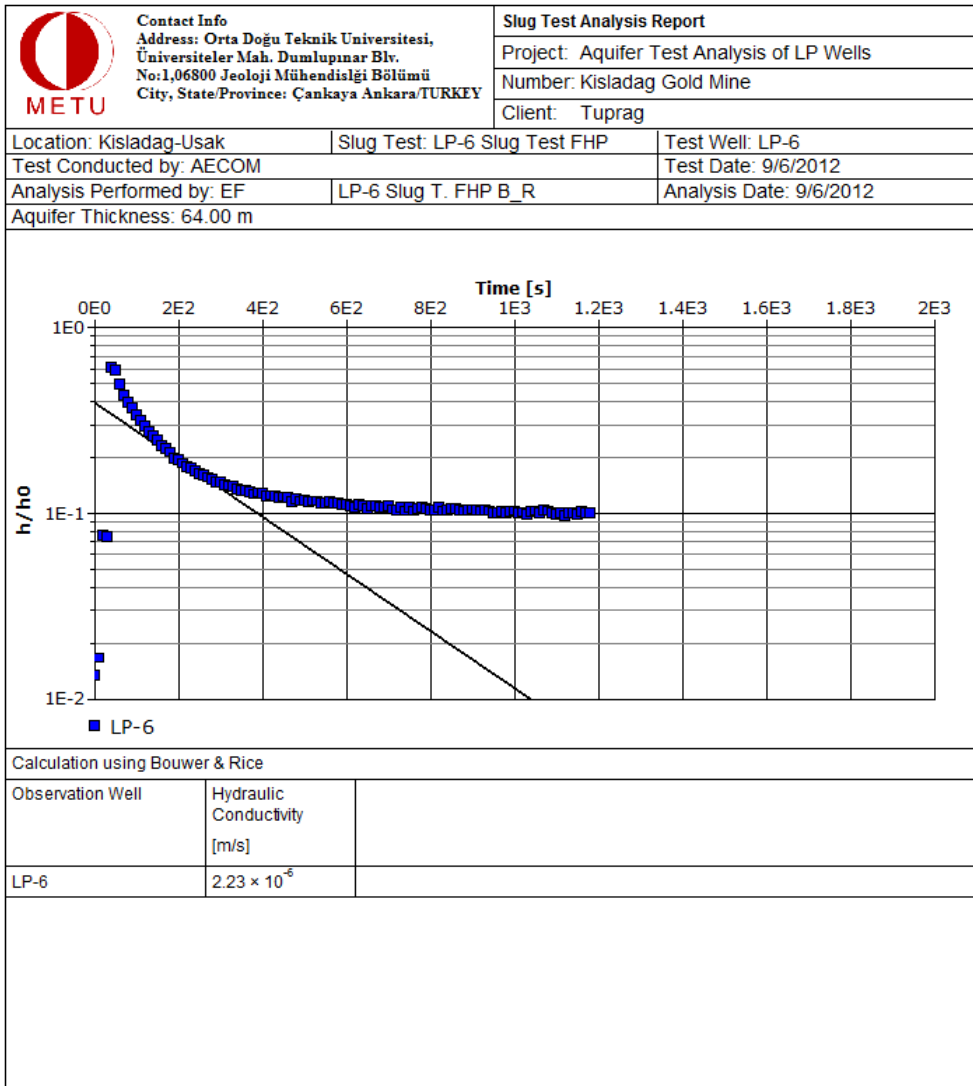


Figure C.24 Pumping test result of LP-6

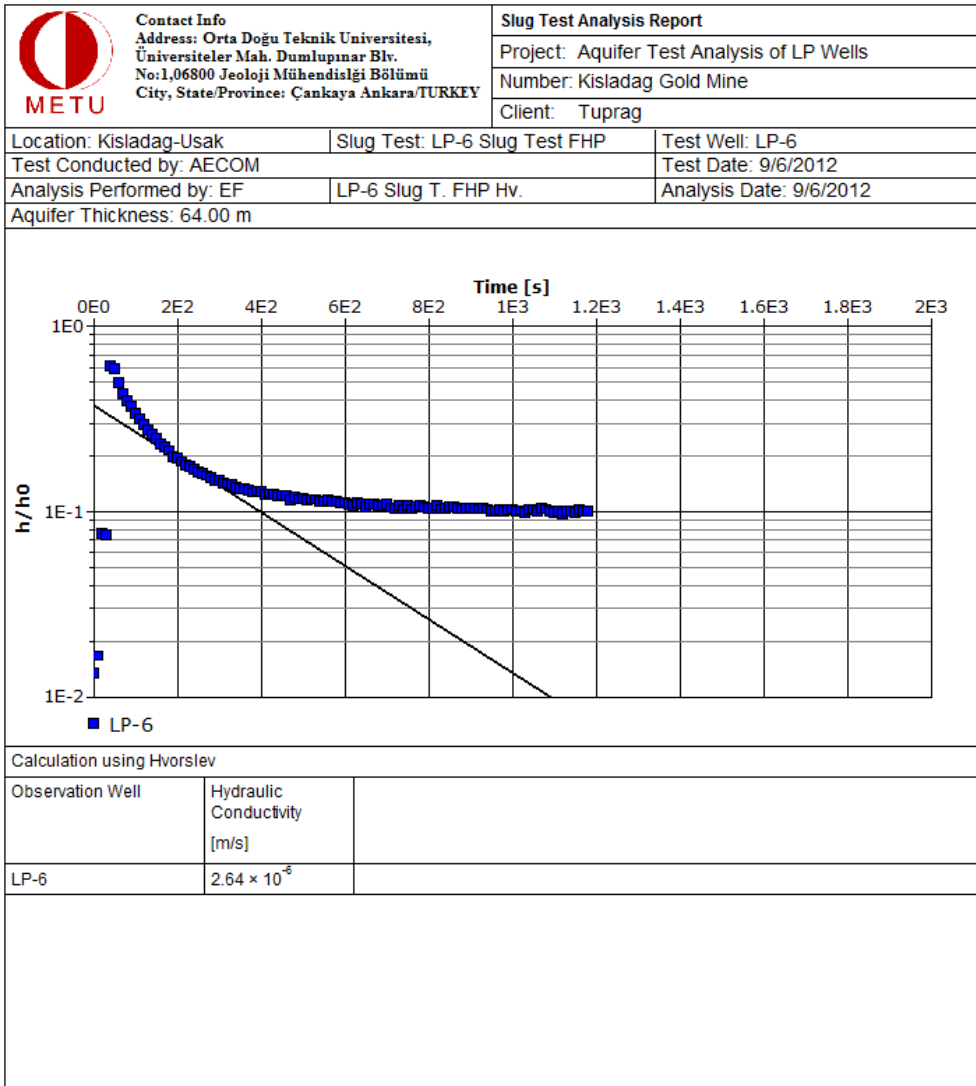


Figure C.3 Slug test result of LP-6 (cont'd)

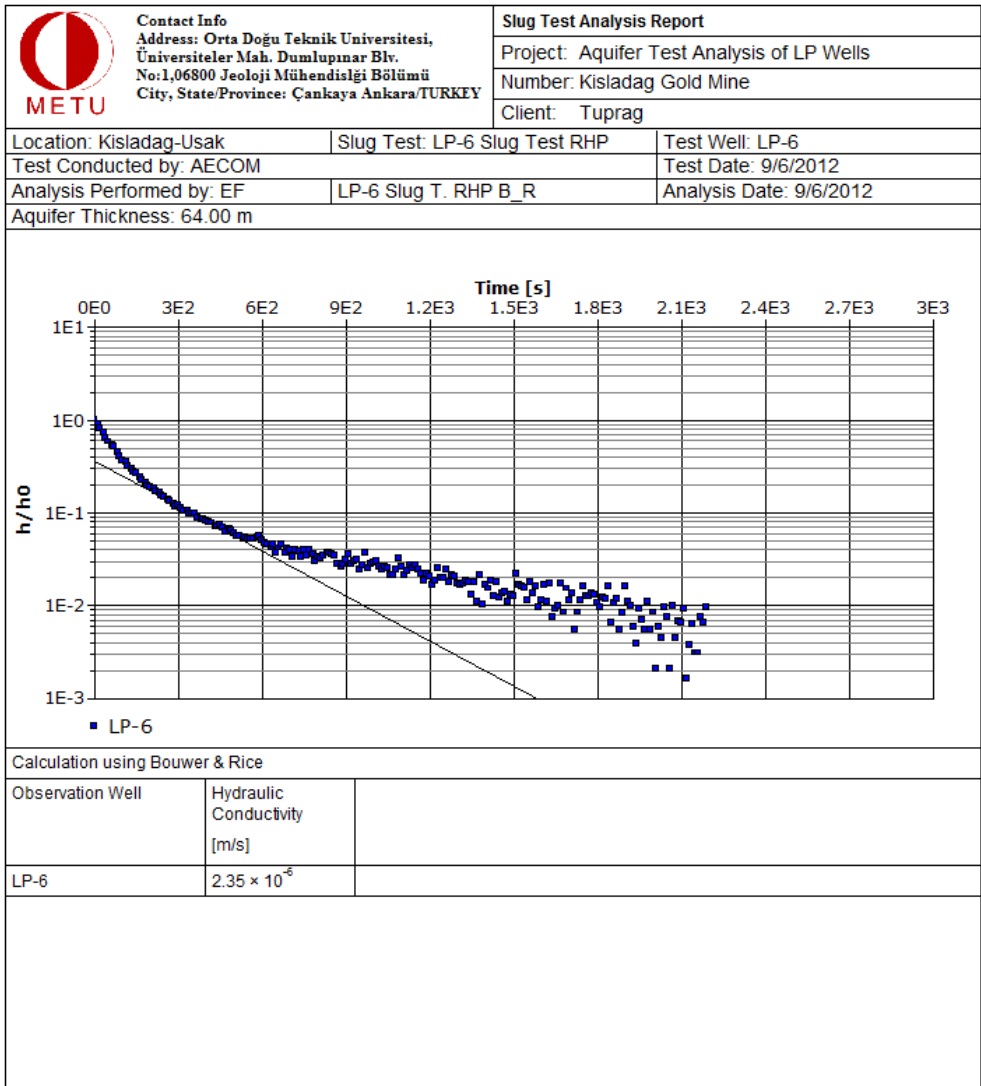


Figure C.3 Slug test result of LP-6 (cont'd)

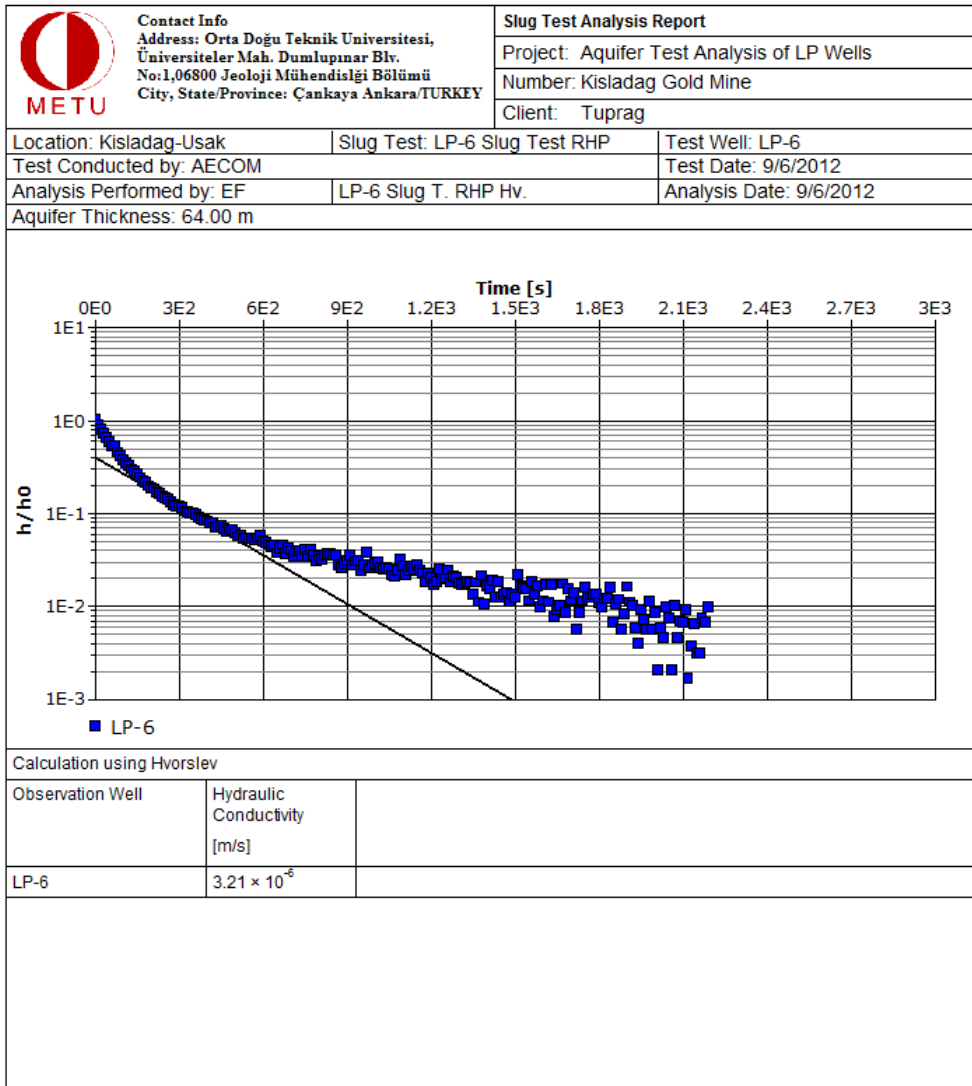


Figure C.3 Slug test result of LP-6 (cont'd)

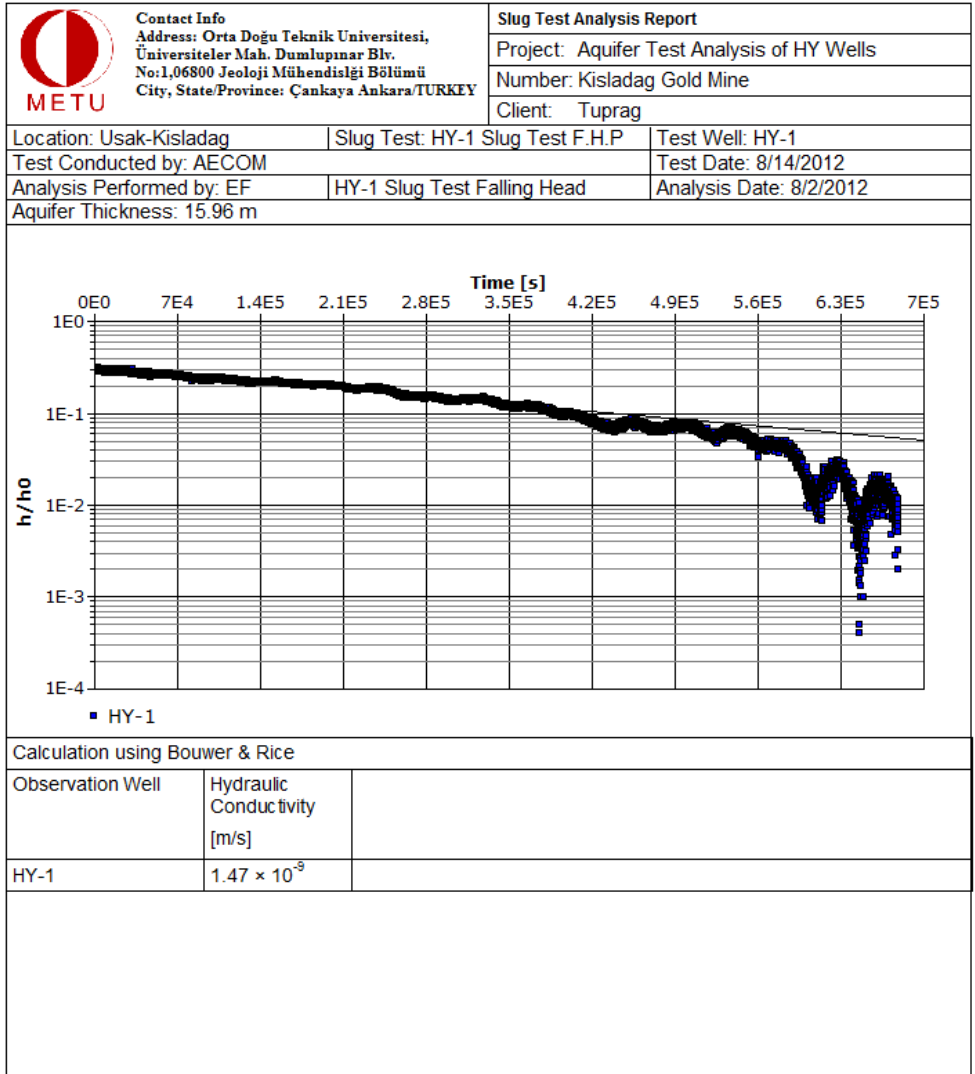


Figure C.25 Slug test result of HY-1

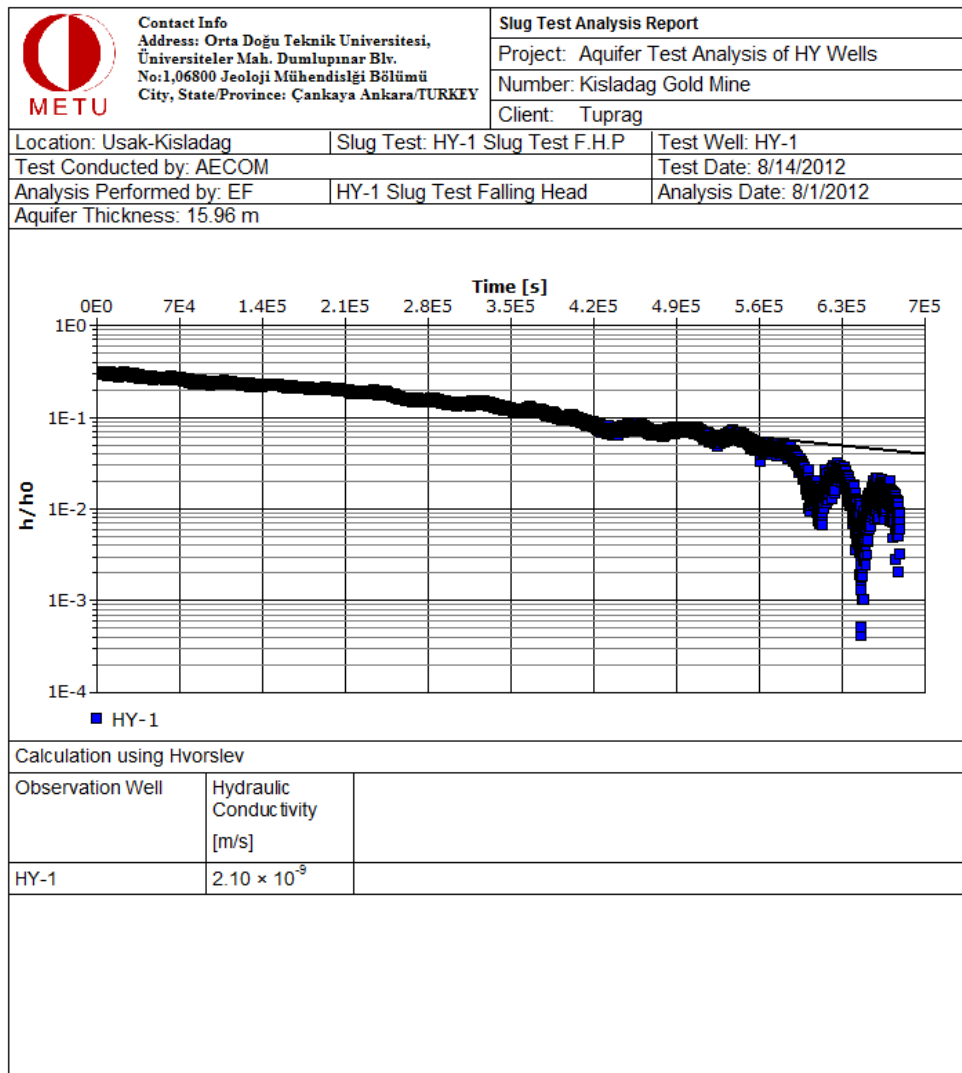


Figure C.4 Slug test result of HY-1(cont'd)

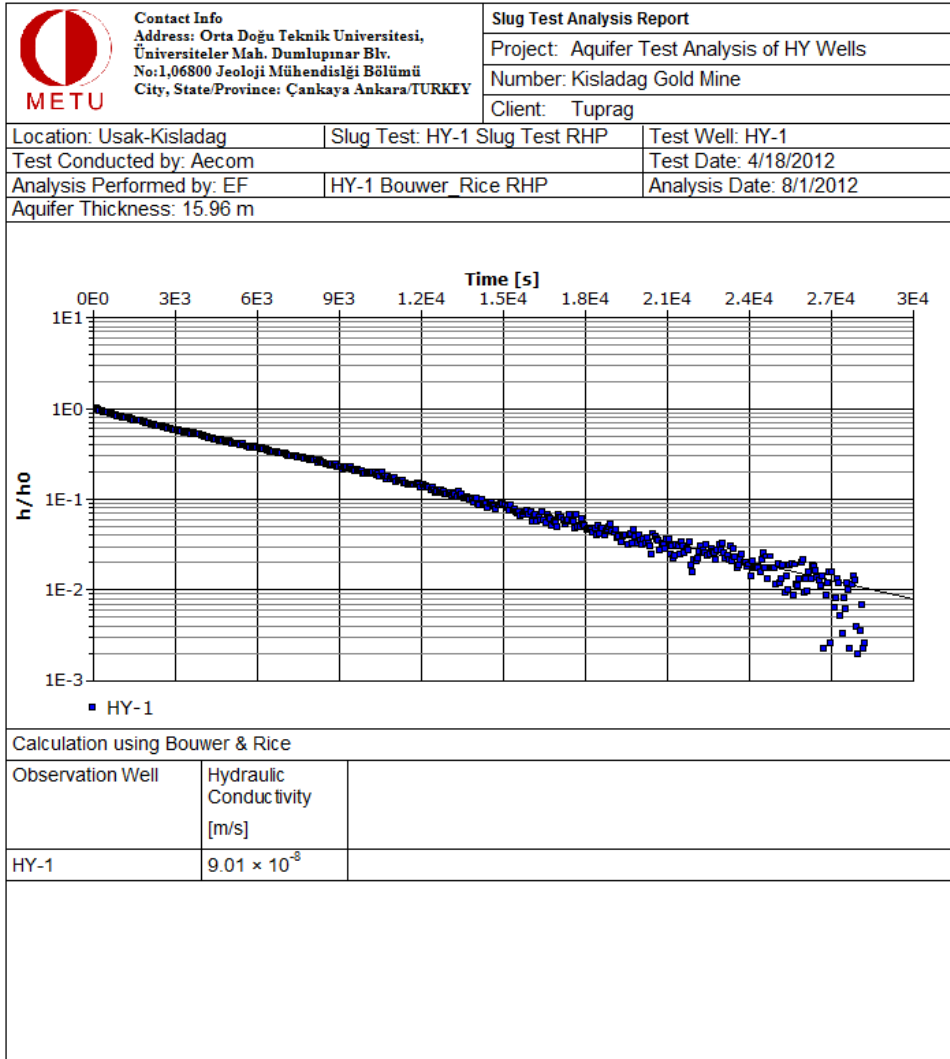


Figure C.4 Slug test result of HY-1(cont'd)

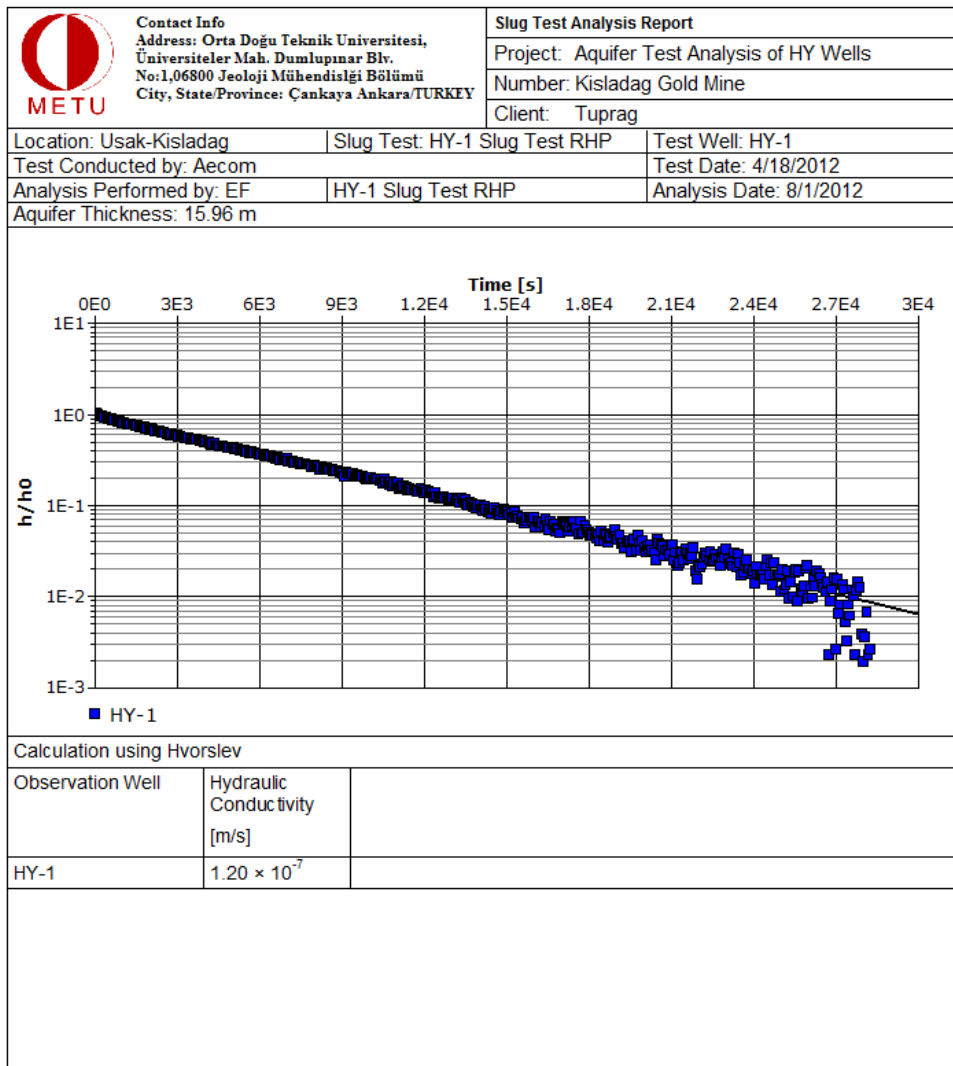


Figure C.4 Slug test result of HY-1(cont'd)

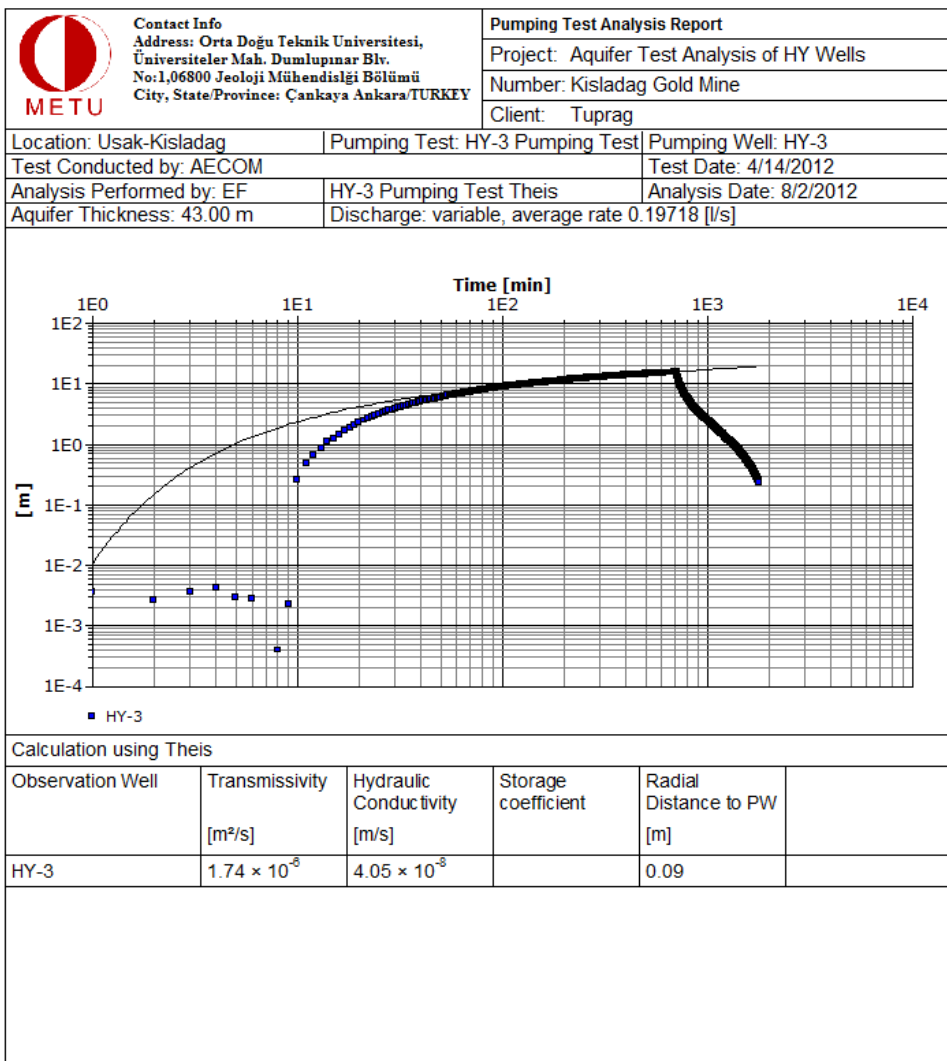


Figure C.26 Pumping test result of HY-3

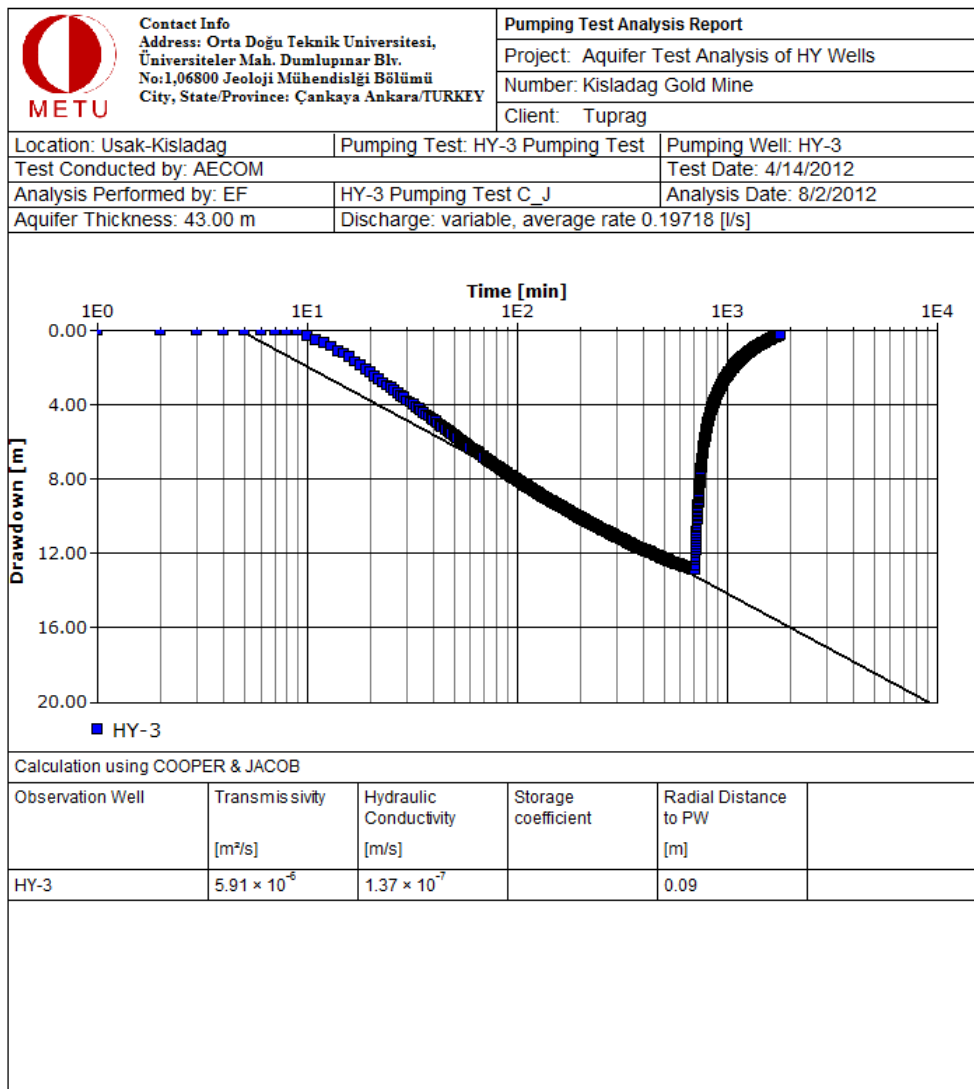


Figure C.5 Pumping test result of HY-3 (cont'd)

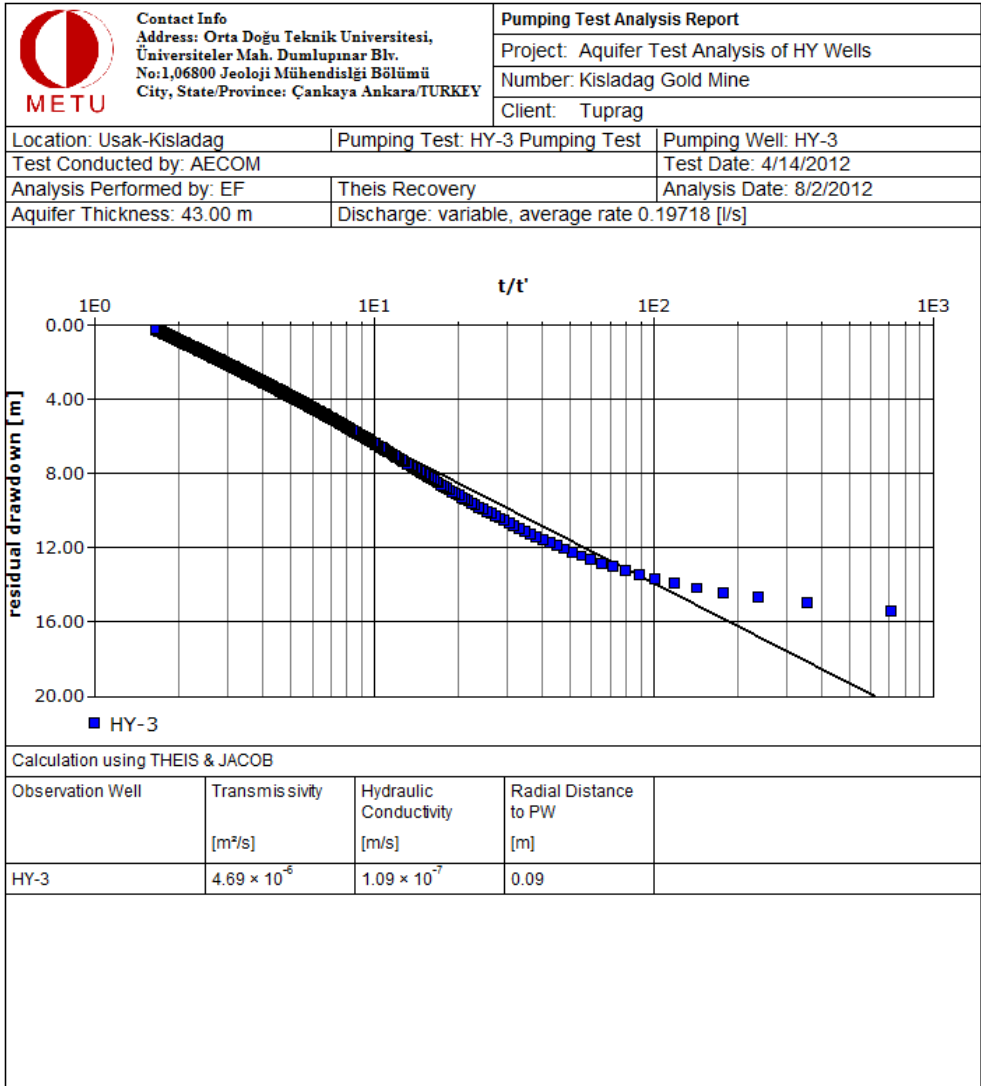


Figure C.5 Pumping test result of HY-3 (cont'd)

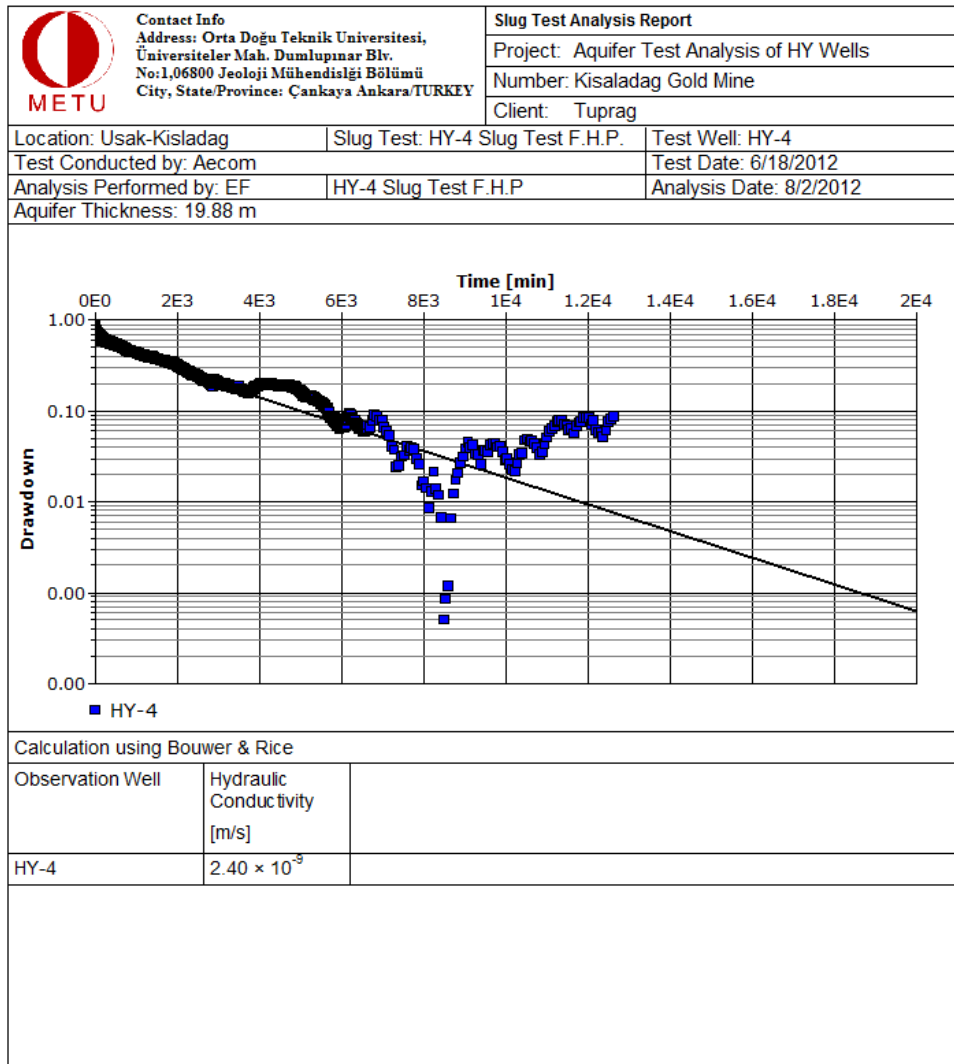


Figure C.27 Slug test result of HY-4

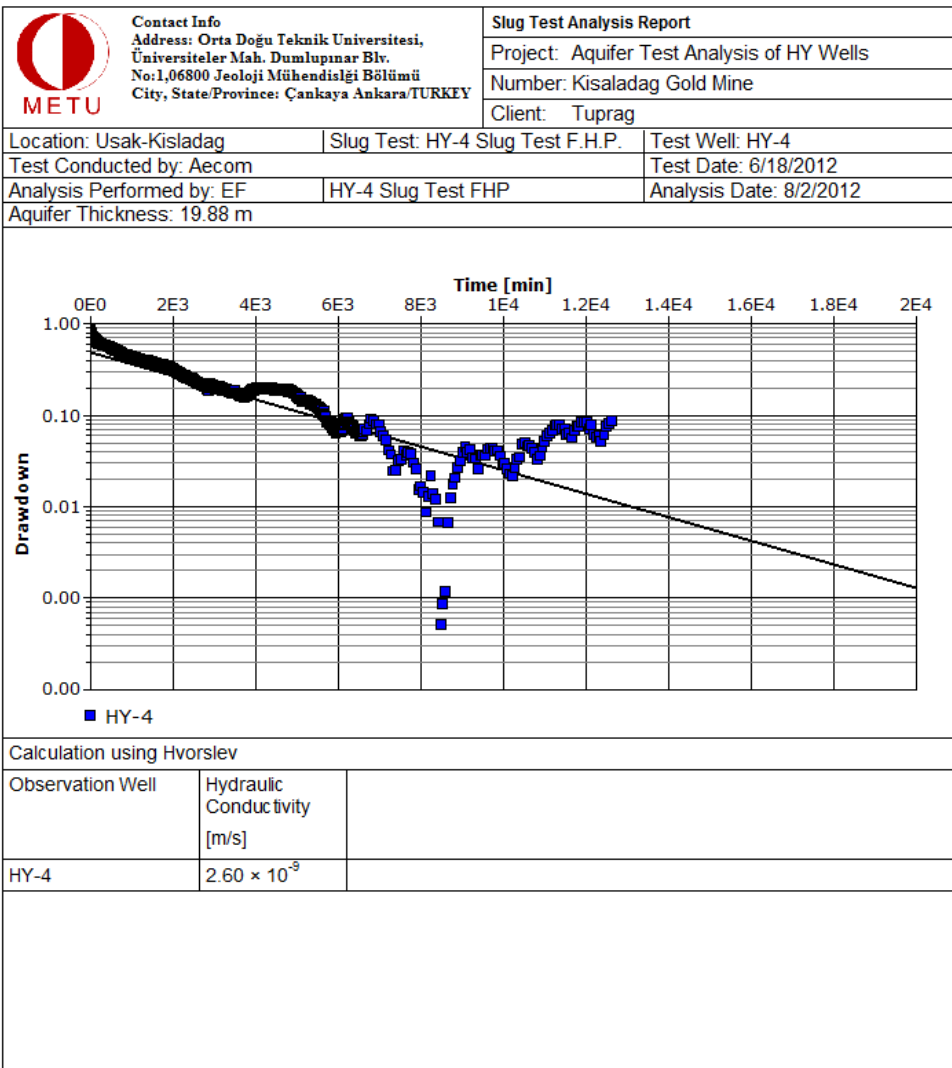


Figure C.6 Pumping test result of HY-4 (cont'd)

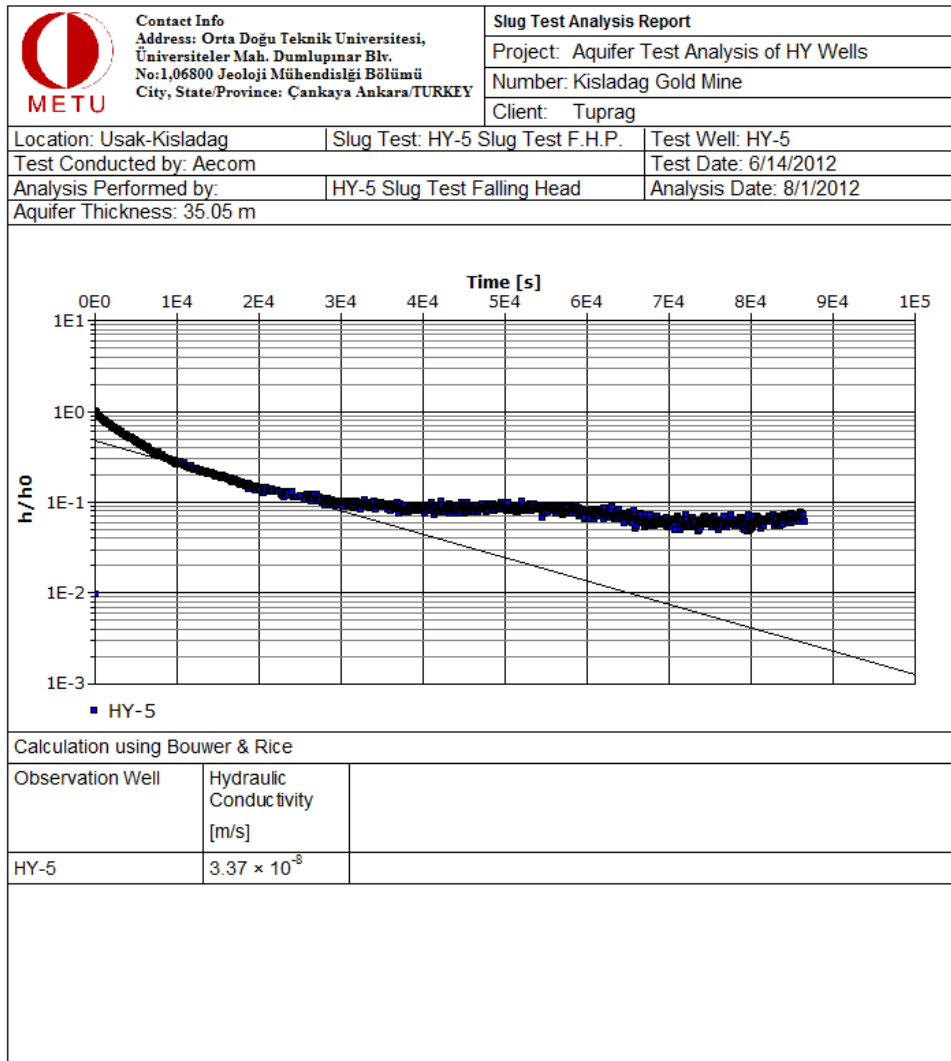


Figure C.28 Pumping test result of HY-5

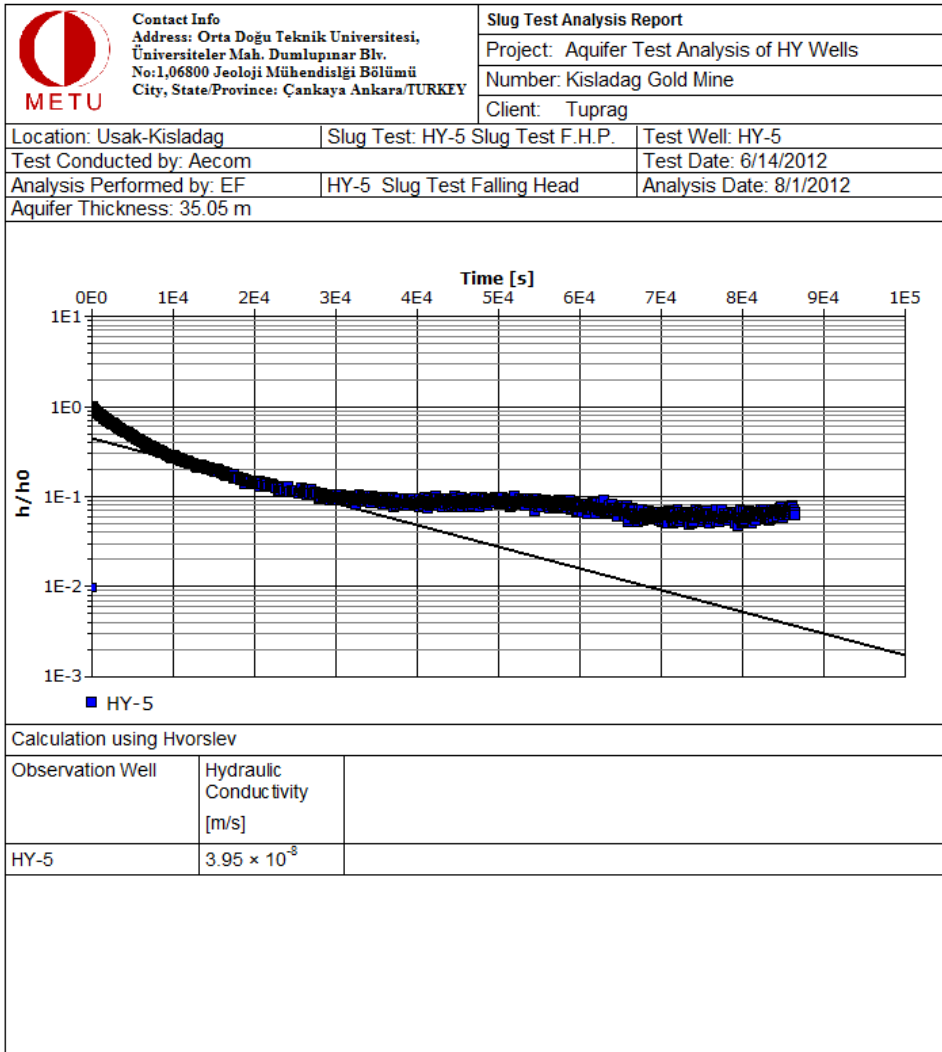


Figure C.7 Pumping test result of HY-5 (cont'd)

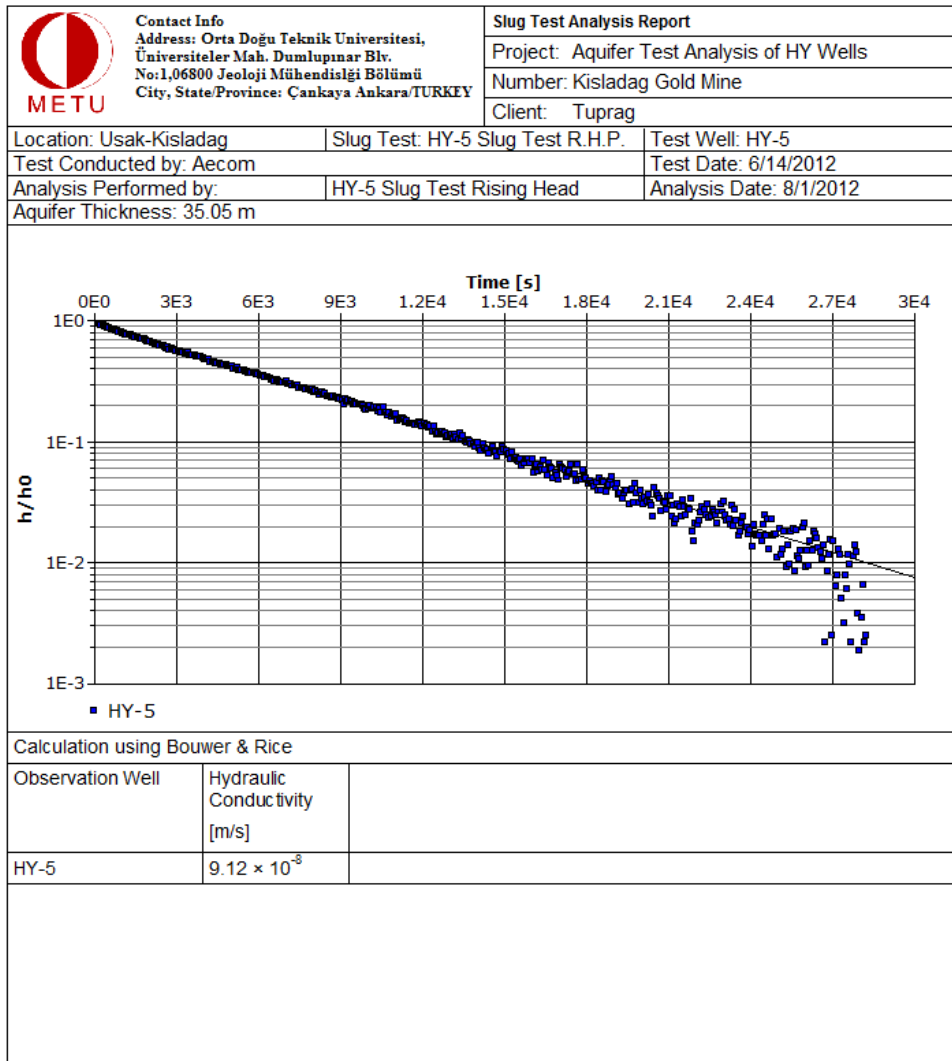


Figure C.7 Pumping test result of HY-5 (cont'd)

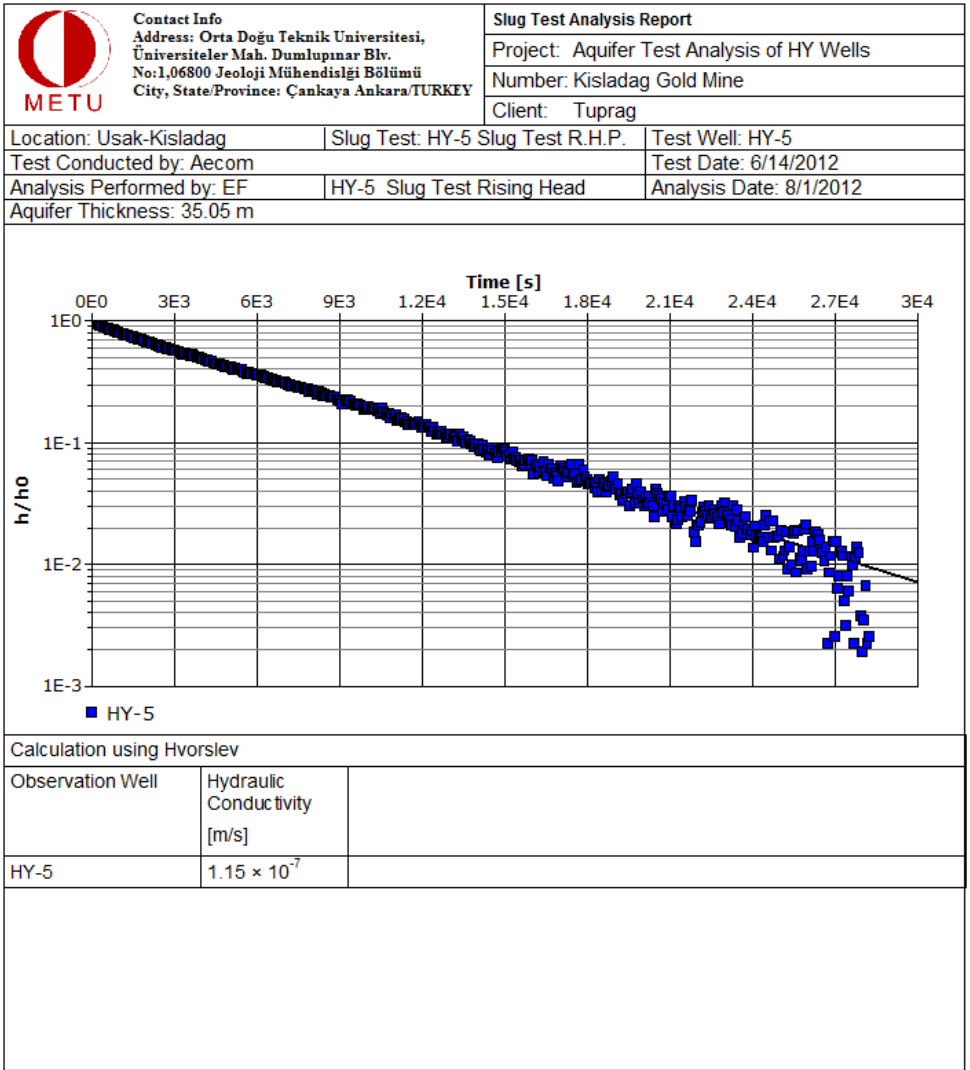


Figure C.7 Pumping test result of HY-5 (cont'd)

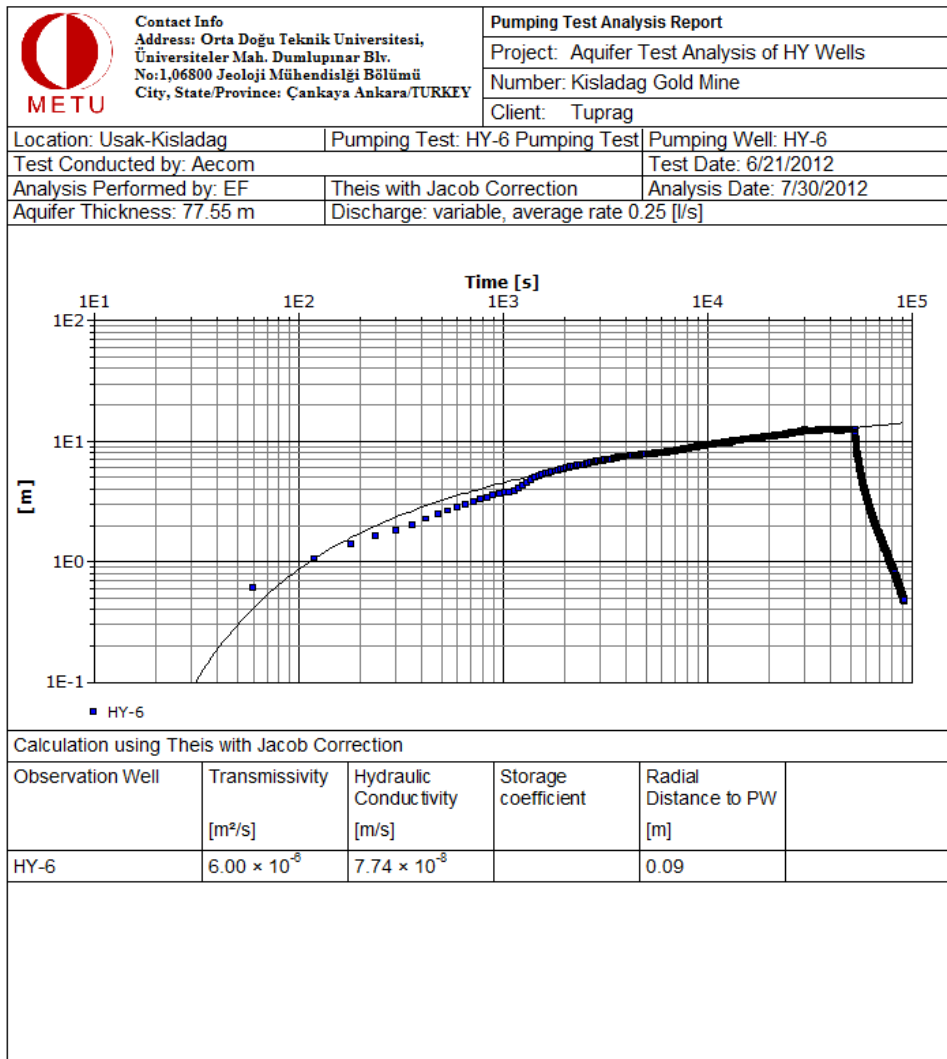


Figure C.29 Pumping test result of HY-6

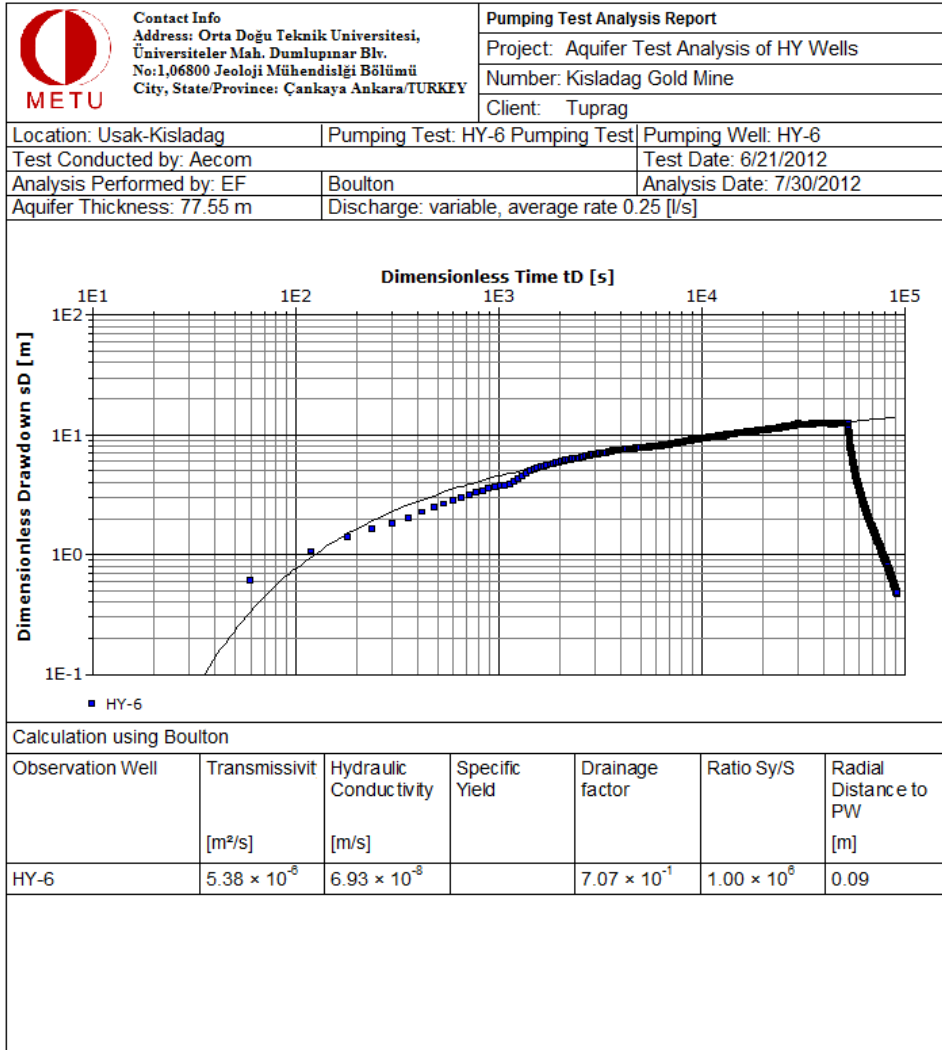


Figure C.8 Pumping test result of HY-6 (cont'd)

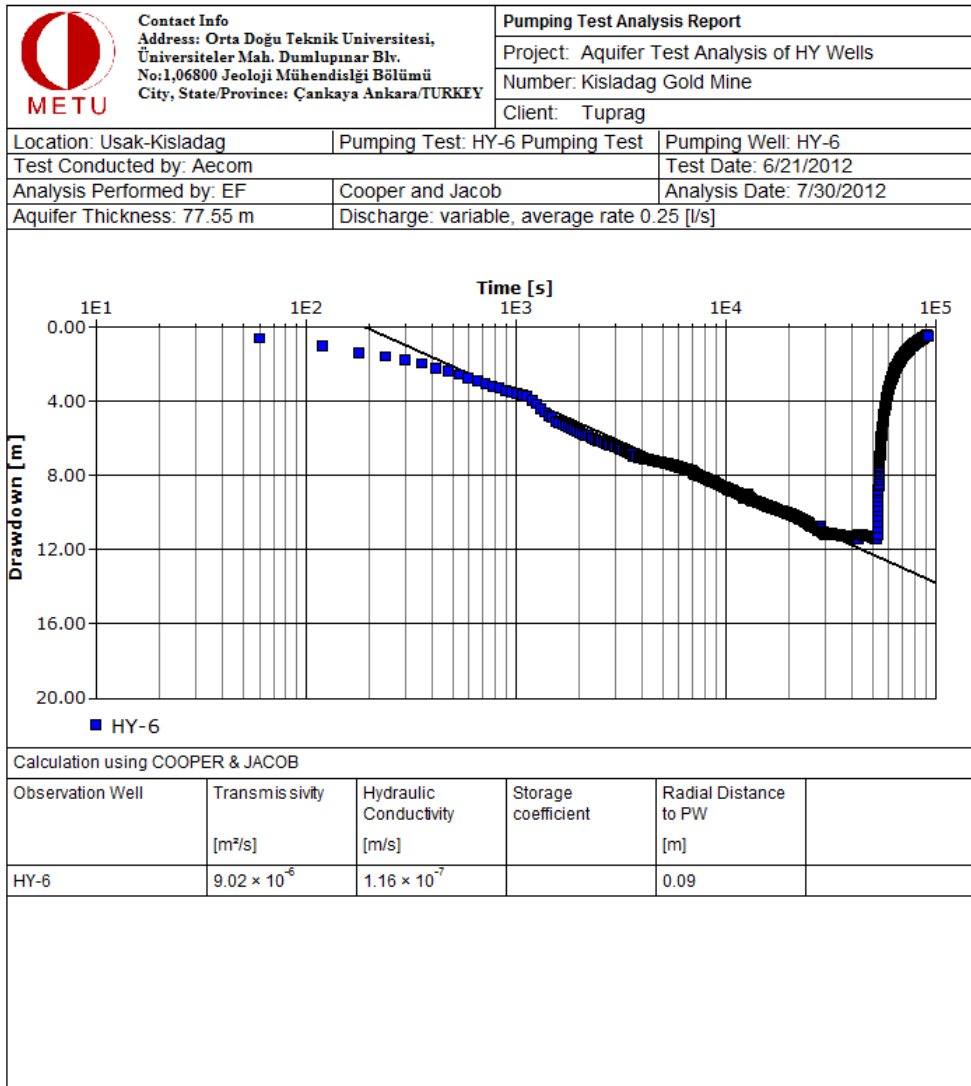


Figure C.8 Pumping test result of HY-6 (cont'd)

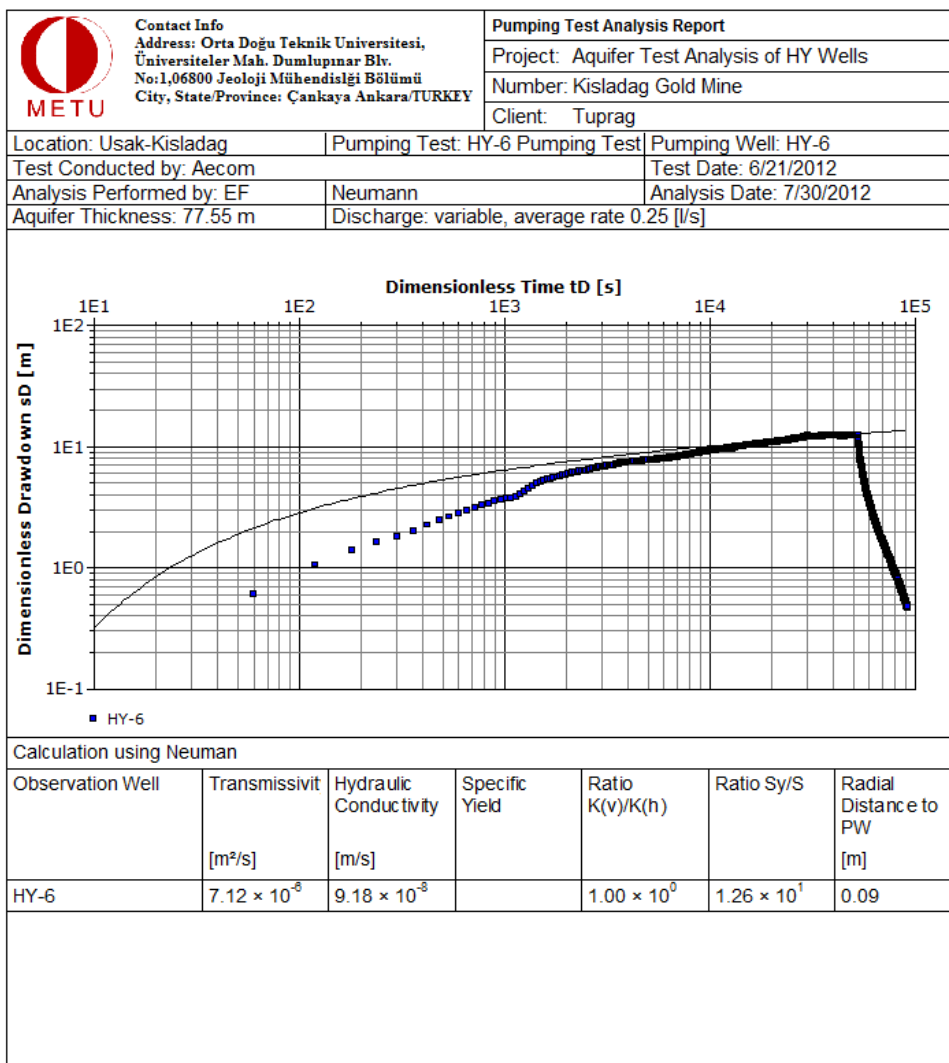


Figure C.8 Pumping test result of HY-6 (cont'd)

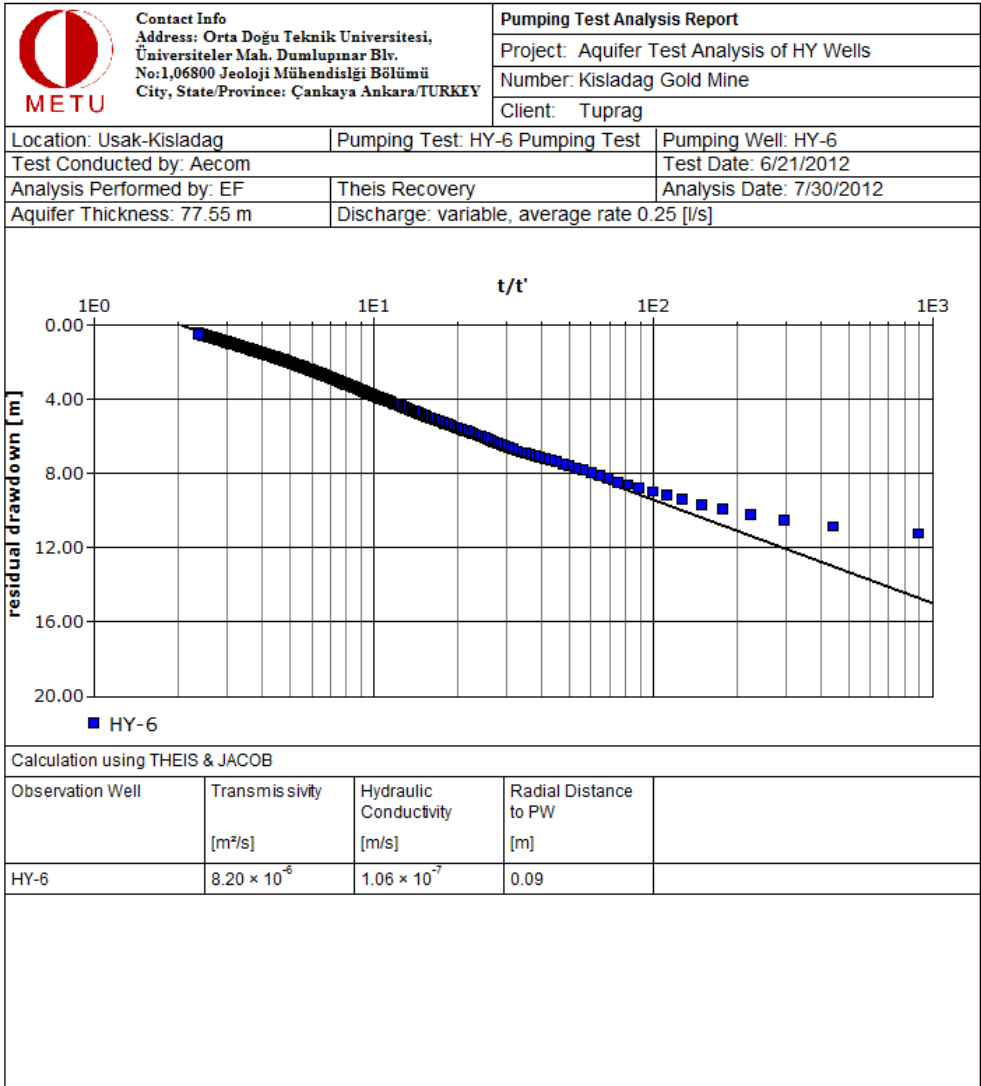
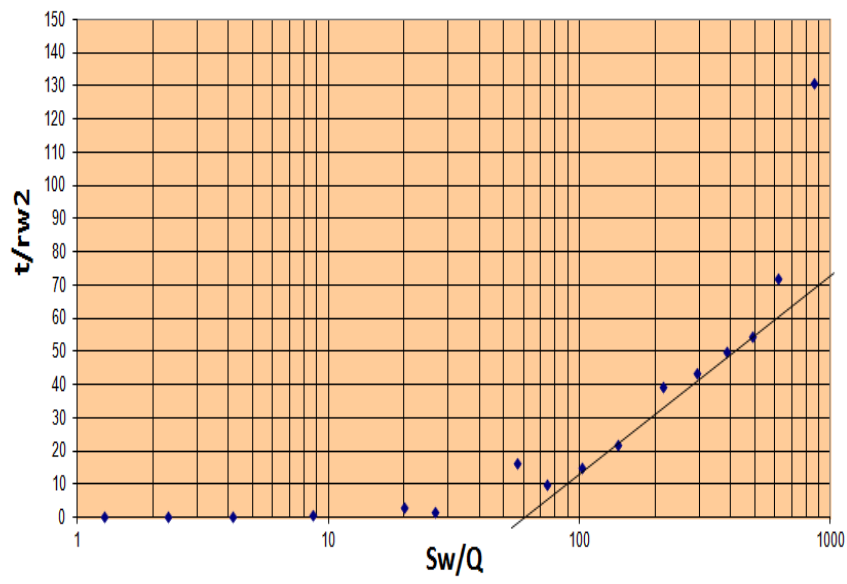


Figure C.8 Pumping test result of HY-6 (cont'd)



Unit Sw/Q	58 ft gal-1 min	
d	180.4461942 ft	
K	0.003368398 ft/d	1.19E-08 m/s
S	0.044210624	

Figure C.30 Free flow test result of HY-7

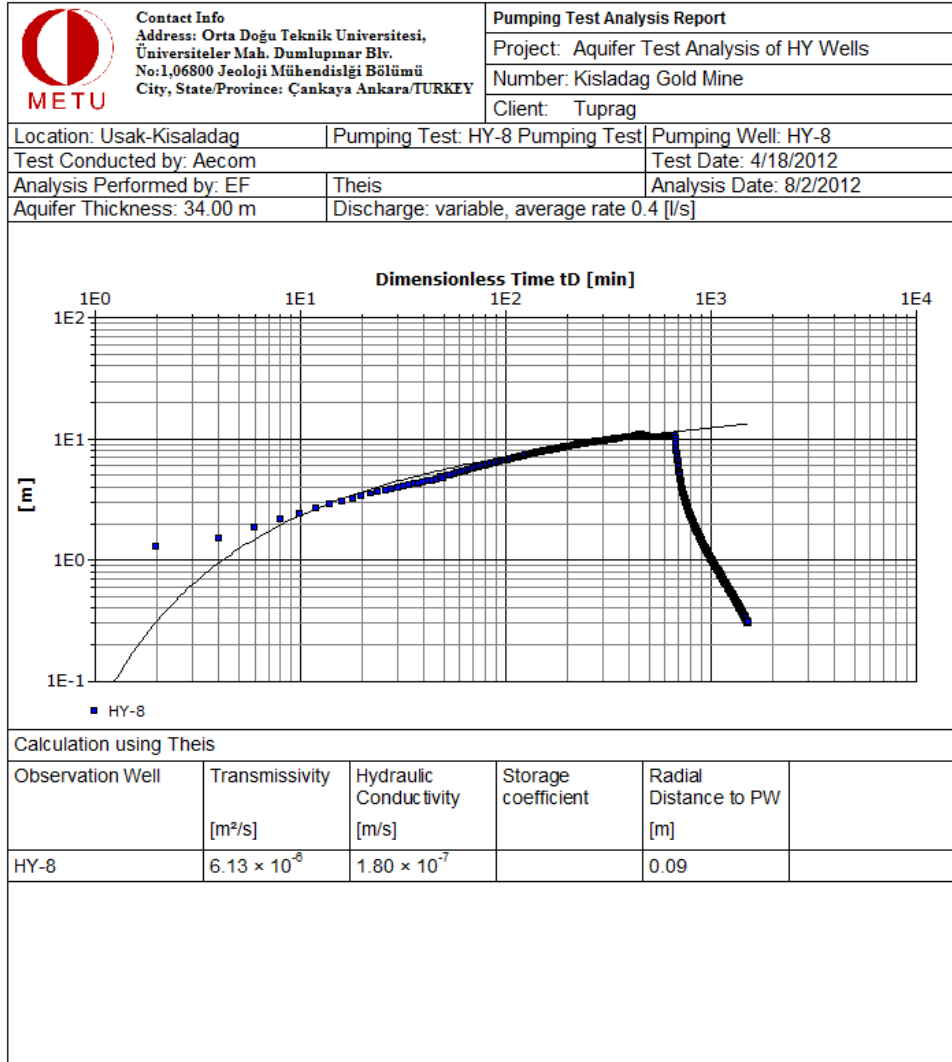


Figure C.31 Pumping test result of HY-8

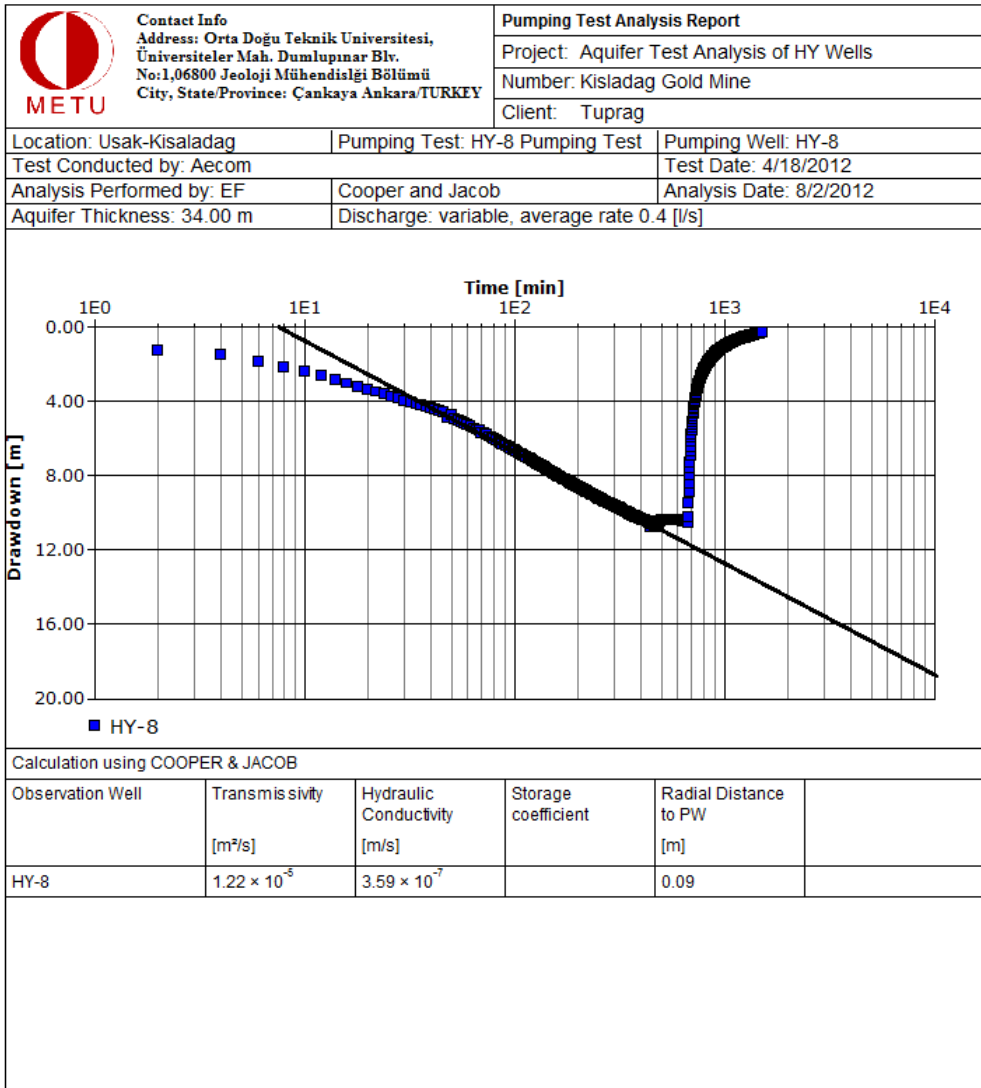


Figure C.10 Pumping test result of HY-8 (cont'd)

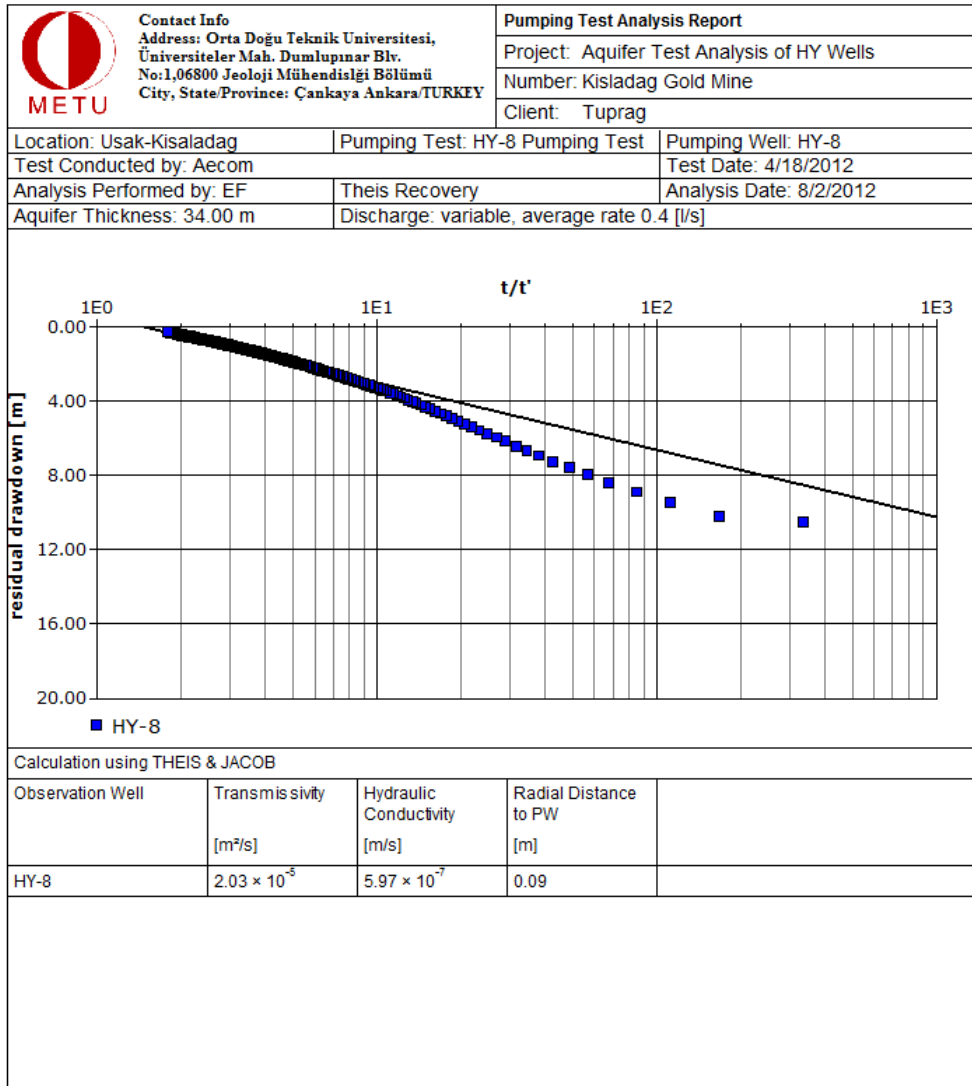


Figure C.10 Pumping test result of HY-8 (cont'd)

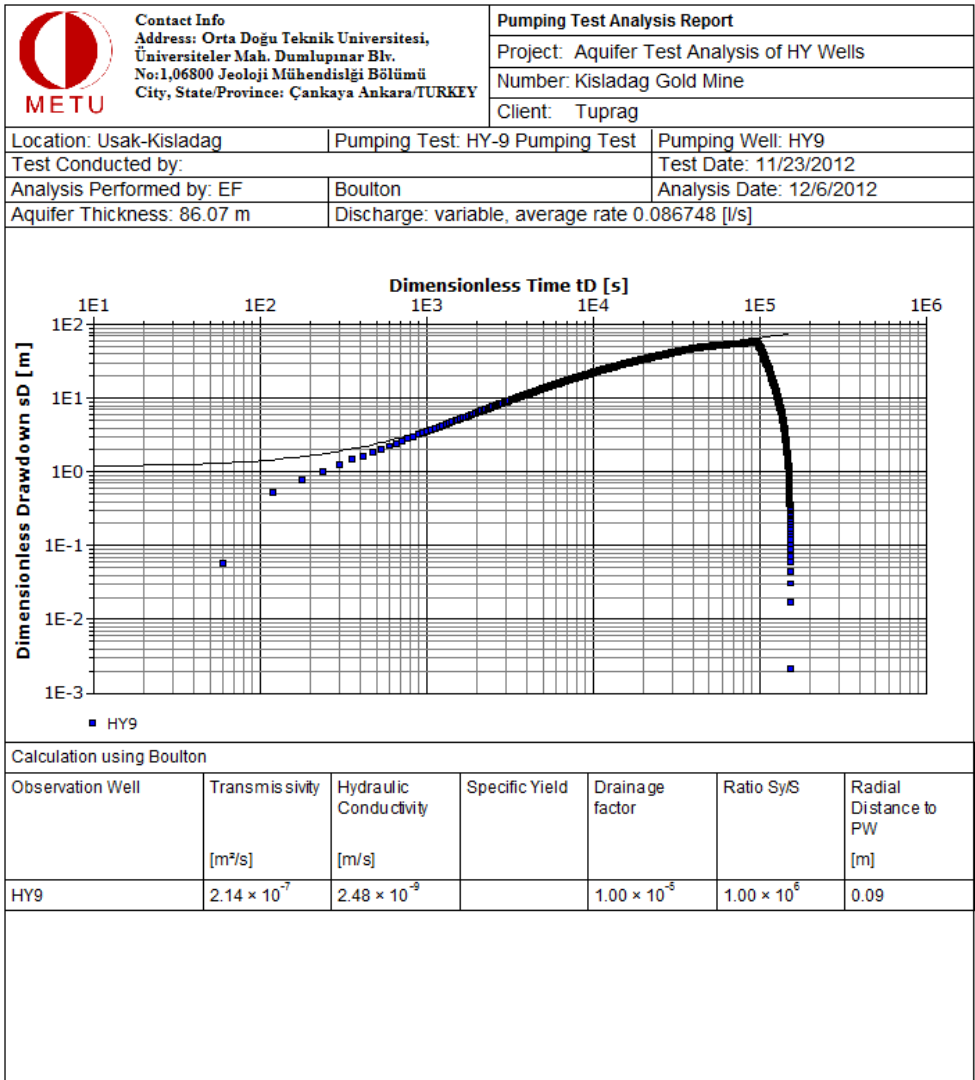


Figure C.32 Pumping test result of HY-9

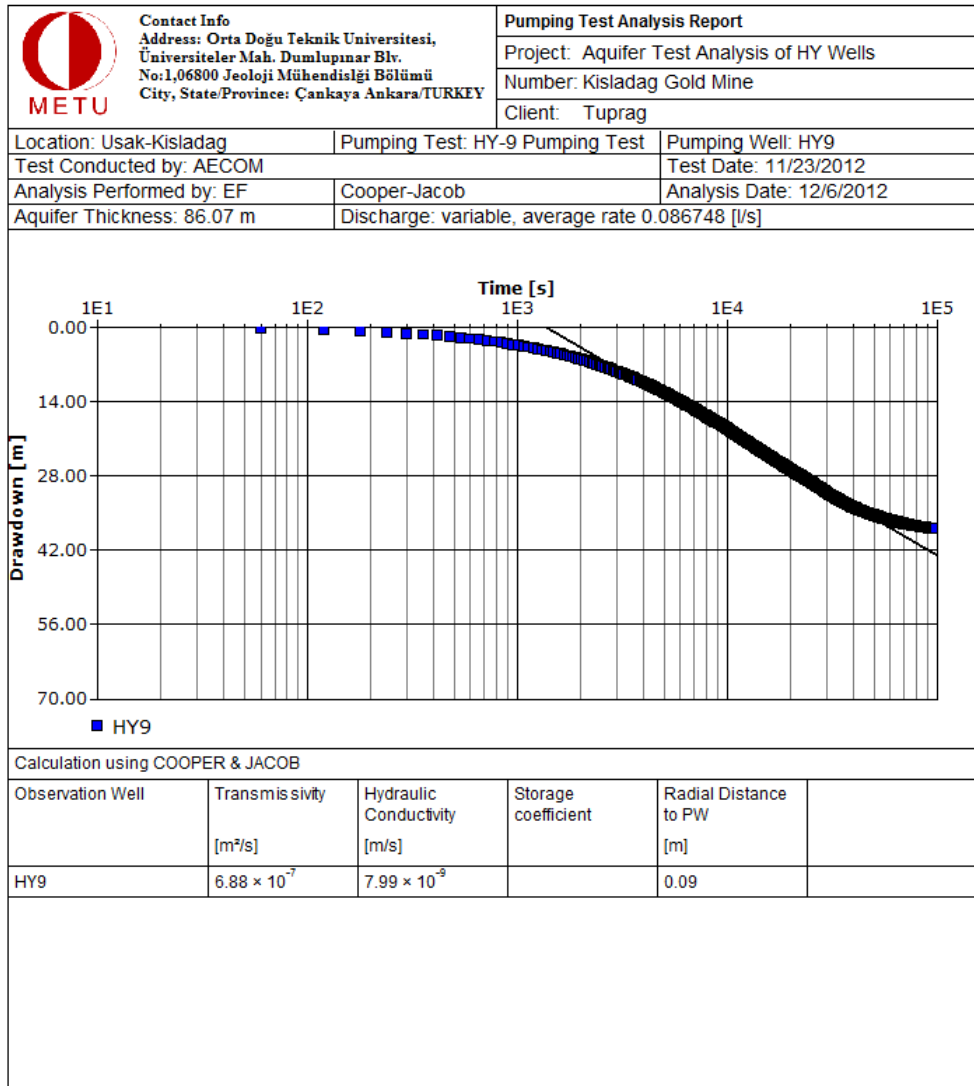


Figure C.11 Pumping test result of HY-9 (cont'd)

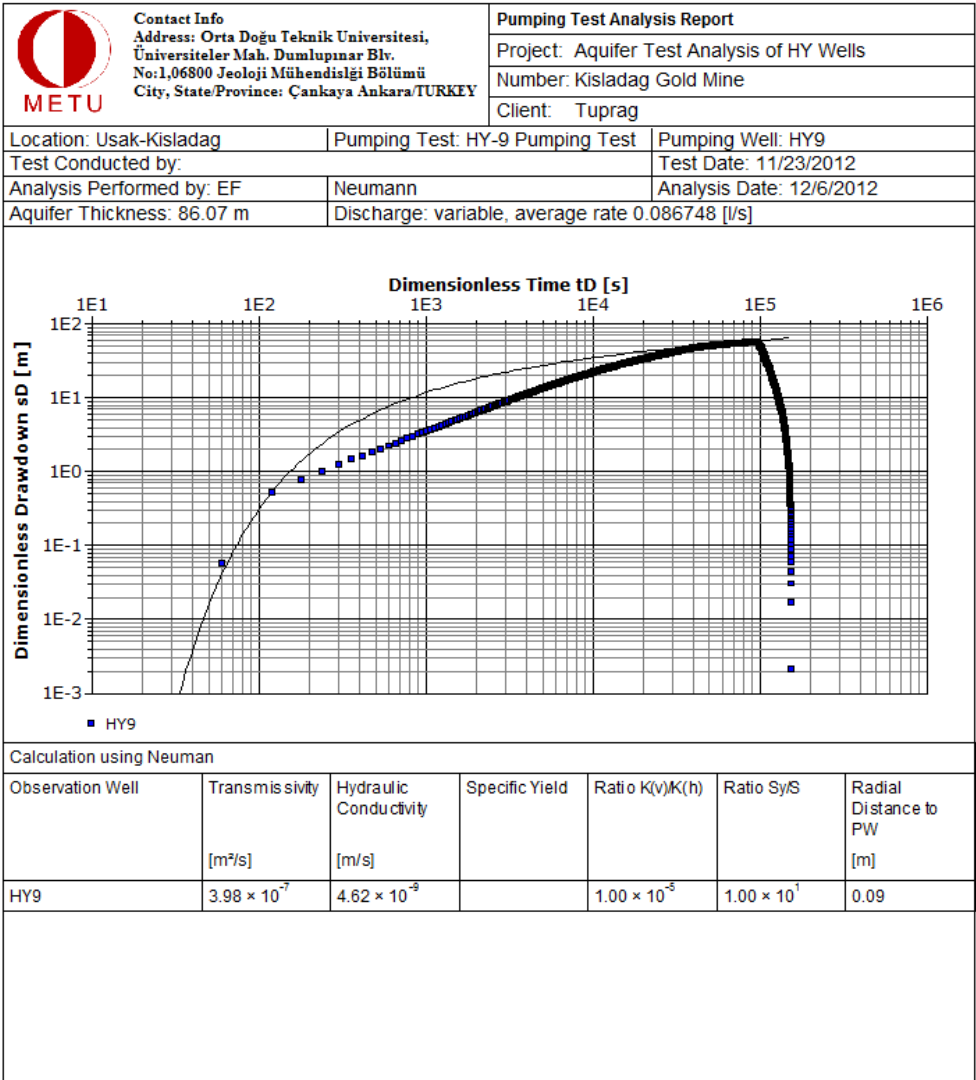


Figure C.11 Pumping test result of HY-9 (cont'd)

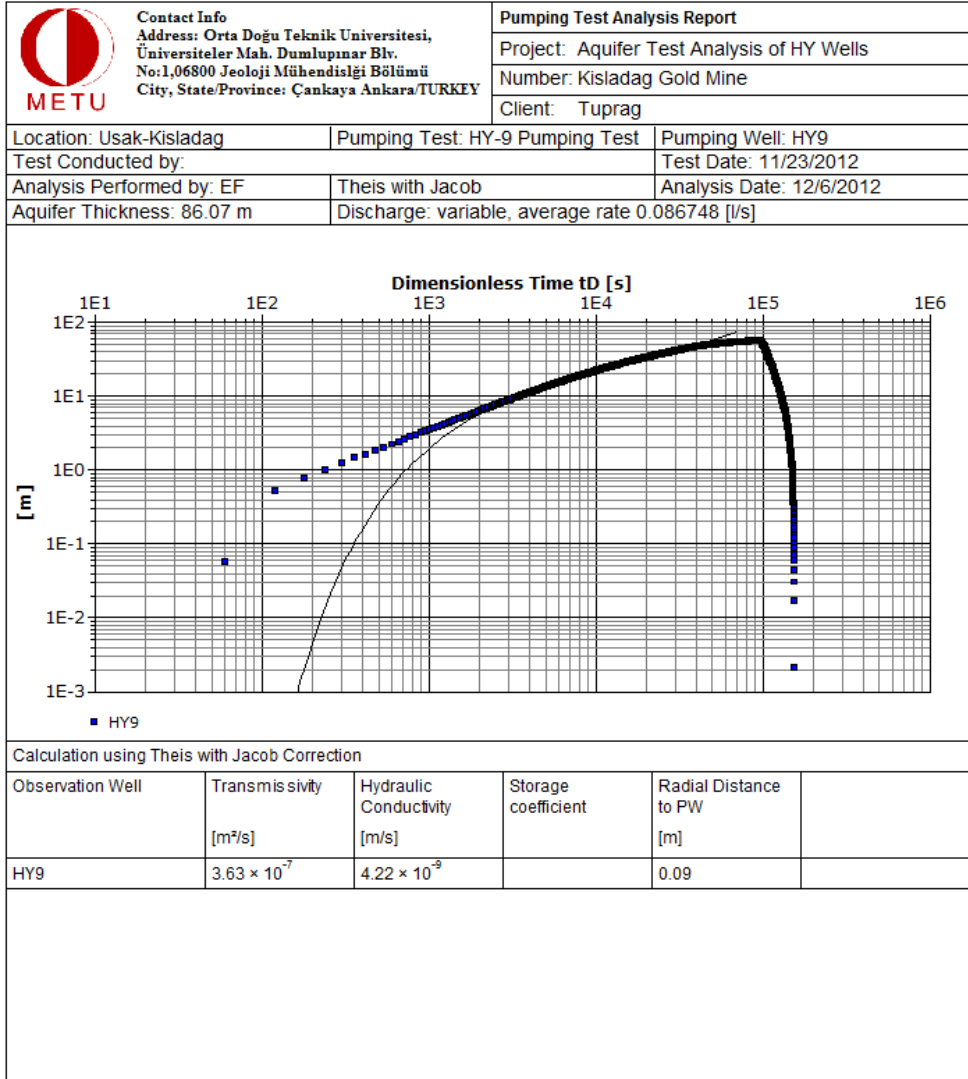


Figure C.11 Pumping test result of HY-9 (cont'd)

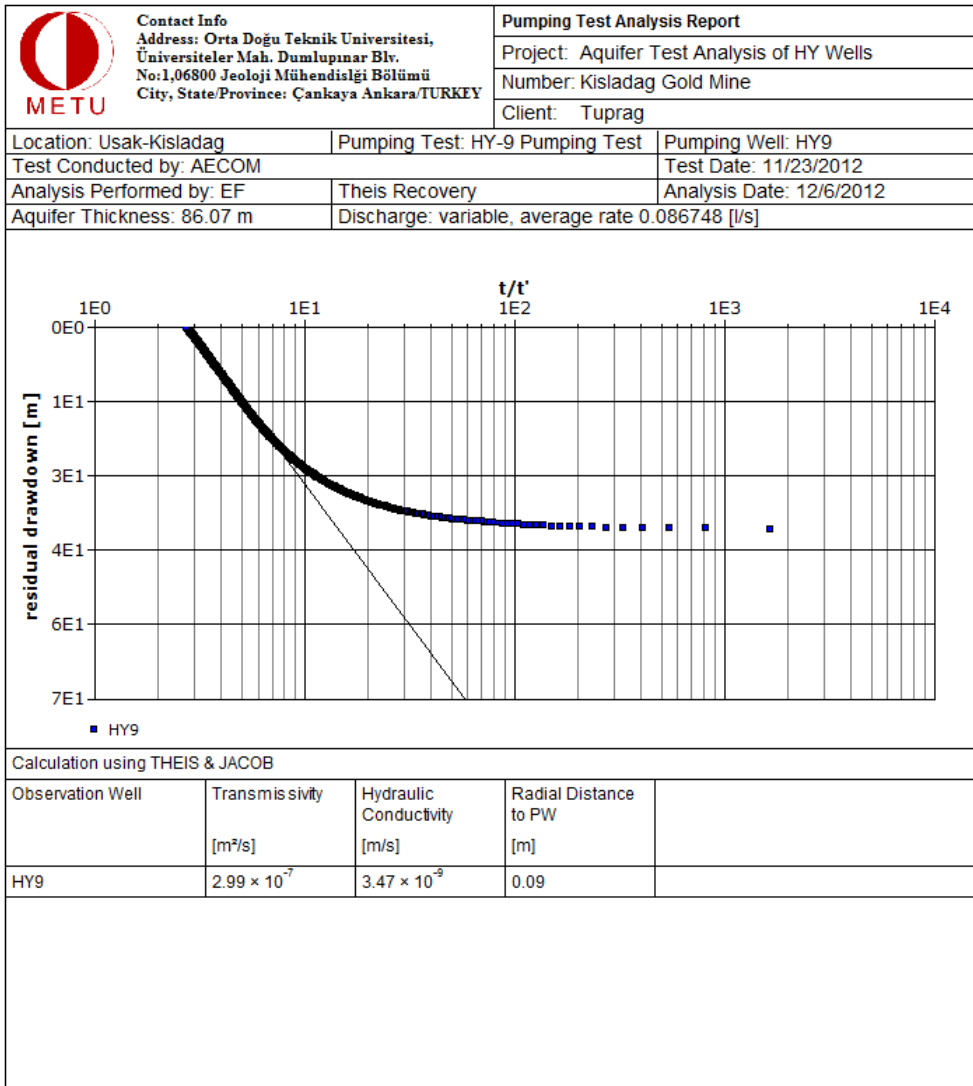


Figure C.11 Pumping test result of HY-9 (cont'd)

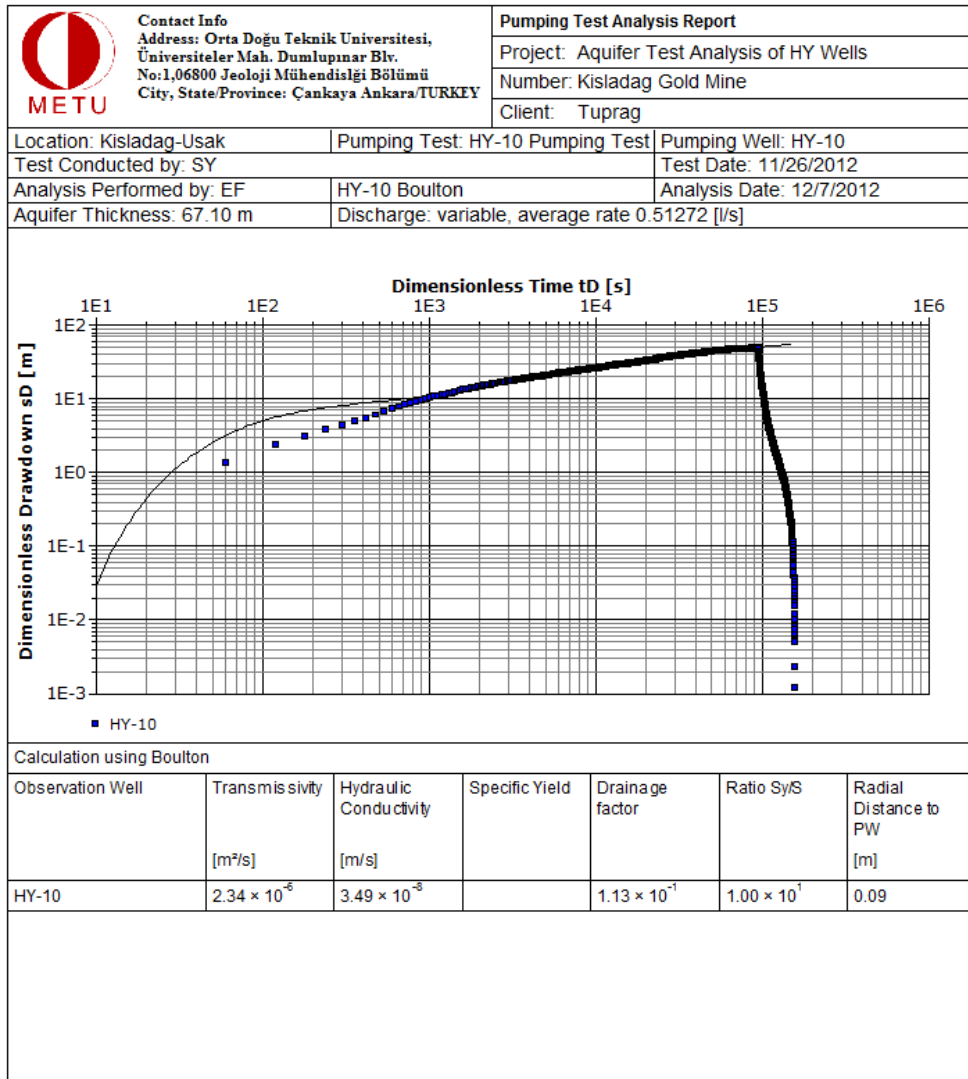


Figure C.33 Pumping test result of HY-10

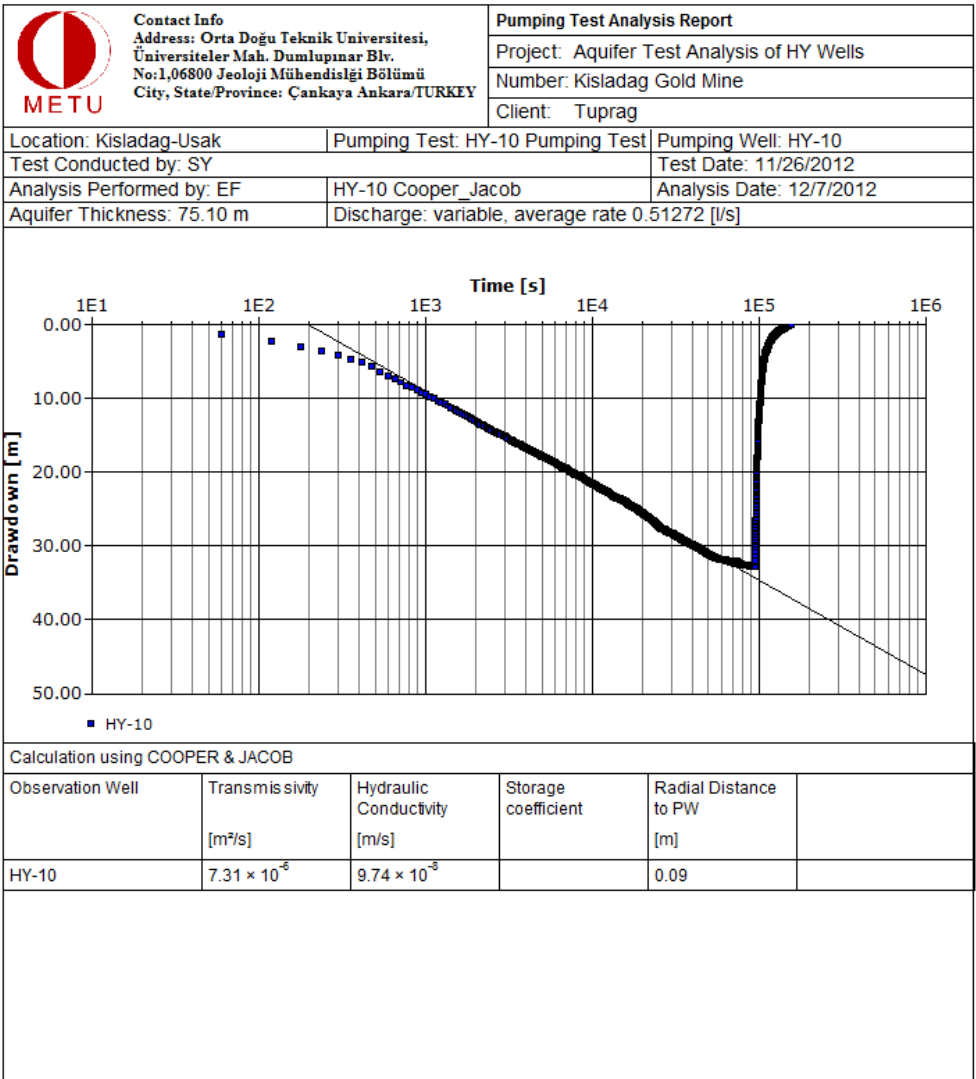


Figure C.12 Pumping test result of HY-10 (cont'd)

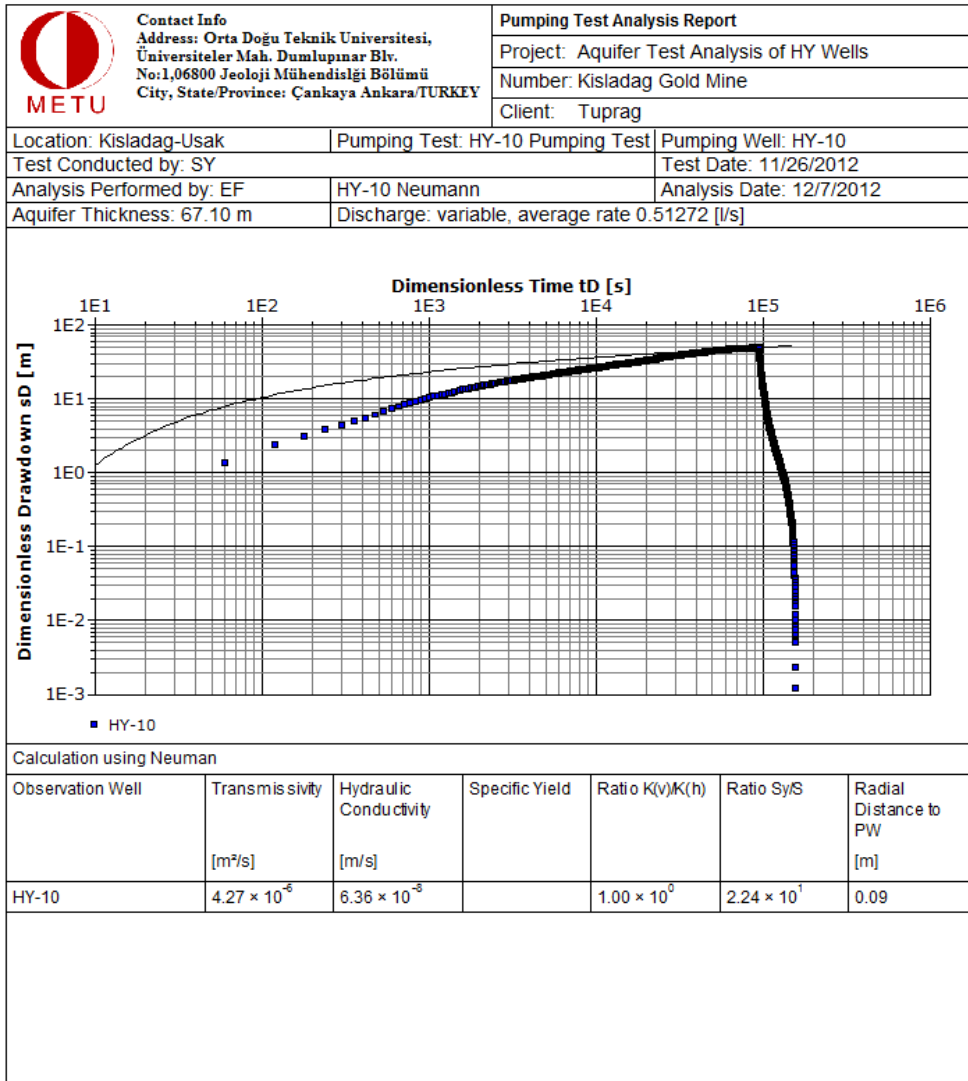


Figure C.12 Pumping test result of HY-10 (cont'd)

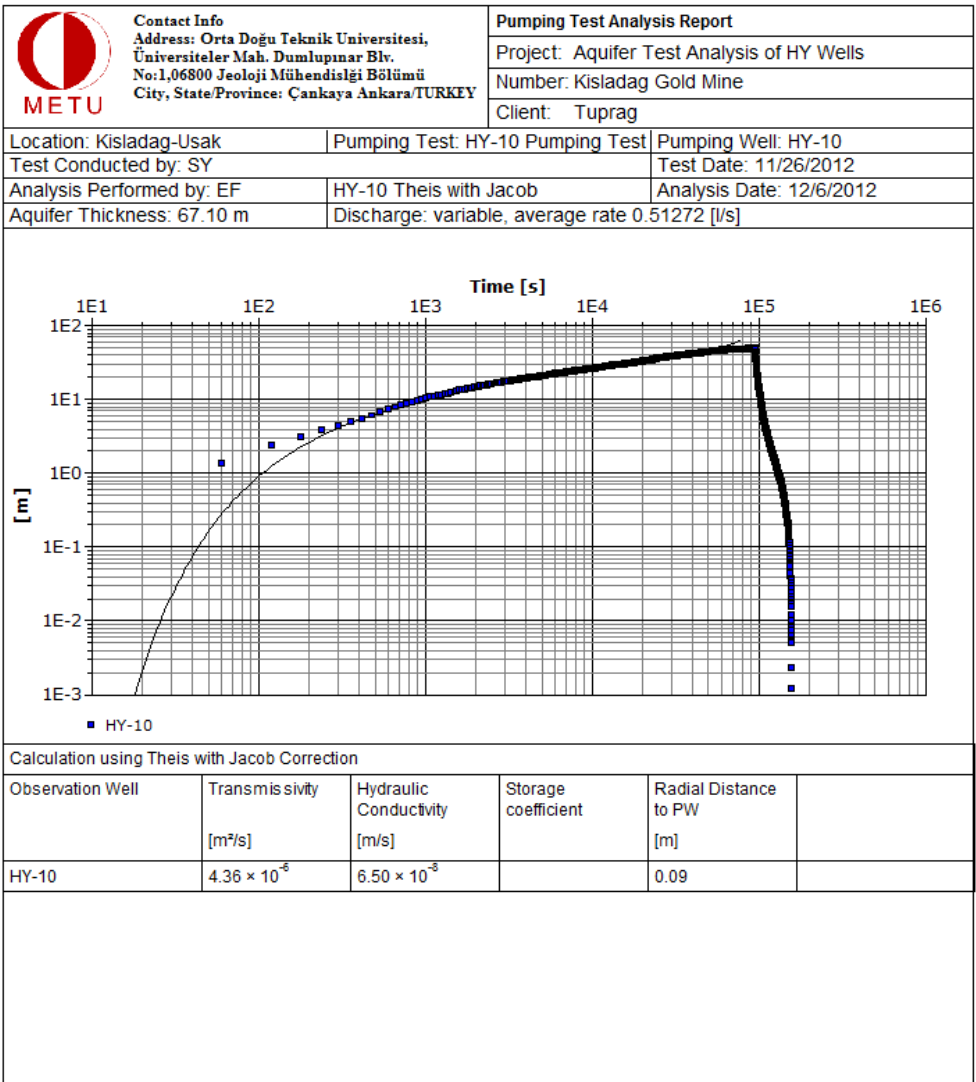


Figure C.12 Pumping test result of HY-10 (cont'd)

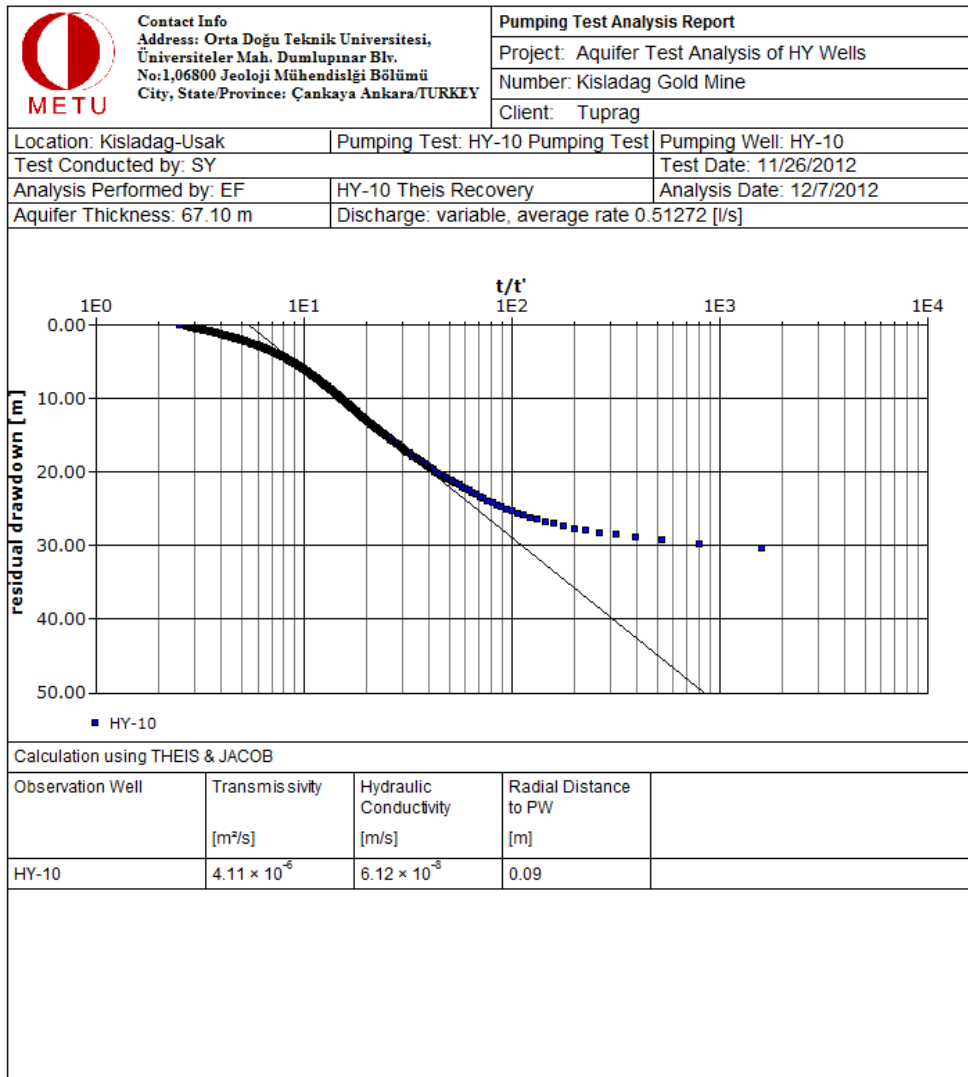


Figure C.12 Pumping test result of HY-10 (cont'd)

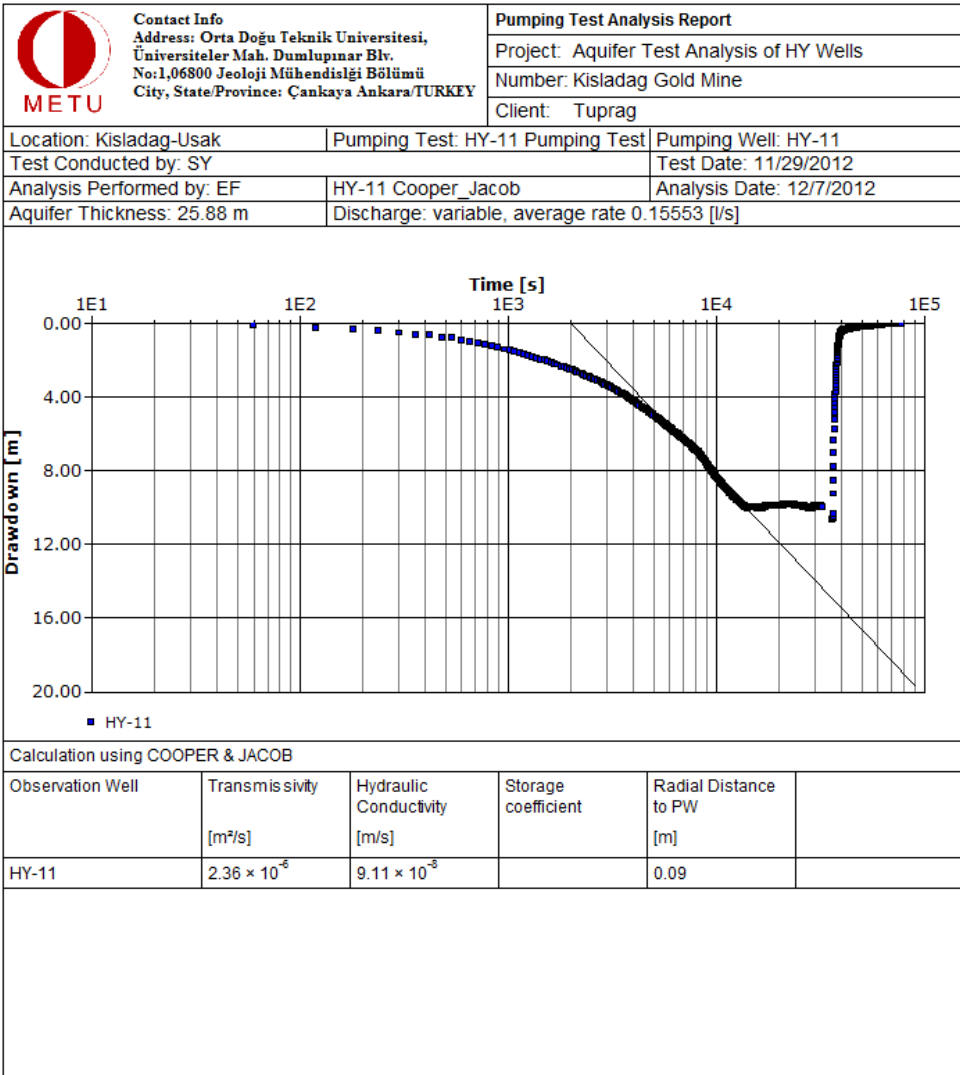


Figure C.34 Pumping test result of HY-11

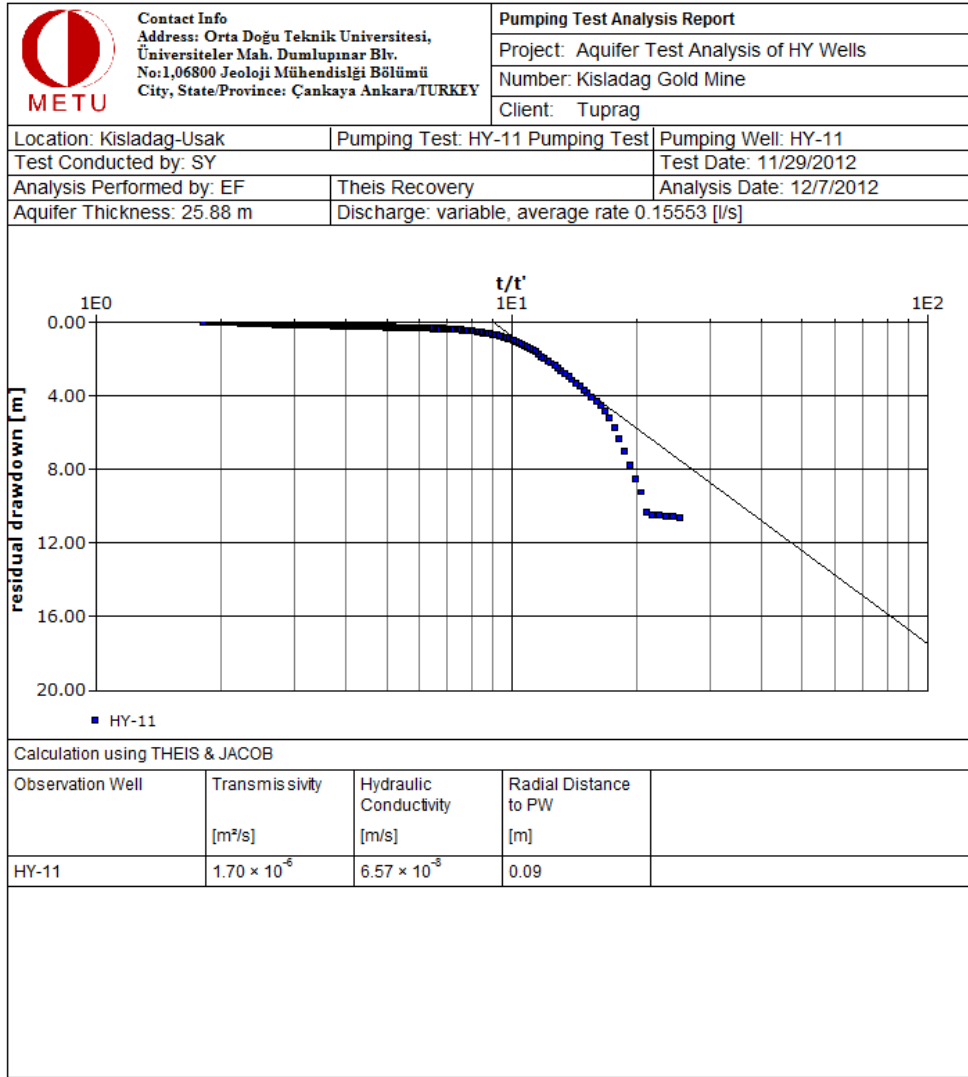


Figure C. 13 Pumping test result of HY-11 (cont'd)